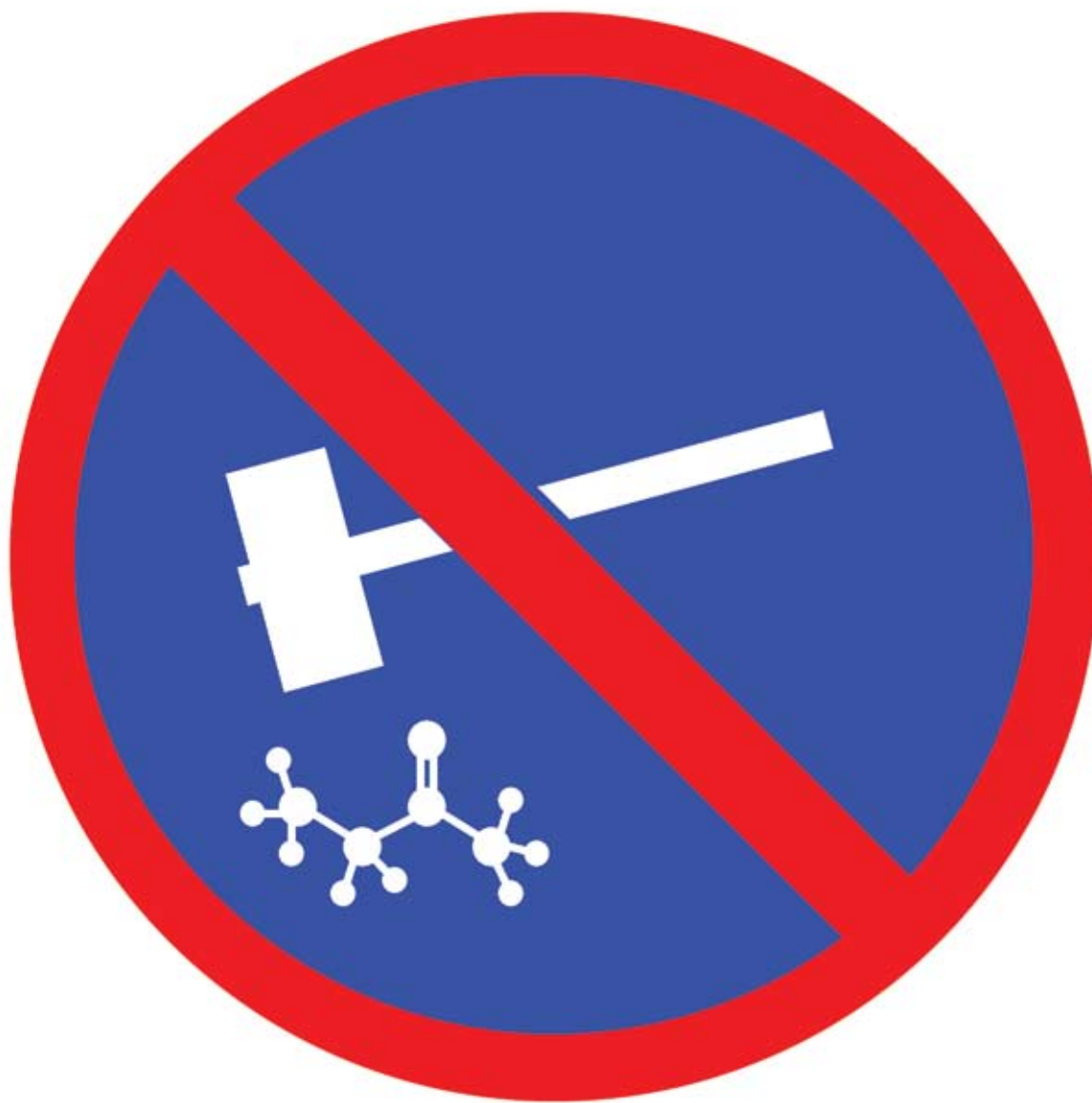


# Green Chemistry

Cutting-edge research for a greener sustainable future

[www.rsc.org/greenchem](http://www.rsc.org/greenchem)

Volume 10 | Number 12 | December 2008 | Pages 1237–1344



ISSN 1463-9262

RSC Publishing

de Klerk  
Fischer–Tropsch refining

Han *et al.*  
Conversion of fructose to  
5-hydroxymethylfurfural



1463-9262(2008)10:12;1-C



# 42nd IUPAC CONGRESS Chemistry Solutions

2–7 August 2009 | SECC | Glasgow | Scotland | UK

On behalf of IUPAC, the RSC is delighted to host the 42nd Congress (IUPAC 2009), the history of which goes back to 1894. RSC and IUPAC members, groups and networks have contributed a wealth of ideas to make this the biggest UK chemistry conference for several years.

As well as a programme including more than 50 symposia, a large poster session and a scientific exhibition, we are planning a series of social and satellite events to enhance networking and discussion opportunities.

Sponsored by  Schering-Plough

## Call for abstracts

This is your chance to take part in IUPAC 2009. Contributions are invited for oral presentation by 16 January 2009 and poster abstracts are welcome until 5 June 2009.

## Themes

- Analysis & Detection
- Chemistry for Health
- Communication & Education
- Energy & Environment
- Industry & Innovation
- Materials
- Synthesis & Mechanisms

## Plenary speakers

Peter G Bruce, University of St Andrews  
Chris Dobson, University of Cambridge  
Ben L Feringa, University of Groningen  
Sir Harold Kroto, Florida State University  
Klaus Müllen, Max-Planck Institute for Polymer Research  
Sir J Fraser Stoddart, Northwestern University  
Vivian W W Yam, The University of Hong Kong  
Richard N Zare, Stanford University

For a detailed list of symposia, keynote speakers and to submit an abstract visit our website.



RSC | Advancing the  
Chemical Sciences



[www.iupac2009.org](http://www.iupac2009.org)

Registered Charity Number 207890

# Green Chemistry

Cutting-edge research for a greener sustainable future

[www.rsc.org/greenchem](http://www.rsc.org/greenchem)

RSC Publishing is a not-for-profit publisher and a division of the Royal Society of Chemistry. Any surplus made is used to support charitable activities aimed at advancing the chemical sciences. Full details are available from [www.rsc.org](http://www.rsc.org)

## IN THIS ISSUE

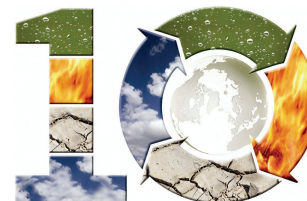
ISSN 1463-9262 CODEN GRCHFJ 10(12) 1237-1344 (2008)



### Cover

See de Klerk, pp. 1249-1279.  
No molecular abuse allowed!  
Refining of unconventional feed material requires proper technology selection to avoid inefficient conversion.

Image reproduced with permission from Arno de Klerk from *Green Chem.*, 2008, **10**, 1249.



## CHEMICAL TECHNOLOGY

### T89

Drawing together research highlights and news from all RSC publications, *Chemical Technology* provides a 'snapshot' of the latest applications and technological aspects of research across the chemical sciences, showcasing newsworthy articles and significant scientific advances.

## Chemical Technology

December 2008/Volume 5/Issue 12

[www.rsc.org/chemicaltechnology](http://www.rsc.org/chemicaltechnology)

## NEWS

### 1247

#### Conference Report: Bridging chemistry and engineering

Martyn Poliakoff and Richard Bourne

SynTOP offers the bright hope of innovation against a threatening background to the chemical industry.



## EDITORIAL STAFF

**Editor**

Sarah Ruthven

**Assistant editor**

Sarah Dixon

**Publishing assistant**

Ruth Bircham

**Team leader, serials production**

Stephen Wilkes

**Technical editor**

Edward Morgan

**Production administration coordinator**

Sonya Spring

**Administration assistants**Clare Davies, Donna Fordham, Kirsty Lunnon,  
Julie Thompson**Publisher**

Emma Wilson

Green Chemistry (print: ISSN 1463-9262; electronic: ISSN 1463-9270) is published 12 times a year by the Royal Society of Chemistry, Thomas Graham House, Science Park, Milton Road, Cambridge, UK CB4 0WF.

All orders, with cheques made payable to the Royal Society of Chemistry, should be sent to RSC Distribution Services, c/o Portland Customer Services, Commerce Way, Colchester, Essex, UK CO2 8HP. Tel +44 (0) 1206 226050; E-mail sales@rscdistribution.org

2008 Annual (print + electronic) subscription price: £947; US\$1799. 2008 Annual (electronic) subscription price: £852; US\$1695. Customers in Canada will be subject to a surcharge to cover GST. Customers in the EU subscribing to the electronic version only will be charged VAT.

If you take an institutional subscription to any RSC journal you are entitled to free, site-wide web access to that journal. You can arrange access via Internet Protocol (IP) address at [www.rsc.org/ip](http://www.rsc.org/ip). Customers should make payments by cheque in sterling payable on a UK clearing bank or in US dollars payable on a US clearing bank. Periodicals postage paid at Rahway, NJ, USA and at additional mailing offices. Airfreight and mailing in the USA by Mercury Airfreight International Ltd., 365 Blair Road, Avenel, NJ 07001, USA.

US Postmaster: send address changes to Green Chemistry, c/o Mercury Airfreight International Ltd., 365 Blair Road, Avenel, NJ 07001. All despatches outside the UK by Consolidated Airfreight.

PRINTED IN THE UK

**Advertisement sales:** Tel +44 (0) 1223 432246; Fax +44 (0) 1223 426017; E-mail [advertising@rsc.org](mailto:advertising@rsc.org)

# Green Chemistry

Cutting-edge research for a greener sustainable future

[www.rsc.org/greenchem](http://www.rsc.org/greenchem)

Green Chemistry focuses on cutting-edge research that attempts to reduce the environmental impact of the chemical enterprise by developing a technology base that is inherently non-toxic to living things and the environment.

## EDITORIAL BOARD

**Chair**

Professor Martyn Poliakoff  
Nottingham, UK

**Scientific Editor**

Professor Walter Leitner  
RWTH-Aachen, Germany

**Associate Editors**

Professor C. J. Li  
McGill University, Canada

**Members**

Professor Paul Anastas  
Yale University, USA  
Professor Joan Brennecke  
University of Notre Dame, USA  
Professor Mike Green  
Sasol, South Africa  
Professor Buxing Han  
Chinese Academy of Sciences,  
China

Dr Alexei Lapkin  
Bath University, UK  
Professor Steven Ley  
Cambridge, UK  
Dr Janet Scott  
Unilever, UK  
Professor Tom Welton  
Imperial College, UK

## ADVISORY BOARD

James Clark, York, UK  
Avelino Corma, Universidad  
Politécnica de Valencia, Spain  
Mark Harmer, DuPont Central  
R&D, USA  
Herbert Hugl, Lanxess Fine  
Chemicals, Germany  
Roshan Jachuck,  
Clarkson University, USA  
Makoto Misono, nite,  
Japan

Colin Raston,  
University of Western Australia,  
Australia  
Robin D. Rogers, Centre for Green  
Manufacturing, USA  
Kenneth Seddon, Queen's  
University, Belfast, UK  
Roger Sheldon, Delft University of  
Technology, The Netherlands  
Gary Sheldrake, Queen's  
University, Belfast, UK

Pietro Tundo, Università ca  
Foscari di Venezia, Italy

## INFORMATION FOR AUTHORS

Full details of how to submit material for publication in Green Chemistry are given in the Instructions for Authors (available from <http://www.rsc.org/authors>). Submissions should be sent via ReSource: <http://www.rsc.org/resource>.

Authors may reproduce/republish portions of their published contribution without seeking permission from the RSC, provided that any such republication is accompanied by an acknowledgement in the form: (Original citation) – Reproduced by permission of the Royal Society of Chemistry.

© The Royal Society of Chemistry 2008. Apart from fair dealing for the purposes of research or private study for non-commercial purposes, or criticism or review, as permitted under the Copyright, Designs and Patents Act 1988 and the Copyright and Related Rights Regulations 2003, this publication may only be reproduced, stored or transmitted, in any form or by any means, with the prior permission in writing of the Publishers or in the case of reprographic reproduction in accordance with the terms of licences issued by the Copyright Licensing Agency in the UK. US copyright law is applicable to users in the USA.

The Royal Society of Chemistry takes reasonable care in the preparation of this publication but does not accept liability for the consequences of any errors or omissions.

The paper used in this publication meets the requirements of ANSI/NISO Z39.48-1992 (Permanence of Paper).

Royal Society of Chemistry: Registered Charity No. 207890

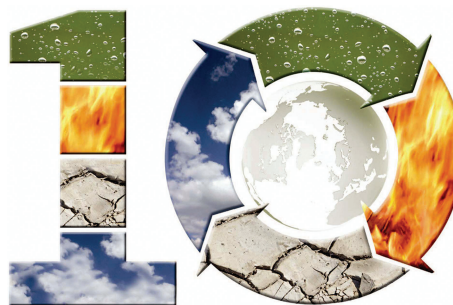


## EDITORIAL

1248

**Environmentally friendly refining**

Mike Green highlights the importance of Fischer–Tropsch refineries and introduces the review by Arno de Klerk on this topic.



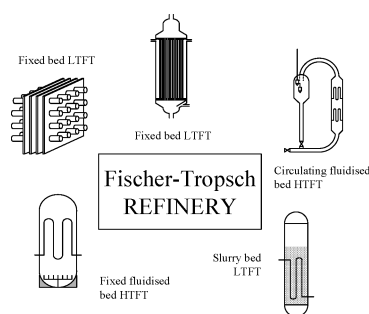
## CRITICAL REVIEW

1249

**Fischer–Tropsch refining: technology selection to match molecules**

Arno de Klerk\*

On a molecular level Fischer–Tropsch syncrude is significantly different from crude oil. Recommendations are made for appropriate refinery technology selection when dealing with the conversion of Fischer–Tropsch syncrude into transportation fuels.



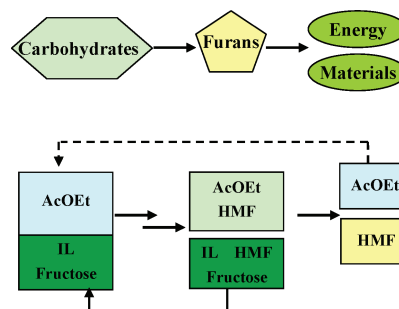
## COMMUNICATIONS

1280

**Conversion of fructose to 5-hydroxymethylfurfural using ionic liquids prepared from renewable materials**

Suqin Hu, Zhaofu Zhang, Yinxi Zhou, Buxing Han,\* Honglei Fan, Wenjing Li, Jinliang Song and Ye Xie

The conversion of fructose to 5-hydroxymethylfurfural (HMF) was achieved efficiently in an ethyl acetate (AcOEt)/biorenewable ionic liquid (IL) biphasic system, the separation process had no cross-contamination and the IL can be reused easily.

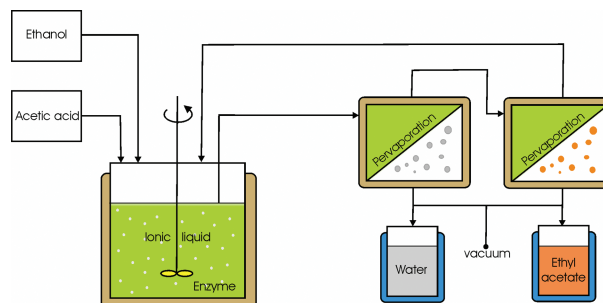


1284

**Waste-free process for continuous flow enzymatic esterification using a double pervaporation system**

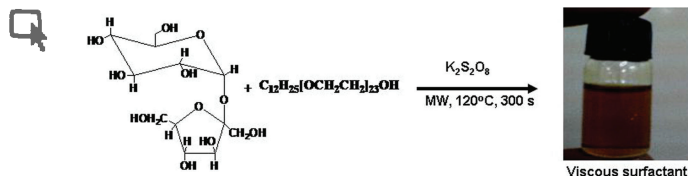
László Gubicza,\* Katalin Bélafi-Bakó, Erika Fehér and Tamás Fráter

A double pervaporation system was developed for the simultaneous removal of water and ethyl acetate produced during continuous enzymatic esterification of acetic acid and ethanol in [bmim]PF<sub>6</sub> ionic liquid.



## COMMUNICATIONS

1288



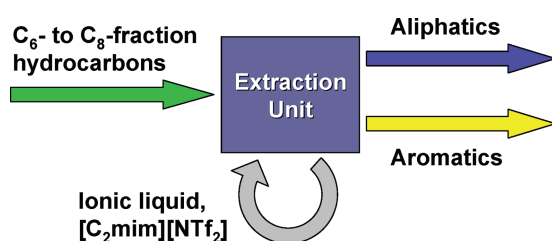
### Facile solvent free synthesis of polymerised sucrose functionalised polyoxyethylene (23) lauryl ether by microwave irradiation

Kamalesh Prasad,\* P. Bahadur, Ramavatar Meena and A. K. Siddhanta

One-pot solvent free synthesis of a polymerised sucrose and polyoxyethylene (23) lauryl ether based viscous surfactant by microwave irradiation (MW) was achieved.

## PAPERS

1294

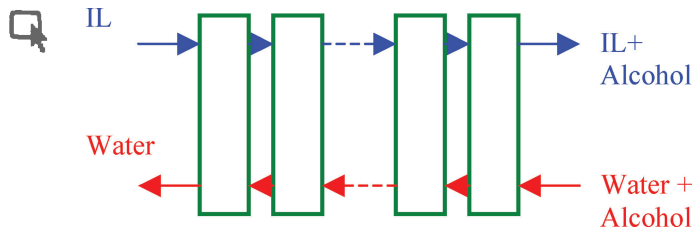


### 1-Ethyl-3-methylimidazolium bis{(trifluoromethyl)sulfonyl}amide as solvent for the separation of aromatic and aliphatic hydrocarbons by liquid extraction – extension to C<sub>7</sub>- and C<sub>8</sub>-fractions

Alberto Arce, Martyn J. Earle,\* Héctor Rodríguez, Kenneth R. Seddon and Ana Soto

The ionic liquid 1-ethyl-3-methylimidazolium bis{(trifluoromethyl)sulfonyl}amide ([C<sub>2</sub>mim][NTf<sub>2</sub>]) constitutes a potential green alternative solvent in liquid extraction processes for the separation of aromatic and aliphatic hydrocarbons with 6–8 carbon atoms in their structures.

1301

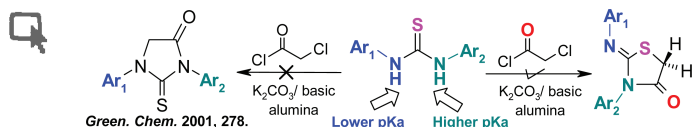


### Extraction of alcohols from water with 1-hexyl-3-methylimidazolium bis(trifluoromethylsulfonyl)imide

Alexandre Chapeaux, Luke D. Simoni, Thomas S. Ronan, Mark A. Stadtherr and Joan F. Brennecke\*

This study provides data on how ionic liquids can be used to separate alcohol and water mixtures at room temperature and pressure.

1307



### It is “2-imino-4-thiazolidinones” and not thiohydantoin as the reaction product of 1,3-disubstituted thioureas and chloroacetylchloride

Ramesh Yella, Harisadhan Ghosh and Bhisma K. Patel\*

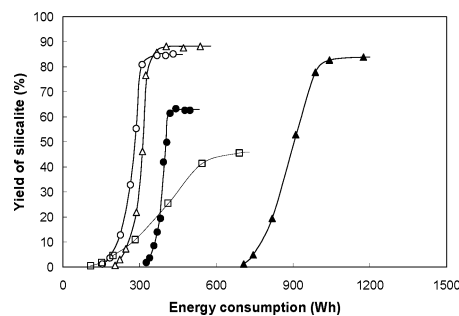
The products obtained by the reaction of 1,3-disubstituted thioureas with chloroacetylchloride are actually 2-imino-4-thiazolidinone derivatives and not thiohydantoin as previously reported. This reaction gives regioselective product and can be performed without any added base.

1313

### Microwave assisted synthesis of silicalite—power delivery and energy consumption

Ko-Yeol Choi,\* Geoffrey Tompsett and W. Curtis Conner

Silicalite was synthesized by microwave heating and two conventional heating methods: an ethylene glycol bath or an electric oven.

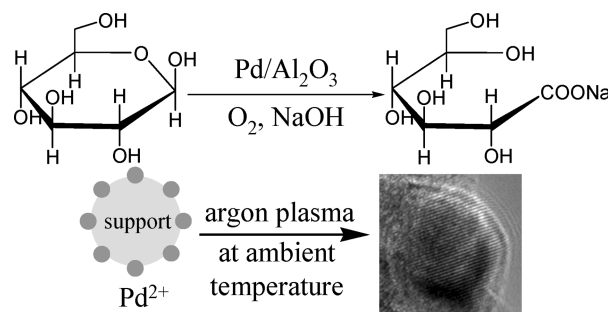


1318

### Selective oxidation of glucose to gluconic acid over argon plasma reduced Pd/Al<sub>2</sub>O<sub>3</sub>

Xi Liang, Chang-jun Liu\* and Pingyu Kuai

The Pd/ $\gamma$ -Al<sub>2</sub>O<sub>3</sub> catalysts reduced by argon glow discharge plasma, which is environmentally benign, energy efficient and economic effective, show higher stability against leaching of active metal into the reaction medium than the conventional hydrogen reduced catalyst.

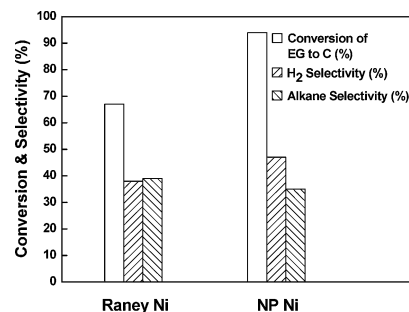


1323

### An environmentally benign and catalytically efficient non-pyrophoric Ni catalyst for aqueous-phase reforming of ethylene glycol

Ling-Jun Zhu, Ping-Jun Guo, Xian-Wen Chu, Shi-Run Yan, Ming-Hua Qiao,\* Kang-Nian Fan, Xiao-Xin Zhang and Bao-Ning Zong\*

A non-pyrophoric Ni catalyst prepared from the Ni<sub>50</sub>Al<sub>50</sub> alloy was more active and more stable than the conventional Raney Ni catalyst in aqueous-phase reforming of ethylene glycol to H<sub>2</sub> and light alkanes.



1331

### Variables affecting homogeneous acid catalyst recoverability and reuse after esterification of concentrated omega-9 polyunsaturated fatty acids in vegetable oil triglycerides

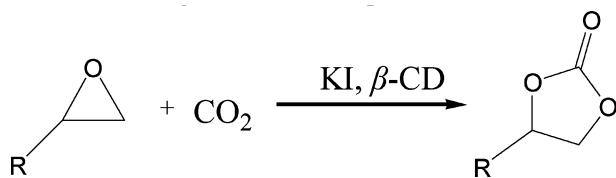
Matthew B. Boucher, Steven A. Unker, Kyle R. Hawley, Benjamin A. Wilhite, James D. Stuart and Richard S. Parnas\*

This study illustrates for the first time the much greater sensitivity of diprotic H<sub>2</sub>SO<sub>4</sub> to water during free fatty acid esterification in the presence of triglycerides, compared to HCl.



## PAPERS

1337



**Synthesis of cyclic carbonates from epoxides and CO<sub>2</sub> catalyzed by potassium halide in the presence of β-cyclodextrin**

Jinliang Song, Zhaofu Zhang, Buxing Han,\* Suqin Hu, Wenjing Li and Ye Xie

KI and β-cyclodextrin (β-CD) shows excellent synergetic effect in promoting cycloaddition of CO<sub>2</sub> with epoxides to produce cyclic carbonates. The catalytic system is very active, selective, stable, greener, and inexpensive.

## ADDITIONS AND CORRECTIONS

1342

Wen-Hua Ou and Zhi-Zhen Huang

Peter D. Vu, Andrew J. Boydston and Christopher W. Bielawski\*

Hua Zhao, Gary A. Baker, Zhiyan Song, Olarongbe Olubajo, Tanisha Crittle and Darkeysha Peters

**Retracted article: An efficient and practical synthesis of chiral imidazolium ionic liquids and their application in an enantioselective Michael reaction**

**Ionic liquids *via* efficient, solvent-free anion metathesis**

**Designing enzyme-compatible ionic liquids that can dissolve carbohydrates**

## AUTHOR INDEX

Arce, Alberto, 1294  
 Bahadur, P., 1288  
 Bélafi-Bakó, Katalin, 1284  
 Boucher, Matthew B., 1331  
 Bourne, Richard, 1247  
 Brennecke, Joan F., 1301  
 Chapeaux, Alexandre, 1301  
 Choi, Ko-Yeol, 1313  
 Chu, Xian-Wen, 1323  
 Conner, W. Curtis, 1313  
 de Klerk, Arno, 1249  
 Earle, Martyn J., 1294  
 Fan, Honglei, 1280

Fan, Kang-Nian, 1323  
 Fehér, Erika, 1284  
 Fráter, Tamás, 1284  
 Ghosh, Harisadhan, 1307  
 Gubicza, László, 1284  
 Guo, Ping-Jun, 1323  
 Han, Buxing, 1280, 1337  
 Hawley, Kyle R., 1331  
 Hu, Suqin, 1280, 1337  
 Kuai, Pingyu, 1318  
 Li, Wenjing, 1280, 1337  
 Liang, Xi, 1318  
 Liu, Chang-jun, 1318

Meena, Ramavatar, 1288  
 Parnas, Richard S., 1331  
 Patel, Bhisma K., 1307  
 Poliakov, Martyn, 1247  
 Prasad, Kamalesh, 1288  
 Qiao, Ming-Hua, 1323  
 Rodríguez, Héctor, 1294  
 Ronan, Thomas S., 1301  
 Seddon, Kenneth R., 1294  
 Siddhanta, A. K., 1288  
 Simoni, Luke D., 1301  
 Song, Jinliang, 1280, 1337  
 Soto, Ana, 1294

Stadtherr, Mark A., 1301  
 Stuart, James D., 1331  
 Tompsett, Geoffrey, 1313  
 Unker, Steven A., 1331  
 Wilhite, Benjamin A., 1331  
 Xie, Ye, 1280, 1337  
 Yan, Shi-Run, 1323  
 Yella, Ramesh, 1307  
 Zhang, Xiao-Xin, 1323  
 Zhang, Zhaofu, 1280, 1337  
 Zhou, Yinxi, 1280  
 Zhu, Ling-Jun, 1323  
 Zong, Bao-Ning, 1323

## FREE E-MAIL ALERTS AND RSS FEEDS

Contents lists in advance of publication are available on the web *via* [www.rsc.org/greenchem](http://www.rsc.org/greenchem) – or take advantage of our free e-mail alerting service ([www.rsc.org/ej.alert](http://www.rsc.org/ej.alert)) to receive notification each time a new list becomes available.



Try our RSS feeds for up-to-the-minute news of the latest research. By setting up RSS feeds, preferably using feed reader software, you can be alerted to the latest Advance Articles published on the RSC web site. Visit [www.rsc.org/publishing/technology/rss.asp](http://www.rsc.org/publishing/technology/rss.asp) for details.

## ADVANCE ARTICLES AND ELECTRONIC JOURNAL

Free site-wide access to Advance Articles and the electronic form of this journal is provided with a full-rate institutional subscription. See [www.rsc.org/ejs](http://www.rsc.org/ejs) for more information.

\* Indicates the author for correspondence: see article for details.



Electronic supplementary information (ESI) is available *via* the online article (see <http://www.rsc.org/esi> for general information about ESI).

# A new journal from RSC Publishing launching in 2009

## Metallomics: Integrated biometal science



060877

This timely new journal will cover the research fields related to metals in biological, environmental and clinical systems and is expected to be the core publication for the emerging metallomics community. Professor Joseph A. Caruso of the University of Cincinnati/Agilent Technologies Metallomics Center of the Americas, and a leading player in the field, will chair the Editorial Board.

From launch, the latest issue will be freely available online to all readers. Free institutional access to previous issues throughout 2009 and 2010 will be available following a simple registration process. Email [metallomics@rsc.org](mailto:metallomics@rsc.org) for further information or visit the website.

**Submit your work now!**

RSC Publishing

Supporting the **ISM**  
 International  
 Symposium  
 on Metallomics

[www.rsc.org/metallomics](http://www.rsc.org/metallomics)

Registered Charity Number 207890





# Journal of Environmental Monitoring

## Focus on Medical Geology & Air- and Biomonitoring

*Journal of Environmental Monitoring (JEM)* issue 12, 2008, is focusing on the areas of Medical Geology & Air- and Biomonitoring.

**Medical Geology** has seen immense growth and maturation allowing biomedical/health professionals and geoscientists to take strong root in the international arena. The journal anticipates publishing many articles in this field. The first two reviews, included in this issue, are:

**The utility of mosquito-borne disease as an environmental monitoring tool in tropical ecosystems**

Andrew Jardine, Angus Cook and Philip Weinstein

**10th Anniversary Critical Review: Naturally occurring asbestos**

Martin Harper

**Air- and Biomonitoring** features six selected papers on exposure monitoring within the preventive framework of identifying and controlling health hazards within the workplace and in the environment presented at AIRMON 2008, held at Geilo, Norway, January 28-31, 2008.

**Highlighted papers:**

**Three dimensional modeling of air flow, aerosol distribution and aerosol samplers for unsteady conditions**

Albert Gilmudtinov and Ilya Zivliskii

**Experimental methods to determine inhalability and personal sampler performance for aerosols in ultra-low windspeed environments**

Darrah K. Schmees, Yi-Hsuan Wu and James H. Vincent

**A study of the bio-accessibility of welding fumes**

Balázs Berlinger, Dag G. Ellingsen, Miklós Náray, Gyula Zárny and Yngvar Thomassen

110807

RSC Publishing

[www.rsc.org/jem](http://www.rsc.org/jem)

Registered Charity Number 207890

# Chemical Technology

Isotopes reveal clues about the birth of the Solar System

## Results that are out of this world

Danish scientists have developed a precise method to test for chromium isotopes in rocks and meteorites. The method will help to reveal more details about the evolution of the Solar System, they claim.

Supernovae explosions in the Solar System generate chromium-50, chromium-52 and chromium-53 isotopes. The amounts of these isotopes vary and are recorded in materials formed as a result of these explosions, such as meteorites, asteroids and planets.

Using thermal ionisation mass spectrometry, Anne Trinquier and colleagues from the Geological Museum at the University of Copenhagen purified and measured chromium isotopes in meteorites at concentrations as low as 10 parts per million, a level of accuracy that has never before been achieved. Their method is simple and quick, which minimises cost and contamination. Also, it uses only a small amount of meteorite, a bonus when the starting material is so hard to replace.

The results enable Trinquier to distinguish between planetary



**Explosive results: isotopes released from supernovae can be measured in meteorites**

bodies that were formed from different mixes of components and hence different explosions, something of great interest to scientists studying cosmochemistry.

'Precise chromium isotope ratio measurements are of great importance in any research related to the formation and early evolution of our Solar System,' comments Thorsten Kleine, an expert in Solar System chronology from the Institute of Isotope Geochemistry and Mineral Resources, ETH Zürich, Switzerland.

Trinquier says the next step is to improve the reproducibility of the results, with the hope that the measurements 'might reveal additional differences between planetesimals [small solar system bodies] and planets and help constrain further our understanding of planetary formation processes and timing'.

Rebecca Brodie

### Reference

A Trinquier, J -L Birck and C L Allègre, *J. Anal. At. Spectrom.*, 2008, DOI:10.1039/b809755k

NASA

## In this issue

### Back to the grindstone

Solid–solid reactions provide a greener route to metal complexes

### Sweet solution for on-card reagent storage

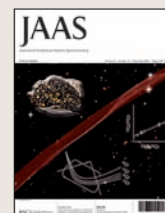
Sugar-dried labelling agents detect malaria on a card

### Interview: Taking the lab to the field

Gillian Greenway talks to Freya Mearns about taking analytical chemistry out of the lab and into the real world

### Instant insight: Photochemistry goes micro

Michael Oelgemöller and Emma Coyle discuss how microreactors may change synthetic organic photochemistry



The latest applications and technological aspects of research across the chemical sciences



# Application highlights

Solid–solid reactions generate new types of metal-organic frameworks

## Back to the grind-stone

UK scientists have studied a greener way to make microporous materials that could lead to new types of metal-organic frameworks.

Stuart James and Anne Pichon, at Queen's University Belfast, investigated a wide range of solvent-free mechanochemical reactions. Mechanochemistry is the initiation of chemical reactions by grinding two or more solids together using, for example, a mechanical ball-mill. Since mechanochemistry avoids the use of solvents, it could be a greener alternative to solution reactions.

James and Pichon surveyed 60 metal complexation reactions between 12 different metal salts and five bridging ligands using a ball-mill to grind the solid components together. They found that many of



the mixtures were highly reactive and gave crystalline products within a few minutes. The study revealed some interesting trends, including an inverse correlation between ligand melting point and reactivity, which could prompt further investigation. They also

**Grinding solids in a ball-mill can generate crystalline products within minutes**

#### Reference

A Pichon and S L James, *CrystEngComm*, 2008, DOI: 10.1039/b810857a

obtained new types of structures than those formed using solvents.

'Mechanochemistry is actually a very old method,' explains James. 'However, most chemists are not tempted to try it because it is counter-intuitive that two solids can react with each other. It's comparatively recent that the impetus for avoiding solvents has become strong enough to start making chemists think again.'

Graham Bowmaker, an expert in mechanochemical synthesis from the University of Auckland, New Zealand, says that James' study 'provides clues about the possible mechanisms of mechanochemical reactions, which in turn will greatly enhance further exploitation of the method'.

Ruth Doherty

## Fundamental Toxicology

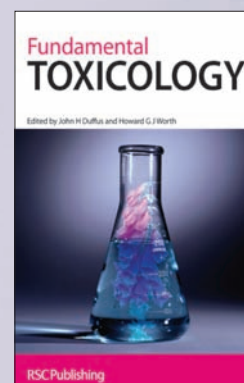
2nd Edition

By J H Duffus and H G J Worth

This popular textbook has been thoroughly revised and updated and includes new information on:

- toxicogenomics
- reproductive toxicology
- behavioural toxicology
- ecotoxicology

Ideal for students and includes special features for lecturers and teachers.



NEW EDITION

Hardback | 2006 | xxvi + 490 pages | ISBN-13: 978 0 85404 614 0 | £39.95 | RSC Member Price £25.75

RSC Publishing

www.rsc.org/books

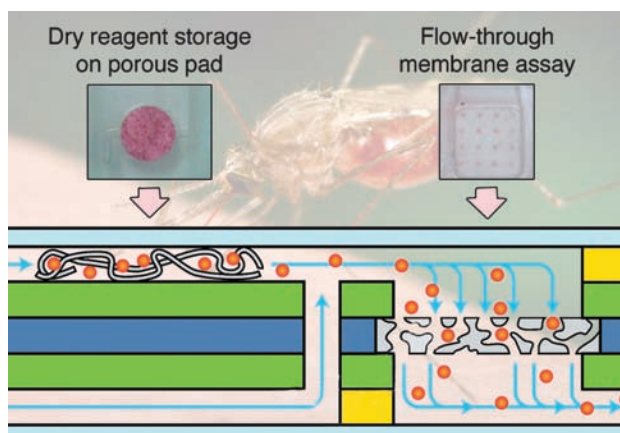
Registered Charity Number 207890

Sugar-dried labelling agents detect malaria on a card

## Sweet solution for on-card reagent storage

US scientists have developed a method for storing dry reagents on low-cost disposable cards. They claim the cards could be used for point-of-care diagnostics in the developing world, where high temperatures and a lack of refrigeration make it difficult to preserve reagent functions.

Paul Yager and colleagues from the University of Washington, Seattle, and Boston College, Chestnut Hill, demonstrated that their storage system works in an automated on-card microfluidic test for malaria. The card's main components are a porous membrane patterned with malaria antibodies and a fibrous pad containing gold-antibody conjugates in sugar. The sugar stabilises the dry conjugates and preserves their function as labelling agents. When Yager pumped samples containing malaria antigens through the card, the conjugates bound to the antigens, causing red spots to form on the



card. They used a scanner to capture images of the cards and calculate the changes in spot intensity.

'The proposed on-card dry reagent storage method is a good solution for reagent storage issues,' says Christopher Ko, an expert in microfluidics and molecular diagnostics at the Samsung Advanced Institute of Technology,

**Malaria antigens cause red spots to form on the card**

**Reference**  
D Y Stevens *et al.*, *Lab Chip*, 2008, DOI: 10.1039/b811158h

Suwon, South Korea. 'Of course, in order to be useful in the developing world, much more, in addition to dry reagent, is needed, such as eliminating the costly microfluidic pumps and scanners used in this study,' he adds.

Yager's team are working to develop a diagnostic system called the DxBox, which consists of a portable reader and disposable test cards. They aim to incorporate both immunoassays and nucleic acid assays on to the cards to allow them to test blood samples for multiple diseases at once.

'Our target markets will be under-resourced communities in areas such as rural India, Brazil and sub-Saharan Africa,' says Dean Stevens, a scientist in Yager's team. 'Our goal is to make the portable reader and each card fit within a reasonable diagnostic budget – a dollar per card would be an ideal, if challenging, goal.'

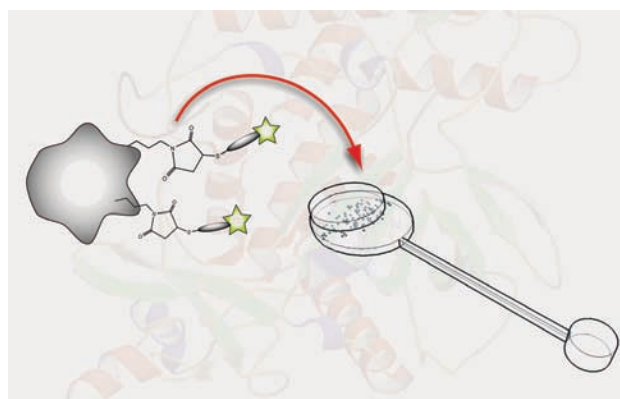
*Freya Mearns*

Bead-based sensor detects deadly poison

## Microfluidics joins fight against bioweapon

US scientists have developed a new sensor capable of detecting trace levels of a lethal neurotoxin. The sensor is quicker and more sensitive than the mouse bioassay currently used for detecting the toxin and, unlike the bioassay, does not require animal sacrifice.

David Beebe and colleagues at the University of Wisconsin–Madison designed a portable microfluidic device that can detect botulinum toxin A (BoNT/A). Although known for its use in Botox cosmetic treatments, BoNT/A is one of the most poisonous naturally occurring substances – eating around 70 micrograms can kill the average person. It causes the muscle paralysis illness botulism, which poses a serious bioterrorism threat. Many people can be affected by a single contaminated food source so a quick and effective detection



method is required.

Beebe's sensor contains toxin-specific beads, which react with a BoNT/A solution to release fluorescently labelled fragments. The solution then flows down a microfluidic channel to a detection port, where evaporation of the solution concentrates

**The beads react with the toxin and release fluorescent fragments**

the fluorescent fragments and amplifies the signal.

Hugh Fan, an expert in microfluidics from the University of Florida, Gainesville, US, appreciates the clever design of the sensor. 'It exploits unique features of enzymatic cleavage on the bead surface and an evaporation-induced flow in a microchannel,' he says. 'The technique can also be extended to other biological assays,' Fan adds, and Megan Frisk from the Beebe group agrees.

'I'm hoping that we can simplify our current microfluidic systems to meet the needs of developing countries, particularly in the area of rapid and reliable tests for tuberculosis and HIV,' she says.

*Roxane Owen*

**Reference**  
M L Frisk *et al.*, *Lab. Chip*, 2008, DOI: 10.1039/b811075a

## Volatile functional groups assist thin film synthesis

# New spin on electronics production

Chemists have taken a significant step closer to the goal of cheap, flexible and printable organic electronic displays, an idea they claim could revolutionise the electronics industry.

A Japanese team, led by Tetsuo Okujima and Noboru Ono at Ehime University, Matsuyama, synthesised thin films of phthalocyanine (Pc) and the related compound, naphthalocyanine (Nc), without using costly ultra-high vacuum techniques.

Pc and Nc are insoluble so Ono and Okujima added functional groups to the molecules to improve solubility. They then dissolved the molecules in an organic solvent and spun the solution rapidly on a glass plate, evaporating the solvent and forming a thin film of the molecules



on the glass. When they heated the films, a retro Diels-Alder reaction released the volatile solubility-imparting groups. The final films were totally insoluble and acted as semiconductors.

The group then made an organic field-effect transistor (OFET)

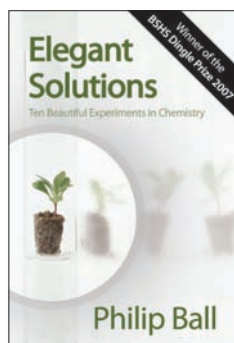
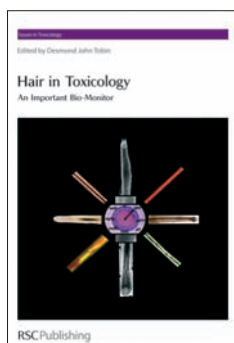
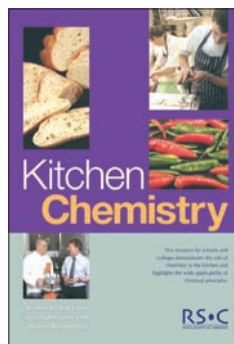
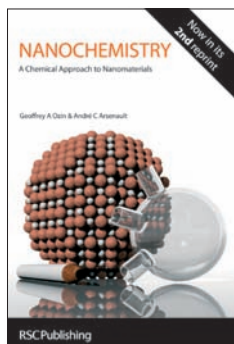
**Heating the spin-coated film converts it to an insoluble semiconductor**

**Reference**  
A Hirao *et al.*, *Chem. Commun.*, 2008, DOI: 10.1039/b811674a

using the films. OFETs are essential components of flexible organic electronic displays, which are starting to appear on the market but are hampered by high-cost production.

Okujima says that his work could result in organic electronic devices becoming cheaper and easier to make. 'This is the first example of solution-processed parent Pc- or Nc-based OFETs which are fabricated easily, at low cost and over a large area,' he explains.

'This work represents a step forward to realising organic semiconductor-based, low-cost, printable and flexible electronics,' says Jerzy Kanicki, an expert in organic electronics at the University of Michigan, Ann Arbor, US. *James Hodge*



# 35% discount

## off books for RSC members

One of the many benefits of RSC membership is a 35% book discount off most RSC titles. The RSC offers a wide range of titles aimed at all levels, including;

- Popular science
- Text books
- Educational books
- High level monographs

**For this and other benefits visit**

RSC Publishing

[www.rsc.org/members](http://www.rsc.org/members)

Registered Charity Number 207890



## Interview

# Taking the lab to the field

*Gillian Greenway talks to Freya Mearns about taking analytical chemistry out of the lab and into the real world*



**Gillian Greenway**

**Professor Gillian Greenway is Head of Environmental Monitoring at the Hull Environment Research Institute and the new president of the Analytical Division of the Royal Society of Chemistry. Her research interests include chemical miniaturisation and environmental analysis.**

#### Who inspired you to become a scientist?

I was really inspired by family. My father and uncles were engineers and my aunt was a pharmacist. I lived near the sea and when we went to the beach to play, my uncle, who was a civil engineer, had us using scientific principles to design dams.

#### What projects are you working on?

My main project is trying to take measurements out of the laboratory and into the environment or to crime scenes. I'm working with engineers and physicists to try to make truly portable systems. Although there have been a lot of lab-on-a-chip proof-of-concepts in the lab, there are still very few instruments that actually work out in the field in a reliable way – trying to convert the lab-based systems into something that works is challenging. The sort of concepts that I'm working on are: trying to make the systems robust, immobilising reagents, including redundancy, using engineering approaches to fault testing, using feedback to find out when things aren't working and determining how to overcome problems. It is also important not just to repeat the way the chemistry is carried out in the lab but to find different ways that will work better in the environment.

#### You work across a broad range of subjects. How do you strike a balance between specialising in one area and knowing enough about the other areas?

I think you do have to specialise in one area, so the key thing is learning to communicate with people from other disciplines. That can be surprisingly difficult. It takes patience because each discipline seems to have its own language; often the same word has different meanings. So it's important to overcome these barriers and be able to tell biologists and engineers, for example, what you need and to understand what they are telling you.

#### What's the trickiest problem you've had to overcome in your research and how did you get around it?

I've got dyspraxia, which is a coordination-specific

learning problem. That means that, practically, I can be a bit of a disaster in the lab. The fact that I became a chemist must show my determination. I need lots of practise with practical skills. Fortunately, I chose a degree with industrial placements and the day-to-day experience in the laboratories gave me the confidence I needed. After that, the number of breakages, spills and floods decreased.

#### What's the role of the Analytical Division?

The role of the Analytical Division is to promote analytical chemistry and science. It's about promoting research in the area and communicating with the public so that people understand the importance of good chemical measurements in their everyday lives. It's also about working with industry, encouraging collaboration between industry and academia, and going into schools and encouraging children to be interested in science. The Analytical Division's there to support the members too, to organise meetings and to help people network. It's been very useful in my career to network through the Royal Society of Chemistry.

#### What would you like to achieve as president?

Obviously, what's really important is to keep promoting analytical science and to get people to understand its importance. Within the Analytical Division, I'd like to get people more involved by getting them enthused and willing to participate and to promote their ideas. We're very lucky in the Analytical Division because we have the Analytical Chemistry Trust Fund (ACTF) – if you have good ideas, you can go to the ACTF to get funds to promote them. We have a lot of initiatives at the moment including the development of a new studentship scheme and the encouragement of science in developing countries.

#### Finally, if you weren't a scientist, what would you be?

I think I would be a teacher. It is a really good feeling when you are able to inspire people although it is hard work.

# A new journal from RSC Publishing launching in 2009

## Integrative Biology

Quantitative biosciences from nano to macro



*Integrative Biology* provides a unique venue for elucidating biological processes, mechanisms and phenomena through quantitative enabling technologies at the convergence of biology with physics, chemistry, engineering, imaging and informatics.

With 12 issues published annually, *Integrative Biology* will contain a mix of research articles including Full papers, Reviews (Tutorial & Critical), and Perspectives. It will be supported by an international Editorial Board, chaired by Distinguished Scientist Dr Mina J Bissell of Lawrence Berkeley National Laboratory.

The current issue of *Integrative Biology* will be freely available to all readers via the website. Free institutional online access to all 2009 and 2010 content of the journal will be available following registration at [www.rsc.org/ibiology\\_registration](http://www.rsc.org/ibiology_registration)

Contact the Editor, Harp Minhas, at [ibiology@rsc.org](mailto:ibiology@rsc.org) or visit the website for more details.

RSC Publishing

[www.rsc.org/ibiology](http://www.rsc.org/ibiology)

Registered Charity Number 207890

## Instant insight

# Photochemistry goes micro

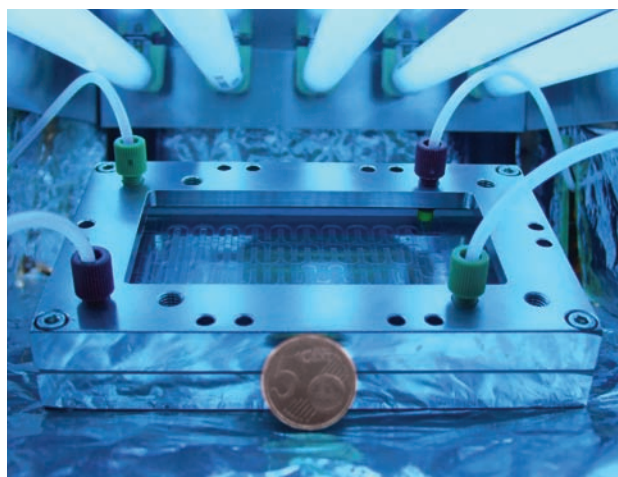
Michael Oelgemöller and Emma Coyle of Dublin City University, Ireland, discuss how microreactors may change synthetic organic photochemistry

At the International Congress of Applied Chemistry in New York in 1912,<sup>1</sup> Giacomo Ciamician, the father of organic photochemistry, presented his spectacular vision of 'The Photochemistry of the Future': 'On the arid lands there will spring up industrial colonies without smoke and without smokestacks; forests of glass tubes will extend over the plains, and glass buildings will rise everywhere; inside of these will take place the photochemical processes that hitherto have been the guarded secret of the plants, but that will have been mastered by human industry which will know how to make them even more abundant fruit than nature, for nature is not in a hurry and mankind is.'

Generally speaking, light can be used to efficiently and selectively induce chemical changes. It can be easily tuned and controlled, literally with a flick of a switch. Photochemistry also allows scientists to construct exotic, high-energy molecules with relative ease. Due to the specialised equipment and reaction conditions, however, chemical transformations with light have been widely ignored by the chemical industry. More than 90 years later, Ciamician's vision is yet to be realised.

Microreactors, otherwise known as microchannelled or microstructured reactors, have recently become widespread in research. Originally developed for analytical applications as the famous 'lab on a chip', these devices have also found promising uses in synthetic organic chemistry.

Since many commercially available microreactors are glass-based and transparent, they can be easily adopted for photochemical applications. Miniature light sources, such as light-emitting diodes, can be used and offer real



**A glass microreactor (Dwell device, mikroglas) under a UV exposure panel (Luzchem). A five Euro-cent coin is used to illustrate the size of the reactor**

advantages over conventional light sources – they are small, energy efficient, come in a range of wavelengths and produce very little heat, thus reducing the need to cool the reaction. Because the reaction channels in a microreactor are shallow, light can penetrate even concentrated solutions. Solution flow rate controls the exposure to light and can be easily varied to rapidly optimise photochemical reactions. Additionally, the reactions can be monitored on-line, for example by analysing the effluent using a UV spectrometer. Microreactors can also be used in parallel to scale-up reactions, a process known as numbering up.

There are a number of different microreactor types available today. As their name suggests, serpentine channel reactors have long, snaking reaction channels, which range from several centimetres to more than a metre in length. The dwell-reactor produced by mikroglas, for example, is the size of an external floppy drive but its reaction channel is 1.15 metres long. The reactor consists

of a reaction channel and a second, cooling channel through which water flows. Another design is the falling film reactor, which generates a thin falling film of solution like a waterfall that passes by the light source. This device is especially advantageous for gas-liquid reactions, such as photooxidations or photohalogenations. Many researchers, however, continue to custom build their own reactors based on their needs and applications.

The photochemical transformations studied to date in microreactors include homogeneous reactions, such as photocyanation and photodecarboxylation; heterogeneous reactions between liquid and gaseous reagents, such as photooxygenations; and photocatalytic processes using semiconductors. In many cases, the selectivities and yields are better than those from large scale experiments, clearly demonstrating the feasibility and superiority of microphotochemistry.

Ciamician's vision may thus be realised in the form of a microchip, rather than the glass buildings he envisaged. By scaling down photochemical reactions using microreactors, photochemical reactions can be conveniently carried out in research laboratories, for example for finding and developing leads for drug discovery. In addition, numbering up, rather than scaling up, may enable photochemical products to be produced industrially.

Read more in 'Micro-photochemistry: photochemistry in microstructured reactors. The new photochemistry of the future?' in issue 11 of Photochemical & Photobiological Sciences<sup>2</sup>

#### References

- 1 G Ciamician, *Science*, 1912, **36**, 385
- 2 E E Coyle and M Oelgemöller, *Photochem. Photobiol. Sci.*, 2008, **7**, 1313 (DOI: 10.1039/b808778d)



# Essential elements

## Board member wins Nobel Prize

The Nobel Prize in Chemistry 2008 has been awarded to Roger Tsien (below right), University of California, San Diego, US, a member of the editorial board for the upcoming RSC journal *Integrative Biology* (to be launched in January 2009), and colleagues for their work in the development of the gene marker green fluorescent protein (GFP).

Harp Minhas, editor of *Integrative Biology*, says: 'Congratulations to Professor Tsien, from all of us at the RSC. We are all immensely pleased that 2008 Nobel Prize winner Roger Tsien is an editorial board member for *Integrative Biology*; his work typifies the quality of material we are seeking in the development of biology through new tools and technologies.'

Derivatives of GFP are used in experiments to observe



cell dynamics and behaviour – their fluorescent glow allows scientists to visualise processes inside cells. Furthermore, as it is non-toxic to cells it can be used in live



cell (in vitro) studies meaning that real time analysis of cells is possible.

GFP is a protein first extracted from the jellyfish *Aequorea victoria* in the 1960s by Osamu Shimomura, who was jointly awarded this year's prize with Tsien and Martin Chalfie. Variants of GFP can fluoresce in different colours, allowing several different proteins in a cell to be studied simultaneously.

Find out more about our new journal *Integrative Biology* at [www.rsc.org/ibiology](http://www.rsc.org/ibiology)

## Did you know...

RSC Publishing has an extensive food science book list comprised of a superb range of monographs, textbooks, professional references and popular science titles – all related to food science and technology. Our exclusive food science titles cater for scientists at all levels and also incorporate many of the food science subdisciplines such as food safety, food preservation and food microbiology. The classic, best selling textbook *Food: The Chemistry of its Components 5th Edition* is the latest title to join RSC Publishing's rapidly expanding food science book list.

### FOOD

The Chemistry of its Components

Tom Coultate



This textbook has been fully revised and updated and includes a foreword written by Heston Blumenthal. Look out for other exciting new food science books in 2009 such as *Kitchen Chemistry* (new volume), *Handbook of Culture Media for Food and Water Microbiology and Nanotechnologies in Food*.

For more information visit [www.rsc.org/books](http://www.rsc.org/books)

## Announcing *Lab on a Chip* prize winners

*Lab on a Chip*, the miniaturisation journal for chemistry, biology and bioengineering, has yet again shown extensive community support by sponsoring some of the most prestigious prizes in the miniaturisation field. At this year's  $\mu$ -TAS meeting in San Diego the journal, together with Corning Inc., awarded the 'Pioneers in Miniaturisation Prize' to Patrick Doyle, professor at the department of chemical engineering at MIT, US. Jean-Louis Viovy from the Institute Curie comments on Doyle's

work: '[Patrick] developed the "stop-flow lithography" technological platform, which I consider a major breakthrough in microfluidics.'

*Lab on a Chip* also awarded the 'Widmer Young Researcher Poster Award' to Maged Fouad for best poster and presentation. Among 589 candidates, this poster titled 'Nanotechnology meets plant biotechnology: carbon nanotubes deliver DNA and incorporate into the plant cell structure' caught the judges' eyes.

A new award named 'Art in

Science' recognised the aesthetic value in scientific illustrations. 'The winner, Yu Wen Huang (Texas A & M University) clearly understood the principles of this award and produced an image that was reminiscent of a tall city building seen in an early morning fog. The picture is an optical effect generated by concentrated double-stranded DNA in the vicinity of a 50 micrometre wide electrode inside a microchannel,' comments Harp Minhas, editor of *Lab on a Chip*, who proudly presented all awards to the winners.

*Chemical Technology* (ISSN: 1744-1560) is published monthly by the Royal Society of Chemistry, Thomas Graham House, Science Park, Milton Road, Cambridge UK CB4 0WF. It is distributed free with *Chemical Communications*, *Journal of Materials Chemistry*, *The Analyst*, *Lab on a Chip*, *Journal of Atomic Absorption Spectrometry*, *Green Chemistry*, *CrystEngComm*, *Physical Chemistry Chemical Physics*, *Energy & Environmental Science* and *Analytical Abstracts*. *Chemical Technology* can also be purchased separately. 2008 annual subscription rate: £199; US \$396. All orders accompanied by payment should be sent to Sales and Customer Services, RSC (address above). Tel +44 (0)1223 432360, Fax +44 (0)1223 426017 Email: [sales@rsc.org](mailto:sales@rsc.org)

**Editor:** Joanne Thomson  
**Deputy editor:** Michael Spenceclayh  
**Associate editors:** Celia Gitterman, Nina Notman  
**Interviews editor:** Elinor Richards  
**Web editors:** Nicola Convine, Michael Townsend, Debora Giovanelli  
**Essential elements:** Daniel Bradnam, Kathrin Hilpert, and Rebecca Jeeves

**Publishing assistant:** Jackie Cockrill  
**Publisher:** Graham McCann

Apart from fair dealing for the purposes of research or private study for non-commercial purposes, or criticism or review, as permitted under the Copyright, Designs and Patents Act 1988 and the copyright and Related Rights Regulations 2003, this publication may only be reproduced, stored or transmitted, in any form or by any means, with the prior permission of the Publisher or in the case of reprographic reproduction in accordance with the terms of licences issued by the Copyright Licensing Agency in the UK. US copyright law is applicable to users in the USA.

The Royal Society of Chemistry takes reasonable care in the preparation of this publication but does not accept liability for the consequences of any errors or omissions. The RSC is not responsible for individual opinions expressed in *Chemical Technology*. Content does not necessarily express the views or recommendations of the RSC.

Royal Society of Chemistry: Registered Charity No. 207890.

RSC Publishing

# Conference Report: Bridging chemistry and engineering

DOI: 10.1039/b814665a

1st SynTOP Conference, Seminaris Hotel, Potsdam, Germany, June 11th–13th, 2008.

It is widely acknowledged that the European chemical industry needs to innovate if it is to maintain its global position in the 21st century. The first conference on Smart Synthesis and Technologies for Organic Processes (1st SynTOP) was intended to contribute to this innovation by “changing organic processes for the better”. SynTOP was the brainchild of Professor Volker Hessel of Eindhoven University of Technology and the Institut für Mikrotechnik Mainz GmbH, ably supported by conference organizers VDI Wissensforum and a programme committee of 6 academic and 2 industrial scientists. Hessel’s by-line of the conference was “bridging chemistry and engineering” and he succeeded admirably in doing so. What distinguished SynTOP from other similar bridging exercises was that the chemists were not those already working close to the chemistry/engineering interface but mainstream synthetic organic chemists. So, for once, there was real dialogue between those making molecules in the lab and those trying to manufacture them. This made the conference of direct relevance to green chemistry.

The tone of the conference was set by two excellent plenary lectures one by a chemist S. V. Ley (Cambridge University, UK) on real applications of flow reactors, and the other by an engineer, M. Matlosz (ENSIC, Nancy, France) on microprocess engineering, process intensification and multi-scale design. The rest of the programme<sup>1</sup> consisted of 35 lectures divided into: Microwave-Assisted Catalysis; Foams, Monoliths, Microcapsules, Micro beads and other Structured Media; Micro and Milli Process Technologies; Micro and Milli Chip Synthesis; Supercritical & Ionic Liquids; and finally, Advanced Organic Synthesis & Process Chemistry & Automation. It was striking that more

than a third of the lectures were presented by speakers from industry or involved industrial co-authors, particularly those from the pharma industries. This gave the conference a real sense of industrial relevance which is not always so clear in green chemistry events. In addition there were posters and a small exhibition of flow equipment.

All lecturers and poster presenters submitted short papers which have been collected into a report.<sup>2</sup> Here we summarise just a few of the interesting points which emerged from the lectures.

- *Flow processes can save energy for low temperature reactions.* Many chemists realise that the short residence times in flow reactors often permit reactions to be run at higher temperatures than in batch reactors, without decomposition of the product. However, far fewer chemists have appreciated that this also means that flow processes do not need to be run at temperatures as low as the analogous batch process, and there is a corresponding saving in the energy needed for refrigeration.

- *Microwaves do not appear to alter chemical reactions.* There are developments in the longstanding controversy over possible differences between reactions promoted by microwave and conventional heating; careful experiments where conditions between the two processes are made as similar as possible suggest that there are negligible differences in the overall chemistry.

- *“Microreactors” do not necessarily have to be small.* Many of the advantages of microreactors in mass and heat transfer have a length scale ca 100  $\mu\text{m}$ . It has now been demonstrated that these advantages can be retained in quite large reactors provided that at least one dimension is of this scale or that a larger volume microstructured mixer is present. For example, one

lecture described just such a “mini” reactor packed with porous metal foam, which was  $\frac{1}{2}$  inch in diameter and 1 metre long!

- *Micoreactors are already beginning to be exploited in industrial processes.* A particularly interesting application involved the addition of a micro-reactor upstream of a conventional reactor, which greatly increased the productivity of the existing process equipment to 1700 kg/h!

- *Innovation need not necessarily be slow.* Provided that a “killer” application has been identified for a new technology (e.g. simulated moving bed chromatography), the technology can spread right across the chemical industry in a matter of just a few years.

- *Micoreactors can help in teaching.* The Technische Universität Ilmenau exhibited a complete table-top microreactor system which allowed delegates to measure reactor residence times during the coffee breaks!

The conference was attended by nearly 100 delegates, with a large proportion from industry. The warmth and liveliness of the discussion between them completely validated Prof. Hessel’s vision. There is a synergy between these organic chemists and process engineers which, if properly exploited, should lead to real innovation in the future.

**Martyn Poliakoff**, and **Richard Bourne**, The School of Chemistry, The University of Nottingham, Nottingham, UK NG7 2RD. E-mail: martyn.poliakoff@nottingham.ac.uk

## References

- 1 Details of the programme and the conference proceedings can be found on the conference website [www.syntop2008.com](http://www.syntop2008.com).
- 2 *1st SynTOP Smart Synthesis and Technologies for Organic Processes*, VDI Berichte 2039, VDI Verlag GmbH, Dusseldorf, 2008.



# Environmentally friendly refining

DOI: 10.1039/b819712c

The recent instability in the price of oil, and the perception (right or wrong) that oil reserves are in decline, means that the search for, and the commercialisation of, alternate technologies for the production of transportation fuels and chemicals is now a reality. The Fischer–Tropsch process for the conversion of synthesis gas to primarily hydrocarbons, but also oxygenates, is already practised in South Africa and Qatar and new large scale facilities are under construction in various parts of the world where large deposits

of coal, gas or biomass are available for conversion to syngas mixtures.

The chemical composition of the mixtures obtained from these gas conversion processes are different to those obtained from oil and as a result the associated down stream refineries will be of a different configuration to the existing conventional units. This provides an opportunity to move away from established concepts and to design such installations from scratch using environmentally friendly technologies. In the review article

published in this issue, Arno de Klerk lifts the lid on what is possible for the next generation of F-T refineries and essentially defines the future.<sup>1</sup> Make no mistake; many of us will be using this type of product in the years to come, so it is a debate well worth having.

**Mike Green**

Sasol, South Africa

## Reference

- 1 A. de Klerk, *Green Chem.*, **10**, DOI: 10.1039/b813233j.

# Fischer–Tropsch refining: technology selection to match molecules

Arno de Klerk\*

Received 4th August 2008, Accepted 15th October 2008

First published as an Advance Article on the web 6th November 2008

DOI: 10.1039/b813233j

On a molecular level Fischer–Tropsch syncrude is significantly different from crude oil. When syncrude is treated as if it is a crude oil, its refining becomes inefficient. Refining technologies developed for crude oil can be employed to refine Fischer–Tropsch syncrude, but in order to conform to green chemistry principles (preventing waste; maximising atom economy; increasing energy efficiency) the technology selection must be compatible with the syncrude composition. The composition of Fischer–Tropsch syncrude is discussed in relation to the molecular requirements of transportation fuels and the refining gap that needs to be bridged. Conversion technologies are evaluated in terms of their refining objective, chemistry, catalysts, environmental issues, feed requirements, and compatibility to Fischer–Tropsch syncrude, in order to suggest appropriate technologies for efficient refining of Fischer–Tropsch products. The conversion technologies considered are: double bond isomerisation, dimerisation/oligomerisation, skeletal isomerisation, etherification, aliphatic alkylation, aromatic alkylation, metathesis, hydrogenation/hydrotreating, hydroisomerisation, hydrocracking, catalytic cracking, coking, thermal cracking, catalytic reforming, aromatisation, alcohol dehydration and olefin hydration.

The transportation sector of the economy is carbon based and unless a breakthrough in engine technology radically changes the nature of transportation fuels, it is likely fuels will remain carbon based. At present, transportation fuels are primarily produced from crude oil, with alternative sources such as renewables, coal and natural gas still having a small market share. In future this will change, since crude oil is not an infinite resource and “peak oil” (oil production reaches a maximum, after which oil production inexorably declines) is approaching.<sup>1</sup> This implies that there will be increasing scope for transportation fuel production from other carbon sources.

---

*Fischer–Tropsch Refinery Catalysis, Sasol Technology Research and Development, PO Box 1, Sasolburg, 1947, South Africa.  
E-mail: arno.deklerk@sasol.com; Fax: +27 11 522–3517; Tel: +27 16 960–2549*

---



Arno de Klerk

*Arno de Klerk is a PhD chemical engineer with MSc in analytical chemistry. His main research interest is the refining of alternative feedstocks. He joined Sasol Technology R & D in 1994 and headed the Fischer–Tropsch Refinery Catalysis group from 2001. He is a registered professional engineer and thrice recipient of the SAICHe Innovation Award.*

Liquid fuels can be produced from non-crude oil carbon sources by direct means, such as direct coal liquefaction, or indirect means, such as biomass gasification followed by hydrocarbon synthesis. One of the key technologies for gas-to-liquid (GTL), coal-to-liquid (CTL) and biomass-to-liquid (BTL) conversion, is Fischer–Tropsch (FT) synthesis. The product from Fischer–Tropsch synthesis is a synthetic crude oil, or syncrude for short. This syncrude, like crude oil, has to be further refined to produce transportation fuels. Yet, despite significant activity in the field of Fischer–Tropsch synthesis, little attention has been paid to the refining of Fischer–Tropsch syncrude. The tacit assumption being made is that Fischer–Tropsch syncrude can be refined along similar lines as crude oil.

There are significant differences between Fischer–Tropsch syncrude and crude oil that in principle allows syncrude refining to be more efficient than crude oil refining.<sup>2</sup> When syncrude is treated as if it is crude oil, refining becomes inefficient and it violates green chemistry principles such as preventing waste, maximising atom economy and increasing energy efficiency.

The predominantly crude oil based refining community is unfamiliar with the composition of Fischer–Tropsch syncrude and there are almost no refining technologies that were specifically developed for this purpose. This makes it challenging to design a syncrude refinery. During the development of such designs, even on a conceptual level, it is difficult not to inadvertently blunder into a technology selection that is environmentally “irresponsible”. It is important to match the molecules to the technology. The aim of this review is to provide the information that can help scientists and engineers do responsible syncrude refinery design, not only from a commercial point of view, but also from an environmental point of view.

## Fischer–Tropsch technology

The industrial application of Fischer–Tropsch technology consists of three integrated operations (Fig. 1): synthesis gas production, Fischer–Tropsch synthesis and refining.

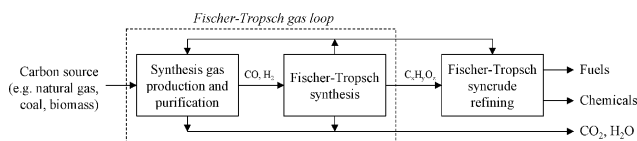


**Fig. 1** The main design features of an industrial Fischer–Tropsch based facility.

### Synthesis gas production and gas loop

Classification of a Fischer–Tropsch facility as gas-to-liquids (GTL) or coal-to-liquids (CTL) makes reference to the feed that is employed for synthesis gas production. When natural gas is reformed to produce synthesis gas, the facility is called a GTL facility and when coal is gasified to produce synthesis gas, it is called a CTL facility. In principle other carbon sources can also be employed for synthesis gas production and in each instance the method of synthesis gas production will be determined by the feed.

The feed selection does not dictate the technology selection for Fischer–Tropsch synthesis. Depending on the feed and technology selected for synthesis gas generation, the design of the gas loop may favour a specific type of Fischer–Tropsch synthesis on account of the  $\text{CO} : \text{H}_2$  ratio of the synthesis gas. Nevertheless, the gas loop may be designed to accommodate any type of Fischer–Tropsch synthesis. The unconverted synthesis gas and products can be recovered and recycled in various ways.<sup>3</sup>

The feed selection and gas loop design has a considerable impact on the refinery.

The nature of the feed and the technology employed for synthesis gas generation may result in the co-production of material that has to be co-refined. In a GTL facility there may be associated natural gas condensates, as is the case with the PetroSA (Mossgas) GTL plant. In a CTL facility there may be coal pyrolysis products, as is the case with the Sasol Synfuels CTL plant. In both instances the refinery design is markedly affected by the need to co-refine these associated products.

Part of the gas loop design involves the stepwise cooling of the primary Fischer–Tropsch products (Fischer–Tropsch syncrude) after synthesis. The nature of the syncrude is such that more than one product phase will form when it is cooled down. Although the syncrude produced during high temperature Fischer–Tropsch (HTFT) synthesis is gaseous at reaction conditions, more than one product phase is formed on cooling (Fig. 2). In the case of large scale HTFT based facilities it is beneficial to make use of cryogenic separation to recover hydrogen, methane, ethylene and ethane. In smaller facilities,  $\text{C}_2$  and lighter products are typically not separately recovered.

Low temperature Fischer–Tropsch (LTFT) syncrude is a two-phase mixture at reaction conditions, but at ambient conditions the syncrude from LTFT synthesis consists of four different product phases (Fig. 3): gaseous (tail gas), organic liquid (condensates), organic solid (wax) and aqueous.

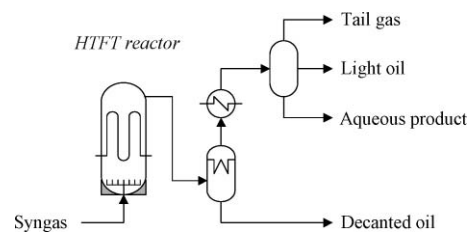


**Fig. 2** Typical stepwise cooling of the syncrude from HTFT synthesis and the resulting product fractions that are formed. In larger HTFT facilities the tail gas may additionally be cryogenically separated.

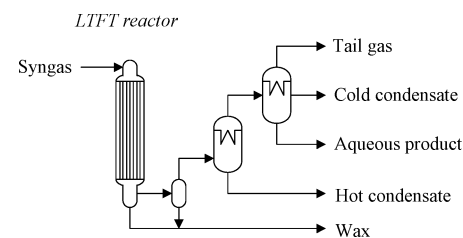


**Fig. 3** Typical stepwise cooling of the syncrude from LTFT synthesis and the resulting product fractions that are formed.

The composition of each product fraction that is recovered from Fischer–Tropsch synthesis is determined by the gas loop design. The feed to the Fischer–Tropsch refinery is therefore not a single syncrude, but different syncrude fractions (Figs. 2 and 3).

### Fischer–Tropsch synthesis

Industrially, Fischer–Tropsch technology is classified as high temperature Fischer–Tropsch (HTFT) or low temperature Fischer–Tropsch (LTFT) synthesis. This classification refers to the operating conditions of the Fischer–Tropsch synthesis. There are presently six different technologies for Fischer–Tropsch synthesis in industrial operation (Table 1).

The syncrude composition from Fischer–Tropsch synthesis is mainly determined by the Fischer–Tropsch catalyst type, iron or cobalt based, and the operating regime, although other factors also have an effect, such as the catalyst promoters, reactor type and synthesis gas composition ( $\text{H}_2 : \text{CO}$  ratio).<sup>3</sup> In theory, infinite variation in syncrude composition is possible, but in practice only two types of syncrude composition are found, namely HTFT and LTFT syncrude. The properties of these syncrudes are different and from a refining perspective there are three aspects of Fischer–Tropsch synthesis that are of importance:

- Probability of chain growth.
- Degree of hydrogenation.
- Secondary product formation.

The carbon number distribution obtained during Fischer–Tropsch synthesis is determined by the probability of chain growth on the catalyst, which is also called the  $\alpha$ -value. The Anderson–Schultz–Flory (ASF) equation is often used to express the carbon number distribution. The carbon number distribution does not obey the ASF description exactly, due to the influence of chain length on desorption kinetics,<sup>4</sup> but it is a good approximation. The operating temperature plays an important role in determining the  $\alpha$ -value, since it controls product desorption from the catalyst surface. Desorption is an endothermic process and at higher temperatures the rate of

**Table 1** Fischer–Tropsch processes currently in industrial operation

Type	FT catalyst	FT reactor type	FT technology	Operator	Commercial operation
HTFT	fused Fe	circulating fluidised bed	Sasol Synthol	PetroSA	Mossel Bay, South Africa
HTFT	fused Fe	fixed fluidised bed	Sasol Advanced Synthol (SAS)	Sasol	Secunda, South Africa
LTFT	precipitated Fe	fixed bed	ARGE <sup>a</sup>	Sasol	Sasolburg, South Africa
LTFT	precipitated Fe	slurry bubble column	Sasol Slurry Bed Process (SSBP)	Sasol	Sasolburg, South Africa
LTFT	Co-SiO <sub>2</sub>	fixed bed	Shell Middle Distillate Synthesis (SMDS)	Shell	Bintulu, Malaysia
LTFT	Co-Al <sub>2</sub> O <sub>3</sub>	slurry bubble column	Sasol Slurry Bed Process (SSBP)	Sasol	Ras Laffan, Qatar

<sup>a</sup> ARGE = Arbeitsgemeinschaft Ruhrchemie-Lurgi.

desorption increases, resulting in a lower  $\alpha$ -value. In general commercial HTFT catalysts have  $\alpha$ -values around 0.65–0.70, while LTFT catalysts have  $\alpha$ -values around 0.85–0.95. This implies that a syncrude from HTFT synthesis would normally have a high naphtha yield and almost no residue (>360 °C boiling material), while a syncrude from LTFT synthesis would include a considerable amount of residue in the form of paraffin wax (Fig. 4).

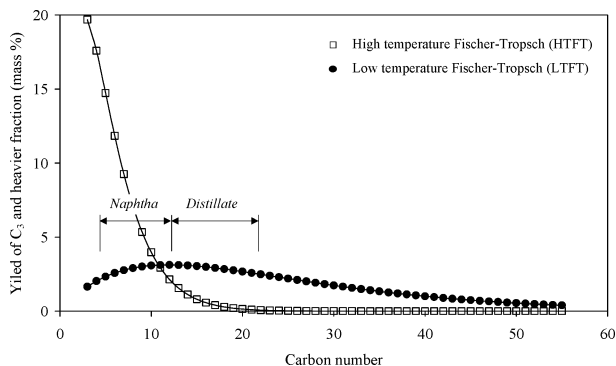


**Fig. 4** Carbon number distributions calculated from the Anderson–Schultz–Flory equation for typical HTFT syncrude ( $\alpha = 0.67$ ) and typical LTFT syncrude ( $\alpha = 0.92$ ). Note that the yields are on a mass basis and are calculated for the C<sub>3</sub> and heavier fraction only.

The degree of product hydrogenation is mainly determined by the hydrogenation activity of the metal employed for the Fischer–Tropsch catalyst. Iron is less hydrogenating than cobalt. Syncrude from iron-based Fischer–Tropsch synthesis is therefore more olefinic and contains more oxygenates than syncrude from cobalt-based Fischer–Tropsch synthesis.

The composition of the syncrude is also influenced by the operating conditions. At low temperature, the syncrude consists mainly of primary Fischer–Tropsch products, namely paraffins, olefins, alcohols, aldehydes and carboxylic acids. The hydrocarbon composition is rich in linear paraffins and linear  $\alpha$ -olefins. As the temperature is increased, more secondary products are formed, such as aromatics and branched aliphatics. The effect of an increase in temperature is especially apparent in the composition of the oxygenates:

- Equilibrium interconversion of the primary oxygenates.
- Ketone formation by carboxylic acid decomposition.
- Iso-alcohol formation by ketone hydrogenation.
- Alcohol dehydration to produce more olefins.

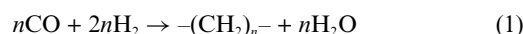
The syncrude from HTFT synthesis is consequently more olefinic, rich in oxygenates (mainly alcohols, carboxylic acids and ketones) and contains aromatics, while syncrude from

**Table 2** Composition (mass%) of straight run naphtha and distillate from different commercial Fischer–Tropsch processes

Composition	Fe-HTFT	Fe-LTFT	Fe-LTFT	Co-LTFT
	SAS	SSBP	ARGE	SSBP
	340 °C	230 °C	230 °C	220 °C
<b>Naphtha (C<sub>5</sub>–C<sub>10</sub>)</b>				
Paraffins	13	29	60	54
Olefins	70	64	32	35
Aromatics	5	0	0	0
Oxygenates	12	7	8	11
<b>Distillate (C<sub>11</sub>–C<sub>22</sub>)</b>				
Paraffins	15	44	66	80
Olefins	60	50	26	15
Aromatics	15	0	0	0
Oxygenates	10	6	8	5

LTFT synthesis contains mainly paraffins, olefins and alcohols (Table 2). Product saturation increases with carbon number and although straight run LTFT naphtha and distillate contains a fair amount of olefins and oxygenates, the heavier products are mostly *n*-paraffin waxes.

One of the major products from Fischer–Tropsch synthesis is water (eqn (1)).



In industrial practice, when the Fischer–Tropsch synthesis product is cooled down, the water is condensed with the hydrocarbons and oxygenates to produce an oil product and an aqueous product. The short chain oxygenates that are very polar, preferentially dissolve in the aqueous product. This aqueous product is typically refined separately from the oil product.

A significant fraction of the syncrude ends up in the aqueous product, 7–10% of HTFT syncrude and around 3% of LTFT syncrude. The difference between HTFT and LTFT synthesis is also reflected in the composition of the aqueous products (Table 3). Apart from the obvious differences in the distribution of oxygenate classes, the compounds within each class are also distributed differently. For example, HTFT synthesis produces very little methanol, while methanol is a major compound in the LTFT aqueous product.<sup>5</sup>

From the preceding discussion it is clear that Fischer–Tropsch synthesis inherently produces commodity chemicals, such as oxygenated solvents (alcohols and ketones) and linear  $\alpha$ -olefins.<sup>5,6</sup> These chemicals can be extracted and sold as high value products. Fischer–Tropsch syncrude can therefore be refined to fuels and/or chemicals, although the subsequent discussion will focus mainly on technology selection for fuels refining.

**Table 3** Composition (mass%) of the Fischer–Tropsch aqueous product

Composition	Fe-HTFT	Fe-LTFT
	Sasol Synthol	ARGE
Compound classes		
Alcohols	70	85
Aldehydes	4	2
Carboxylic acids	14	10
Ketones	12	3
Alcohol distribution		
Methanol	1	22
Ethanol	47	45
Propanol	14	10
C <sub>4</sub> and heavier	8	8

### Fischer–Tropsch refining

There is considerable variation in the design of commercial Fischer–Tropsch refineries for upgrading the syncrude to useful products.<sup>7</sup> Historically, both transportation fuels and chemicals were produced and the configuration of each refinery reflected the fuel specifications and chemical markets of its time.

This review will focus on the technologies needed to produce present day transportation fuels.

### Transportation fuels

The transportation fuel classes that are generally produced during fuels refining are: motor-gasoline, jet fuel (aviation turbine fuel) and diesel fuel. Each of these classes will be considered in order to highlight the molecular requirements of these fuels. It should be noted that once refined, Fischer–Tropsch derived transportation fuels are no different to crude oil derived transportation fuels. On a molecular level it falls within the same band of variation as is found in the refined products that are produced from different crude oil types and Fischer–Tropsch derived fuels have to meet the same fuel specifications.

#### Motor-gasoline

There are four compound classes allowed in motor-gasoline, namely paraffins (including naphthenes), olefins, aromatics and oxygenates. Fuel specifications have placed a limit on all of these compound classes, except for the paraffins. The molecular composition within each class is not regulated, but the maximum benzene content and the composition of the oxygenates (alcohols and ethers) are regulated. In addition to these, specific limits have also been set for sulfur and lead.

Typical limits are: olefins (max. 18 vol%), aromatics (max. 35 vol%) and oxygenates (max. 2.7 mass% as O; 10–15 vol% as oxygenates). Comparing these specifications with the composition of straight run naphtha (Table 2) from both HTFT and LTFT synthesis, it is clear that the olefin content is much higher than allowed and that the aromatic content is much lower than allowed. The oxygenates also include compound classes that are undesirable for motor-gasoline, such as aldehydes, ketones and short chain carboxylic acids. Furthermore, the aliphatic hydrocarbons are mainly *n*-paraffins and linear  $\alpha$ -olefins, which affect the properties of the motor-gasoline.

The properties of the motor-gasoline are regulated through a number of specifications, the most important being the octane number, vapour pressure and distillation range. These property requirements affect the way in which the feed molecules must be refined and in what way the fuel composition can be manipulated:

(a) Octane number. Aromatics and oxygenates inherently have high octane numbers. The octane number of olefins is more structure sensitive. For olefins to have octane numbers close to that required by the fuel specifications, the olefins must have some branching and the C=C double bond should preferably be internal. From an octane number perspective the worst kind of olefin is a linear  $\alpha$ -olefin. The octane number of paraffins is extremely structure sensitive and in general octane number increases with an increase in degree of branching and decrease in carbon number.

(b) Vapour pressure. The vapour pressure determines the extent to which low molecular weight hydrocarbons can be included in the motor-gasoline blend, as well as the nature of the oxygenates that can be accommodated. For example, ethers are less polar than alcohols and have a smaller vapour pressure contribution.

(c) Distillation range. The distillation range and properties like the density range, limit the carbon number distribution of the fuel. As a consequence, motor-gasoline consists mainly of molecules in the range C<sub>5</sub>–C<sub>10</sub>, with some C<sub>4</sub>'s that can be blended in to the vapour pressure limit.

From the preceding discussion it can be anticipated that the refining technologies that will be needed to produce motor-gasoline should be able to transform linear molecules into branched molecules or aromatics. There is also a need to change the carbon number distribution of HTFT syncrude in the naphtha range (Fig. 4) to more material on the heavier side. The oxygenate composition should also be altered to exclude unwanted oxygenate classes. These transformations do not constitute serious refining challenges.

#### Jet fuel

The main compound class that is regulated, is aromatics, since aromatic compounds are soot precursors that can lead to poor combustion. Particulate matter generated by poor combustion can damage the turbine and the aromatic content of Jet A-1 is limited to maximum 25 vol% aromatics and less than 3 vol% naphthalenes (diaromatics). Synthetic jet A-1, as produced by Fischer–Tropsch synthesis, must conform to a more stringent specification, which requires the aromatic content to be in the range 8–22 vol%.

Apart from limits imposed on acidity and sulfur content, olefins and hetroatom containing compounds are not directly regulated, but indirectly regulated by the thermal stability requirements. This is a key property, since the fuel is used as heat exchange fluid in the engine and airframe. Any molecules that have a tendency to form gum must be excluded from the fuel, such as aldehydes and ketones.

The freezing point specification of Jet A-1 (<–47 °C) is needed to ensure that the fuel remains pumpable at the low temperature conditions experienced during high altitude flight. It places a limit on the amount of linear hydrocarbons, since



these compounds have high freezing points. Some branching is required. For example, *n*-decane has a freezing point of  $-29.6^{\circ}\text{C}$ , but 2-methylnonane has a freezing point of  $-74.7^{\circ}\text{C}$ .

There are also other properties that are important, such as the distillation curve, energy content, density and viscosity. These properties determine the spray and evaporation characteristics of the jet fuel. Molecular composition plays a role in determining these properties, but the degree to which these properties can be manipulated, is limited. In general it can be said that it is easy to refine Fischer–Tropsch syncrude to jet fuel.

### Diesel fuel

Sulfur and polynuclear aromatics are regulated in diesel fuel and neither affects the refining of Fischer–Tropsch syncrude, which is practically free of sulfur and only in the instance of HTFT syncrude contains some ( $<0.5\%$ ) polynuclear aromatic material.

The key performance measure of diesel fuel is its cetane number and on a molecular level it is a measure of the ease with which the molecule can be thermally decomposed in the presence of air at high temperature and pressure. The cetane number is therefore a measure of the inherent thermal stability of the molecule and its autoxidation propensity. Cetane number improves when moving from aromatics to naphthenes (cycloparaffins) to paraffins and increases with increasing carbon number.<sup>8</sup> Since linear hydrocarbons have high cetane numbers, Fischer–Tropsch distillates ( $170\text{--}360^{\circ}\text{C}$ ) generally have a cetane number exceeding that required by diesel fuel specifications.

The narrow density and viscosity ranges that are specified for diesel fuel are necessary to meet engine emission targets. The fuel density and viscosity determine the amount of fuel that is injected and thereby the combustion behaviour. This presents a refining problem for LTFT syncrude that contains almost no aromatics and typically has a distillate density of around  $770\text{--}780\text{ kg m}^{-3}$ . It is less of a problem for HTFT syncrude, which contains aromatics.

Other diesel fuel properties that are important include cold flow, lubricity, flash point and distillation range. Fischer–Tropsch syncrude has poor cold flow properties on account of its high linear hydrocarbon content and just like in the case of jet fuel, some branching must be introduced. Boundary layer lubricity is related to the polarity of the compounds present in the diesel fuel<sup>9</sup> and good lubricity is provided by 1-alcohols and long chain carboxylic acids that are present in Fischer–Tropsch syncrude. Flash point and distillation range are not so much determined by molecular properties as by the cut point during refining.

It is possible to meet Euro-4-type diesel fuel specifications ( $820\text{--}845\text{ kg m}^{-3}$ ;  $\geq 51$  cetane number) with HTFT syncrude, but contrary to common perception, it is not possible to meet these specifications with LTFT syncrude when using standard refining technologies.

### Additives, blending and niche applications

It is not always possible, or economically viable to meet all the fuel specifications by refining only. When the molecular properties of the Fischer–Tropsch syncrude are such that it is difficult to achieve a specific fuel property, it may be more

efficient and environmentally responsible to fix the deficiency with an additive, or by blending with fuels derived from a different source. For example, in coal-to-liquids facilities that employ low temperature gasification, the associated coal pyrolysis products can be beneficially blended with the Fischer–Tropsch material to adjust density and viscosity of the distillate.<sup>10</sup> A similar situation exists with respect to crude oil derived material.

The unique properties of Fischer–Tropsch syncrude lends itself to refining for niche applications. This is especially true for the distillate range material from LTFT synthesis. It is more beneficial to refine LTFT syncrude to smaller market special diesel fuel grades,<sup>11</sup> which do not penalise Fischer–Tropsch distillate for its low density and low aromatic content, rather than to try and meet general diesel fuel specifications. However, the perception that LTFT distillate can be employed to blend away off-specification crude oil derived diesel fuel is not true in markets with strict diesel fuel specifications, like Europe. It is only true for crude oil derived diesel fuels that are close to specification in markets with less stringent specifications. For example, if a crude oil derived diesel fuel has a sulfur content that is  $10\text{ }\mu\text{g g}^{-1}$  above the sulfur specification, a blend containing 3% LTFT distillate will upgrade the crude oil derived diesel fuel to meet a sulfur specification of  $\leq 350\text{ }\mu\text{g g}^{-1}\text{ S}$ , but a blend with 50% LTFT distillate is required to meet a sulfur specification of  $\leq 10\text{ }\mu\text{g g}^{-1}\text{ S}$ .

Other such applications of Fischer–Tropsch derived material include the production of a “Battle Use Fuel of the Future” (BUFF). This is a multipurpose kerosene type fuel, very similar to Jet A-1 in properties, which is required by the United States Department of Defence for use in aircraft, tanks and other military vehicles to simplify fuel supply logistics. There is significant interest in Fischer–Tropsch syncrude as feed material for BUFF due to the potential energy security that can thus be provided.<sup>12</sup>

For motor-gasoline production, there are also co-refining synergies with crude oil that can be exploited. HTFT syncrude is a good source of olefins and alcohols (Tables 2 and 3). The olefins and alcohols can be beneficially employed in a crude oil refinery to boost production in some high-octane refining technologies such as aliphatic alkylation and etherification.

### Refining technologies in a Fischer–Tropsch context

Fischer–Tropsch syncrude can be refined to fuels and/or chemicals. In this section only technologies for fuels refining will be considered, although some of these technologies may be equally applicable to chemicals refining.

In the past there has been little incentive to develop Fischer–Tropsch specific refining technologies, due to the small number of Fischer–Tropsch refineries. This situation has not changed much and commercial Fischer–Tropsch operators had to adapt crude oil refining technology to make it compatible with Fischer–Tropsch feed materials. This often took the form of hydrogenating the olefins and oxygenates to hydrocarbons, so that the Fischer–Tropsch feed becomes similar to a paraffinic crude oil feed.

Some exceptions are noted, such as the development of a technology and catalyst for the hydrocracking of

Fischer–Tropsch wax by Shell<sup>13</sup> and the development of the conversion of olefins to distillate (COD) process by the Central Energy Fund of South Africa.<sup>14</sup> The former process is employed in the Shell Bintulu refinery, while the latter process is employed in the PetroSA (Moss gas) refinery. In addition to these two technologies, there is also the development of the dry C84–3 solid phosphoric acid (SPA) catalyst by Süd-Chemie Sasol Catalysts for use in the olefin oligomerisation units at Sasol Synfuels,<sup>15</sup> as well as the mild isomerisation and deoxygenation technologies employed for Fischer–Tropsch refining.<sup>16</sup> Other technology developments were mostly for chemicals production, such as those applied in the Sasol linear  $\alpha$ -olefin processes.<sup>17</sup>

Technology selection for use with Fischer–Tropsch streams cannot draw on the broad experience base that is available to the crude oil refining industry and the commercial implementation of a technology in a Fischer–Tropsch refinery does not imply that there is a good technology fit. A thorough understanding of the composition of the Fischer–Tropsch feed, including its trace components, the chemistry of the process and the catalysis involved, are all needed to make a proper technology selection. It will also indicate what level of customisation is necessary before the technology can reliably be implemented in a Fischer–Tropsch refinery. This type of analysis is not presently available from literature or technology licensors.

The refining technologies that are evaluated in this review, will be discussed in terms of the following:

- Refining objective of the technology.
- Chemistry involved.
- Catalysts employed.
- Feed requirements.
- Environmental issues.
- Technology compatibility to Fischer–Tropsch syncrude.
- Prospects for future application.

### Double bond isomerisation

The octane numbers of olefins are dependent on the position of the double bond. In general the octane numbers of linear  $\alpha$ -olefins are considerably lower than that of linear internal olefins (Table 4).<sup>18</sup> When a feed material has a high linear  $\alpha$ -olefin content, as is the case with Fischer–Tropsch syncrude, double bond isomerisation can improve the octane number significantly. The octane gain is less for branched olefins.

Double bond isomerisation at low temperature favours the formation of internal olefins from  $\alpha$ -olefins. It is an almost thermoneutral conversion, with an exothermic heat of reaction

**Table 4** Research octane number (RON) and motor octane number (MON) of some linear olefins to illustrate the octane gain by double bond isomerisation of the linear  $\alpha$ -olefin to a linear internal olefin

C#	Olefin	RON	MON	$\Delta$ relative to $\alpha$ -olefin
C <sub>6</sub>	1-hexene	76.4	63.4	—
	<i>trans</i> -2-hexene	92.7	80.8	16.9
	<i>trans</i> -3-hexene	94.0	80.1	17.2
C <sub>7</sub>	1-heptene	54.5	50.7	—
	<i>trans</i> -2-heptene	73.4	68.8	18.5
	<i>trans</i> -3-heptene	89.8	79.3	32.0
C <sub>8</sub>	1-octene	28.7	34.7	—
	<i>trans</i> -2-octene	56.3	56.5	24.7
	<i>trans</i> -3-octene	72.5	68.1	38.6
	<i>trans</i> -4-octene	73.3	74.3	42.1

( $-\Delta H_r$ ) in the order of 5–10 kJ mol<sup>-1</sup>. The reaction is acid catalysed and takes place *via* a carbocation intermediate, but it can also take place *via* a carbanion intermediate or a radical intermediate in different reaction environments (Fig. 5).

Industrially, double bond isomerisation is catalysed by solid acid catalysts with sufficient Brønsted acidity for olefin protonation. Numerous examples of potential catalysts have been recorded in the extensive review by Dunning,<sup>20</sup> with more recent literature reporting studies on catalyst classes such as sulfonic acid resins,<sup>21</sup> various zeolites<sup>22</sup> and mixed oxides.<sup>23</sup> Double bond isomerisation by non-acidic catalysts are less common, although isomerisation over basic zeolites<sup>24</sup> and in alkaline media<sup>25</sup> have been reported.

Acid catalysed double bond isomerisation has previously been used in refineries to upgrade products with a high linear  $\alpha$ -olefin content.<sup>16</sup> These applications used bauxite or silica-alumina materials and were not environmentally friendly on account of their high operating temperatures (>340 °C)<sup>26</sup> and high frequency of regeneration. Such a high operating temperature is not needed for double bond isomerisation, but were used since these processes also doubled as heteroatom conversion technologies.

It is possible to conduct double bond isomerisation at milder operating conditions by using a catalyst with stronger acidity. With catalysts such as acidic resins, or even silica-alumina materials, isomerisation can be performed at below 100 °C.<sup>27</sup> However, olefin oligomerisation can become a significant side-reaction.<sup>28</sup> Furthermore, unless the catalyst is only weakly acidic, the process can only be considered for C<sub>4</sub>–C<sub>6</sub> olefin feeds, since C<sub>7</sub> and heavier olefins are prone to catalytic cracking.<sup>29</sup>

Double bond isomerisation can also be performed as a side-reaction during partial hydrogenation of mono-olefins and

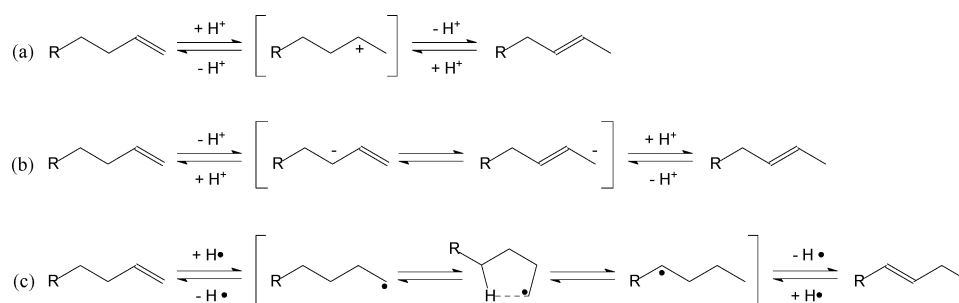


**Fig. 5** Double bond isomerisation mechanisms by (a) carbocation, (b) carbanion, and (c) radical intermediates.

dienes over palladium<sup>30</sup> and nickel<sup>31</sup> catalysts. These are not the only hydrogenating metals capable of inducing double bond isomerisation, but they are most active. The reported order of isomerisation activity of reduced metals are: Pd > Ni > Rh, Ru > Os, Ir, Pt.<sup>32</sup> The isomerisation mechanism is different to those already mentioned and involves hydrogen exchange on a metal surface (Fig. 6).

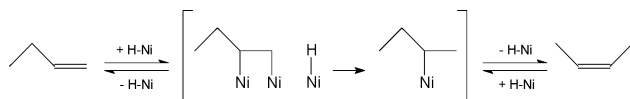


Fig. 6 Metal catalysed double bond isomerisation.

Since naphtha range Fischer–Tropsch primary products are rich in linear  $\alpha$ -olefins, there is a good technology fit with double bond isomerisation technology. Catalyst selection is crucial though, since Fischer–Tropsch derived naphtha feeds contain oxygenates. Alcohols may be dehydrated to produce olefins and the water thus formed may either be beneficial, as in the case of silica-alumina,<sup>33</sup> or detrimental, as in the case of acidic resins.<sup>34</sup> In the case of hydrogenation catalysts, application is limited to light naphtha streams that are low in oxygenates, and specifically low in carboxylic acids, since carboxylic acids can lead to catalyst deactivation by metal leaching.<sup>35</sup>

Although double bond isomerisation technology has been proven with Fischer–Tropsch derived feed, its prospect for future application is slim. From Table 4, it is clear that even with the significant gain in octane number that can be achieved, linear internal olefins still have moderate to poor octane numbers. The resulting octane deficit cannot be corrected by the addition of tetraethyl lead, as was the case when this technology was developed. Its usefulness is further restricted by the fuel specifications that limit the olefin content of motor-gasoline.

### Skeletal isomerisation of olefins

Skeletal isomerisation of olefins involves the conversion of linear olefins into branched olefins. It is employed as a feed pretreatment step for isobutene dimerisation to produce high octane motor-gasoline and for etherification with alcohols to produce high octane fuel ethers, such as methyl tertiary butyl ether (MTBE) and tertiary amyl methyl ether (TAME).

Industrial processes have been developed with mostly *n*-butenes and *n*-pentenes in mind.<sup>36</sup> Studies on the skeletal isomerisation of *n*-hexenes are more limited,<sup>37</sup> since these compounds are not generally used as fuel ethers.

There are two mechanistic routes by which the skeletal isomerisation takes place (Fig. 7), namely monomolecular isomerisation *via* a protonated cyclopropane intermediate and a bimolecular process involving dimerisation, followed by skeletal isomerisation and cracking.<sup>36</sup> The contribution of each of these two mechanisms depends on the feed material. The monomolecular mechanism is the dominant mechanism whereby pentene and heavier feeds are isomerised. Skeletal rearrangement *via* a monomolecular mechanism requires a carbon chain length of at least 5 carbon atoms to avoid the formation of a primary carbocation intermediate. Conversely the bimolecular mechanism is expected to be the dominant mechanism for butene isomerisation. In practice, the skeletal isomerisation of butene

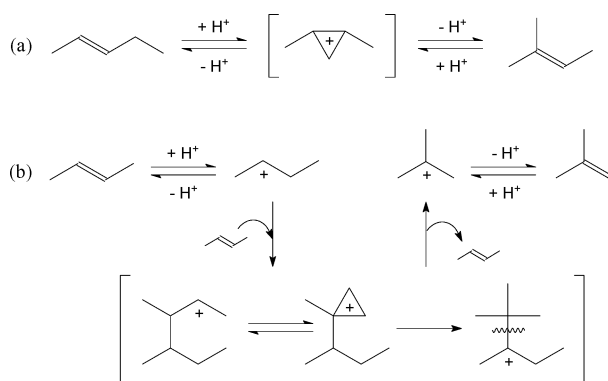


Fig. 7 Skeletal isomerisation by (a) monomolecular rearrangement through a protonated cyclopropane intermediate, and (b) bimolecular mechanism involving dimerisation, isomerisation and cracking.

is more complex and the details of the mechanism are still being debated.<sup>38</sup>

**Butene skeletal isomerisation.** Various catalysts have been investigated for the skeletal isomerisation of *n*-butene,<sup>39</sup> and it has been shown that ferrierite is by far the most selective for high temperature isomerisation, but it requires operating temperatures of 350 °C and higher. The overall efficiency of the process is somewhat eroded by side-product formation (10%). At typical operating temperatures there is a gradual loss of catalyst activity due to coking,<sup>40</sup> and for commercial processes, cycle lengths in the order of 500 hours have been reported.<sup>41</sup> Catalyst activity can generally be restored by controlled carbon burn-off.

Butene skeletal isomerisation is a fairly clean process in terms of solid waste, but its high operating temperature and frequent catalyst regeneration makes it energy intensive, which increases its environmental footprint. There is also no specific advantage (or disadvantage) to process Fischer–Tropsch butenes compared to crude oil derived feed, such as cracker-derived raffinate-II. With the decline in MTBE use globally, it will only be considered in an octane-constrained refinery in conjunction with a selective dimerisation process (“indirect alkylation”)<sup>42</sup> to produce alkylate-type product.

**Pentene skeletal isomerisation.** The skeletal isomerisation of *n*-pentene is more facile and a wider selection of commercial technologies is available. The technologies are based on different catalysts, such as acidic molecular sieves (UOP), ferrierite (Lyondell) and alumina (IFP/Axens).<sup>36,41</sup>

From a thermodynamic, as well as an environmental point of view, it is better to operate at lower temperatures. At lower temperatures the process is less energy intensive, catalyst coking is reduced and the equilibrium concentration of branched olefins is higher. The UOP Pentosom™ process, which employs an acidic molecular sieve catalyst, makes use of this advantage and has a start-of-run temperature of less than 300 °C. Unfortunately, this benefit is not available to the Fischer–Tropsch refiner. It was found that the oxygenates typically present in feed materials derived from Fischer–Tropsch synthesis, adsorb strongly on the catalyst and require a temperature of at least 320 °C to desorb.<sup>43</sup> This reduces the cycle length from 1 year, that is obtainable with cracker-derived feed, to only 1–2 months with Fischer–Tropsch derived feed. Ferrierite is also negatively affected by oxygenates, but conversely, oxygenates were actually found to

be beneficial during alumina catalysed skeletal isomerisation.<sup>44</sup> This was indeed found in practice and the alumina based ISO-5™ process that was implemented at Sasol Synfuels was found to work well with Fischer–Tropsch pentenes. The ISO-5™ process has an operating temperature around 410 °C and makes use of continuous catalyst regeneration (CCR) to burn off coke that has been formed on the catalyst. On account of the high operating temperature and significant side-product formation (10–15%) of this alumina based process, like other olefin skeletal isomerisation processes, it is not considered especially environmentally friendly.

Pentene skeletal isomerisation technology is only important if future motor-gasoline specifications allow the inclusion of ethers in the form of pentene derived ethers.

### Dimerisation and oligomerisation of olefins

The solubility of short chain hydrocarbons in naphtha is quite high and on account of their high octane numbers (Table 5)<sup>18</sup> it is desirable to include these compounds in motor-gasoline. There is unfortunately a limit on the amount of short chain hydrocarbons that can be accommodated in motor-gasoline due to vapour pressure constraints. In industrial practice, some butanes are typically blended into motor-gasoline until the final blend reaches the vapour pressure specification of the fuel.

**Table 5** Research octane number (RON), motor octane number (MON) and Reid vapour pressure (RVP) at 37.8 °C of the C<sub>2</sub>–C<sub>4</sub> hydrocarbons

C#	Compound	RON	MON	RVP/kPa
C <sub>2</sub>	Ethylene	100.4	75.6	>2000
	Ethane	111.4	100.7	>2000
C <sub>3</sub>	Propylene	102.5	75.6	1570
	Propane	112.1	97.1	1300
C <sub>4</sub>	1-Butene	97.4	80.8	435
	<i>cis</i> -2-Butene	100.0	83.5	315
	<i>n</i> -Butane	93.8	89.6	355
	Isobutane	101.3	97.6	500

This still leaves much of the light material available for extraction as chemicals (ethylene and propylene), or to be sold as fuels, namely liquid petroleum gas (propane and butane) and synthetic natural gas (methane and ethane). In cases where the refinery is far from petrochemical markets, it may be preferable to convert these light products into liquid fuels. Olefin oligomerisation technology (that includes olefin dimerisation) provides a way of doing so, although its application is limited to olefinic compounds only.

In Fischer–Tropsch refining context, olefin oligomerisation is a key technology, especially for HTFT synthesis, where C<sub>2</sub>–C<sub>4</sub> olefins constitute 25% of the total syncrude production. It enables the conversion of these olefins to liquid products and provides a convenient way to manipulate the motor-gasoline to diesel fuel production ratio of the refinery.

Olefin dimerisation is a highly exothermic reaction, with a heat of reaction in the order of 85–105 kJ mol<sup>-1</sup>. The type of catalysis that is employed for the conversion determines the mechanism (Fig. 8) and thereby the product distribution and quality. The mechanisms that are shown in Fig. 8 are simplified descriptions that do not show how stereochemistry and branching are influenced. Detailed mechanistic variations have been reported to account for specific types of catalysis and catalysts.<sup>45</sup>

There is quite a large selection of olefin oligomerisation technologies to choose from.<sup>46</sup> Some general pointers that can be followed in selecting an appropriate technology are:

(a) The carbon number distribution of the product is determined by both the catalyst and operating conditions. If the catalyst is very active, or the conversion is conducted at a high temperature, it is likely that the carbon number distribution will be thermodynamically, rather than kinetically controlled. Thermodynamically, oligomerisation is favoured by low temperature and high pressure. Processes operating at a high temperature would consequently require high pressure to produce heavier products. The carbon number distribution may also be determined by the mechanism.

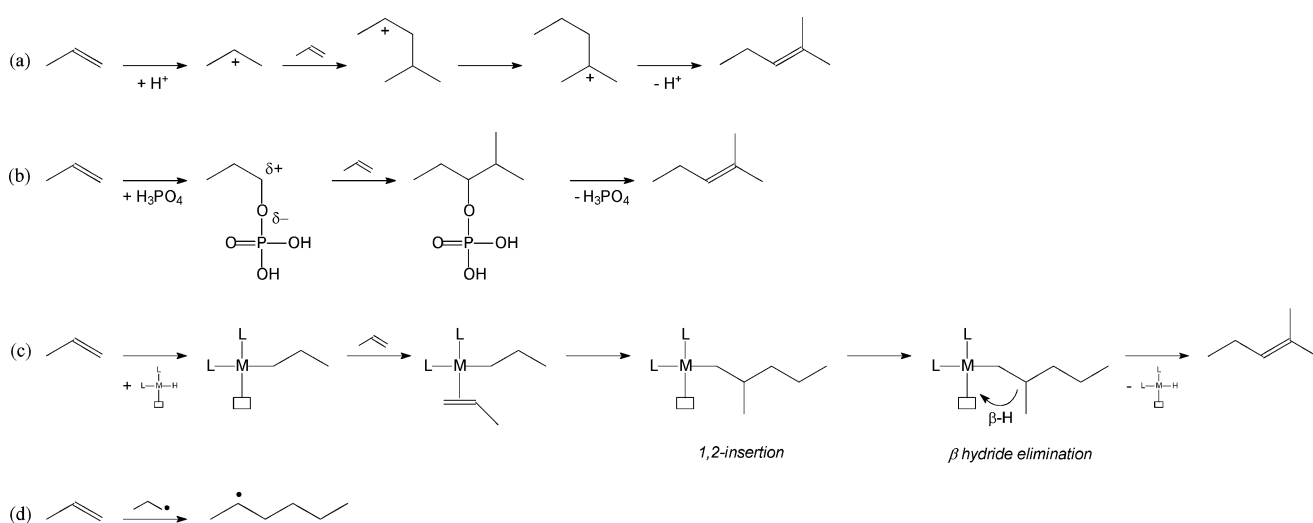


**Fig. 8** Olefin oligomerisation by the (a) classic Whitmore-type carbocation mechanism, (b) ester-based mechanism, (c) by organometallic catalysis involving 1,2-insertion and  $\beta$ -hydride elimination, and (d) radical propagation. Note that the influence of these mechanisms on stereochemistry and branching requires a more detailed description and is not apparent from this simplified description.



(b) The mechanism plays an important role in determining how each dimerisation step takes place. The mechanism is therefore linked to the type of catalyst being employed. Of especial importance is its control over the degree of branching of the product, that is, the number of alkyl side-chains on the carbon backbone of the product. For diesel fuel production and chemical applications, a low degree of branching is generally preferred. Cetane number decreases with increasing degree of branching. Nonetheless, some branching is required for acceptable cold flow properties. In jet fuel production, some branching is imperative, since linear hydrocarbons have much higher freezing points than branched hydrocarbons. If motor-gasoline is the desired product, a high degree of branching is required, since the octane number of motor-gasoline increases with increasing degree of branching. It is important to note that the differing dependence of product quality on degree of branching implies that an oligomerisation process is inherently predisposed to produce either good quality motor-gasoline, or good quality diesel fuel, but not both.

(c) Although the catalyst type determines the mechanism, the geometry may also play a role. When the catalyst has a pore constrained geometry, it may impose transition state selectivity on the mechanism, thereby changing the nature of the products that can form. Catalyst geometry is typically used to control the degree of branching. The acid strength of the catalyst is also relevant and may in some instances be changed by the feed quality. Acid strength determines the relative rate of cracking compared to oligomerisation, skeletal isomerisation rate, hydrogen transfer propensity and the temperature at which the transition from the kinetic to thermodynamic control takes place. Industrially, catalyst lifetime is important and the process configuration and reactor cycle length is also linked to the catalyst selection.

(d) The feed composition to an oligomerisation process should be carefully considered, since some catalysts are sensitive to the nature of the olefinic feed. The conversion and selectivity over such catalysts may be vastly different depending on the feed. The influence of the feed on catalyst performance can also be extended to tolerance of feed impurities. For example, in Fischer–Tropsch refining context, it is important to take note of the response of a catalyst to oxygenates.

In order to facilitate technology selection, it is necessary to consider the different olefin oligomerisation technologies separately. Each technology has its own processing aims, feed requirements and can be expected to yield products (motor-gasoline, jet fuel, diesel fuel or chemicals) in different ratios and of different qualities.

**Acidic resin catalysts.** The development of technology to make use of sulfonated styrene-divinylbenzene based resins, such as Amberlyst 15, for olefin oligomerisation, received a boost with the phase out of MTBE in some areas.<sup>47</sup> Processes like NExOCTANE™ (Fortum Oy)<sup>48</sup> was developed to convert MTBE units to dimerisation units that operated at similar conditions (<100 °C, liquid phase) and used the same catalyst. Other technology suppliers include Snamprogetti/CDTech, UOP and Lyondell.<sup>49</sup> Instead of etherifying the isobutene, it is selectively dimerised to trimethylpentenes that can be hydrogenated to

give high-octane trimethylpentanes (RON of 99–101 and MON of 96–99).<sup>48</sup> This makes the technology an environmentally friendly alternative to aliphatic alkylation for the production of alkylate-quality high-octane paraffins. Its application for alkylate-type production in Fischer–Tropsch context has been evaluated previously.<sup>50</sup>

To maximise dimerisation selectivity and limit heavy oligomer formation, the reaction is moderated by the addition of polar compounds, typically *tert*-butanol.<sup>51</sup> Only branched olefins are targeted for conversion, with isobutene being the main feed material. The feed needs to be free of typical acid catalyst poisons, but oxygenates in general does not seem to be a problem. Few side-reactions were noted on Amberlyst 15 at 70 °C and 0.4 MPa.<sup>34</sup> The application of acidic resin catalysed oligomerisation of Fischer–Tropsch feed benefits from the moderate oxygenate tolerance of this system.

**Zeolite catalysts.** The well-known “Mobil Olefins to Gasoline and Distillate” (MOGD)<sup>52</sup> and “Conversion of Olefins to Distillate” (COD)<sup>14</sup> processes, both make use of a H-ZSM-5 (MFI-type zeolite) based catalyst. The chemistry and catalysis of olefin oligomerisation over H-ZSM-5 has been studied extensively, with the pioneering work of Garwood<sup>53</sup> clearly showing its equilibration properties at high temperature. At low temperature, typically below 230 °C, H-ZSM-5 catalyses oligomerisation with limited cracking, resulting in the formation of oligomers that are multiples of the monomer. At higher temperatures the carbon number distribution of the product is equilibrated.<sup>54</sup> In the temperature region where the feed is “equilibrated”, the process is insensitive to the carbon number distribution of the olefins in the feed. The operating conditions (temperature and pressure) and product recycling can then be used to determine the product distribution.<sup>55</sup>

Oxygenates are known to reduce catalyst activity,<sup>56</sup> but this does not preclude the use of H-ZSM-5 with Fischer–Tropsch feed material. The COD process operates commercially with an oxygenate containing HTFT feed.

Both the MOGD and COD processes employ conditions around 200–320 °C and 5 MPa. The distillate produced by oligomerisation is hydrogenated to a high quality diesel, with >51 cetane number and good cold flow properties.<sup>14,52,57</sup> The motor-gasoline is of a lower quality (RON = 81–85, MON = 74–75) when employing Fischer–Tropsch derived feed that is low in isobutene.<sup>14,58</sup> The linearity of the oligomers, which is responsible for the good cetane number of the diesel fuel and poor octane number of the olefinic motor-gasoline, is due to the pore constraining geometry of ZSM-5.<sup>58</sup>

Despite the low coking propensity of H-ZSM-5 catalysts, the catalyst has to be regenerated every 3–6 months by controlled coke burn-off. The catalyst lifetime extends over multiple cycles and overall the process does not raise environmental concern.

The ExxonMobil Olefins to Gasoline (EMOGAS™) technology is another zeolite-based process that has recently been introduced. In the absence of nitrogen bases, it is claimed to have a catalyst lifetime of 1 year and has been designed for retrofitting solid phosphoric acid units.<sup>59</sup> The zeolite-type (not H-ZSM-5) has not been stated explicitly, although ExxonMobil patent applications suggest that it is a zeolite of the MFS-type (H-ZSM-57) or TON-type (Theta-1/H-ZSM-22). The carbon

number distribution of the product is similar to that of SPA, with little material boiling above 250 °C.<sup>60</sup>

Other zeolites have also been investigated for olefin oligomerisation, but generally deactivate too fast to be of commercial value in this type of service.<sup>61</sup>

**Amorphous silica-alumina (ASA) catalysts.** The IFP/Axens Polynaphtha™ process was originally designed for use with an amorphous silica-alumina catalyst (IP811). This process can also be licensed with a zeolite-based catalyst (IP501).

The most obvious difference between ASA and zeolite catalysts used for oligomerisation, is their less pore constrained geometry, since ASA is not crystalline. There are other differences too, that allow ASA to yield a very different product from oligomerisation. These include its apparent lower acid strength, hydrogen transfer propensity<sup>62</sup> and reaction mechanism that is different to the classic Whitmore-type carbocation mechanism. The latter is evidenced by its *cis*-selective nature for double bond isomerisation and the differences in products obtained from the oligomerisation of linear  $\alpha$ -olefins and linear internal olefins.<sup>63</sup>

It has been found that ASA catalysts work well with Fischer–Tropsch feeds, including oxygenate containing feed materials.<sup>64</sup> The distillate thus produced has a higher density (810 kg m<sup>-3</sup>; much needed in Fischer–Tropsch refining) than any of the other oligomerisation catalysts. The hydrogenated distillate also has good cold flow properties, but with a cetane number of only 28–30. The naphtha properties are feed dependent and short chain olefins yield a better quality motor-gasoline (RON = 92–94, MON = 71–72) than H-ZSM-5. Similar catalyst cycle lengths and regenerability as H-ZSM-5 has been demonstrated in service as an olefin oligomerisation catalyst, making ASA based oligomerisation technology as environmentally friendly as H-ZSM-5 based technology.

There is also a fair amount of interest in making use of the more structured ASA derivatives, like MCM-41, for olefin oligomerisation.<sup>65</sup> These catalysts have large pores and are not geometrically constraining, but have not yet been applied industrially for this purpose.

One variation on ASA catalysts that is interesting for chemical applications is the Hüls Octol process, which uses a nickel promoted silica-alumina molecular sieve catalyst (Montmorillonite).<sup>66</sup> For chemicals applications, the Octol B catalyst is employed that yields a more linear product, while for fuels applications, the Octol A catalyst that gives a more branched product is preferred.<sup>67</sup> The addition of nickel to the catalyst introduces a different reaction mechanism, namely 1,2-insertion and  $\beta$ -hydride elimination, which implies that more than one mechanism is operative in parallel.

**Solid phosphoric acid (SPA) catalysts.** The Catalytic Polymerisation (CatPoly) technology of UOP was the first of many solid acid catalysed olefin oligomerisation technologies to be commercialised.<sup>68</sup>

The catalyst is manufactured by impregnating a natural silica source such as kieselguhr (diatomaceous earth) with phosphoric acid.<sup>15</sup> The active phase is a viscous layer of phosphoric acid on the support, with the support itself being inactive.<sup>69</sup>

Olefin oligomerisation takes place *via* an ester mechanism, whereby a phosphoric acid ester stabilises the polarised hydrocarbon intermediate.<sup>70</sup> The operating temperature and amount

of water in the feed determine the ratio of different phosphoric acid species on the catalyst, which in turn determines its activity and selectivity behaviour.<sup>71</sup> The technology was nevertheless reported to be insensitive to the feed composition (C<sub>2</sub>–C<sub>5</sub> olefins) and the olefinic motor-gasoline thus produced invariably had a RON in the range of 95–97 and MON in the range of 81–82.<sup>72</sup> This does not imply that the olefin oligomers produced by different olefinic feeds are isostructural – they are not. It was found that the quality of the hydrogenated motor-gasoline is very dependent on feed and operating conditions.<sup>73</sup> This is relevant to Fischer–Tropsch refining, since it is likely that at least some of the olefinic motor-gasoline will have to be hydrogenated to meet the olefin specification of motor-gasoline. Surprisingly it was found that a low temperature isomerisation pathway is operative during 1-butene oligomerisation, which results in the formation of a significant fraction of trimethylpentenes.<sup>74</sup>

It is possible to produce a hydrogenated motor-gasoline with 86–88 octane from a 1-butene rich Fischer–Tropsch feed. SPA oligomerisation can consequently be considered for producing alkylate-type product from Fischer–Tropsch olefins, even though there is little isobutene in the feed.<sup>50</sup> Even higher octane alkylate-type products can be obtained when operating at low temperature (<140 °C) with an isobutene-rich feed, for example the UOP InAlk™-process (“indirect alkylation”).<sup>42</sup>

SPA oligomerisation is not a distillate producing technology,<sup>75</sup> although distillate yield can be improved by manipulating the water content and operating conditions.<sup>76</sup> The distillate has a low cetane number (25–30), but excellent cold flow properties, making it a good jet fuel, but poor diesel fuel.

Since the SPA catalyst is influenced by water, only a limited amount of oxygenates can be tolerated in the feed and catalyst activity is inhibited at high oxygenate concentration. This limits application of SPA in a Fischer–Tropsch refinery to the conversion of light olefin streams that are almost free of oxygenates. Attempts to use it with Fischer–Tropsch derived naphtha gave poor results<sup>77</sup> and some oxygenate classes were found to be especially detrimental to the SPA catalyst.<sup>78</sup>

SPA is a cheap catalyst and the spent catalyst is not regenerated. The process is nevertheless environmentally friendly, because the catalyst is produced from natural silica and is disposed of in a beneficial way. The spent catalyst is neutralised with ammonia to produce ammonium phosphate plant fertiliser and it does not generate solid waste.

**Homogeneous catalysts.** Olefin oligomerisation by the Dimersol™ process from IFP/Axens, is presently one of very few refinery technologies where homogeneous organometallic catalysis are applied industrially.<sup>46</sup>

The Dimersol™ process makes use of a nickel-based Ziegler-type catalyst system and olefin oligomerisation takes place by a  $\beta$ -hydride elimination mechanism.<sup>79</sup> There are a number of variants of the Dimersol™ process:<sup>80</sup>

(a) Dimersol™ E for the oligomerisation of ethylene and FCC off-gas (C<sub>2</sub>/C<sub>3</sub> olefin mixture) to motor-gasoline. This type of technology was in commercial operation in the HTFT refinery of Sasol in Secunda to convert excess ethylene to motor-gasoline. It was installed as a risk-mitigation option to avoid flaring of ethylene. The plant became redundant in the 1990’s and was officially written off early in the 2000’s.

(b) Dimersol™ G for the oligomerisation of propylene and C<sub>3</sub>/C<sub>4</sub> olefin mixtures to motor-gasoline.<sup>81</sup>

(c) Dimersol™ X for butene oligomerisation to linear octenes for plasticiser alcohol manufacturing.<sup>82</sup>

Because the technology makes use of a homogeneous organometallic catalyst system, it is sensitive to any impurities that will complex with the nickel. Amongst others, it is sensitive to dienes, alkynes, water and sulfur, which should not exceed 5–10 μg g<sup>-1</sup> in the feed.<sup>81</sup> It is possible to increase the catalyst dosing to offset deactivation by feed impurities, an advantage of using a homogeneous catalyst, but at an operating cost penalty.

The catalyst has to be removed from the reaction product by a caustic wash, which increases the environmental footprint of Dimersol™. In a more recent incarnation of this technology, called Difasol™, the catalyst is contained in an ionic liquid phase,<sup>79</sup> which makes catalyst separation easier. The Difasol™ process does not generate the same amount of caustic effluent as the Dimersol™ process. In a lifetime test conducted over a period of 5500 hours, it was found that the nickel catalyst consumption in the Difasol™ process was only 10% of that found with the Dimersol™ process, while that co-catalyst consumption was half.<sup>83</sup>

There may be a competitive advantage to employ the Dimersol™ X and Difasol™ technologies for chemicals production from Fischer–Tropsch derived butenes, on account of their low isobutene content. For fuels production, these technologies hold no advantage.

**Thermal (no catalyst).** The thermal oligomerisation of cracker gas streams to motor-gasoline had been practised widely in the past,<sup>84</sup> but has since been completely replaced by catalytic oligomerisation. This happened not only due to the higher efficiency of the catalytic processes, but also due to the lower octane number (MON = 77) obtained by thermal oligomerisation.

The reaction takes place by a radical mechanism,<sup>85</sup> which results in the formation of products that have a low degree of branching. This explains the low octane number of the motor-gasoline produced by thermal oligomerisation. Branching is not introduced by isomerisation of radicals<sup>86</sup> and there is consequently similarities to Lewis acid catalysed oligomerisation, such as with BF<sub>3</sub>.<sup>87</sup> Thermal oligomerisation of linear α-olefins, as is prevalent in HTFT products, results in lubricating oils with good viscosity properties.<sup>88</sup> Mechanistically, thermal oligomerisation is better suited to the production of distillates and lubricating oils from Fischer–Tropsch products, as was indeed shown.<sup>89</sup>

The technology unfortunately requires high temperatures. A method to overcome this shortcoming by heat-integrating thermal oligomerisation with high temperature Fischer–Tropsch synthesis has been suggested, which makes the overall process more energy efficient.<sup>89</sup> Attempts to further reduce the energy requirements by making use of radical initiators, such as di-tertiary butyl peroxide, failed due to low initiator productivity.<sup>90</sup>

## Etherification

Fuel ethers are high-octane blending components that provide a convenient way to improve motor-gasoline quality. The inclusion of oxygenates in motor-gasoline is unfortunately also

**Table 6** Blending research octane number (RON), motor octane number (MON) and vapour pressure at 37.8 °C of some fuel alcohols and ethers

Compound <sup>a</sup>	RON	MON	Blending vapour pressure/kPa
Ethanol	120	99	154
MTBE	118	101	55
ETBE	118	101	40
TAME	115	100	25

<sup>a</sup> MTBE = methyl *tert*-butyl ether (2-methoxy-2-methylpropane); ETBE = ethyl *tert*-butyl ether (2-ethoxy-2-methylpropane); TAME = tertiary amyl methyl ether (2-methoxy-2-methylbutane).

a politically sensitive subject and relying on oxygenates to meet octane specifications should be made judiciously.

With the mandatory inclusion of oxygenates in reformulated fuels, as promulgated in legislation such as the Clean Air Act Amendment of 1990 in the United States, refiners mainly had a choice between alcohols and ethers. Both alcohols (C<sub>1</sub>–C<sub>4</sub>) and ethers (C<sub>4</sub>–C<sub>5</sub> olefin derived) are high-octane blending components. Ethers were preferred over alcohols for a number of technical reasons:

(a) Ethers have a lower phase separation tendency in the presence of small amounts of water. This gives ethers better storage and transport stability than alcohols.

(b) The production of fuels ethers is a convenient way to reduce the amount of volatile short chain olefins in motor-gasoline.

(c) Ethers have a lower blending vapour pressure than the alcohols (Table 6).<sup>91</sup>

Despite the technical merits of using fuel ethers for motor-gasoline, etherification technology selection is subject to political expediency. A case in point is the debate around methyl *tert*-butyl ether (MTBE), darling oxygenate of the 1990's, which was eventually banned from motor-gasoline in large parts of the United States, but not in Europe.<sup>92</sup> The subsequent discussion will focus on the technical aspects.

Etherification as practised industrially, is an equilibrium limited reaction between an alcohol and an olefin containing a C=C bond on a tertiary carbon (Fig. 9).

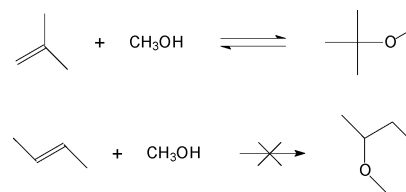


**Fig. 9** Etherification reaction between an olefin and an alcohol.

The etherification reaction is catalysed by an acid and the conversion is equilibrium limited, with ether formation being favoured by low temperature.<sup>93</sup> The catalyst that is most often used for etherification, is Amberlyst 15, a sulfonic acid exchanged divinylbenzene-styrene copolymer resin catalyst from Rohm and Haas. Other acidic resin catalysts<sup>91</sup> and zeolites<sup>94</sup> can also be used.

The process has to be operated with an excess of alcohol to reduce olefin oligomerisation as side reaction. When an excess

of alcohol is used, the catalyst protonates the alcohol and the alcohol becomes the protonating agent,<sup>95</sup> thereby preventing the formation of oligomers. The alcohol also acts as solvating agent, breaking the hydrogen bonds between sulfonic acid groups and thereby reducing the acid strength of the catalyst.<sup>96</sup> This also reduces oligomerisation as a side-reaction.

From a technical point of view, methanol is the preferred alcohol for etherification, since it does not form an azeotrope with water and it results in a higher ether concentration at etherification equilibrium. For example, the equilibrium constant for MTBE is 32 at 70 °C, but for ETBE it is only 18 at 70 °C.<sup>97</sup> The selection of the olefin feed is refinery dependent, with isobutene and isopentenes being the preferred olefins (depending on local legislation). It is also possible to make use of a mixed olefin stream and the etherification of all reactive olefins in fluid catalytic cracking (FCC) derived naphtha has been investigated.<sup>98</sup> By doing so, it simplifies feed preparation, but it complicates product separation. This is not useful in Fischer–Tropsch context, where it has been shown that most hexyl ethers derived from Fischer–Tropsch naphtha have low octane numbers.<sup>99</sup>

The etherification reaction can be affected by basic compounds that can neutralise the acid sites, as well as dienes and oxygenates found in Fischer–Tropsch syncrude. Dienes are very reactive and can form heavy polymers under etherification conditions. Various oxygenates can inhibit the etherification reaction and can participate in side-reactions,<sup>34</sup> often forming water, which is also known to inhibit conversion.<sup>100</sup> Etherification of C<sub>5</sub> and C<sub>6</sub> olefins with methanol are nevertheless successfully applied on industrial scale with HTFT feed, but only tertiary amyl methyl ether (TAME) is employed as fuel ether.

Etherification is an environmentally friendly technology. It is not energy intensive and it is quite selective. Future application in Fischer–Tropsch refineries will mostly depend on fuel specifications, which may preclude the use of some fuel ethers.

### Aliphatic alkylation

Aliphatic alkylation is one of the most important technologies for the production of high-octane paraffins. With fuel specifications putting increasingly tighter limits on non-paraffin compound classes, the viability of motor-gasoline production in a refinery becomes more and more reliant on the quality of the paraffins in the base stock.

Aliphatic alkylation entails the alkylation of isobutane with an olefin (preferably butene) to produce a highly branched paraffin. It is an acid catalysed reaction (Fig. 10), with hydrofluoric acid (HF) and sulfuric acid (H<sub>2</sub>SO<sub>4</sub>) being the two catalysts employed industrially.<sup>101</sup>

The biggest drawback of current aliphatic alkylation technologies is their significant environmental footprint. Liquid acid processes are not considered environmentally friendly, especially not HF processes, despite significant advances in addressing environmental concerns. Due to the current lack of alternative technologies, these liquid acid processes are tolerated. This may well change in future.

The field of aliphatic alkylation has seen incremental advances since its development, but a comparison of reviews shows that the same technologies that were commercially available in the

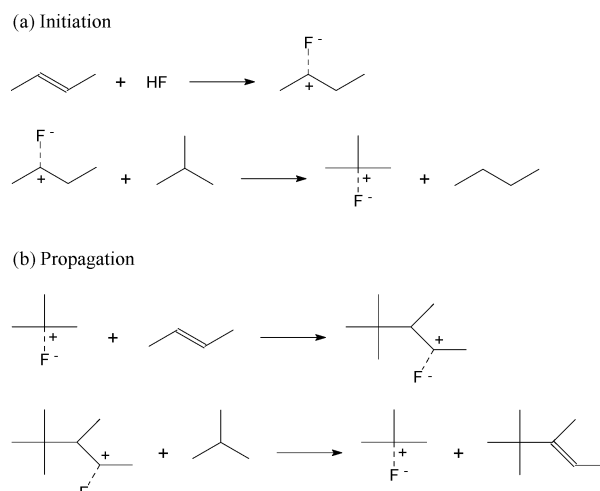


**Fig. 10** Aliphatic alkylation mechanism illustrated by the initiation and propagation steps involved during hydrofluoric acid (HF) catalysed alkylation of isobutane with 2-butene.

1950's,<sup>102</sup> are still the technologies available today.<sup>101</sup> The projected development of solid acid catalysts for this process, “[t]he trend is definitely toward solid catalysts operating at temperature that do not require refrigeration” (1958),<sup>102</sup> has not yet come to pass.<sup>103</sup> One of the main reasons why solid acid catalysed aliphatic alkylation processes have not yet found industrial use, is the rapid rate of catalyst deactivation and the inability to guarantee a high on-stream availability. The high on-stream availability of alkylation units is often imperative on account of the critical role of alkylate as a high-octane paraffinic blending component that is necessary to meet motor-gasoline specifications.

Aliphatic alkylation units based on HF catalysts are more feed sensitive than H<sub>2</sub>SO<sub>4</sub> units and the feed must be dried (<20 μg g<sup>-1</sup> H<sub>2</sub>O) to limit corrosion. The effect of oxygenates as feed impurities are still inadequately understood,<sup>101</sup> but oxygenates can generally be seen as a source of water from acid catalysed side-reactions. Olefinic feed impurities, such as ethylene and dienes, can increase the acid consumption. A high isobutene content in the feed is also detrimental, because it rapidly oligomerises to form heavy products.

The type of olefin that is used for alkylation has a significant influence on the acid consumption<sup>104</sup> and octane number of the product (Table 7).<sup>101</sup> Typical acid consumption of HF and H<sub>2</sub>SO<sub>4</sub> units are 0.82 and 60 kg per ton product respectively.<sup>101</sup>

Of specific importance to the Fischer–Tropsch refiner is that the most abundant butene isomer, namely 1-butene, is the least desirable olefin for HF alkylation (Table 7). The opposite is true for alkylation over H<sub>2</sub>SO<sub>4</sub>, where the quality of alkylate being produced from 1-butene with 99% H<sub>2</sub>SO<sub>4</sub> is better than that from 2-butene.<sup>105</sup>

Aliphatic alkylation not only requires olefins, but also isobutane. There is little isobutane in Fischer–Tropsch syncrude and even if all the *n*-butane in syncrude is hydroisomerised, only part of the total butene product could be used for alkylation. A different situation exists when the Fischer–Tropsch syncrude is co-refined with an alternative source of butanes. For example, in the case of the PetroSA HTFT refinery in Mossel Bay, South Africa, natural gas provides an external source of butanes for the HF alkylation unit.<sup>106</sup>



**Table 7** Typical research octane numbers (RON) and motor octane numbers (MON) of alkylate produced by alkylation of isobutane with various olefins over HF and H<sub>2</sub>SO<sub>4</sub>. The alkylate quality is influenced by operating conditions, acid purity and feed purity that are not shown

Olefin in feed	HF alkylation		H <sub>2</sub> SO <sub>4</sub> alkylation	
	RON	MON	RON	MON
Propylene	91–92	89.5–90	89	87.1
1-Butene	94.4	91.6	97.8	93.9
2-Butenes	97.8	94.6		
Isobutene	95.9	93.4	93.2	90.3
<i>n</i> -Pentenes	82.5	91	88	
Isopentene	—	—	91.2	88.8
Mixed pentenes	90–91.5	89–90	—	—

Aliphatic alkylation has been evaluated as potential technology for Fischer–Tropsch refining and it was found to be lacking in many respects.<sup>50</sup> It has been concluded that selective olefin dimerisation (“indirect alkylation”) combined with hydrogenation of the product is the preferred route for alkylate production.

### Aromatic alkylation

Aromatic alkylation is not normally associated with refining, but rather with petrochemical production. However, with the increasingly more stringent regulation of benzene content in motor-gasoline, various options for benzene reduction have been considered, including benzene alkylation.<sup>107</sup> One of the advantages of benzene alkylation over alternatives such as benzene extraction and benzene hydrogenation, is that it retains the octane value of benzene.

The alkylation of benzene with an olefin is an acid catalysed reaction (Fig. 11). There are various commercial processes for the alkylation of benzene with either ethylene or propylene and the catalysts most often used are solid phosphoric acid (SPA) and zeolite-type materials such as H-ZSM-5 (Mobil-Badger 1980’s), H-MCM-22 (Mobil-Ratheon/Mobil-Badger 1990’s), HY-zeolite (CDTech) and modified-H-Beta (Enichem).<sup>108</sup>

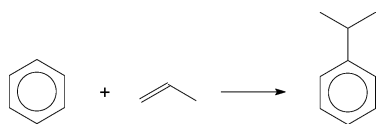


**Fig. 11** Aromatic alkylation illustrated by the acid catalysed reaction of propylene with benzene to produce cumene.

The main difference between SPA and zeolite catalysed processes is that SPA has a low multiple alkylation tendency, while zeolite-based processes require a transalkylation reactor after the alkylation reactor to increase the yield of mono-alkylated products.<sup>109</sup> The low multiple alkylation tendency of SPA is related to the alkylation mechanism and that linear olefins have a much higher alkylation than oligomerisation rate.<sup>110</sup>

The degree of alkylation can also be controlled by the aromatic to olefin ratio in the process. Aromatic alkylation processes are generally operated at an aromatic to olefin ratio of around 5 : 1 to 8 : 1 to limit olefin oligomerisation and multiple alkylation as side-reactions. A benzene conversion of less than 20% per pass is achieved, which necessitates benzene recycling and the benzene should be sufficiently pure to enable such recycling. This mode of operation makes sense for chemicals production, but when

aromatic alkylation is employed for fuels production, the final product is a mixture and the side-reactions are not necessarily undesirable. Side-reactions can be beneficially employed, for example, it has been shown that fully synthetic Jet-A1 can be produced over SPA by co-feeding benzene with propylene at low aromatic to olefin ratio.<sup>111</sup> Multiple alkylation is therefore not necessarily a problem during fuels refining.

The choice of olefin for alkylation and the degree of alkylation are dependent on the desired product (motor-gasoline, jet fuel or diesel fuel) and the product properties (Table 8).<sup>8,18</sup>

Most alkylation processes have been designed for pure feed materials, since their intended application is the chemicals industry. Catalyst selection for aromatic alkylation to produce fuels must take the sensitivity of the catalyst towards feed impurities into account. Zeolites are in general more sensitive to heteroatom impurities than SPA.

Olefin oligomerisation and benzene alkylation can be combined in a single refining step to reduce refinery benzene levels and produce motor-gasoline and jet fuel blending components. It has been reported that >80% conversion of benzene to alkylated benzenes was found during industrial operation over SPA.<sup>112</sup> It has also been noted that propylene is the preferred olefin for alkylation. Although butene-rich feeds can also be employed, benzene conversion is lower.

For fuels refining, SPA-based aromatic alkylation is recommended over zeolite-based processes, contrary to the trend for chemicals production.<sup>108</sup> Aromatic alkylation over SPA requires a lower operating temperature, requires no transalkylation reactor, is more resistant to feed impurities and can be operated at a much lower aromatic to olefin ratio. All of these factors make SPA less energy intensive and more environmentally friendly than zeolite-based processes.

Future application of aromatic alkylation technology in Fischer–Tropsch refinery design is likely, because it allows the synthesis of alkylbenzenes as high quality transportation fuels, while creating a platform for chemical growth.

### Metathesis

Metathesis technologies have not been developed with fuels refining in mind. Yet, considering the abundance of olefins in Fischer–Tropsch syncrude, it may find application in shifting the carbon number distribution around its mean. Unlike olefin oligomerisation that only produces heavier olefins from lighter olefins, or cracking that only produces lighter olefins from heavier hydrocarbons, metathesis produces heavier and lighter olefins, while retaining the same average molecular mass in the product as in the feed. The metathesis reaction, which is a form

**Table 8** Boiling point ( $T_b$ ), research octane number (RON), motor octane number (MON), freezing point ( $T_m$ ), density ( $\rho$ ) and cetane number (CN) of some alkylbenzenes

Compound	$T_b/^\circ\text{C}$	RON	MON	$T_m/^\circ\text{C}$	$\rho/\text{kg m}^{-3}$	CN
Ethylbenzene	136	107.4	97.9	–95	874	8
Cumene	152	113	99.3	–96	869	15
<i>sec</i> -Butylbenzene	173	106.8	95.7	–75	866	6
<i>tert</i> -Butylbenzene	169	>115	107.4	–58	871	–1
<i>m</i> -Diethylbenzene	181	>115	97	–84	868	9
<i>m</i> -Diisopropylbenzene	203	—	—	–61	856	–7

of olefin disproportionation, requires an unsymmetric olefin or a mixture of olefins to result in productive disproportionation (Fig. 12).<sup>113</sup>

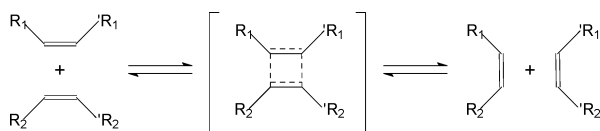


Fig. 12 Olefin disproportionation (metathesis) reaction.

Metathesis finds application in the olefins business for the conversion of ethylene and 2-butene to propylene, or *vice versa* by the Olefins Conversion Technology (OCT) licensed by ABB Lummus and Meta-4™ process of IFP/Axens. It is also employed for the production of linear  $\alpha$ -olefins by the Shell Higher Olefins Process (SHOP), as well as 1-hexene by the OCT-process.<sup>114</sup>

The most commonly used heterogeneous metathesis catalysts are based on  $\text{WO}_3$  (OCT),  $\text{MoO}_3$  (SHOP) and  $\text{Re}_2\text{O}_7$  (Meta-4™). The need for frequent catalyst regeneration<sup>115</sup> increases the energy consumption of the process and makes it less environmentally friendly. It has also been noted that oxygenates change the catalytic behaviour of some metathesis catalysts,<sup>116</sup> which detracts from its use in a Fischer–Tropsch environment.

One specific application where metathesis technology may be considered is for the conversion of ethylene to heavier olefins. This is necessary when the Fischer–Tropsch facility is far from petrochemical markets and the ethylene has to be used within the refinery. Nevertheless, even in this specific application it is doubtful whether metathesis would be preferred over technologies such as aromatic alkylation or olefin hydration for converting ethylene in the refinery.

## Hydrotreating

Hydrotreating is the mainstay of refining. Broadly defined, hydrotreating is the reaction of any feed with hydrogen and it is the conversion technology most frequently employed to convert heteroatom containing compounds into hydrocarbons.

Hydrotreating fulfils two functions in the refinery, both related to the removal of specific functional groups. Firstly, it is useful as a feed pretreatment step for refinery operations that are sensitive to impurities. For example, hydrogenation of dienes to mono-olefins as feed pretreatment before an acid catalysed conversion step to prevent the formation of heavy polymers. Secondly, it is used to meet final product specifications in terms of composition. For example, the hydrogenation of sulfur containing compounds in order to meet the sulfur specification of transportation fuel.<sup>117</sup>

Hydrotreating can be classified in terms of its function, which is also a convenient way of indicating the fields of hydrotreating that are most relevant to Fischer–Tropsch refining:

(a) Hydrodesulfurisation (HDS).<sup>118</sup> There is essentially no sulfur compounds in Fischer–Tropsch syncrude. This type of hydrotreating is relevant only when Fischer–Tropsch is co-refined with sulfur containing materials, for example from crude oil, direct coal liquefaction, low temperature coal gasification or coal pyrolysis.

(b) Hydrodenitrogenation (HDN).<sup>119</sup> The same as for HDS applies; Fischer–Tropsch syncrude is essentially free of nitrogen containing compounds.

(c) Hydrodeoxygenation (HDO).<sup>120</sup> This is one of the most important fields of hydrotreating relevant to Fischer–Tropsch syncrude. Some applications include the selective conversion of carbonyl compounds to alcohols in the Fischer–Tropsch aqueous product,<sup>121</sup> deep deoxygenation of waxes for food applications<sup>122</sup> and oxygenate conversion for the production of transportation fuels.<sup>123</sup>

(d) Hydrodearomatisation (HDA).<sup>124</sup> The polynuclear aromatic content of Fischer–Tropsch syncrude is low. This class of hydrotreatment is nonetheless relevant in specific applications, such as the upgrading of the atmospheric residue from HTFT synthesis.

(e) Hydrogenation of olefins (HYD).<sup>125</sup> This is an important class of hydrotreating on account of the high olefin content of Fischer–Tropsch syncrude. Its two main applications are the hydrogenation of the products from olefin oligomerisation<sup>126</sup> and in conjunction with HDO, hydrotreating of straight run syncrude to transportation fuels.<sup>123</sup>

(f) Hydrodemetallisation (HDM).<sup>127</sup> The main metals in Fischer–Tropsch syncrude are iron and sodium, which are present as metal carboxylates. Unfortunately HDM catalysts are ineffective at the removal of these metals.<sup>128</sup>

Hydrotreating is invariably exothermic and the specific heat release is related to the compound type being hydrogenated. When Fischer–Tropsch naphtha and distillate cuts are hydrotreated, the heat release can be very high. This not only requires a reactor design that is capable of proper heat management, but also necessitates careful catalyst selection ensure that the reaction rate is not too high. In this respect the hydrotreating of Fischer–Tropsch materials tend to require less active catalysts in order to avoid hot spot formation and hydrogen starvation at the catalyst surface. This presents a problem, since catalyst manufacturers are generally discontinuing lower activity catalysts in favour of very high activity catalysts.

During hydrotreating, hydrogen addition occurs. In the case of HDS, HDO and HDN, hydrogen sulfide ( $\text{H}_2\text{S}$ ), water ( $\text{H}_2\text{O}$ ) and ammonia ( $\text{NH}_3$ ) are co-produced, which have to be removed downstream of the hydrogenation reactor. The rate of heteroatom removal for isostructural compounds is generally in the order  $\text{HDS} > \text{HDO} > \text{HDN}$ .<sup>120</sup> This order may change when the compounds are not isostructural.

Most commercial refinery hydrotreating catalysts are bi- or trimetallic, with NiMo, NiW, CoMo and NiCoMo on alumina being the main types encountered in practice.<sup>129</sup> On account of the sulfur content of crude oil, these catalysts are all designed to be operated as sulfided metal catalysts and are called sulfided catalysts for short.<sup>130</sup> A smaller group of hydrotreating catalysts are used for selective hydrogenation and are used in the absence of sulfur. These unsulfided catalysts are generally based on Ni, Pd or Pt on alumina.

The selection of hydrotreating catalysts is very application specific.<sup>131</sup> In practice hydrotreaters are not loaded with a single type of catalyst, but with different layers, each performing a specific function. However, it is not only the catalyst activity that is important, but also its deactivation behaviour with the intended feed.<sup>132</sup> Special catalyst types are often loaded on

top of the main catalyst beds to help with feed distribution and to remove feed impurities that can lead to deposit formation. Catalyst grading with an HDM catalyst on top to trap metals and avoid pressure drop problems is therefore common practice.

In a Fischer–Tropsch refinery, HDO and HYD are the main hydrotreating duties required, whereas in crude oil refineries it is HDS and HDN. The absence of sulfur in Fischer–Tropsch syncrude creates a problem for most hydrotreating catalysts, since they have been designed as sulfided catalysts. Standard crude oil refinery hydrotreating catalysts and technology is consequently poorly suited for direct application to Fischer–Tropsch feeds. This can be overcome in two ways, by either using only unsulfided catalysts, or by adding sulfur compounds to the feed to keep the sulfided catalysts in a sulfided state. It is clear that from an environmental point of view the latter is undesirable. Ironically, it is the latter approach that is followed in practice. This is mainly due to the action of the carboxylic acids in Fischer–Tropsch syncrude that necessitates special catalyst properties, but oxygenates in general may cause problems with unsulfided catalysts not designed for HDO.<sup>35,128</sup> The environmental footprint of hydrotreating in a Fischer–Tropsch refinery can therefore be significantly reduced if unsulfided catalysts can be developed that are stable and active in the presence of oxygenates.

Another aspect relevant to the hydroprocessing of Fischer–Tropsch syncrude is demetallisation. In syncrude the metals are present mainly as metal carboxylates that are produced during corrosion and catalyst leaching. These metal carboxylate species can be stable under hydrotreating conditions and are not removed by standard HDM catalysts. The stability of the metal carboxylates depends on both the metal, as well as the chain length of the carboxylate. Removal of the metal carboxylates does not require hydrogenation, since it follows a thermal decomposition pathway.<sup>133</sup> At temperatures below their decomposition temperature the metal carboxylates can cause scaling in preheaters and result in catalyst bed plugging. When the metal carboxylates decompose, the metal oxide that is formed will deposit on the catalyst and may be reactive under hydrotreating conditions. When a sulfiding agent is added to keep the catalyst in a sulfided state, stable sulfides can be formed. The decomposition of iron carboxylates to yield

stable iron sulfides is especially troublesome in Fischer–Tropsch refineries.<sup>128</sup>

## Hydroisomerisation

The process of hydroisomerisation increases the degree of branching of hydrocarbons under hydrogenating conditions. This is achieved by rearrangement of the carbon chain in an analogous way to olefin skeletal isomerisation.

Hydroisomerisation is divided into four categories based on the type of feed material being processed. This classification may initially seem arbitrary, but it is actually based on fundamental catalytic considerations. The categories are:

(a) Hydroisomerisation of *n*-butane to isobutane for use in aliphatic alkylation units.

(b) C<sub>5</sub>–C<sub>6</sub> hydroisomerisation to improve the octane number of light straight run (LSR) naphtha.

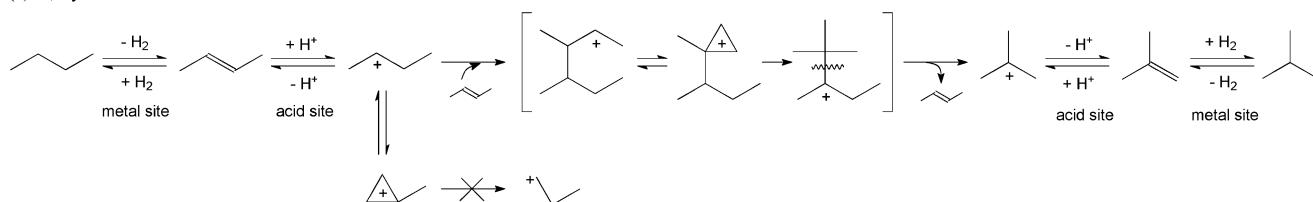
(c) C<sub>7</sub> isomerisation to improve the octane number of this difficult to refine cut, which is poorly converted by catalytic reforming, but not amenable to upgrading by standard C<sub>5</sub>–C<sub>6</sub> hydroisomerisation technology. This type of technology is not yet commercially available, despite research activity in this field.<sup>134</sup>

(d) Hydroisomerisation of waxy paraffins, or catalytic dewaxing, to improve their cold flow properties and optionally to produce lubricating oil. The application depends on the carbon chain length of the feed material.

Hydroisomerisation catalysts are bifunctional, since both metal sites and acid sites are necessary for the reaction to proceed (Fig. 13).

The metal sites are responsible for dehydrogenation of the paraffin to produce an olefin. The olefin can then be skeletally isomerised on the acid site, which is the rate determining step. The metal sites are then again responsible for the hydrogenation of the olefin.<sup>135</sup> The balance between metal and acid sites are important for catalyst performance, since it determines the partial pressure of olefins on the catalyst surface and thereby the probability that acid catalysed side-reactions can take place, such as olefin oligomerisation and cracking.<sup>136</sup> The optimum metal to acid ratio, as well as acid site strength is different for the different classes of hydroisomerisation catalysts and a different isomerisation mechanism may even be operative, like in the case

(a) C<sub>4</sub> Hydroisomerisation



(b) C<sub>5</sub>+ Hydroisomerisation

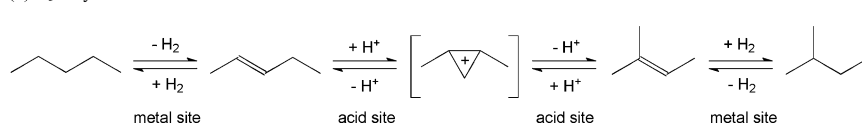


**Fig. 13** Hydroisomerisation mechanism of (a) *n*-butane that proceeds through a bimolecular mechanism to avoid the formation of a primary carbocation, and (b) *n*-pentane and heavier paraffins that can proceed through a monomolecular mechanism.

of butane isomerisation.<sup>137</sup> Butane cannot rearrange without passing through a primary carbocation intermediate, which is very unstable. The same mechanistic limitations as discussed for olefin skeletal isomerisation therefore applies.

The cracking propensity of C<sub>6</sub> and lighter aliphatics is low, because these molecules are too short to easily produce a tertiary carbocation intermediate during cracking.<sup>29</sup> The probability of cracking to produce less stable secondary or primary carbocation intermediates, is correspondingly lower. Once the carbon chain length is C<sub>7</sub> or longer, cracking can readily proceed, since a tertiary carbocation is easily produced during cracking. Hydroisomerisation of waxy paraffins, which by definition have a chain length longer than C<sub>7</sub>, is consequently always accompanied by some losses due to cracking.

There is sufficient variation in hydroisomerisation catalysts and technologies that each has to be considered separately.

**C<sub>4</sub> hydroisomerisation**<sup>138</sup>. The principal technology for *n*-butane isomerisation to isobutane is the chlorinated Pt/Al<sub>2</sub>O<sub>3</sub> catalysed Butamer™ process of UOP. It operates at 180–220 °C, 1.5–2.0 MPa, space velocity of 2 h<sup>-1</sup> and with a hydrogen to hydrocarbon ratio of 0.5–2.0. There are generally two reactors, the first reactor operating at a higher temperature to increase the reaction rate and the second reactor at a lower temperature improve the isobutane equilibrium concentration. The conversion to isobutane is thermodynamically limited and side-product formation is less than 2%. In order to maintain the acidity of the catalyst, constant chlorination is required, which increases the environmental footprint of this technology. It is important to ensure that the feed is water-free. Water can react with the chlorided alumina to produce hydrochloric acid (HCl), which is corrosive and also leads to catalyst deactivation due to loss of strong acidity. The feed should therefore be free of oxygenates that can potentially form water at the reaction conditions.

The potential application of C<sub>4</sub> hydroisomerisation in a Fischer–Tropsch refinery is limited, since it is typically used in conjunction with aliphatic alkylation. It has also already been pointed out that there are more efficient refining pathways for alkylate production than aliphatic alkylation.<sup>50</sup>

**C<sub>5</sub>–C<sub>6</sub> hydroisomerisation**<sup>138,139</sup>. There are three main classes of catalysts that are presently used for C<sub>5</sub>–C<sub>6</sub> paraffin hydroisomerisation, namely chlorinated Pt/Al<sub>2</sub>O<sub>3</sub> (e.g. UOP I-8/I-80, Procatalyse IS 612, Albemarle AT-20), Pt/mordenite

(e.g. Süd-Chemie Hysopar, Procatalyse IS 632, UOP HS-10) and Pt/SO<sub>4</sub><sup>2-</sup>/ZrO<sub>2</sub> (e.g. UOP LPI-100, Süd-Chemie Hysopar-SA).

The chlorinated Pt/Al<sub>2</sub>O<sub>3</sub> catalysts have similar requirements, advantages and drawbacks as those already listed for C<sub>4</sub> hydroisomerisation. The main advantage is the low operating temperature (120–180 °C), which favours the isomerisation equilibrium. The main drawback, apart from the environmental concern related to the use of a chlorinated system, is the sulfur and water sensitivity of the catalyst.<sup>140</sup>

This led to the development of Pt/mordenite zeolite catalysts, which are much more resistant to sulfur and water. The drawback of a Pt/mordenite catalyst is that it requires a higher operating temperature (250–280 °C), which is less favourable in terms of the isomerisation equilibrium. Although sulfur is not a problem in a Fischer–Tropsch environment, oxygenates and water are ever-present, giving Pt/mordenite a competitive feed advantage. This catalyst type is also more environmentally friendly, since it requires no chlorination and has an exceptionally long catalyst lifetime (service life of 10 years).

Sulfated zirconia catalysts have some tolerance to sulfur and water (<35 μg g<sup>-1</sup>)<sup>141</sup> and operate at lower temperature (180–240 °C) than the zeolitic system. A catalyst cycle length of 18 months before regeneration has been reported.

The isomerisation equilibrium advantage that is gained by a catalyst operating at a low temperature, can be offset by recycling the unconverted *n*-paraffins. Various processing options are available to do so.<sup>142</sup>

In most refineries the C<sub>5</sub>–C<sub>6</sub> paraffins are present as a light straight run (LSR) naphtha mixture and the inclusion of C<sub>7</sub> paraffins is generally limited to <2%. During normal operation with a mixed C<sub>5</sub>–C<sub>6</sub> feed, the isomerisation of the *n*-pentane is equilibrium limited, while the isomerisations of the C<sub>6</sub> paraffins are slower and kinetically limited. Of all the C<sub>5</sub>–C<sub>6</sub> compounds in LSR, *n*-hexane has by far the worst octane number (Table 9)<sup>18</sup> and most process configurations aim at maximising the conversion of *n*-hexane.

Benzene is often found in LSR, because it has a very high vapour pressure and is reasonably close in boiling point to *n*-hexane (80 vs 69 °C). The benzene is hydrogenated to cyclohexane over hydroisomerisation catalysts. This is a very exothermic reaction with a large associated adiabatic temperature increase over the catalyst bed. Depending on the nature of the catalyst, the benzene content in the feed is generally limited (<2%). With proper heat management zeolite based catalysts are able to deal with higher benzene levels in the feed. Hydroisomerisation

**Table 9** Research octane number (RON), motor octane number (MON) and Reid vapour pressure (RVP) at 37.8 °C of the C<sub>5</sub>–C<sub>6</sub> paraffins

C#	Compound	RON	MON	RVP/kPa	Δ octane relative to <i>n</i> -paraffin
C <sub>5</sub>	<i>n</i> -Pentane	61.7	62.6	107	—
	2-Methylbutane	92.3	90.3	141	29.2
	2,2-Dimethylpropane	85.5	80.2	253	20.7
	Cyclopentane	101.3	84.9	68	31.0
C <sub>6</sub>	<i>n</i> -Hexane	24.8	26.0	34	—
	2-Methylpentane	73.4	73.5	47	48.1
	3-Methylpentane	74.5	74.3	42	49.0
	2,2-Dimethylbutane	91.8	93.4	68	67.2
	2,3-Dimethylbutane	103.5	94.3	51	73.5
	Cyclohexane	83.0	77.2	23	54.7
	Methylcyclopentane	91.3	80.0	31	60.3



technology may therefore be used to reduce refinery benzene levels, but it should be noted that the octane value of cyclohexane is low (Table 9).

In general, C<sub>5</sub>–C<sub>6</sub> hydroisomerisation technology is clean, efficient and delivers a significant octane improvement. From a fuels blending perspective its only drawback is the high vapour pressure of the isomerised products. There is also a good technology fit with Fischer–Tropsch syncrude due to its high linear hydrocarbon content. However, most straight run C<sub>5</sub>–C<sub>6</sub> hydrocarbons from HTFT and LTFT are olefins, not paraffins. This presents a problem, since it would imply that hydroisomerisation would require olefin hydrogenation as a feed pretreatment step. This thinking is being challenged and it was shown that a Pt/modernite catalyst could be employed for hydroisomerisation of olefinic feed without prior feed hydrogenation.<sup>143</sup> The mechanism (Fig. 13) shows that isomerisation proceeds *via* an olefinic intermediate and it is possible to beneficially use the heat of hydrogenation to preheat the olefinic feed. In this way the inlet temperature to the reactor can be lowered, thereby limiting side-reactions at the top of the catalyst bed where the olefin partial pressure is the highest.

**Catalytic dewaxing**<sup>144</sup>. Long chain paraffin hydrocracking and hydroisomerisation always occur in parallel. Catalysts that are tailored for hydroisomerisation, generally have lower acid strength to promote isomerisation but not cracking. The operating conditions for hydroisomerisation is milder than for hydrocracking, and for Fischer–Tropsch materials dewaxing can typically be performed in the temperature range 280–360 °C and 3–6 MPa pressure. The reaction conditions, feed and catalyst selection can be optimised to maximise lubricating oil production. The sulfur-free nature of LTFT waxes makes them ideal feed materials for unsulfided noble metal catalysed hydroisomerisation, which is similar to that used for hydrocracking.

## Hydrocracking

The shrinking market for residues (boiling point >360 °C) as heavy fuels, more stringent sulfur specifications and high crude oil price, necessitated refiners to convert residues into products in the distillate and naphtha boiling ranges. One way of accomplishing this is by hydrocracking. The aim of hydrocracking is threefold:

- It cracks the heavy material to lighter boiling material.
- It removes heteroatoms (S, N, O) by both hydrotreating and hydrocracking.

(c) It reduces the aromatic content, especially polynuclear aromatic content, to meet final product specifications.

The conversion of residue material into lighter boiling fractions requires C–C bond scission, which in turn requires high temperatures, even in the presence of a catalyst. In order to convert the residue at lower temperatures than required for acid catalysed paraffin cracking, hydrocracking employs bifunctional catalysts. These bifunctional catalysts have both metal and acid sites. As mentioned during the discussion of hydroisomerisation, the performance of bifunctional catalysts is determined by the balance between the metal sites and the acid sites.<sup>136</sup> The mechanism of hydrocracking follows the same basic steps as outlined for hydroisomerisation in Fig. 13, but rather than hydrogenating the branched olefin directly, the branched olefin is cracked by  $\beta$ -scission, before it is hydrogenated (Fig. 14).<sup>145</sup> Cracking by  $\beta$ -scission of the olefin is not the only mechanism that is operative, but it is the dominant mechanism during hydrocracking. Cracking *via* a pentacoordinated carbocation is an important mechanistic route too, but cracking of a carbocation that is formed by olefin protonation is much faster and therefore dominant during hydrocracking.

It can be expected that the metal to acid site ratio of hydrocracking catalysts will typically be less than that of hydroisomerisation catalysts and that the acid sites will be stronger. The metal sites on hydrocracking catalysts are also responsible for heteroatom removal by HDS, HDO and HDN. The metal sites are similarly responsible for the hydrogenation of coke precursors, such as aromatics that are thermodynamically favoured at high temperatures.

The conditions necessary for hydrocracking is determined by the feed quality and catalyst type, but in general hydrocrackers are operated in the range 360–440 °C, 7–15 MPa and with a space velocity of around 0.3–2.0 h<sup>-1</sup>.<sup>146</sup> Hydrogen is co-fed in a ratio of 800–1800 normal m<sup>3</sup> h<sup>-1</sup> per 1 m<sup>3</sup> h<sup>-1</sup> of liquid feed.

Two classes of hydrocracking catalysts can be found, namely sulfided base-metal catalysts and unsulfided noble metal catalysts. Sulfided hydrocracking catalysts usually consist of NiMo or NiW (CoMo is less often employed) on an acidic amorphous silica-alumina (ASA) or zeolitic support. Sulfur acts as a poison for noble metal catalysts, but with proper feed pretreatment (that is not necessary for Fischer–Tropsch syncrude), unsulfided noble metal hydrocracking catalysts using Pd or Pt on ASA or zeolitic supports can be used. These catalysts are well-suited for wax hydrocracking.

Hydrocracking of LTFT waxes is unique in that the feed is sulfur-free and consists of mainly linear paraffins, with small

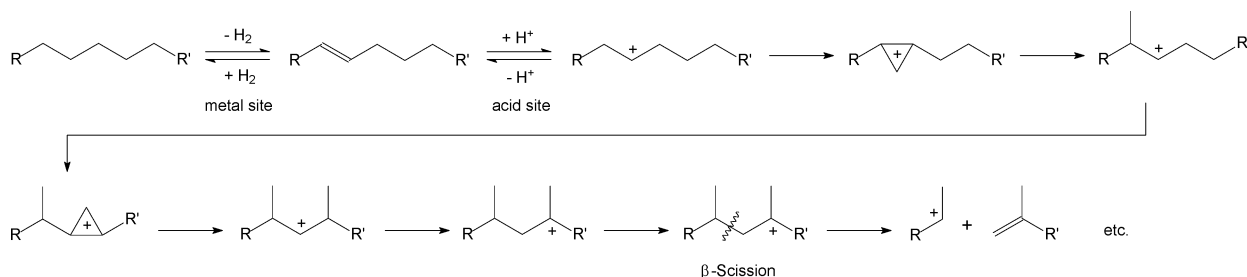


**Fig. 14** Reaction sequence of hydrocracking. The paraffin is dehydrogenated on a metal site and the olefin thus formed is then protonated on an acid site. Skeletal isomerisation generally precedes cracking by  $\beta$ -scission. The reaction sequence is terminated by deprotonation and hydrogenation.

amounts of olefins and oxygenates. Unsulfided base metal hydrocracking catalysts seem to be ideal for this application, but both Ni-based and Co-based hydrocracking catalysts display high methane selectivity.<sup>147</sup> In contrast, unsulfided noble metal catalysts seem to work very well, not only on small scale,<sup>148</sup> but also on commercial scale, as used in the Shell Middle Distillate Synthesis (SMDS) process in Bintulu, Malaysia.<sup>149</sup> The hydrocracking of LTFT waxes is much more facile than crude derived residues and lower temperatures (300–370 °C) and lower pressures (3–7 MPa) can be used.<sup>148,149,150</sup> It is consequently somewhat surprising that the Oryx gas-to-liquids facility does not employ an unsulfided noble metal hydrocracking catalyst. Chevron's Isocracking™ technology has been selected,<sup>151</sup> which employs a sulfided base metal hydrocracking catalyst operating at medium pressure. Since the wax is sulfur-free, the process requires sulfur addition to the LTFT feed to maintain the catalyst in its active state.

The oxygenates that are present in Fischer–Tropsch products adsorb strongly on hydrocracking catalysts to cause some inhibition, but this can be beneficially used as selectivity modifier.<sup>152</sup>

Hydrocracking of HTFT residue is fundamentally different to hydrocracking of LTFT wax and it resembles crude oil hydrocracking. The HTFT residue fraction contains more than 25% aromatics, although its polynuclear aromatic content is low (<1%). The same principles employed for the hydrocracking of crude oil residues can be applied to HTFT residue, but less severe operating conditions are required on account of the low sulfur and nitrogen content of HTFT residue.

The heavy fraction from both HTFT and LTFT synthesis contains some metals as metal carboxylates. It has already been pointed out that HDM catalysts are ineffective for metal carboxylate removal.<sup>128</sup> There is consequently scope for the application of different reactor technologies to overcome the problems associated with metals deposition in fixed bed reactors.

In general it can be said that hydrocracking has a good fit with Fischer–Tropsch product refining and especially with LTFT wax refining. Although it is a fairly energy intensive processing step, unsulfided hydrocracking is otherwise an environmentally friendly technology.

### Catalytic cracking

Catalytic cracking was originally commercialised as a fixed bed process, but was soon thereafter replaced by fluid catalytic cracking (FCC). Fluid catalytic cracking is used for the conversion of heavy residues to lighter material that is more hydrogen rich in comparison to the feed. It is often the main source of short chain olefins in a crude oil refinery and its operation is usually focused on the production of motor-gasoline. In larger refineries that are close to petrochemical producers, additional revenue can be generated by selling the propylene produced during FCC as a chemical feedstock. Refinery propylene, mainly derived from FCC, presently supplies 25% of the European propylene market, 50% of the North American market and 20% of the Asian market.<sup>153</sup>

HTFT residue can in principle be upgraded by standard FCC technology, but it constitutes only 5% of the total syncrude and it is unlikely to be economically justifiable. On the other hand,

about half of LTFT syncrude is residue material (wax) and FCC is of interest as upgrading technology.

The catalytic cracking of Fischer–Tropsch wax has been investigated by a number of groups.<sup>154</sup> Of specific interest is that an economic comparison of FCC and hydrocracking for the upgrading of Fischer–Tropsch wax, indicated that a Fischer–Tropsch refinery based on FCC, with its more olefinic product slate, is more economical than one based on hydrocracking.<sup>155</sup> This is contrary to the perception that has been created by the exclusive use of hydrocracking technology for the upgrading of wax in LTFT based gas-to-liquids facilities.<sup>13,149,151</sup> Yet, it is understandable, since these facilities do not produce transportation fuels like in a normal fuels refinery, but naphtha and a high cetane number distillate blending stock.

Catalytic cracking is a high temperature acid catalysed process. Most FCC catalysts are based on Y zeolite (10–50%) mixed with a diluent, such as kaolin, to reduce the catalyst cost. The zeolite and diluent are contained in a matrix or binder made from silica, alumina or silica-alumina. The catalyst may additionally contain additives, such as pseudoboehmite to increase cracking activity. During FCC operation various other catalysts (catalyst additives) may be added to the catalyst mixture to customise it for the specific feed or adjust the product slate.<sup>156</sup> The additives are not necessarily incorporated into the catalyst, but are co-fed with the catalyst. Some of these additives are combustion promoters (Pt or Pd salts), SO<sub>x</sub> transfer agents (basic metallic oxides), metal traps and octane improvers (H-ZSM-5 zeolite).

Catalytic cracking is similar to hydrocracking in that it uses acid catalysed cracking by β-scission to break C–C bonds and reduce the molecular weight of the product. The ease of cracking increases with the degree of branching,<sup>29</sup> which is introduced by skeletal isomerisation of the carbocation, as shown in Fig. 14. In addition to the β-scission mechanism, cracking can also take place by protolysis, or α-scission (Fig. 15).

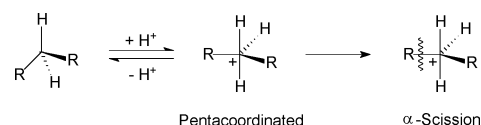


**Fig. 15** Cracking by protolysis involving the direct protonation of a paraffin to form a pentacoordinated carbocation that cracks by α-scission.

Protonation of a paraffin will yield a pentacoordinated carbon that can crack by α-scission to yield products different from β-scission, including products that would otherwise require a primary carbocation intermediate to form *via* β-scission. The contribution of protolysis is determined by the availability of other carbocation creating pathways and is especially important during initial conversion, before a carbocation covered catalyst surface is created.<sup>157</sup>

Another important process during catalytic cracking is hydrogen transfer. During hydrogen transfer one molecule is dehydrogenated, while the other molecule is hydrogenated. Acid catalysts in general have poor hydrogen desorbing capability and in instances when molecular hydrogen (H<sub>2</sub>) is detected in FCC products, thermal cracking cannot be ruled out.<sup>157</sup> Hydrogen transfer does not involve C–C bond scission, but affects the product selectivity to paraffins, olefins and aromatics. This

process drives carbon rejection during catalytic cracking, since heavy aromatics (coke) are formed on the catalyst surface, while the lighter cracked products are hydrogen enriched. This is also the primary catalyst deactivation mechanism<sup>158</sup> and the reason why FCC technology includes continuous catalyst regeneration (CCR).

FCC is performed at high temperature (480–550 °C), low pressure (0.1–0.3 MPa) and short contact time (<10 s). The yield structure is influenced by the operating conditions, as well as the nature of the feed. The reactivity of the different hydrocarbon classes during catalytic cracking are as follows:<sup>156</sup> polynaphthenes ≈ mononuclear aromatics > mononaphthenes > branched paraffins > *n*-paraffins > dinuclear aromatics.

Although it has been shown that LTFT wax is a good feed material for FCC,<sup>154</sup> the reason for using FCC to upgrade wax has to be different to that of residue upgrading in a crude oil refinery. FCC can in principle be considered for the production of chemicals,<sup>159</sup> or when LTFT syncrude has to be converted into motor-gasoline, but one has to question the rationale for using a carbon rejection technology with a hydrogen-rich feed material. Furthermore, the high hydrogen content of LTFT material is not conducive to coke formation and additional fuel will have to be burned in the catalyst regenerator to make the FCC heat balance work. This goes against the green chemistry principles of atom economy, prevention of waste and energy efficiency.

On a fundamental level FCC has a poor technology fit with Fischer–Tropsch feed. Nevertheless, the use of FCC technology may still be required by specific refinery configurations and the future application of FCC with Fischer–Tropsch feed cannot be ruled out.

### Coking

Coking is used to convert heavy residues to coke and lighter fuel products. The coke has a high carbon to hydrogen ratio, making it suitable for metallurgical applications, but it may also be used for heating. It can therefore be seen as an extreme carbon rejection technology, because about 30% of the feed mass is rejected as coke<sup>160</sup> (in FCC it is only about 4%). Since the coke is effectively the rejected carbon and contains most of the sulfur and metals, the lighter products are comparatively hydrogen enriched and partially desulfurised, making them more amenable to conventional refining to transportation fuels. Contrary to what the name suggests, the aim of coking in a refinery is not to produce coke, but to produce hydrogen enriched distillates. The lighter products are rich in olefins, which makes coking also a source of olefins for motor-gasoline production.

Coking is a non-catalytic thermal process that relies on homolytic bond scission to form radicals for the reaction to proceed. The likelihood of bond rupture at a given temperature is determined by the bond dissociation energy, which is in the range of 320–375 kJ mol<sup>-1</sup> for most of the aliphatic C–C bonds (Table 10).<sup>161</sup> Some oxygenates have even lower bond dissociation energies. As the thermal decomposition proceeds, radicals can recombine to produce more stable products that are not thermally decomposed at the same temperature, such as aromatics and light hydrocarbon gases. In this way the light fraction is hydrogen enriched, while the aromatics poly-condense and are hydrogen depleted to form coke.

**Table 10** Homolytic bond dissociation energy (BDE) of hydrocarbon C–H and C–C bonds at 25 °C

Bond dissociation reaction	BDE/kJ mol <sup>-1</sup>
<i>C–H bonds in paraffins</i>	
CH <sub>4</sub> → ·CH <sub>3</sub> + H·	439
C <sub>2</sub> H <sub>6</sub> → ·CH <sub>2</sub> CH <sub>3</sub> + H·	423
C <sub>3</sub> H <sub>8</sub> → ·CH(CH <sub>3</sub> ) <sub>2</sub> + H·	413
<i>tert</i> -C <sub>4</sub> H <sub>10</sub> → ·C(CH <sub>3</sub> ) <sub>3</sub> + H·	404
<i>C–C bonds in paraffins</i>	
C <sub>2</sub> H <sub>6</sub> → ·CH <sub>3</sub> + ·CH <sub>3</sub>	377
C <sub>3</sub> H <sub>8</sub> → ·CH <sub>2</sub> CH <sub>3</sub> + ·CH <sub>3</sub>	372
C <sub>4</sub> H <sub>10</sub> → ·CH <sub>2</sub> CH <sub>3</sub> + ·CH <sub>2</sub> CH <sub>3</sub>	368
<i>tert</i> -C <sub>4</sub> H <sub>10</sub> → ·CH(CH <sub>3</sub> ) <sub>2</sub> + ·CH <sub>3</sub>	371
<i>C–H bonds in olefins</i>	
CH <sub>2</sub> =CH <sub>2</sub> → ·CH=CH <sub>2</sub> + H·	463
CH <sub>3</sub> CH=CH <sub>2</sub> → ·CH <sub>2</sub> CH=CH <sub>2</sub> + H·	372
<i>C–C bonds in olefins</i>	
CH <sub>3</sub> CH=CH <sub>2</sub> → ·CH=CH <sub>2</sub> + ·CH <sub>3</sub>	424
C <sub>2</sub> H <sub>5</sub> CH=CH <sub>2</sub> → ·CH=CH <sub>2</sub> + ·CH <sub>2</sub> CH <sub>3</sub>	418
(CH <sub>3</sub> ) <sub>2</sub> CHCH=CH <sub>2</sub> → ·CH=CH <sub>2</sub> + ·CH(CH <sub>3</sub> ) <sub>2</sub>	415
C <sub>2</sub> H <sub>5</sub> CH=CH <sub>2</sub> → ·CH <sub>2</sub> CH=CH <sub>2</sub> + ·CH <sub>3</sub>	320 <sup>1</sup>
<i>C–H bonds in aromatics</i>	
C <sub>6</sub> H <sub>6</sub> (benzene) → ·C <sub>6</sub> H <sub>5</sub> + H·	472
C <sub>6</sub> H <sub>5</sub> CH <sub>3</sub> (toluene) → ·CH <sub>2</sub> C <sub>6</sub> H <sub>5</sub> + H·	375
<i>C–C bonds in aromatics</i>	
C <sub>6</sub> H <sub>5</sub> CH <sub>3</sub> (toluene) → ·C <sub>6</sub> H <sub>5</sub> + ·CH <sub>3</sub>	433
C <sub>6</sub> H <sub>5</sub> CH <sub>2</sub> CH <sub>3</sub> (ethylbenzene) → ·CH <sub>2</sub> C <sub>6</sub> H <sub>5</sub> + ·CH <sub>3</sub>	325

<sup>1</sup>The allyl radical (·CH<sub>2</sub>CH=CH<sub>2</sub>) is resonance stabilised.

An operating temperature of 485–505 °C is typically used in cokers, which is well above the temperature that is needed to initiate thermal bond scission in Fischer–Tropsch derived feed materials. The feed composition determines the coke yield and feed materials with a high Conradson carbon residue (ASTM D189) produces more coke.

There are mainly two types of coking, namely delayed coking and flexicoking. In delayed coking the process is operated batchwise, with coke being produced as by-product. The feed is heated to cracking temperatures in a furnace and then allowed to soak in drums to complete the thermal conversion of the feed. In flexicoking the process is continuous, with almost complete conversion of the feed into gaseous and liquid products. The coking is performed in a fluidised bed, with the coke being fed to a gasifier to produce a low heating value gas.<sup>160</sup>

Coking is energy intensive, which is its main drawback from an environmental point of view.

Fischer–Tropsch materials are hydrogen rich and therefore have a low Conradson carbon content. This makes Fischer–Tropsch syncrude a poor feed for coking. On a fundamental level coking makes no sense in Fischer–Tropsch context, since it is a carbon rejection technology. However, when co-refining products such as crude oil or coal tar, coking may be considered.

### Thermal cracking

Historically thermal cracking processes were classified as gas-phase or mixed-phase. Gas-phase processes typically operated at temperatures around 620 °C and at low pressure, while mixed-phase processes operated in the temperature range 450–540 °C.<sup>19</sup> Steam cracking (gas-phase) is generally associated with the petrochemical industry for the production of ethylene, as well as for the production of products such as propylene and

butadiene.<sup>162</sup> In fuels refineries a less severe form of thermal cracking is found, namely visbreaking (mixed-phase). The term “visbreaking” is derived from “viscosity breaking”, since this form of thermal cracking had previously been used to reduce the viscosity of fuel oils.<sup>163</sup>

Thermal cracking has also been used in some of the German Fischer–Tropsch plants<sup>19,164</sup> and has since then found its way into other Fischer–Tropsch refinery strategies. In this respect it is presently considered as upgrading pathway for LTFT naphtha, with specific feed benefits being claimed for the cracking of such naphtha.<sup>165</sup> Cracking of LTFT waxes has been investigated as way to produce fuels,<sup>166</sup> candle wax<sup>167</sup> and lubricating oils.<sup>164,168</sup>

The process is non-catalytic and follows a radical mechanism (Fig. 16), with propagation steps that may involve reactions such as intermolecular radical transfer, intramolecular decomposition and thermal dimerisation. Intramolecular isomerisation is also possible, as shown in Fig. 5, although this type of isomerisation is limited to isomerisation of the radical position by 1–4 and 1–5 hydrogen transfer, which does not affect the skeletal structure.<sup>86</sup>

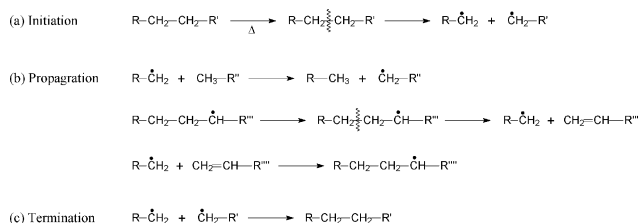


**Fig. 16** Thermal cracking follows a radical mechanism. Propagation may take place by hydrogen atom abstraction (radical transfer), intramolecular cracking to produce an  $\alpha$ -olefin and radical addition to an olefin (thermal oligomerisation).

The cracking mechanism is the same as for coking, but with the difference that recombination reactions leading to hydrogen ( $\text{H}_2$ ) rejection in order to form aromatic molecules (coke precursors) are generally limited. Aromatic compounds can in principle be formed,<sup>169</sup> but thermal cracking processes are operated in such a way that the residence time is limited to avoid excessive formation of coke. By doing so, aromatics are not allowed to poly-condense and thermal cracking effectively becomes a hydrogen rejection technology.

At cracking temperatures in the range 420–500 °C it was found that the product distribution from the thermal cracking of Fischer–Tropsch waxes can be adequately described by the Rice–Kossiakoff<sup>170</sup> cracking mechanism and Voge–Good<sup>171</sup> approximation for the chain length dependence of the thermal cracking rate.<sup>167</sup>

Oxygenates are readily thermally cracked and cracking may either be initiated by hydrocarbon decomposition, or direct homolytic bond dissociation of the oxygenate. It should be noted that there are significant differences between the bond dissociation energies of oxygenates and oxygenate radicals. For example, it requires 349 kJ mol<sup>-1</sup> to convert butanone into an acetyl and ethyl radical,<sup>161</sup> but only 40 kJ mol<sup>-1</sup> to liberate CO from the acetyl radical.<sup>172</sup> These differences in bond dissociation energy become very important when thermally cracking oxygenate rich HTFT material.

Apart from the energy intensive nature of thermal cracking, it is a clean technology. In comparison to hydrocracking, it is less efficient for fuels refining, but has been shown to have some advantages over hydrocracking when it comes to chemicals refining. The <370 °C boiling fraction from thermal cracking of LTFT hard wax has a high linear  $\alpha$ -olefin content (about 40%) and that the medium wax fraction co-produced can find application as candle wax.<sup>167</sup>

### Catalytic reforming

Initially catalytic reforming was developed to upgrade low octane naphtha to a high octane product that is rich in aromatic compounds.<sup>173</sup> The hydrogen that is co-produced during this process has since become equally important,<sup>174</sup> due to the increasing pressure on refineries to increase their hydroconversion severity.<sup>175</sup>

Two types of catalytic reforming are distinguished which have markedly different response to the nature of the feed, namely platinum promoted chlorided alumina (Pt/Cl/Al<sub>2</sub>O<sub>3</sub>) and non-acidic platinum promoted L-zeolite (Pt/L-zeolite). The former is bifunctional, containing acid and metal sites, while the latter is monofunctional, containing only metal sites.

The reaction network is quite complex and is discussed in detail in literature.<sup>176</sup> Multiple reaction pathways are possible and the main reaction classes found during catalytic reforming are:

(a) Dehydrogenation–hydrogenation, which is the addition or removal of hydrogen by metal sites.

(b) Hydroisomerisation, which results in a rearrangement of the skeletal structure, as shown in Fig. 13, and requires both metal and acid sites.

(c) Aromatisation, which may involve dehydrogenation of a cycloparaffin or dehydrocyclisation whereby a ring-structure is created during dehydrogenation. Both processes occur on metal sites.

(d) Cracking, hydrocracking and hydrogenolysis, which are various ways of reducing the carbon chain length of the product by either acid or metal sites. These are undesirable side-reactions during catalytic reforming.

The rate limiting step in catalytic reforming is alkane activation,<sup>177</sup> which is an endothermic process and one of the reasons why catalytic reforming is performed at high temperature. Another reason for employing high temperature is that aromatics formation is thermodynamically favoured. By increasing the temperature (severity of operation) the octane number of the final product can be increased and catalytic reformers are typically operated in such a way that the product (reformate) is of sufficiently high octane number to meet octane demand in the refinery.

**Pt/Cl/Al<sub>2</sub>O<sub>3</sub> reforming.** Almost all the catalytic reformers found in crude oil refineries use Pt/Cl/Al<sub>2</sub>O<sub>3</sub> based bifunctional catalysts. The first platinum based reforming process to be used for refining was the UOP Platforming<sup>TM</sup> process that came on stream in 1949.<sup>178</sup> The platinum is often stabilised by the addition of a second metal, which in most cases is rhenium, tin or iridium. The support material is acidified by the addition of chloro-alkanes (such as CCl<sub>4</sub> or C<sub>2</sub>Cl<sub>4</sub>), which also helps to retard platinum agglomeration and aids platinum re-dispersion



during regeneration.<sup>174</sup> The acidity of the support is necessary to catalyse isomerisation reactions, such as the conversion of alkylcyclopentanes to cyclohexane species that is a prerequisite for aromatisation. This requires the feed to be free of water and oxygenates (refer to the hydroisomerisation discussion). As with all noble metal catalysts, the catalyst is also sensitive to sulfur poisoning and the feed should preferably contain no sulfur.

Typical operating ranges are 490–525 °C and 1.4–3.5 MPa for semi-regenerative (SR) reforming and 525–540 °C and 0.3–1.0 MPa for reformers with continuous catalyst regeneration (CCR).<sup>173,174,179</sup>

The feed plays an important role in determining the severity of operation that is necessary to achieve the desired reformate octane number. Naphthenes (cyclo-paraffins) react much faster than acyclic paraffins, since it requires less reaction steps to form a 6-membered ring structure that can directly be dehydrogenated to produce an aromatic. Feed materials containing a high concentration of naphthenes are called rich naphthas. The richness of a naphtha is often expressed by the number  $N + 2A$ , where  $N$  refers to the percentage naphthenes in the feed and  $A$  refers to the percentage aromatics in the feed. Rich naphthas require less severe conditions than lean naphthas to obtain the same reformate octane number.

The carbon chain length of the paraffins in the feed also has an impact, with paraffin reactivity for catalytic reforming by Pt/Cl<sup>-</sup>/Al<sub>2</sub>O<sub>3</sub> catalysts increasing in the order C<sub>6</sub> < C<sub>7</sub> << C<sub>8</sub> ≈ C<sub>9</sub> and heavier. In general C<sub>6</sub>–C<sub>7</sub> compounds are not considered desirable feed due to their low reactivity and in the case of C<sub>6</sub> its high benzene selectivity. It can therefore be said that the aromatics yield over Pt/Cl<sup>-</sup>/Al<sub>2</sub>O<sub>3</sub> reforming catalysts is mainly determined by the operating temperature,  $N + 2A$  number and the average carbon chain length of the hydrocarbons in the feed.

Straight run Fischer–Tropsch naphtha contains oxygenates and olefins. It is consequently necessary to hydrotreat the naphtha before it can be employed as reformer feed, despite the naphtha being sulfur-free. LTFT naphtha contains no aromatics (Table 2) and little naphthenes, and even HTFT naphtha, which contains some aromatics and naphthenes, has an  $N + 2A$  number of less than 30. This makes Fischer–Tropsch naphtha especially poor feed for Pt/Cl<sup>-</sup>/Al<sub>2</sub>O<sub>3</sub> reforming. The conversion of synthetic naphtha therefore results in much higher gas-make and lower aromatics yield when compared to crude derived feed at similar conversion.<sup>173</sup> This can only partially be compensated for by the severity of reforming, since coke formation and gas-make increases rapidly with an increase in temperature. For example, it has been reported that reforming of HTFT naphtha with an end point of 180 °C results in a liquid yield of only 70–75% at a research octane number of around 80.<sup>180</sup>

Catalytic reforming over Pt/Cl<sup>-</sup>/Al<sub>2</sub>O<sub>3</sub> clearly has a poor technology fit with Fischer–Tropsch syncrude. Furthermore, despite it being a key refining technology, it is not an environmentally friendly technology. It is energy intensive and requires the continuous addition of chloro-alkanes to keep the catalyst active. Although it is employed industrially with Fischer–Tropsch feed materials, it should not in future be the reforming technology of choice.

**Pt/L-zeolite reforming.** Catalytic reforming over non-acidic, monofunctional Pt/L-zeolite catalysts were developed

much later<sup>181</sup> than catalytic reforming over acidic bifunctional Pt/Cl<sup>-</sup>/Al<sub>2</sub>O<sub>3</sub> catalysts. Technologies based on Pt/L-zeolite catalysts, such as Aromax™ (Chevron Phillips Chemical company)<sup>182</sup> and RZ-Platforming™ (UOP),<sup>183</sup> are mainly employed for chemicals production on account of their very high aromatics selectivity with C<sub>6</sub>–C<sub>8</sub> naphtha and especially with C<sub>6</sub>–C<sub>7</sub> linear paraffinic feed. Non-acidic reforming catalysts are consequently very active for the conversion of light naphtha fractions, for which Pt/Cl<sup>-</sup>/Al<sub>2</sub>O<sub>3</sub> catalysts show poor activity.

Pt/L-zeolite reforming catalysts have no acidity and any residual acidity in the L-zeolite structure is typically removed by ion exchange with potassium and/or barium. The absence of acidity eliminates acid catalysed side-reactions and the mechanism is dependent on metal sites only. The very high (around 90%) aromatics selectivity of *n*-paraffin conversion over L-zeolite is ascribed to the shape selectivity of the zeolite structure, which ensures end-on attachment of the molecule.<sup>184</sup> End-on attachment is a prerequisite for 1,6-ring closure to selectively produce benzene from *n*-hexane (Fig. 17).

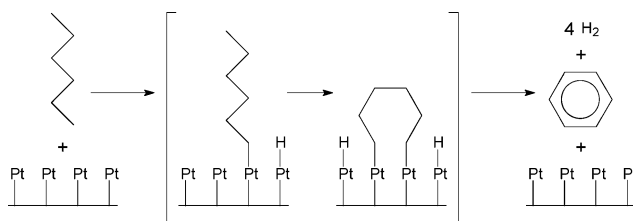


Fig. 17 Aromatisation of *n*-hexane to benzene over non-acidic Pt/L-zeolite catalyst by selective end-on attachment and 1,6-ring closure.

The operating conditions of Pt/L-reforming is similar to that of reforming over Pt/Cl<sup>-</sup>/Al<sub>2</sub>O<sub>3</sub>, but it requires no chloro-alkane addition. The main drawback of non-acidic Pt/L-zeolite catalysts, however, are their extreme sensitivity to sulfur poisoning.<sup>185</sup> This requires additional precautions to remove sulfur in the feed to levels below 0.05 μg g<sup>-1</sup>.

Sulfur removal presents no difficulty when this technology is employed with Fischer–Tropsch derived feed, since it is already sulfur-free. The effect of oxygenates on a Pt/L-zeolite has been studied and it was found that oxygenates and CO suppressed conversion, while water had no effect.<sup>186</sup> This indicated that Fischer–Tropsch feeds, even containing some oxygenates, are good feed materials for Pt/L-zeolite reforming. Fischer–Tropsch naphtha is also rich in linear hydrocarbons, and very high aromatics selectivities can be expected. This has indeed been demonstrated, with a hydrotreated HTFT naphtha yielding better than predicted hydrogen and aromatics yields during piloting with the Aromax™ technology. The suitability of this technology to refine Fischer–Tropsch products has also been voiced for quite some time by one of the key figures in the development of Fischer–Tropsch technology.<sup>187</sup>

From the discussion it should be clear that non-acidic Pt/L-zeolite based reforming is the preferred technology for converting Fischer–Tropsch naphtha into aromatics.

### Aromatisation

The aromatisation of light hydrocarbons (C<sub>3</sub>–C<sub>5</sub>) is related to reforming, but such units are generally not associated with

fuels refineries. The aim of this type of aromatisation is to convert normally gaseous paraffins, mainly liquid petroleum gas (LPG) range  $C_3$ – $C_4$ , to aromatic-rich liquid hydrocarbons. Like in the case of catalytic reforming, an added advantage is the co-production of hydrogen.

It has been shown that light paraffins can be activated and aromatised on H-ZSM-5, without the rapid deactivation being seen on many other acidic zeolites. ZSM-5 not only has a lower coking tendency, but it also has a much larger coke capacity than some of the less coking zeolites. More coke lay down is therefore required before complete deactivation occurs.<sup>188</sup>

Processes like the M2 Forming process of Mobil, employed H-ZSM-5 as catalyst for aromatisation.<sup>189</sup> This intrinsically limits the aromatics yield, since hydrogen rejection has to occur by hydrogen transfer to olefins, rather than by desorption of molecular hydrogen.<sup>190</sup> When a metal is added to the H-ZSM-5 to produce a bifunctional catalyst, the hydrogen can be desorbed as  $H_2$  and the aromatics yield is substantially increased.<sup>191</sup> The role of the different catalyst sites in the aromatisation mechanism is shown in Fig. 18.

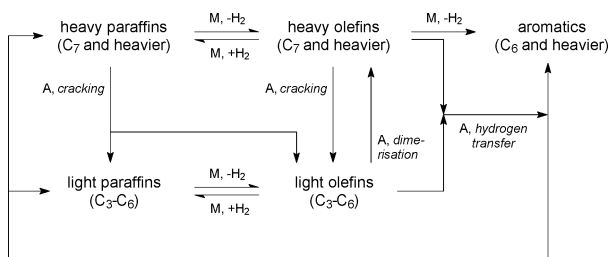


**Fig. 18** Reaction network during aromatisation on a bifunctional metal promoted acidic zeolite catalyst, such as Zn/H-ZSM-5. (A, denotes an acid site and M denotes a metal site).

All modern aromatisation processes make use of metal promoted catalysts and are either based on Zn/H-ZSM-5 (for example the Alpha process of Asahi) or Ga/H-ZSM-5 (for example the Cyclar process of BP).

Operating conditions are typically in the range 450–520 °C and less than 1 MPa pressure.

Aromatisation processes are also characterised by periodic operation. Each production cycle (in the order of 2 days), is followed by a regeneration cycle during which the coke on the catalyst is removed by controlled coke burn-off. During coke burn-off, some water is generated that causes hydrothermal dealumination of the zeolite and eventually results in catalyst deactivation.<sup>192</sup> Numerous reaction–regeneration cycles are nevertheless possible, albeit being dependent on the water partial pressure and exposure time to water vapour during regeneration.<sup>193</sup> Water vapour that is produced during coke-combustion is unavoidable, but the water partial pressure is in practice controlled by the water content of the nitrogen recycle gas used to dilute the air used for coke combustion. It is impractical to remove all the water vapour from this high temperature gas stream. In this respect aromatisation within a Fischer–Tropsch refinery has an advantage, since it is practical to make use of fresh nitrogen on a once-through basis. The air separation units associated with synthesis gas production for Fischer–Tropsch synthesis, also produces nitrogen as by-product. It is consequently not necessary to recycle nitro-

gen, since nitrogen is available as fatal by-product from air separation.

From the reaction network (Fig. 18) it can be seen that any hydrocarbon feed material can in principle be used. It is generally not economical to use a  $C_5$  and heavier liquid hydrocarbon feed. Metal promoted ZSM-5 aromatisation processes have a liquid yield of around 60–70%, which implies a significant loss of liquid volume when the feed material is a liquid hydrocarbon stream.

The use of aromatisation for the upgrading of light Fischer–Tropsch fractions has been previously suggested<sup>3</sup> and the upgrading of HTFT naphtha has also been investigated. In the latter application it was found that the oxygenates present in HTFT naphtha is detrimental to the catalyst lifetime, causing not only hydrothermal dealumination, but also selective loss of the metal from the catalyst.<sup>194</sup>

The environmental footprint of LPG aromatisation is determined mainly by the high operating temperature and frequent catalyst regeneration. Future use within a Fischer–Tropsch refinery will primarily depend on the availability of light paraffins, which may be produced as a by-product from processes such as hydrocracking.

### Alcohol dehydration and olefin hydration

Aliphatic alcohols are primary Fischer–Tropsch products and alcohol dehydration is an unconventional conversion technology that is relevant to Fischer–Tropsch refining. By dehydrating the alcohols to olefins, refining can be simplified. This is especially beneficial in reducing the complexity of Fischer–Tropsch aqueous product refining.<sup>195</sup> By converting the alcohols into olefins, the separation of alcohol–water azeotropes can be avoided. The olefins are easily separated from the water and the olefins can then be co-processed with the rest of the Fischer–Tropsch olefins.

Another application of alcohol dehydration that is becoming important is the partial dehydration of alcohols to ethers, which are employed as high cetane additives for diesel fuel.<sup>49,196</sup> Ether formation is accompanied by an increase in chain length of the product and this is also a convenient way to shift naphtha range alcohols into distillate range ethers.

It should be noted that the reverse reaction, namely olefin hydration, may also be relevant in a Fischer–Tropsch context. Ethylene hydration to ethanol is a useful way to convert ethylene into a transportable product when the Fischer–Tropsch refinery is not close to a petrochemical market. The ethanol itself can also be added to the fuel.

Dehydration is an acid catalysed endothermic reaction. During alcohol dehydration, hydrogen is rejected in the form of water, thereby converting the alcohols into olefins. There are two mechanistic pathways (Fig. 19). The first pathway is a direct monomolecular dehydration of the alcohol to an olefin. The second pathway is a bimolecular dehydration to the ether, which may then be followed by monomolecular dehydration to produce an olefin.<sup>197</sup> Methanol, because it contains only a single carbon atom, can only dehydrate to the ether and not directly to an olefin.

Strictly speaking the dehydration reaction is reversible, but the equilibrium favours dehydration. For example, ethanol

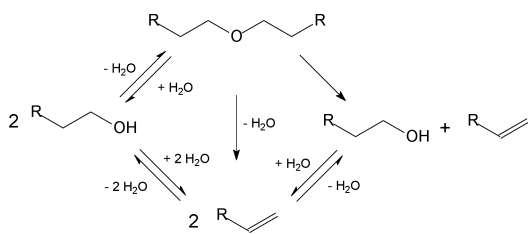


**Fig. 19** Alcohol dehydration by indirect bimolecular dehydration to an ether and direct monomolecular dehydration to an olefin.

dehydration to diethyl ether and ethylene are the least favourable of the dehydration reactions, but at 300 °C equilibrium constants are 3.9 and 320 respectively.<sup>198</sup> The water that is produced during the reaction therefore has little impact on the equilibrium conversion.

**Alcohol dehydration.** Since alcohol dehydration produces water in an equimolar ratio to the olefin being produced, the catalysts that can be considered for alcohol dehydration should be water-tolerant.<sup>199</sup> Industrially, the catalyst that is most often employed for alcohol dehydration is alumina.<sup>200</sup> Alumina is stable in the presence of large amounts of water at the operating conditions required for dehydration.

Operating conditions are usually in the range 300–400 °C and near atmospheric pressure. The dehydration temperature depends on the feed. The conversion of ethanol to ethylene requires a higher temperature than is required for any of the heavier alcohols. It is also far easier to dehydrate branched alcohols than linear alcohols. The operating temperature can be lowered by using a more acidic catalyst, but side-reactions, such as olefin oligomerisation, may then become a problem.

During industrial operation, water is typically co-fed with the alcohols to reduce the adiabatic temperature decrease. Co-feeding water has the additional benefit of diluting the surface concentration of the alcohol and olefinic products.<sup>201</sup> This type of operation has been practised on industrial scale with mixed HTFT alcohols. It is a clean conversion, albeit being energy intensive.

Dehydration of alcohols to ethers is performed at lower temperatures (<300 °C) and higher pressures. When operating at very low temperature (<130 °C) high ether selectivity can be obtained, with acidic resins being the preferred catalysts in this type of application. This is a clean conversion and it is more environmentally friendly than complete dehydration from an energy usage perspective.

It is also possible to convert alcohols in the presence of other Fischer–Tropsch oxygenates. It has been reported that the dehydration of alcohols on  $\eta$ -alumina was not affected by the presence of carbonyls and carboxylic acids.<sup>202</sup> These oxygenates are also converted, but it was found that the alumina catalyst deactivated in a matter of days for such conversions, albeit without affecting the catalyst's activity for the alcohol dehydration reaction. It was consequently possible to selectively dehydrate the alcohols to olefins without converting the other oxygenates.

**Olefin hydration.** Ethylene hydration is a commercial phosphoric acid catalysed process.<sup>203</sup> Propylene can also be hydrated to produce isopropanol,<sup>204</sup> but is less important in a fuels refining

context, since propylene has numerous other refining pathways. Like dehydration, hydration catalysts also need to be water-tolerant and only a limited number of catalysts have been investigated for this purpose.<sup>205</sup>

Application of ethylene hydration in a Fischer–Tropsch refinery has one additional advantage, namely that the side-products can be co-processed with the Fischer–Tropsch aqueous product. This implies a significant capital saving for such technology and allows operation of the hydration technology in such a way that side-product formation is not constraining.

## Discussion

### Technology selection

In the preceding discussion, different refining technologies were evaluated in terms of their compatibility with Fischer–Tropsch syncrude as feed material and their environmental friendliness. Since the term “environmentally friendly” can become charged with emotion and filled with political undertones, its meaning in the present context will be made clear. It is used as a term to describe the collective impact of aspects that would make a technology less efficient or cause it to generate more waste products than necessary for the conversion of interest. In general it is good engineering practice to select the most environmentally friendly refining technology for a given task.

The ultimate selection of conversion technologies for use within a Fischer–Tropsch refinery must consider the overall refining efficiency. The refining intent will shift emphasis between technologies, and Fischer–Tropsch refinery design is a topic in its own right. Nevertheless, the present evaluation forms the basis for rational and responsible technology selection.

The following specific aspects have been considered in making a recommendation of the suitability of the different technologies previously discussed for the refining of Fischer–Tropsch syncrude (Table 11):

(a) Fischer–Tropsch compatibility. If a technology is compatible with Fischer–Tropsch syncrude, it implies that the least effort will have to be expended in feed pretreatment and that the conversion itself will be suited to deal with type of molecules present in the feed. Although this does not render the technology environmentally friendly, it is likely to be less wasteful than other technologies having the same aim, but a poorer suitability for processing Fischer–Tropsch syncrude.

(b) Waste generation. All irreversible processes or activities generate waste (second law of thermodynamics), whether it is wasted energy or “low energy” by-products. It is therefore not helpful to consider waste generation *per se*, but to rather focus on the generation of waste in excess of the norm. For example, let us consider the solid waste generated by the unloading of a spent catalyst from a conversion process. There will be an industry norm for the amount and nature of the solid waste resulting from this type of operation. Deviations from this norm could be positive, like less waste or more biodegradable waste, or it can be negative, like the generation of excessive amounts of spent catalyst or more hazardous waste.

(c) Chemicals addition. The nature of refining is such that it deals with chemicals, some of which are hazardous. The type of chemicals that will be highlighted as increasing the

**Table 11** Compatibility of refining technologies for processing Fischer–Tropsch syn crude and an evaluation of their environmental impact when employed in conjunction with Fischer–Tropsch syn crude

Refining technology	Environmental impact					
	Catalyst	Fischer–Tropsch compatibility	Waste	Chemicals	Energy use	Recommendation for Fischer–Tropsch refining
Double bond isomerisation	alumina	good	low	none	high	subject to fuel olefin specification
Butene skeletal isomerisation	ferrierte	average	low <sup>a</sup>	none	high	only when octane constrained
Pentene skeletal isomerisation	alumina	good	low <sup>b</sup>	none	high	pretreatment for etherification
	acidic mol. sieve	average <sup>c</sup>	low	none	moderate	pretreatment for etherification <sup>b</sup>
Olefin di-/oligomerisation	acidic resin	average	low	none	low	isobutene “indirect alkylation” <sup>b</sup>
	H-ZSM-5	good	low	none	moderate	high cetane, low density distillate
	MFS/TON	average	low	none	low	not recommended (SPA is better)
	ASA	good	low	none	low	low cetane, high density distillate
	SPA	good	low	none	low	low cetane, high density distillate
	homogeneous	average	moderate	catalyst/NaOH	low	“alkylate” from <i>n</i> -butenes; jet fuel
	thermal	good	low	none	high	not recommended, except for chemicals
	acidic resin	average	low	none	low	subject to fuel ether specification
Etherification	HF	poor <sup>d</sup>	moderate	HF	low	not recommended
Aliphatic alkylation	H <sub>2</sub> SO <sub>4</sub>	poor <sup>d</sup>	high	H <sub>2</sub> SO <sub>4</sub>	low	not recommended (better than HF)
Aromatic alkylation	SPA	good	low	none	low	benzene reduction; jet fuel
	zeolites	average	low	none	moderate	not recommended (SPA is better)
Metathesis	metal oxide	average	low	none	moderate	needed when carboxylic acids in feed
Hydrotreating	sulfided	average	low <sup>f</sup>	DMDs <sup>g</sup>	moderate <sup>g</sup>	preferred if no carboxylic acids in feed
	unsulfided	average	low <sup>f</sup>	none	low	only needed with aliphatic alkylation
Butane hydroisomerisation	Pt/Cl <sup>-</sup> /Al <sub>2</sub> O <sub>3</sub>	average	low <sup>h</sup>	chloro-alkane	moderate	not recommended (Pt/MOR is better)
C <sub>5</sub> -C <sub>6</sub> hydroisomerisation	Pt/Cl <sup>-</sup> /Al <sub>2</sub> O <sub>3</sub>	poor <sup>i</sup>	low <sup>h</sup>	chloro-alkane	low	not recommended (Pt/MOR is better)
	Pt/metal oxide	poor <sup>i</sup>	low	none	low	not recommended for isomerate production
	Pt/mordenite	average	low	none	low	high cetane distillate
Hydrocracking	sulfided	average	low <sup>f</sup>	DMDs <sup>g</sup>	high	high cetane distillate
	unsulfided	good	low <sup>f</sup>	none	high	useful for motor-gasoline from LFTT
Catalytic cracking	zeolite	poor <sup>j</sup>	low	none	high	not recommended
Coking	thermal	poor <sup>j</sup>	low	none	high	not recommended, except for chemicals
Thermal cracking	thermal	good	low	none	high	not recommended (Pt/L is better)
Catalytic reforming	Pt/Cl <sup>-</sup> /Al <sub>2</sub> O <sub>3</sub>	poor <sup>k</sup>	low <sup>h</sup>	chloro-alkane	high	aromatic motor-gasoline; chemicals
	non-acidic Pt/L	good	low	none	high	LPG (not naphtha) to aromatics
Aromatisation	M/H-ZSM-5	average <sup>l</sup>	low	none	high	aqueous product refining
Alcohol dehydration	alumina	good	low	none	moderate <sup>l</sup>	fuel ethers
	acidic resin	average	low	none	low	far from ethylene market; ethanol
Olefin hydration	H <sub>3</sub> PO <sub>4</sub> /support	average	moderate	H <sub>3</sub> PO <sub>4</sub>	moderate	

<sup>a</sup> Side-product formation is 10%. <sup>b</sup> Side product formation is 10–15%. <sup>c</sup> Oxygenates in feed adsorbs strongly on catalyst, decreasing its operating window. <sup>d</sup> No butane source due to high olefin to paraffin ratio, selective dimerisation better fit for alkylate production. <sup>e</sup> Depends on type of metal oxide. Re<sub>2</sub>O<sub>7</sub> (low), MoO<sub>3</sub> (moderate), WO<sub>3</sub> (moderate/high). <sup>f</sup> Depending on the feed, water is a significant by-product. <sup>g</sup> Fischer–Tropsch syn crude is sulfur free, dimethyl disulfide (DMDs) is needed to keep catalyst sulfided. <sup>h</sup> Products contain Cl introduced by chloro-alkane addition. <sup>i</sup> Oxygenates in naphtha require feed pretreatment for removal. <sup>j</sup> It is a carbon rejection technology employed with a hydrogen rich feed. <sup>k</sup> Naphtha has a low (<30) *N*+2*A* ratio, resulting in high gas make for high octane motor-gasoline production. <sup>l</sup> Depends on the feed, ethanol dehydration (high), other alcohols (moderate).



environmental footprint of the technology, are those that are either present in very large volumes, or those that are destructively added (non-catalytic) to make the process work. It should be noted that in some instances this is done to gain energy efficiency and a trade-off is involved.

(d) Energy requirements. Processes that are energy intensive, or operate at high temperature, are considered less environmentally friendly, since they indirectly generate waste. High temperature processes are usually, but not necessarily more energy intensive than low temperature processes. In general the energy use is considered high if the operating temperature exceeds 350 °C. A proper evaluation of the energy use of processes has to take waste heat recovery into account. It is recognised that proper quantitative analysis is necessary to correctly rank technologies with respect to their energy requirements, but such a detailed analysis has not been attempted. There may also be other trade-offs involved, for example the use of hazardous chemicals to allow lower temperature operation.

### Fischer–Tropsch refinery design

Although Fischer–Tropsch refinery design falls outside the scope of the present review, the summary presented in Table 11 makes it clear that a Fischer–Tropsch refinery will look very different to a crude oil refinery.

In a modern crude oil refinery (Fig. 20), the topping-reforming-cracking-visbreaking-alkylation-isomerisation (TR-CVAI) designs of the 1990's are typically supplemented with additional residue upgrading technologies and may include units for the production of oxygenated motor-gasoline. Technologies such as fluid catalytic cracking, visbreaking (thermal cracking), Pt/Cl<sup>-</sup>/Al<sub>2</sub>O<sub>3</sub> catalytic reforming and aliphatic alkylation are all key technologies in crude oil refineries. Yet, these same technologies have poor compatibility with Fischer–Tropsch syncrude. This does not imply that such technologies cannot be used in conjunction with Fischer–Tropsch refining, but that such refinery designs would be sub-optimal.

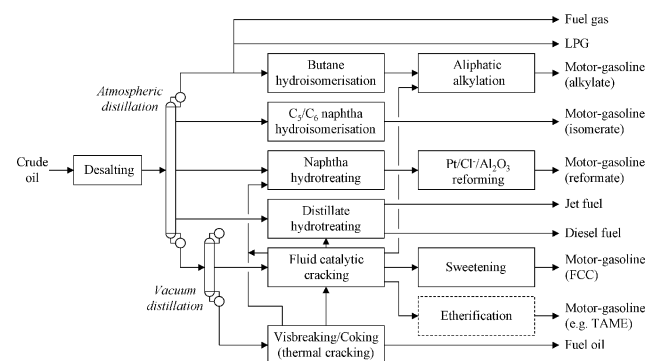


**Fig. 20** Generic design of a modern crude oil refinery. The design does not represent any specific refinery, but illustrates the refining pathways and conversion units typically required in order to refine crude oil to transportation fuels.

The design of a Fischer–Tropsch refinery will consequently have to be different if it is to be efficient. This point has previously been made.<sup>2</sup>

It is helpful to put Fischer–Tropsch refinery technology selection into context by looking at a generic Fischer–Tropsch

refinery (Fig. 21). In the design shown, high temperature Fischer–Tropsch syncrude is converted into transportation fuels that meet the current European specifications. The products therefore do not require blending to be sold in the retail market, unlike the hydrocracker-only LTFT designs employed in gas-to-liquids facilities such as Shell Bintulu and Oryx GTL.<sup>7</sup>

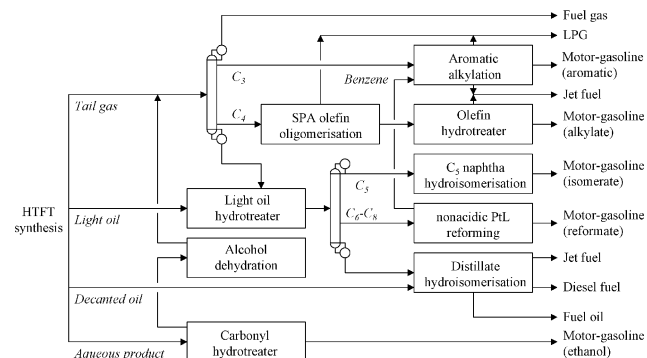


**Fig. 21** Generic design of a modern high temperature Fischer–Tropsch refinery that produces only on specification transportation fuels. This design does not represent any specific refinery. The tail gas is not separated by cryogenic cooling which limits refining of C<sub>2</sub> and lighter products.

The stepwise cooling of the HTFT syncrude (previously shown in Fig. 2) produces four different feed fractions for the refinery (Fig. 21). As a consequence the oil fraction of the HTFT syncrude is sufficiently pre-fractionated to be directly routed to conversion units, without first passing through an atmospheric distillation unit. The aqueous product is converted to ethanol and olefins by selective carbonyl to alcohol hydrogenation and alcohol dehydration.<sup>121</sup> Neither of these units are found in a crude oil refinery. Dimerisation/oligomerisation and aromatic alkylation are the key olefin conversion technologies responsible for converting normally gaseous olefins into liquid products. Although some crude oil refineries have olefin oligomerisation units to convert light FCC olefins to olefinic motor-gasoline, the combination of olefin oligomerisation and aromatic alkylation is not common in crude oil refineries. Hydrotreating units can be found in both Fischer–Tropsch and crude oil refineries, but the refining focus in a Fischer–Tropsch refinery is different; hydrotreaters are mainly used for olefin and oxygenate conversion. The catalytic reformer makes use of a nonacidic PtL-zeolite type catalyst (not Pt/Cl<sup>-</sup>/Al<sub>2</sub>O<sub>3</sub>). Distillate hydroisomerisation to improve cold flow properties is preferably conducted over a noble metal catalyst with mild acidity. Only the technologies for C<sub>3</sub> naphtha hydroisomerisation are common to both crude oil (Fig. 20) and Fischer–Tropsch (Fig. 21) refinery designs.

### Conclusions

The suitability of various conversion technologies to process Fischer–Tropsch syncrude has been evaluated. The evaluation focused on the compatibility of the feed on a molecular level to the chemistry and catalysis of the process, as well as its environmental impact in terms of waste, chemical addition and energy requirements. Some specific aspects that can be highlighted are:

(a) The relative importance of conversion technologies for Fischer–Tropsch refining varies depending on the type of syncrude to be refined. The two main classes of Fischer–Tropsch technology, namely high temperature Fischer–Tropsch (HTFT) and low temperature Fischer–Tropsch (LTFT), produce syncrudes that are significantly different in terms of composition (olefin, aromatic and oxygenate content) and carbon number distribution.

(b) It is possible to adapt technologies that were developed for crude oil refining, for the refining of Fischer–Tropsch syncrude. When doing so, provision must be made for the high concentration of olefins and oxygenates in the <360 °C boiling material, as well as the aliphatic nature of the heavier fractions of LTFT syncrude.

(c) Fischer–Tropsch syncrude lends itself to the production of motor-gasoline, jet fuel, niche fuels and chemicals. Contrary to common perception, Fischer–Tropsch syncrude is not well suited for the production of Euro-4-type diesel fuel (820–845 kg m<sup>-3</sup>; ≥51 cetane number), on account of its low naphthene and aromatic content.

(d) Catalyst types that are well-suited for the conversion of Fischer–Tropsch syncrude include less acidic catalysts such as alumina, solid phosphoric acid (SPA) and non-acidic Pt/L-zeolite. Catalysts with strong acidity tend to result in increased side-product formation due to the reactive nature of the syncrude.

(e) Some important crude oil refining technologies, such as Pt/Cl<sup>-</sup>/Al<sub>2</sub>O<sub>3</sub>, catalytic reforming, aliphatic alkylation, fluid catalytic cracking (FCC) and coking, display poor compatibility with Fischer–Tropsch syncrude.

(f) The most important conversion technologies for Fischer–Tropsch refining are olefin dimerisation/oligomerisation, aromatic alkylation, pentene skeletal isomerisation with etherification, hydrotreating (oxygenates and olefins), hydroisomerisation, hydrocracking, nonacidic Pt/L-zeolite reforming and alcohol dehydration.

## References

- 1 R. C. Duncan, Big jump in ultimate recovery would ease, not reverse, postpeak production decline, *Oil Gas J.*, 2004, **102**(27), 18; A. Petzet, World oil production to peak in 15–25 years, AAPG told, *Oil Gas J.*, 2007, **105**(16), 50; T. Nicholls, The peak is nigh, *Petroleum Econ.*, 2008, **75**(4), 40.
- 2 A. de Klerk, Environmentally friendly refining: Fischer–Tropsch versus crude oil, *Green Chem.*, 2007, **9**, 560.
- 3 *Fischer–Tropsch technology (Stud. Surf. Sci. Catal. 152)*, ed. A. P. Steynberg and M. E. Dry, Elsevier, Amsterdam, 2004.
- 4 F. G. Botes, Proposal of a new product characterization model for the iron-based low-temperature Fischer–Tropsch synthesis, *Energy Fuels*, 2007, **21**, 1379.
- 5 M. E. Dry, Chemicals produced in a commercial Fischer–Tropsch process, *Am. Chem. Soc. Symp. Ser.*, 1987, **328**, 18.
- 6 A. P. Steynberg, W. U. Nel and M. A. Desmet, Large scale production of high value hydrocarbons using Fischer–Tropsch technology, *Stud. Surf. Sci. Catal.*, 2004, **147**, 37; A. de Klerk, L. P. Dancuart and D. O. Leckel, Chemicals refining from Fischer–Tropsch synthesis, *Proc. World Petrol. Congr.*, 2005, **18**, cd185.
- 7 A. de Klerk, Refining of Fischer–Tropsch syncrude: lessons from the past, *Prepr. Pap.-Am. Chem. Soc. Div. Petrol. Chem.*, 2008, **53**(2), 105.
- 8 R. C. Santana, P. T. Do, M. Santikunaporn, W. E. Alvarez, J. D. Taylor, E. L. Sughrie and D. E. Resasco, Evaluation of different reaction strategies for the improvement of cetane number in diesel fuels, *Fuel*, 2006, **85**, 643.
- 9 G. Knothe and K. R. Steidley, Lubricity of components of biodiesel and petrodiesel. The origin of biodiesel lubricity, *Energy Fuels*, 2005, **19**, 1192.
- 10 D. O. Leckel, Catalytic hydroprocessing of coal-derived gasification residues to fuel blending stocks: Effect of reaction variable and catalyst on hydrodeoxygenation (HDO), hydrodenitrogenation (HDN), and hydrodesulfurization (HDS), *Energy Fuels*, 2006, **20**, 1761.
- 11 H. O. Hardenberg, Thoughts on an ideal diesel fuel from coal, *S. Afr. Mech. Eng.*, 1980, **30**, 34.
- 12 C. A. Forest; and P. A. Muzzell, Fischer–Tropsch fuels: Why are they of interest to the United States military?, *SAE Technol. Pap. Ser.*, 2005, 2005-01-1807; D. Lamprecht, Fischer–Tropsch fuel for use by the U.S. military as battlefield-use fuel of the future, *Energy Fuels*, 2007, **21**, 1448.
- 13 J. Eilers, S. A. Posthuma and S. T. Sie, The Shell middle distillate synthesis process (SMDS), *Catal. Lett.*, 1990, **7**, 253.
- 14 E. Köhler, F. Schmidt, H. J. Wernicke, M. De Pontes and H. L. Roberts, Converting olefins to diesel - the COD process, *Hydrocarbon Technol. Int.*, 1995, Summer, 37.
- 15 J. H. Coetzee, T. N. Mashapa, N. M. Prinsloo and J. D. Rademan, An improved solid phosphoric acid catalyst for alkene oligomerization in a Fischer–Tropsch refinery, *Appl. Catal. A*, 2006, **308**, 204.
- 16 F. H. Bruner, Synthetic gasoline from natural gas. Composition and quality, *Ind. Eng. Chem.*, 1949, **41**, 2511; M. D. Schlesinger and H. E. Benson, Upgrading Fischer–Tropsch products, *Ind. Eng. Chem.*, 1955, **47**, 2104; J. C. Hoogendoorn and J. M. Salomon, Sasol: World's largest oil-from-coal plant. III, *Br. Chem. Eng.*, 1957, Jul, 368.
- 17 *Process Economics Program Report 12D, Linear Alpha Olefins*, SRI: Menlo Park, 2001; K. McGurk, *S. Afr. Chem. Eng. Congr. Sun City, South Africa*, 2003, P082.
- 18 *ASTM DS 4B. Physical, constants of hydrocarbons and non-hydrocarbon compounds*, 2nd edn, ASTM, Philadelphia, PA, 1991.
- 19 F. Asinger, *Mono-olefins chemistry and technology*, Pergamon, Oxford, 1968.
- 20 H. N. Dunning, Review of olefin isomerization, *Ind. Eng. Chem.*, 1953, **45**, 551.
- 21 R. S. Karinen, M. S. Lylykangas and A. O. I. Krause, Reaction equilibrium in the isomerization of 2,4,4-trimethyl pentenes, *Ind. Eng. Chem. Res.*, 2001, **40**, 1011.
- 22 J. N. Kondo and K. Domen, IR observations of adsorption and reactions of olefins on H-form zeolites, *J. Mol. Catal. A*, 2003, **199**, 27.
- 23 D. J. Rosenberg, B. Bachiller-Baeza, T. J. Dines, T. J. and J. A. Anderson, Nature of surface sulfate species and the generation of active sites on silica-zirconia mixed-oxide catalysts, *J. Phys. Chem. B*, 2003, **107**, 6526.
- 24 J. Li and R. J. Davis, On the use of 1-butene double-bond isomerisation as probe reaction on cesium-loaded zeolite X, *Appl. Catal. A*, 2003, **239**, 59.
- 25 J. C. Cowen, Isomerization reactions of drying oils, *Ind. Eng. Chem.*, 1949, **41**, 294.
- 26 C. J. Helmers and G. M. Brooner, Catalytic desulfurization and reforming of naphthas over bauxite, *Petroleum Process.*, 1948, **3**, 133.
- 27 P. J. Lucchesi, D. L. Baeder and J. P. Longwell, Stereospecific isomerization of butene-1 to butene-2 over SiO<sub>2</sub>-Al<sub>2</sub>O<sub>3</sub> catalyst, *J. Am. Chem. Soc.*, 1959, **81**, 3235; D. Kalló and I. Preszler, *n*-Butene isomerization on acidic ion-exchange resin, *J. Catal.*, 1968, **12**, 1.
- 28 A. Corma, Inorganic solid acids and their use in acid catalyzed hydrocarbon reactions, *Chem. Rev.*, 1995, **95**, 559.
- 29 J. S. Buchanan, J. G. Santiesteban and W. O. Haag, Mechanistic considerations in acid-catalyzed cracking of olefins, *J. Catal.*, 1996, **158**, 279.
- 30 E. R. Cousins, W. A. Guice and R. O. Feuge, Positional isomers formed during the hydrogenation of methyl linoleate under various conditions, *J. Amer. Oil Chem. Soc.*, 1959, **36**, 24; M. Pecque and R. Maurel, Hydrogénation catalytique. IV. Hydrogénation, en phase liquide de couples d'oléfines isomères de position, *Bull. Soc. Chim. Fr.*, 1969, **6**, 1882; A. J. Sederman, M. D. Mantle, C. P. Dunkley, Z. Huang and L. F. Gladden, *In situ* MRI study of 1-octene

- isomerisation and hydrogenation within a trickle-bed reactor, *Catal. Lett.*, 2005, **103**, 1.
- 31 G. H. Twigg, The mechanism of catalytic exchange reactions between deuterium and olefins, *Trans. Faraday Soc.*, 1939, **35**, 934; T. I. Taylor and V. H. Dibeler, Catalyzed reactions of unsaturated hydrocarbons with hydrogen and deuterium, *J. Phys. Chem.*, 1951, **55**, 1036; L. F. Albright and J. Wisniak, Selectivity and isomerization during partial hydrogenation of cottonseed oil and methyl oleate: effect of operating variables, *J. Am. Oil Chem. Soc.*, 1962, **39**, 14; M. S. Lylykangas, P. A. Rautanen and A. O. I. Krause, Liquid-phase hydrogenation kinetics of isooctenes on Ni/Al<sub>2</sub>O<sub>3</sub>, *AIChE J.*, 2003, **49**, 1508.
- 32 M. Pecque and R. Maurel, R., Hydrogénation catalytique. III. Cinétique, de l'hydrogénation avec isomérisation, *Bull. Soc. Chim. Fr.*, 1969, **6**, 1878.
- 33 J. N. Finch and A. Clark, The effect of water content of silica-alumina catalyst on 1-butene isomerization and polymerization, *J. Phys. Chem.*, 1969, **73**, 2234.
- 34 D. Smook and A. de Klerk, Inhibition of etherification and isomerization by oxygenates, *Ind. Eng. Chem. Res.*, 2006, **45**, 467.
- 35 A. D. Pienaar and A. de Klerk, Nickel catalyst stability toward carboxylic acids, *Ind. Eng. Chem. Res.*, 2008, **47**, 4962.
- 36 S. M. Ozmen, H. Abrevaya, P. Barger, M. Benthani and M. Kojima, Skeletal isomerization of C<sub>4</sub> and C<sub>5</sub> olefins for increased ether production, *Fuel Reformulation*, 1993, **3**(5), 54; H. H. Mooiweer and K. P. de Jong, Skeletal isomerisation of olefins with the zeolite Ferrierite as catalyst, *Stud. Surf. Sci. Catal.*, 1994, **84**, 2327; J.-L. Duplan, P. Amigues, J. Verstraete and C. Travers, Kinetic studies of the skeletal isomerization of *n*-pentenes over the ISO-5 process catalyst, *Proc. Ethylene Prod. Conf.*, 1996, **5**, 429.
- 37 D. Li, M. Li, Y. Chu, H. Nie and Y. Shi, Skeletal isomerization of light FCC naphtha, *Catal. Today*, 2003, **81**, 65; F. Sandelin, I. Eilos, E. Harlin, J. Hiltunen, J. Jakkula, J. Makkonen and M. Tiitta, A CFB unit for skeletal isomerization of linear C<sub>4</sub>-C<sub>6</sub> olefins on ferrierite catalysts, *Proc. 14th Int. Zeolite Conf. Cape Town, ZA*, 2004, 2157.
- 38 P. Meriaudeau, R. Bacaud, L. N. Hung and A. T. Vu, Isomerisation of butene in isobutene on ferrierite catalyst: A mono- or bimolecular process?, *J. Mol. Catal. A*, 1996, **110**, L177; J. Houzvička and V. Ponec, Skeletal isomerization of butene: On the role of the bimolecular mechanism, *Ind. Eng. Chem. Res.*, 1997, **36**, 1424; M. Guisnet, P. Andy, N. S. Gnep, C. Travers and E. Benazzi, Comments on "Skeletal isomerization of butene: On the role of the bimolecular mechanism, *Ind. Eng. Chem. Res.*, 1998, **37**, 300; J. Houzvička and V. Ponec, Rebuttal to the comments of M. Guisnet, *et al.* on "Skeletal isomerization of butene: On the role of the bimolecular mechanism, *Ind. Eng. Chem. Res.*, 1998, **37**, 303.
- 39 V. R. Choudhary, Catalytic isomerization of *n*-butene to isobutene, *Chem. Ind. Dev.*, 1974, **8**(7), 32.
- 40 K. P. de Jong, H. H. Mooiweer, J. G. Buglass and P. K. Maarsen, Activation and deactivation of the zeolite ferrierite for olefin conversion, *Stud. Surf. Sci. Catal.*, 1997, **111**, 127.
- 41 J. B. Wise and D. Powers, Highly selective olefin skeletal isomerization process, *Am. Chem. Soc. Symp. Ser.*, 1994, **552**, 273.
- 42 J. M. Meister, S. M. Black, B. S. Muldoon, D. H. Wei and C. M. Roeseler, Optimize alkylate production for clean fuels, *Hydrocarbon Process.*, 2000, **79**(5), 63.
- 43 M. Cowley, Skeletal isomerization of Fischer-Tropsch-derived pentenes: The effect of oxygenates, *Energy Fuels*, 2006, **20**, 1771.
- 44 S. Rossini, R. Catani, U. Cornaro, A. Guercio, R. Miglio and V. Piccoli, Oxygenates and nitriles effects on some catalysts for the skeletal isomerization of C<sub>4</sub> and C<sub>5</sub> olefins, *Prepr. Pap.-Am. Chem. Soc. Div. Petrol. Chem.*, 1997, **42**(3), 588.
- 45 M. Sanati, C. Hörnell and S. G. Järås, The oligomerization of alkenes by heterogeneous catalysts, *Catalysis*, 1999, **14**, 236.
- 46 P. Leprince, Oligomerization in *Petroleum Refining Vol.3 Conversion Processes*, ed. P. Leprince, Editions Technip, Paris, 2001, p.321.
- 47 A. K. Kolah, Q. Zhiwen and S. M. Mahajani, Dimerized isobutene: an alternative to MTBE, *Chem. Innov.*, 2001, **31**(3), 15.
- 48 R. H. Nielsen, *NEXOCTANE™ isooctane process; Process Economic Program review 2003-12*, SRI, Menlo Park, CA, 2003; R. Birkhoff, M. Nurminen, *NEXOCTANE™ technology for isooctane production in Handbook of Petroleum Refining Processes*, ed. R. A. Meyers, McGraw-Hill, New York, 2004, p.1.3.
- 49 M. Marchionna and M. Di Girolamo, High quality fuel components from C<sub>4</sub> hydrocarbons, *DGMK Conf. Munich, Germany*, 2004, 125.
- 50 A. de Klerk and P. L. de Vaal, Alkylate technology selection for Fischer-Tropsch syncrude refining, *Ind. Eng. Chem. Res.*, 2008, **47**, 6870.
- 51 M. Marchionna, M. Di Girolamo and R. Patrini, Light olefins dimerization to high quality gasoline components, *Catal. Today*, 2001, **65**, 397; M. L. Honkela and A. O. I. Krause, Influence of polar components in the dimerization of isobutene, *Catal. Lett.*, 2003, **87**, 113.
- 52 S. A. Tabak and F. J. Krambeck, Shaping process makes fuels, *Hydrocarbon Process.*, 1985, **64**(9), 72.
- 53 W. E. Garwood, Conversion of C<sub>2</sub>-C<sub>10</sub> to higher olefins over synthetic zeolite ZSM-5, *Am. Chem. Soc. Symp. Ser.*, 1983, **218**, 383.
- 54 R. J. Quann, L. A. Green, S. A. Tabak and F. J. Krambeck, Chemistry of olefin oligomerization over ZSM-5 catalyst, *Ind. Eng. Chem. Res.*, 1988, **27**, 565; A. de Klerk, Oligomerization of 1-hexene and 1-octene over solid acid catalysts, *Ind. Eng. Chem. Res.*, 2005, **44**, 3887.
- 55 S. A. Tabak, F. J. Krambeck and W. E. Garwood, Conversion of propylene and butylene over ZSM-5 catalyst, *AIChE J.*, 1986, **32**, 1526.
- 56 C. T. O'Connor, S. T. Langford and J. C. Q. Fletcher, The effect of oxygenates on the propene oligomerization activity of ZSM-5, *Proc. 9th Int. Zeolite Conf. Montreal, Canada*, 1992, 463.
- 57 C. Knottenbelt, Moss gas "gas-to-liquids" diesel fuels - an environmentally friendly option, *Catal. Today*, 2002, **71**, 437.
- 58 A. de Klerk, Properties of synthetic fuels from H-ZSM-5 oligomerisation of Fischer-Tropsch type feed materials, *Energy Fuels*, 2007, **21**, 3084.
- 59 G. K. Chitnis, A. B. Dandekar, B. S. Umansky, G. B. Brignac, J. Stokes and W. A. Leet, ExxonMobil olefins to gasoline EMOGAS™ technology for polymerization units, *NPRA 103rd National Meeting, San Francisco*, 2005, AM-05-77.
- 60 G. K. Chitnis, A. B. Dandekar, B. S. Umansky, G. B. Brignac, J. Stokes and W. A. Leet, Polymerisation progress, *Hydrocarbon Eng.*, 2005, **10**(6), 21.
- 61 C. T. O'Connor, Oligomerization in *Handbook of Heterogeneous Catalysis*, ed. G. Ertl, H. Knözinger and J. Weitkamp, VCH: Weinheim, 1997, 2380.
- 62 S. J. Miller, Olefin oligomerization over high silica zeolites, *Stud. Surf. Sci. Catal.*, 1987, **38**, 187.
- 63 M. Golombok and J. de Bruijn, Dimerization of *n*-butenes for high octane gasoline components, *Ind. Eng. Chem. Res.*, 2000, **39**, 267.
- 64 A. de Klerk, Oligomerization of Fischer-Tropsch olefins to distillates over amorphous silica-alumina, *Energy Fuels*, 2006, **20**, 1799; A. de Klerk, Effect of oxygenates on the oligomerisation of Fischer-Tropsch olefins over amorphous silica-alumina, *Energy Fuels*, 2007, **21**, 625.
- 65 S. Peratello, M. Molinari, G. Bellussi and C. Perego, Olefins oligomerization: thermodynamics and kinetics over a mesoporous silica-alumina, *Catal. Today*, 1999, **52**, 271; R. Catani, M. Mandreoli, S. Rossini and A. Vaccari, Mesoporous catalysts for the synthesis of clean diesel fuels by oligomerisation of olefins, *Catal. Today*, 2002, **75**, 125; J. M. Escola, R. van Grieken, J. Moreno and R. Rodriguez, Liquid-phase oligomerization of 1-hexene using Al-MTS catalysts, *Ind. Eng. Chem. Res.*, 2006, **45**, 7409.
- 66 F. Nierlich, J. Neumeister, T. Wildt, R. W. Droste, F. Obenaus, Oligomerization of olefins. Patent ZA 90/3391 (1990, Huels Aktiengesellschaft).
- 67 F. Nierlich, Oligomerize for better gasoline, *Hydrocarbon Process.*, 1992, **71**(2), 45.
- 68 V. N. Ipatieff and G. Egloff, Polymer gasoline has higher blending value than pure iso-octane, *Oil Gas J.*, 1935, **33**(52), 31; V. N. Ipatieff, B. B. Corson and G. Egloff, Polymerization, a new source of gasoline, *Ind. Eng. Chem.*, 1935, **27**, 1077.
- 69 T. R. Krawietz, P. Lin, K. E. Lotterhos, P. D. Torres, D. H. Barich, A. Clearfield and J. F. Haw, Solid phosphoric acid catalyst: A multinuclear NMR and theoretical study, *J. Am. Chem. Soc.*, 1998, **120**, 8502.
- 70 L. Schmerling and V. N. Ipatieff, The mechanism of the polymerization of alkenes, *Adv. Catal.*, 1950, **2**, 21; A. de Klerk, Reactivity differences of octenes over solid phosphoric acid, *Ind. Eng. Chem. Res.*, 2006, **45**, 578.



- 71 A. de Klerk, D. O. Leckel and N. M. Prinsloo, Butene oligomerisation by phosphoric acid catalysis: Separating the effects of temperature and catalyst hydration on product selectivity, *Ind. Eng. Chem. Res.*, 2006, **45**, 6127.
- 72 V. N. Ipatieff and B. B. Corson, Gasoline from ethylene by catalytic polymerization, *Ind. Eng. Chem.*, 1936, **28**, 860; W. F. Deeter, Propene polymerization for motor-gasoline production, *Oil Gas J.*, 1950, 23 March, 252; V. N. Ipatieff and R. E. Schaad, Mixed polymerization of butenes by solid phosphoric acid catalyst, *Ind. Eng. Chem.*, 1938, **30**, 596; P. C. Weinert and G. Egloff, Catalytic polymerization and its commercial application, *Petroleum Process.*, 1948, June, 585.
- 73 A. de Klerk, D. J. Engelbrecht and H. Boikanyo, Oligomerization of Fischer–Tropsch olefins: Effect of feed and operating conditions on hydrogenated motor-gasoline quality, *Ind. Eng. Chem. Res.*, 2004, **43**, 7449.
- 74 A. de Klerk, Isomerization of 1-butene to isobutene at low temperature, *Ind. Eng. Chem. Res.*, 2004, **43**, 6325.
- 75 A. de Klerk, Distillate production by oligomerization of Fischer–Tropsch olefins over Solid Phosphoric Acid, *Energy Fuels*, 2006, **20**, 439.
- 76 N. M. Prinsloo, N. M., Solid, phosphoric acid oligomerisation: Manipulating diesel selectivity by controlling catalyst hydration, *Fuel Process. Technol.*, 2006, **87**, 437.
- 77 T. N. Mashapa and A. de Klerk, Solid Phosphoric Acid catalysed conversion of oxygenate containing Fischer–Tropsch naphtha, *Appl. Catal. A*, 2007, **332**, 200.
- 78 A. de Klerk, R. J. J. Nel and R. Schwarzer, Oxygenate conversion over Solid Phosphoric Acid, *Ind. Eng. Chem. Res.*, 2007, **46**, 2377.
- 79 J. A. Chodorge, J. Cosyns, F. Hughes, H. Olivier-Bourbigou, Dimerisation of C<sub>4</sub> olefins for the manufacture of isononanol, *DGMK-Conference, Aachen, Germany*, 1997, 227.
- 80 Y. Chauvin, J. Gaillard, J. Léonard, P. Bonnifay and J. W. Andrews, Another use for Dimersol, *Hydrocarbon Process.*, 1982, **61**(5), 110.
- 81 Y. Chauvin, J. F. Gaillard, D. V. Quang and J. W. Andrews, IFP's Dimersol process handles C<sub>3</sub> and C<sub>4</sub> olefin cuts, *Petroleum Petrochem. Int.*, 1973, **13**(10), 108; P. M. Kohn, Process provides option for nonleaded-gas makers, *Chem. Eng.*, 1977, 23 May, 114.
- 82 J. Leonard and J. F. Gaillard, Make octenes with Dimersol X, *Hydrocarbon Process.*, 1981, **60**(3), 99; J. F. Boucher, G. Follain, D. Fulop and J. Gaillard, Dimersol X process makes octenes for plasticizer, *Oil Gas J.*, 1982, 29 March, 84.
- 83 F. Favre, A. Forestière, F. Hughes, H. Olivier-Bourbigou and J. A. Chodorge, Butenes dimerization: from monophasic Dimersol to biphasic Difasol, *Oil Gas*, 2005, **31**(2), 83.
- 84 C. R. Wagner, Production of gasoline by polymerization of olefins, *Ind. Eng. Chem.*, 1935, **27**, 933; J. S. Carey, Commercial aspects of the unitary thermal polymerization process, *Refiner Nat. Gas. Manuf.*, 1936, **15**, 549.
- 85 C. D. Hurd, Pyrolysis of unsaturated hydrocarbons, *Ind. Eng. Chem.*, 1934, **26**, 50.
- 86 E. Ranzi, M. Dente, S. Pierucci and G. Biardi, Initial product distributions from pyrolysis of normal and branched paraffins, *Ind. Eng. Chem. Fundam.*, 1983, **22**, 132.
- 87 J. A. Brennan, Wide-temperature range synthetic hydrocarbon fluids, *Ind. Eng. Chem. Prod. Res. Dev.*, 1980, **19**, 2.
- 88 F. M. Seger, H. G. Doherty and A. N. Sachanen, Noncatalytic polymerization of olefins to lubricating oils, *Ind. Eng. Chem.*, 1950, **42**, 2446.
- 89 A. de Klerk, Thermal upgrading of Fischer–Tropsch olefins, *Energy Fuels*, 2005, **19**, 1462.
- 90 M. Cowley, Oligomerisation of olefins by radical initiation, *Org. Process Res. Dev.*, 2007, **11**, 286.
- 91 P. Travers, Olefin etherification in *Petroleum Refining Vol.3 Conversion Processes*, ed. P. Leprince, Editions Technip, Paris, 2001, p.291.
- 92 E. J. Swain and U. S. MTBE, production at a record high in 1998, *Oil Gas J.*, 1999, **97**(24), 99; A. Thayer, MTBE decline hits producers hard, *Chem. Eng. News*, 2003, **28 July**, 12; C. Hodge, More evidence mounts for banning, not expanding, use of ethanol in US gasoline, *Oil Gas J.*, 2003, **101**(38), 18; Anon, Senate approves ethanol mandate and MTBE ban as part of energy bill, *Chemical Market Reporter*, 2003, **263**(24), 16; R. Lamberth, 2003 was a year of transition for the MTBE, fuels industry, *Oil Gas J.*, 2004, **102**(2), 52; L. Kumins, Energy system limits future ethanol growth, *Oil Gas J.*, 2007, **105**(44), 18.
- 93 J. F. Izquierdo, F. Cunill, M. Vila, J. Tejero and M. Iborra, Equilibrium constants for methyl *tert*-butyl ether liquid-phase synthesis, *J. Chem. Eng. Data*, 1992, **37**, 339; L. K. Rihko, J. A. Linnekoski and A. O. I. Krause, Reaction equilibria in the synthesis of 2-methoxy-2-methylbutane and 2-ethoxy-2-methylbutane in the liquid phase, *J. Chem. Eng. Data*, 1994, **39**, 700; K. L. Jensen and R. Datta, Ethers from Ethanol. 1. Equilibrium thermodynamic analysis of the liquid-phase ethyl *tert*-butyl ether reaction (ETBE), *Ind. Eng. Chem. Res.*, 1995, **34**, 392.
- 94 J. G. Goodwin Jr, S. Natesakhawat, A. A. Nikolopoulos and S. Y. Kim, Etherification on zeolites: MTBE synthesis, *Catal. Rev. Sci. Eng.*, 2002, **44**, 287.
- 95 F. Ancillotti, M. M. Mauri, E. Pescarollo and L. Romagnoni, Mechanisms in the reaction between olefins and alcohols catalyzed by ion exchange resins, *J. Mol. Catal.*, 1978, **4**, 37.
- 96 R. Thornton and B. C. Gates, Catalysis by matrix-bound sulfonic acidic groups: Olefin and paraffin formation from butyl alcohols, *J. Catal.*, 1974, **34**, 275.
- 97 F. Cunill, M. Vila, J. F. Izquierdo, M. Iborra and J. Tejero, Effect of water presence on methyl *tert*-butyl ether and ethyl *tert*-butyl ether liquid-phase synthesis, *Ind. Eng. Chem. Res.*, 1993, **32**, 564.
- 98 A. Wyczessany, Chemical equilibria in the process of etherification of light FCC gasoline with methanol, *Ind. Eng. Chem. Res.*, 1995, **34**, 1320; L. K. Rihko and A. O. I. Krause, Etherification of FCC light gasoline with methanol, *Ind. Eng. Chem. Res.*, 1996, **35**, 2500.
- 99 A. de Klerk, Etherification of C<sub>6</sub> Fischer–Tropsch material for linear  $\alpha$ -olefin recovery, *Ind. Eng. Chem. Res.*, 2004, **43**, 6349.
- 100 E. du Toit and W. Nicol, The rate inhibiting effect of water as a product of reactions catalysed by cation exchange resins: formation of mesityl oxide from acetone as case study, *Appl. Catal. A*, 2004, **277**, 219.
- 101 A. Corma and A. Martínez, Chemistry, catalysts, and processes for isoparaffin-olefin alkylation. Actual situation and future trends, *Catal. Rev.-Sci. Eng.*, 1993, **35**, 483; J. -F. Joly, Aliphatic alkylation. In P. Leprince, Ed. *Petroleum Refining Vol.3 Conversion Processes*, Editions Technip: Paris, 2001, p.257; R. H. Nielsen, *Alkylation for motor fuels. Process Economic Program report 88B*, SRI: Menlo Park, 2001.
- 102 E. K. Jones, Commercial alkylation of paraffins and aromatics, *Adv. Catal.*, 1958, **10**, 165.
- 103 J. Weitkamp and Y. Traa, Isobutane/butene alkylation on solid catalysts. Where do we stand?, *Catal. Today*, 1999, **49**, 193; S. I. Hommeltoft, Isobutane alkylation. Recent developments and future perspectives, *Appl. Catal. A*, 2001, **221**, 421.
- 104 L. F. Albright, Alkylation of isobutane with C<sub>3</sub>-C<sub>5</sub> olefins: Feedstock consumption, acid usage, and alkylate quality for different processes, *Ind. Eng. Chem. Res.*, 2002, **41**, 5627.
- 105 K. W. Li, R. E. Eckert and L. F. Albright, Alkylation of isobutane with light olefins using sulfuric acid. Operating variables affecting physical phenomena only, *Ind. Eng. Chem. Process Des. Dev.*, 1970, **9**, 434.
- 106 K. Terblanche, The Moss gas challenge, *Hydrocarbon Eng.*, 1997, March, 2.
- 107 A. R. Goetzler, A. Hernandez-Robinson, S. Ram, A. A. Chin, M. N. Harandi and C. M. Smith, Refiners have several options for reducing gasoline benzene, *Oil Gas J.*, 1993, **91**(13), 63; A. de Klerk and R. J. J. Nel, Benzene reduction in a fuels refinery: An unconventional approach, *Energy Fuels*, 2008, **22**, 1449.
- 108 T. F. Degnan Jr, C. M. Smith and C. R. Venkat, Alkylation of aromatics with ethylene and propylene: recent developments in commercial processes, *Appl. Catal. A*, 2001, **221**, 283; C. Perego and P. Ingallina, Recent advances in the industrial alkylation of aromatics: new catalysts and new processes, *Catal. Today*, 2002, **73**, 3.
- 109 M. A. Cesar, G. Chou, *Cumene. Process Economics Program, report 219*, SRI, Menlo Park, CA, 1999.
- 110 M. Cowley, A. de Klerk, R. J. J. Nel and J. D. Rademan, Alkylation of benzene with 1-pentene over solid phosphoric acid, *Ind. Eng. Chem. Res.*, 2006, **45**, 7399; R. J. J. Nel and A. de Klerk, Selectivity differences of hexene isomers in the alkylation of benzene over solid phosphoric acid, *Ind. Eng. Chem. Res.*, 2007, **46**, 2902.
- 111 T. M. Sakuneka, A. de Klerk and R. J. J. Nel, Synthetic jet fuel production by combined propene oligomerization and aromatic



- alkylation over solid phosphoric acid, *Ind. Eng. Chem. Res.*, 2008, **47**, 1828.
- 112 T. M. Sakuneka, R. J. J. Nel and A. de Klerk, Benzene reduction by alkylation in a Solid Phosphoric Acid catalysed olefin oligomerization process, *Ind. Eng. Chem. Res.*, 2008, **47**, 7178.
- 113 C. T. Adams and S. G. Bandenberger, Mechanism of olefin disproportionation, *J. Catal.*, 1969, **13**, 360.
- 114 J. C. Mol, Industrial applications of olefin metathesis, *J. Mol. Catal. A*, 2004, **213**, 39; A. Wood, C<sub>2</sub>H<sub>4</sub> process boosts profits by 30%, *Chem. Eng. Progress*, 2002, **98**(7), 19.
- 115 M. N. Kwini and J. M. Botha, Influence of feed components on the activity and stability of cobalt molybdenum alumina metathesis catalyst, *Appl. Catal. A*, 2005, **280**, 199.
- 116 C. van Schalkwyk, A. Spamer, D. J. Moodley, T. Dube, J. Reynhardt, J. M. Botha and H. C. M. Vosloo, Factors that could influence the activity of a WO<sub>3</sub>/SiO<sub>2</sub> catalyst: part III, *Appl. Catal. A*, 2003, **255**, 143.
- 117 G. Heinrich, S. Kasztelan, Hydrotreating in *Petroleum Refining Vol.3 Conversion Processes*, ed. P. Leprince, Editions Technip, Paris, 2001, p.533.
- 118 R. R. Chianelli, Fundamental studies of transition metal sulfide hydrodesulfurization catalysts, *Catal. Rev.-Sci. Eng.*, 1984, **26**, 361; T. C. Ho, Deep HDS of diesel fuel: Chemistry and catalysis, *Catal. Today*, 2004, **98**, 3.
- 119 T. C. Ho, Hydrodenitrogenation catalysis, *Catal. Rev.-Sci. Eng.*, 1988, **30**, 117; G. Perot, The reactions involved in hydrodenitrogenation, *Catal. Today*, 1991, **10**, 447; R. Prins, Y. Zhao, N. Sivasamkar and P. Kukula, Mechanism of C–N bond breaking in hydrodenitrogenation, *J. Catal.*, 2005, **234**, 509.
- 120 E. Furimsky, Catalytic hydrodeoxygenation, *Appl. Catal. A*, 2000, **199**, 147.
- 121 R. J. J. Nel and A. de Klerk, Fischer–Tropsch aqueous phase refining by catalytic alcohol dehydration, *Ind. Eng. Chem. Res.*, 2007, **46**, 3558.
- 122 F. H. A. Bolder, Fischer–Tropsch wax hydrogenation over a sulfided nickel-molybdenum catalyst, *Energy Fuels*, 2007, **21**, 1396.
- 123 D. Lamprecht, Hydrogenation of Fischer–Tropsch synthetic crude, *Energy Fuels*, 2007, **21**, 2509.
- 124 A. Stanislaus and B. H. Cooper, Aromatic hydrogenation catalysis: A review, *Catal. Rev.-Sci. Eng.*, 1994, **36**, 75.
- 125 M. Brémaud, L. Vivier, G. Pérot, V. Harlé and C. Bouchy, Hydrogenation of olefins over hydrotreating catalysts. Promotion effect on the activity and on the involvement of H<sub>2</sub>S in the reaction, *Appl. Catal. A*, 2005, **289**, 44.
- 126 M. S. Lylykangas, P. A. Rautanen and A. O. I. Krause, Hydrogenation and deactivation kinetics in the liquid-phase hydrogenation of isooctenes on Pt/Al<sub>2</sub>O<sub>3</sub>, *Ind. Eng. Chem. Res.*, 2004, **43**, 1641; M. S. Lylykangas, P. A. Rautanen and A. O. I. Krause, Liquid-phase hydrogenation kinetics of isooctenes on Co/SiO<sub>2</sub>, *Appl. Catal. A*, 2004, **259**, 73; A. de Klerk and M. J. Strauss, Opportunities for efficiency improvement in high temperature Fischer–Tropsch hydroprocessing units, *Prepr. Pap.-Am. Chem. Soc. Div. Fuel Chem.*, 2008, **53**(1), 313.
- 127 F. M. Dautzenberg and J. C. de Deken, Modes of operation in hydrodemetallization, *Am. Chem. Soc. Symp. Ser.*, 1987, **344**, 233; H. Toulhoat, R. Szymanski and J. C. Plumail, Interrelations between initial pore structure, morphology and distribution of accumulated deposits, and lifetimes of hydrodemetallisation catalysts, *Catal. Today*, 1990, **7**, 531; F. X. Long, B. S. Gevert and P. Abrahamsen, Mechanistic studies of initial decay of hydrodemetallization catalysts using model compounds – effects of adsorption of metal species on alumina support, *J. Catal.*, 2004, **222**, 6.
- 128 A. de Klerk, Hydroprocessing peculiarities of Fischer–Tropsch syncrude, *Catal. Today*, 2008, **130**, 439.
- 129 Anon, OGJ international refining catalyst compilation-2003, *Oil Gas J.*, 2003, 6 Oct, 1.
- 130 O. Weisser, Sulfide catalysts, their properties and uses, *Int. Chem. Eng.*, 1963, **3**, 388.
- 131 E. Furimsky, Selection of catalysts and reactors for hydroprocessing, *Appl. Catal. A*, 1998, **171**, 177.
- 132 E. Furimsky and F. E. Massoth, Deactivation of hydroprocessing catalysts, *Catal. Today*, 1999, **52**, 381.
- 133 R. C. Mehrothra, R. Bohra, *Metal carboxylates*, Academic Press, London, 1983; S. Rajadurai, Pathways for carboxylic acid decomposition on transition metal oxides, *Catal. Rev.-Sci. Eng.*, 1994, **36**, 385.
- 134 A. Chica and A. Corma, Hydroisomerization of pentane, hexane, and heptane for improving the octane number of gasoline, *J. Catal.*, 1999, **187**, 167; T. Okuhara, Skeletal isomerization of *n*-heptane to clean gasoline, *J. Jpn. Petrol. Inst.*, 2004, **47**(1), 1.
- 135 F. Chevalier, M. Guinet and R. Maurel, Tracer study of the isomerization of paraffins on bifunctional catalysts, *Proc. 6th Int. Congr. Catal.*, 1977, 478.
- 136 J. W. Thybaut, C. S. Narasimhan, J. F. Denayer, G. V. Baron, P. A. Jacobs, J. A. Martens and G. B. Marin, Acid-metal balance of a hydrocracking catalyst: Ideal versus nonideal behavior, *Ind. Eng. Chem. Res.*, 2005, **44**, 5159.
- 137 H. Y. Chu, M. P. Rosynek and J. H. Lunsford, Skeletal isomerization of hexane over Pt/H-Beta zeolites: Is the classical mechanism correct?, *J. Catal.*, 1998, **178**, 352; Y. Ono, A survey of the mechanism in catalytic isomerization of alkanes, *Catal. Today*, 2003, **81**, 3.
- 138 C. Travers, Isomerization of light paraffins in *Petroleum Refining Vol.3 Conversion Processes*, ed. P. Leprince, Editions Technip, Paris, 2001, p.229.
- 139 F. M. Floyd, M. F. Gilbert, M. Pérez and E. Köhler, Light naphtha isomerisation, *Hydrocarbon Eng.*, 1998, **Sep**, 42; P. J. Kuchar, R. D. Gillespie, C. D. Gosling, W. C. Martin, M. J. Cleveland and P. J. Bullen, P. J., Developments, in isomerisation, *Hydrocarbon Eng.*, 1999, **Mar**, 50; M. J. Hunter, Light naphtha isomerisation to meet 21st century gasoline specifications, *Oil Gas*, 2003, **29**(2), 97; H. Weyda and E. Köhler, E., Modern, refining concepts - an update on naphtha-isomerization to modern gasoline manufacture, *Catal. Today*, 2003, **81**, 51.
- 140 C. Slade and S. Zuidendorp, Recognizing deactivation mechanisms in paraffin isomerizations, *Catalysts Courier*, 2006, **64**, 10.
- 141 T. Kimura, T. Development, of Pt/SO<sub>4</sub><sup>2-</sup>/ZrO<sub>2</sub> catalyst for isomerization of light naphtha, *Catal. Today*, 2003, **81**, 57.
- 142 N. A. Cusher, UOP Penex process; UOP TIP and once-through zeolitic isomerization processes; Par-isom process in *Handbook of Petroleum Refining Processes*, ed. R. A. Meyers, McGraw-Hill, New York, 2004, pp.9.15; 9.29; 9.41.
- 143 D. Lamprecht and A. de Klerk, Hydroisomerisation of 1-pentene to iso-pentane in a single reactor, *Mexican Congr. Chem. React. Eng. Ixtapa-Zihuatanejo, Mexico*, 2008.
- 144 P. M. Morgan, D. G. van der Merwe, R. Goosen, D. O. Leckel, H. Saayman, H. Loubser and J. J. Botha, The production of high quality base oils from Sasol hydrocrackates, *S. Afr. Mech. Eng.*, 1999, **49**, 11; V. Calemma, S. Peratello and C. Perego, Hydroisomerization and hydrocracking of long chain *n*-alkanes on Pt/amorphous SiO<sub>2</sub>-Al<sub>2</sub>O<sub>3</sub> catalyst, *Appl. Catal. A*, 2000, **190**, 207; Z. Zhou, Y. Zhang, J. W. Tierney and I. Wender, Hybrid zirconia catalysts for conversion of Fischer–Tropsch waxy products to transportation fuels, *Fuel Process. Technol.*, 2003, **83**, 67; V. Calemma, S. Peratello, F. Stroppa, R. Giardino and C. Perego, Hydrocracking and hydroisomerization of long-chain *n*-paraffins. Reactivity and reaction pathway for base oil formation, *Ind. Eng. Chem. Res.*, 2004, **43**, 934.
- 145 S. T. Sie, Acid-catalysed cracking of paraffinic hydrocarbons. 1. Discussion of existing mechanisms and proposal of a new mechanism, *Ind. Eng. Chem. Res.*, 1992, **31**, 1881; S. T. Sie, Acid-catalysed cracking of paraffinic hydrocarbons. 2. Evidence for the protonated cyclopropane mechanism from catalytic cracking experiments, *Ind. Eng. Chem. Res.*, 1993, **32**, 397; S. T. Sie, Acid-catalysed cracking of paraffinic hydrocarbons. 3. Evidence for the protonated cyclopropane mechanism from hydrocracking/hydroisomerization experiments, *Ind. Eng. Chem. Res.*, 1993, **32**, 403.
- 146 A. Billon, P.-H. Bigeard, Hydrocracking in *Petroleum Refining Vol.3 Conversion Processes*, ed. P. Leprince, Editions Technip, Paris, 2001, p.333.
- 147 G. E. Langlois, R. F. Sullivan and C. J. Egan, The effect of sulfiding a nickel on silica-alumina catalyst, *J. Phys. Chem.*, 1966, **70**, 3666; W. Böhringer, A. Kotsiopoulos, M. de Boer, C. Knottenbelt and J. C. Q. Fletcher, On the application of non-sulfided base metal catalysts for normal paraffin hydrocracking, *Proc. S. Afr. Chem. Eng. Congr. Durban*, 2006, OralPDO27.
- 148 D. O. Leckel and M. Liwanga-Ehumbu, Diesel-selective hydrocracking of an iron-based Fischer–Tropsch wax fraction (C<sub>15</sub>–C<sub>45</sub>) using a MoO<sub>3</sub>-modified noble metal catalyst, *Energy Fuels*, 2006,

- 20, 2330; D. O. Leckel, Noble metal wax hydrocracking catalysts supported on high-siliceous alumina, *Ind. Eng. Chem. Res.*, 2007, **46**, 3505.
- 149 F. J. M. Schrauwen, Shell middle distillate synthesis (SMDS) process in *Handbook of Petroleum Refining Processes*, ed. R. A. Meyers, McGraw-Hill: New York, 2004, pp. 15.25.
- 150 D. O. Leckel, Hydrocracking of iron-catalyzed Fischer–Tropsch waxes, *Energy Fuels*, 2005, **19**, 1795; D. O. Leckel, Low pressure hydrocracking of coal-derived Fischer–Tropsch waxes to fuels, *Energy Fuels*, 2007, **21**, 1425.
- 151 M. Quinlan, New product hits the road, *Petroleum Economist*, 2006, **73**(6), 7.
- 152 D. O. Leckel, Selectivity effect of oxygenates in hydrocracking of Fischer–Tropsch waxes, *Energy Fuels*, 2007, **21**, 662.
- 153 S. Zinger, The propylene market is hooked on suppliers from refineries and new technology, *World Petrochem. Conf. Houston*, 2006.
- 154 I. Kopolakis and B. W. Wojciechowski, The catalytic cracking of a Fischer–Tropsch synthesis product, *Can. J. Chem. Eng.*, 1985, **63**, 269; J. Abbot and B. W. Wojciechowski, Catalytic cracking on HY and HZSM-5 of a Fischer–Tropsch product, *Ind. Eng. Chem. Prod. Res. Dev.*, 1985, **24**, 501; T. M. Leib, J. C. W. Kuo, W. E. Garwood, D. M. Nace, W. R. Derr and S. A. Tabak, Upgrading of Fischer–Tropsch waxes to high quality transportation fuels, *AIChE Ann. Meeting, Washington DC*, 1988, paper 61d; W. J. Reagan, Gasoline range ether synthesis from light naphtha products of fluid catalytic cracking of Fischer–Tropsch wax, *Prepr. Pap.-Am. Chem. Soc. Div. Fuel Chem.*, 1994, **39**(2), 337; M. M. Schwartz, The selective catalytic cracking of Fischer–Tropsch liquids to high value transportation fuels, *DOE Contract no. DE-AC22-91PC90057 - Final report*, 1995; X. Dupain, R. A. Krul, M. Makkee and J. A. Moulijn, Are Fischer–Tropsch waxes good feedstocks for fluid catalytic cracking units?, *Catal. Today*, 2005, **106**, 288; X. Dupain, R. A. Krul, C. J. Schaverien, M. Makkee and J. A. Moulijn, Production of clean transportation fuels and lower olefins from Fischer–Tropsch synthesis waxes under fluid catalytic cracking conditions. The potential of highly paraffinic feedstocks for FCC, *Appl. Catal. B*, 2006, **63**, 277.
- 155 G. N. Choi, S. J. Kramer, S. S. Tam, J. M. Fox, III and W. J. Reagan, Fischer–Tropsch indirect coal liquefaction design/economics - mild hydrocracking vs. fluid catalytic cracking, *Prepr. Pap.-Am. Chem. Soc. Div. Fuel Chem.*, 1996, **41**(3), 1079.
- 156 R. Bonifay, C. Marcilly, Catalytic cracking in *Petroleum Refining Vol.3 Conversion Processes*, ed. P. Leprince, Editions Technip, Paris, 2001, p.169.
- 157 A. Corma, J. Planelles, J. Sánchez-Marín and F. Tomás, The role of different types of acid site in the cracking of alkanes on zeolite catalysts, *J. Catal.*, 1985, **93**, 30.
- 158 K. A. Cumming and B. W. Wojciechowski, Hydrogen transfer, coke formation, and catalyst decay and their role in the chain mechanism of catalytic cracking, *Catal. Rev.-Sci. Eng.*, 1996, **38**, 101.
- 159 K. Eng, S. Heidenreich, S. Swart and F. Möller, Clean fuels and petrochemicals at SASOL via SUPERFLEX™, *Proc. World Petrol. Congr.*, 2005, **18**, cd122.
- 160 R. Swindell, Coking in *Petroleum Refining Vol.3 Conversion Processes*, ed. P. Leprince, Editions Technip: Paris, 2001, p.381.
- 161 S. J. Blanksby and G. B. Ellison, Bond dissociation energies of organic molecules, *Acc. Chem. Res.*, 2003, **36**, 255.
- 162 A. Chauvel, G. Lefebvre, *Petrochemical processes. 1. Synthesis-gas derivatives and major hydrocarbons* Editions Technip: Paris, 1989.
- 163 P. Leprince, Visbreaking of residues in *Petroleum Refining Vol.3 Conversion Processes*, ed. P. Leprince, Editions Technip, Paris, 2001, p.365; J. G. Speight, *The chemistry and technology of petroleum*, 4th edn, CRC Press, Boca Raton, 2007.
- 164 W. A. Horne, Review of German synthetic lubricants, *Ind. Eng. Chem.*, 1950, **42**, 2428.
- 165 L. P. Dancuart, J. F. Mayer, M. J. Tallman and J. Adams, Performance of the Sasol SPD naphtha as steam cracking feedstock, *Prepr. Pap.-Am. Chem. Soc. Div. Petrol. Chem.*, 2003, **48**(2), 132.
- 166 C. S. Snodgrass and M. Perrin, The production of Fischer–Tropsch coal spirit and its improvement by cracking, *J. Inst. Petrol. Technologists*, 1938, **24**, 289.
- 167 A. de Klerk, Thermal cracking of Fischer–Tropsch waxes, *Ind. Eng. Chem. Res.*, 2007, **46**, 5516.
- 168 G. H. Dazeley and C. C. Hall, Production of olefins by the cracking of Fischer–Tropsch waxes and their conversion into lubricating oils, *Fuel*, 1948, **27**(2), 50.
- 169 V. Schneider and P. K. Frolich, Mechanism of formation of aromatics from lower paraffins, *Ind. Eng. Chem.*, 1931, **23**, 1405.
- 170 A. Kossiakoff and F. O. Rice, Thermal decomposition of hydrocarbons, resonance stabilization and isomerization of free radicals, *J. Am. Chem. Soc.*, 1943, **65**, 590.
- 171 H. H. Voge and G. M. Good, Thermal cracking of higher paraffins, *J. Am. Chem. Soc.*, 1949, **71**, 593.
- 172 J. Berkowitz, G. B. Ellison and D. Gutman, Three methods to measure RH bond energies, *J. Phys. Chem.*, 1994, **98**, 2744.
- 173 M. Lapinski, L. Baird, R. James, UOP Platforming process in *Handbook of Petroleum Refining Processes*, ed. R. A. Meyers, McGraw-Hill, New York, 2004, pp. 4.3.
- 174 G. Martino, Catalytic reforming in *Petroleum Refining Vol.3 Conversion Processes*, ed. P. Leprince, Editions Technip, Paris, 2001, p.101.
- 175 J. J. Alves and G. P. Towler, Analysis of refinery hydrogen distribution systems, *Ind. Eng. Chem. Res.*, 2002, **41**, 5759.
- 176 B. H. Davis, Alkane dehydrocyclization mechanism, *Catal. Today*, 1999, **53**, 443.
- 177 F. Zaera, Selectivity in hydrocarbon catalytic reforming: a surface chemistry perspective, *Appl. Catal. A*, 2002, **229**, 75.
- 178 M. J. Sterba and V. Haensel, Catalytic reforming, *Ind. Eng. Chem. Prod. Res. Dev.*, 1976, **15**, 2.
- 179 R. L. Peer, R. W. Bennett, D. E. Felch and E. von Schmidt, UOP Platforming leading octane technology into the 1990's, *Catal. Today*, 1993, **18**, 473; P. R. Pujadó, M. Moser, M. Catalytic reforming in *Handbook of petroleum processing*, ed. D. S. J. Jones and P. R. Pujadó, Springer, Dordrecht, 2006, p.217.
- 180 J. S. Swart, G. J. Czajkowski and R. E. Conser, Sasol upgrades Synfuels with refining technology, *Oil Gas J.*, 1981, **79**(35), 62.
- 181 J. R. Bernard, J. Nury, Method of dehydrocyclizing aliphatic hydrocarbons. United States patent 4,104,320 (1 Aug 1978).
- 182 T. R. Hughes, R. L. Jacobson, P. W. Tamm and W. C. Buss, Aromatization of hydrocarbons over platinum alkaline earth zeolites, *Stud. Surf. Sci. Catal.*, 1986, **28**, 725; T. R. Hughes, R. L. Jacobson and P. W. Tamm, Catalytic processes for octane enhancement by increasing the aromatics content of gasoline, *Stud. Surf. Sci. Catal.*, 1988, **38**, 317.
- 183 J. D. Swift, M. D. Moser, M. B. Russ and R. S. Haizmann, The RZ Platforming process: something new in aromatics technology, *Hydrocarbon Technol. Int.*, 1995, Autumn, 86.
- 184 S. J. Tauster and J. J. Steger, Molecular die catalysis: Hexane aromatization over Pt/KL, *J. Catal.*, 1990, **125**, 387.
- 185 T. Fukunaga and V. Ponc, The nature of the high sensitivity of Pt/KL catalysts to sulfur poisoning, *J. Catal.*, 1995, **157**, 550.
- 186 M. E. Dry, R. J. Nash and C. T. O'Connor, The effect of oxygenates on the n-hexane aromatization activity of Pt/KL, *Proc. 12th Int. Zeolite Conf. Baltimore*, 1998, 2557.
- 187 M. E. Dry, Practical and theoretical aspects of the catalytic Fischer–Tropsch process, *Appl. Catal. A*, 1996, **138**, 319; M. E. Dry, Present and future applications of the Fischer–Tropsch process, *Appl. Catal. A*, 2004, **276**, 1.
- 188 P. C. Mihindou-Koumba, H. S. Cerqueira, P. Magnoux and M. Guisnet, Methylcyclohexane transformation over HFAU, HBEA, and HMF1 zeolites: II. Deactivation, and coke formation, *Ind. Eng. Chem. Res.*, 2001, **40**, 1042.
- 189 N. Y. Chen and T. Y. Yan, M2 Forming - A process for aromatization of light hydrocarbons, *Ind. Eng. Chem. Process Des. Dev.*, 1986, **25**, 151.
- 190 C. M. Tsang, P.-S. Dai, F. P. Mertens and R. H. Petty, Saturation of olefinic products by hydrogen transfer during propylene conversion, *Prepr. Pap.-Am. Chem. Soc. Div. Petrol. Chem.*, 1994, **39**(3), 367.
- 191 T. Mole, J. R. Anderson and G. Creer, The reaction of propane over ZSM-5-H and ZSM-5-Zn zeolite catalysts, *Appl. Catal.*, 1985, **17**, 141.
- 192 A. de Lucas, P. Canizares, A. Durán and A. Carrero, Dealumination of HZSM-5 zeolites: Effect of steaming on acidity and aromatization activity, *Appl. Catal. A*, 1997, **154**, 221.
- 193 T. Sano, K. Suzuki, H. Shoji, S. Ikai, K. Okabe, T. Murakami, S. Shin, H. Hagiwara and H. Takaya, Dealumination of ZSM-5 zeolites with water, *Chem. Lett. Jpn.*, 1987, 1421.

- 194 A. de Klerk, Deactivation behaviour of Zn/ZSM-5 with a Fischer–Tropsch derived feedstock in *Catalysis in application*, ed. S. D. Jackson, J. S. J. Hargreaves and D. Lennon, RSC, Cambridge, 2003, p. 24.
- 195 R. J. J. Nel and A. de Klerk, Fischer–Tropsch aqueous phase refining by catalytic alcohol dehydration, *Ind. Eng. Chem. Res.*, 2007, **46**, 3558.
- 196 F. Cunill, J. Tejero, C. Fité, M. Iborra and J. F. Izquierdo, Conversion, selectivity, and kinetics of the dehydration of 1-pentanol to di-*n*-pentyl ether catalyzed by a microporous ion-exchange resin, *Ind. Eng. Chem. Res.*, 2005, **44**, 318.
- 197 H. Knözinger and R. Köhne, Catalytic dehydration of aliphatic alcohols on  $\gamma$ -Al<sub>2</sub>O<sub>3</sub>, *J. Catal.*, 1964, **3**, 559; B. Shi and B. H. Davis, Alcohol dehydration: Mechanism of ether formation using an alumina catalyst, *J. Catal.*, 1995, **157**, 359; B. Shi, H. A. Dabbagh and B. H. Davis, Alcohol dehydration. Isotope studies of the conversion of 3-pentanol, *J. Mol. Catal. A*, 1999, **141**, 257.
- 198 C. S. Cope and B. F. Dodge, Equilibria in the hydration of ethylene at elevated pressures and temperatures, *AIChE J.*, 1959, **5**, 10; C. S. Cope, Equilibria in the hydration of ethylene and of propylene, *AIChE J.*, 1964, **10**, 277.
- 199 T. Okuhara, Water-tolerant solid acid catalysts, *Chem. Rev.*, 2002, **102**, 3641.
- 200 H. Knözinger, Dehydration of alcohols on aluminum oxide, *Angew. Chem., Int. Ed.*, 1968, **7**, 791.
- 201 M. E. Winfield, Catalytic dehydration and hydration in *Catalysis Vol. VII*, ed. P. H. Emmett, Reinhold, New York, 1960, p.93.
- 202 F. H. A. Bolder and H. Mulder, Dehydration of alcohols in the presence of carbonyl compounds and carboxylic acids in a Fischer–Tropsch hydrocarbons matrix, *Appl. Catal. A*, 2006, **300**, 36.
- 203 L. M. Elkin, W. S. Fong, P. L. Morse, *Synthetic ethanol and isopropanol: Ethanol, synthetic ethanol, fermentation, isopropanol, Process Economics Program report 53A*, SRI, Menlo Park, 1979.
- 204 E. Neier and J. Woellner, Isopropyl alcohol by direct hydration, *Chemtech*, 1973, Feb, 95.
- 205 Y. Izumi, Hydration/hydrolysis by solid acids, *Catal. Today*, 1997, **33**, 371.

# Conversion of fructose to 5-hydroxymethylfurfural using ionic liquids prepared from renewable materials†

Suqin Hu, Zhaofu Zhang, Yinxi Zhou, Buxing Han,\* Honglei Fan, Wenjing Li, Jinliang Song and Ye Xie

Received 19th June 2008, Accepted 7th October 2008

First published as an Advance Article on the web 23rd October 2008

DOI: 10.1039/b810392e

Efficient conversion of fructose to 5-hydroxymethylfurfural is a key step for using carbohydrates to produce liquid fuels and value-added chemicals. Here we show that some ionic liquids synthesized from cheap renewable materials are very efficient for the conversion of fructose to HMF. The yield and selectivity could be higher than 90% as the reaction was conducted in an ethyl acetate/renewable IL biphasic system and the separation process had no cross-contamination. Moreover, the IL can be reused easily.

Diminishing fossil fuel reserves and growing concerns about global warming indicate that sustainable resources are needed in the near future.<sup>1</sup> Biomass is abundant, renewable, and is distributed widely in nature, which are promising alternatives for the sustainable supply of liquid fuels and valuable intermediates (such as alcohols, aldehydes, ketones, and carboxylic acids) to the chemical industry for production of drugs and polymeric materials.<sup>2</sup> Carbohydrates comprise the main class of biomass compounds.<sup>3</sup> Utilization of biomass requires efficient methods to convert carbohydrates into a variety of chemical compounds.<sup>4</sup>

It is known that the direct production of useful organic compounds from five and six-carbon carbohydrates is difficult. 5-Hydroxymethylfurfural (HMF **2**), which is obtained from carbohydrates (e.g. glucose, sucrose and fructose (**1**)) by dehydration, is an important “bridge” for efficient use of carbohydrates (Scheme 1).<sup>4–6</sup> As a versatile intermediate, HMF can be converted to 2,5-furandicarboxyl acid (**3**), 2,5-dihydroxy methylfuran (**4**), 2,5-bis(hydroxymethyl)tetrahydrofuran (**5**), dimethylfuran (**6**) and other liquid alkanes by oxidation, hydrogenation,

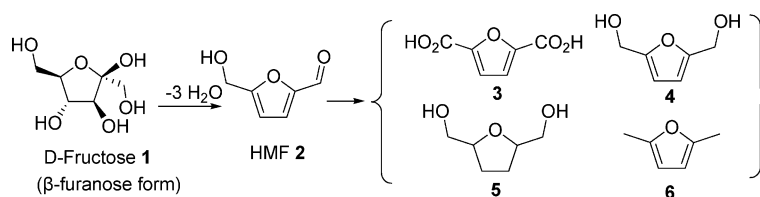
hydrogenolysis or aldol condensation.<sup>2,7</sup> The derivatives **3**, **4** and **5** can replace some important traditional building blocks to produce polyesters, and dimethylfuran **6** has a great potential for use as a liquid transportation fuel.<sup>1,3</sup>

Fructose is a carbohydrate obtained directly from biomass or by the isomerization of glucose. The conversion of fructose to HMF has been carried out in some polar organic solvents, such as dimethylsulfoxide,<sup>8</sup> dimethylformamide,<sup>9</sup> and sub-critical or high temperature water.<sup>10,11</sup> Utilization of these high-boiling point solvents of high polarity needs large amount of energy in the isolation of HMF produced, and the selectivity to HMF in water is usually low. To enhance the selectivity and facilitate the extraction of HMF, biphasic systems of water and organic solvent were used recently.<sup>1–3,12,13</sup> Mineral acid or zeolite were used as the catalysts and butanol or methylisobutylketone with boiling points of 117–118 °C as the organic phases, and processes were operated above 180 °C.<sup>1,2,13</sup>

Room temperature ionic liquids (ILs), which are organic salts with melting point of lower than 100 °C, have attracted much attention in recent years.<sup>14–18</sup> ILs have some unusual properties, such as negligible vapor pressure, nonflammability, high thermal and chemical stability, and adjustable solvent power for organic and inorganic substances. It was reported that some ILs have strong solvent power for carbohydrates.<sup>19,20</sup> With the increasing concern about the environmental protection and sustainable development, some ILs have been synthesized from biorenewable materials, such as amino acid-based<sup>21,22</sup> and choline chloride (ChoCl)-based ILs.<sup>23</sup> In addition, the structure of ILs can be designed and modified to achieve desired properties. For example, acidic ILs have been synthesized and used to catalyze chemical reactions.<sup>24</sup> Recently, Moreau *et al.* reported that 1-H-3-methyl imidazolium chloride can be used as both solvent and catalyst for the conversion of fructose to HMF with satisfactory yield.<sup>25</sup> It was found that metal halides in 1-alkyl-3-methylimidazolium chloride are effective catalysts for converting fructose to HMF, among which chromium(II) chloride was uniquely effective, leading to the conversion of glucose to HMF with a yield near 70%.<sup>4</sup>

Beijing National Laboratory for Molecular Sciences, Institute of Chemistry, Chinese Academy of Sciences, Beijing, 100080, China.  
E-mail: hanbx@iccas.ac.cn; Fax: (+) 86-10-62562821

† Electronic supplementary information (ESI) available: Materials, analysis methods, experimental procedures, structure of ILs (Scheme S1), details of ChoCl-based ILs (Table S1), and more data of the experiments in ChoCl/citric acid or in the biphasic system (Table S2 and S3). See DOI: 10.1039/b810392e



Scheme 1 HMF as the intermediate between carbohydrate and liquid fuel and value-added chemicals.



Production of HMF from fructose with efficient and green routes at mild conditions is a challenging topic of great importance. In this work we found that some ILs prepared from natural, cheap and biorenewable materials are very efficient for the conversion of fructose to HMF. Another very interesting aspect of this work is that the reaction was conducted in an ethyl acetate (AcOEt)/renewable IL biphasic system to promote the yield and selectivity without any cross-contamination, and the IL could be easily reused, which results from unique phase behavior of the reaction system.

We started our work to use a number of ILs and two pyridinium salts as both catalysts and solvents for the conversion of fructose to HMF at 80 °C for 1 h, including 1-H-3-methylimidazolium chloride ([HMim]Cl),<sup>25</sup> 1-butyl-3-methylimidazolium hydrosulfate ([BMim]HSO<sub>4</sub>), ethylammonium nitrate (EtNH<sub>3</sub>NO<sub>3</sub>), 1,1,3,3-tetramethylguanidinium trifluoroacetate (TMG TFA), 1,1,3,3-tetramethylguanidinium lactate (TMG LAC), ChoCl-based deep eutectic mixtures which also belong to ILs (Table S1 in the ESI†),<sup>23,26,27</sup> pyridine hydrochloride (PyHCl), and pyridine p-toluenesulfate (PyTSA).<sup>28</sup> They include Brønsted acids, Lewis acids (ChoCl/metal chlorides), and bases (ChoCl/urea, TMG TFA and TMG LAC). The results are presented in Fig. 1. The results indicate that most Brønsted acidic ILs were very effective for fructose conversion (91–100%) except for PyTSA and EtNH<sub>3</sub>NO<sub>3</sub>. [BMim]HSO<sub>4</sub> was most active and obtained 100% fructose conversion, 56.4% HMF yield, and some by-products such as levulinic acid, furfural were produced. The reaction mixture was solid at 80 °C as PyTSA was used due to the high melting point of PyTSA (117–119 °C), which resulted in the low yield and conversion. Although PyHCl has higher melting point than PyTSA, the reaction mixture with PyHCl at 80 °C was changed into homogeneous liquid after the reaction proceeded several minutes because PyHCl is hygroscopic and the reaction produces water. Therefore, 92.1% fructose conversion and 75.4% HMF selectivity were obtained in PyHCl and were similar to that in [HMim]Cl. The Lewis acids ZnCl<sub>2</sub> and CrCl<sub>3</sub>

in ChoCl/metal chloride ILs were not efficient in producing HMF. And as the basic ILs, ChoCl/urea, TMG TFA and TMG LAC, were not active for the conversion of fructose either.

It is interesting that some ILs prepared entirely from cheap and renewable materials, ChoCl/malonic acid, ChoCl/oxalic acid and ChoCl/citric acid monohydrate (simply called citric acid in the following), are very effective for the reaction, and the ILs are easy to prepare on the large scale.<sup>27</sup> The functional parts of these ILs are the dicarboxylic or tricarboxylic acids and have relatively stronger acidity. Above 90% fructose conversion was reached at mild condition (80 °C, 1 h). Especially, 91.1% conversion and 83.8% selectivity were obtained in ChoCl/citric acid, and citric acid can be produced on a large scale by the biochemical method using agricultural byproducts.

In the above work, the molar ratio of ILs to fructose is 5. We also studied the effect of ChoCl/citric acid or PyHCl to fructose molar ratio on the conversion and selectivity, and the best results were obtained when the molar ratios of ChoCl/citric acid or PyHCl to fructose were 5 and 6 (see the ESI†). The main reason may be that a solvation shell was formed when organic compound was surrounded by about 5 IL molecules<sup>29</sup> and it would facilitate the reaction.<sup>25</sup>

The above results indicate that ChoCl/citric acid is the best among the ILs used. We further studied the effects of reaction time and temperature on the reaction in the IL, and the results are presented in the ESI.† It was demonstrated that when the reaction time exceeded 1 h at 80 °C, the HMF yield was nearly independent of time. The fructose conversion was improved slightly, but the HMF selectivity decreased slightly as reaction time changed from 1 to 3 h. Subsequently, we tested the stability of HMF in ChoCl/citric acid at this temperature by adding 52.6 mg of HMF into 1.47 g of ChoCl/citric acid and stirred for 1 h, and 98.5% HMF could be recovered, indicating that the HMF is rather stable at the experimental condition. When temperature was increased from 70 to 100 °C, fructose conversion increased from 45.3% to 94.6%, but the

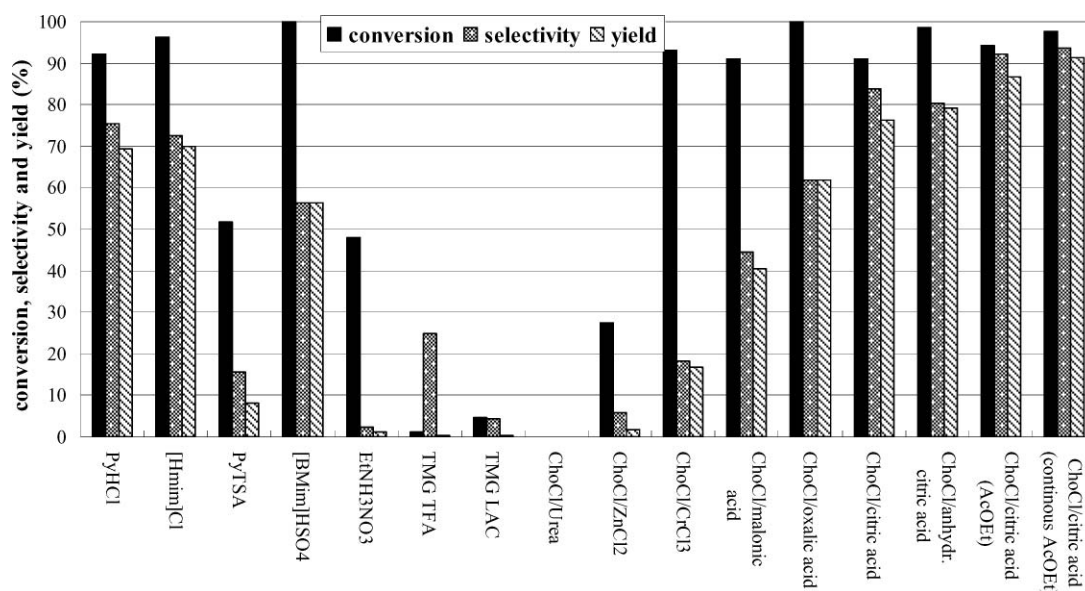


**Fig. 1** Conversion of fructose to HMF in various ILs: fructose (99%) 91.0 mg and 0.5 mmol, ILs 2.5 mmol, 80 °C, 1 h. The results of the two right columns correspond to entries 3 and 7 of Table 1.

HMF selectivity was decreased from 91.2% to 80.0%, and the highest HMF yield was obtained at 80 °C.

Considering that water may affect the reaction, we also used anhydrous citric acid to replace the citric acid monohydrate to obtain ChoCl/anhydrous citric acid. Compared with ChoCl/citric acid prepared using the hydrated citric acid, the HMF yield and fructose conversion were improved by 3% and 7%, respectively (Fig. 1). A little amount of water indeed has a negative effect on this dehydration reaction, but the effect was not significant. However, the viscosity of ChoCl/anhydrous citric acid is higher than that of ChoCl/citric acid, which is not beneficial to the mass transfer in the reaction. Moreover, production of anhydrous citric acid needs more processes and more energy cost than that of monohydrate in industry. To sum up the above information, use of the monohydrate citric acid is more advantageous than the anhydrous one, and our further study was carried out using ChoCl/citric acid.

In the second part, we concentrated on how to improve HMF yield and selectivity in ChoCl/citric acid, to facilitate the extraction of HMF and reuse of the IL. Ethyl acetate (AcOEt) is a widely-used solvent in industry because it is cheap and displays low toxicity. More interestingly, we found in this work that the product HMF is soluble in AcOEt, while the solubility of the IL and reactant fructose in AcOEt is negligible. Moreover, the reactant is soluble in the IL, and AcOEt is only slightly soluble in the IL (<1.8 wt%). This unique phase behavior is very favorable for conducting a biphasic reaction in the AcOEt/IL (ChoCl/citric acid) system because separation can be easily performed without cross contamination. In addition, the boiling point of AcOEt is relatively low, which can reduce the energy cost and avoid thermal decomposition or polymerization of the products during the product isolation process. The reaction was conducted in the biphasic system at 80 °C in batch style (Fig. 2A) with a reaction time of 1 h, and results are presented in Table 1. In this system, the product HMF was extracted by AcOEt, and fructose existed in the IL-rich phase. The HMF yield reached 86.8%, which is 9% larger than that without use of AcOEt (Table 1, entries 1 and 3). Especially, the selectivity exceeded 90% (Table 1, entries 2–4). Table 1 also indicates that, as expected, addition of more AcOEt is favorable to the extraction of the product. It should be known that the percent of extraction was less than 65% because HMF distributes between the AcOEt phase and the IL phase.

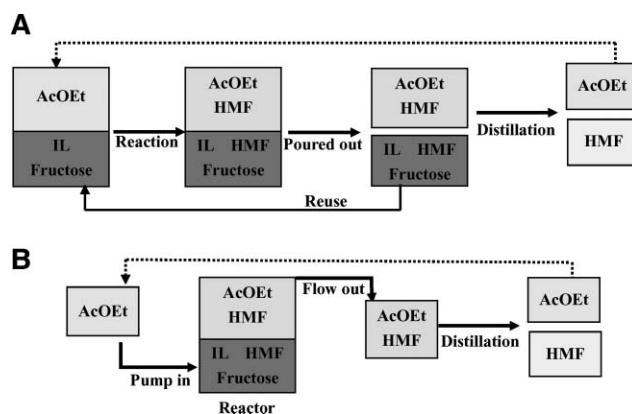


**Fig. 2** (A) Process of the biphasic system. It shows the formation of the biphasic system of AcOEt and ChoCl/citric acid (IL); the reaction in the system; the separation of the two phases and reuse of IL phase; the distillation of AcOEt to obtain HMF and recycle of AcOEt. (B) Sketch for continuous extraction process by pumping AcOEt during the reaction. AcOEt was pumped into the reactor; the biphasic system was formed; the solution of HMF in AcOEt flowed out; separation of HMF and AcOEt by distillation and recycle of AcOEt.

We also explored the intermittent extraction during the biphasic reaction: adding fresh AcOEt ( $W_{\text{AcOEt}}/W_{\text{IL}} = 1$ ) into the IL phase in the beginning of the reaction, pouring the AcOEt phase out after the biphasic system had reacted for 20 min at 80 °C, repeating two times and the total reaction time was 1 h (Table 1, entry 5). The total amount of AcOEt and reaction time were the same as that of the reaction at  $W_{\text{AcOEt}}/W_{\text{IL}} = 3$  with a reaction time of 1 h (Table 1, entry 4). Clearly, the yield in AcOEt of the intermittent extraction process was higher than that of the batch process, although the total yields of the two processes were nearly the same. Based on this result, we developed a continuous extraction route in which fresh AcOEt (0.2 mL/min) was pumped into the IL mixture after the reaction had run for the desired time (Fig. 2B). The AcOEt phase began to flow out from the reactor after pumping AcOEt for 15 min. The reaction and pumping of AcOEt lasted until the total reaction time reached 1 h. In this manipulation 91.4% HMF yield was obtained and the percent of extraction reached 70–80% (Table 1, entries 6 and 7). Compared with the intermittent extraction, the continuous route used a greater amount of AcOEt, but it was easier to manipulate. Both styles of extraction can extract most

**Table 1** HMF converted from fructose in the biphasic system of AcOEt and ChoCl/citric acid. The experiments were carried out at 80 °C for 1 h with 91.0 mg of fructose (99%) and 1.47 g of ChoCl/citric acid

Entry	$W_{\text{AcOEt}}/W_{\text{IL}}^a$	Total yield (%)	Conversion (%)	Selectivity (%)	Yield in AcOEt (%)	Extraction rate $^b$ (%)
1	0	77.8	93.2	83.5	—	—
2 <sup>c</sup>	1	85.4	92.5	92.3	31.9	37.4
3 <sup>c</sup>	2	86.8	94.2	92.1	47.7	55.0
4 <sup>c</sup>	3	85.6	93.2	91.8	55.6	64.9
5 <sup>d</sup>	1 + 1 + 1	82.1	91.7	89.5	63.0	77.0
6 <sup>e</sup>	6.1	80.7	89.8	89.9	64.3	80.0
7 <sup>e</sup>	4.9	91.4	97.6	93.6	66.0	72.2

<sup>a</sup>  $W_{\text{AcOEt}}/W_{\text{IL}}$  is the ratio of weight of AcOEt to weight of IL. <sup>b</sup> Extraction rate is the ratio of yield in AcOEt to the total yield. <sup>c</sup> AcOEt was added into the IL phase in the beginning of the reaction. <sup>d</sup> The intermittent extraction: fresh AcOEt ( $W_{\text{AcOEt}}/W_{\text{IL}} = 1$ ) added into the IL phase and the AcOEt phase poured out after the biphasic system reacted for 20 min, repeated 2 times and the total reaction time was 1 h. <sup>e</sup> The continuous extraction: AcOEt (0.2 mL/min) pumped into the IL mixture after the reaction had run for 10 and 20 min, respectively.

of the HMF out from the IL. After extraction the product HMF can be isolated easily from AcOEt because the amounts of IL and reactant in AcOEt are negligible as discussed above. The AcOEt could be reused (Fig. 2).

The IL can be reused directly after pouring out the AcOEt phase from the reactor. Fig. 3 gives the results for the reuse of the IL. The cycles were processed in both intermittent and continuous extracting manipulations. We examined the amount of HMF in AcOEt which represents the factual obtained amount of HMF after separation. The recycled IL still had a very high activity. The amount of HMF in AcOEt of Run 2 was more than that of Run 1 due to the direct reuse of IL which contained residual HMF. After repeating the run several times, the yield decreased slightly. This was due to the increase of water content in the IL because the reaction produced water. The water has a very important effect on the dehydration. It was shown above that the HMF yield in ChoCl/citric acid anhydrous was more than that in the ChoCl/citric acid monohydrate. After repeating the run 3 times, about 0.072 g water was produced and was equal to 4 mmol, which was 8 times the fructose in mole; enough to affect the dehydration. This was confirmed by the fact that the activity of the IL reached the level of that in the first run after being dried under vacuum at 50 °C for 24 h.

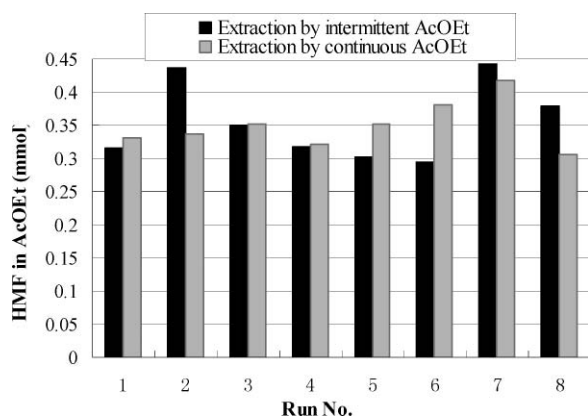


**Fig. 3** ■ The results of recycling of ChoCl/citric acid in the system of intermittent extraction. The condition was the same as that of entry 5 in Table 1. After the 6th run, the IL phase was dried to remove water under vacuum at 50 °C for 24 h and used for the next run, indicating that the yield increased after the water was removed. ■ The results of recycling of ChoCl/citric acid in the system of continuous extraction by pumping AcOEt during the reaction. After the 4th run, the IL phase was dried to remove water under vacuum at 50 °C for 24 h and used for the next run, indicating that the yield increased after the water was removed. The condition was same as that of entry 7 in Table 1.

In summary we found that some ILs prepared from natural, cheap and biorenewable materials are very efficient for the conversion of fructose to HMF. Another very interesting aspect of this work is that the reaction was conducted in an ethyl acetate/renewable IL biphasic system to promote the yield and selectivity to 90% without any cross-contamination, and the IL

could be easily reused, which results from the unique phase behavior of the reaction system.

## Acknowledgements

The work was supported by National Natural Science Foundation of China (20533010) and Chinese Academy of Sciences (KJCX2.YW.H16).

## Notes and references

- 1 Y. Róman-Leshkov, C. J. Barrett, Z. Y. Liu and J. A. Dumesic, *Nature*, 2007, **447**, 982.
- 2 Y. Róman-Leshkov, J. N. Chheda and J. A. Dumesic, *Science*, 2006, **312**, 1933.
- 3 J. N. Chheda, G. W. Huber and J. A. Dumesic, *Angew. Chem. Int. Ed.*, 2007, **46**, 7164.
- 4 H. B. Zhao, J. E. Holladay, H. Brown and Z. C. Zhang, *Science*, 2007, **316**, 1597.
- 5 T. Werpy and G. Petersen, *Top Value Added Chemicals from Biomass*, U. S. Department, of Energy report No. DOE/GO-102004-1992, Golden, CO, 2004 ([www.Osti.gov/bridge](http://www.Osti.gov/bridge)).
- 6 M. Biker, J. Hirth and H. Vogel, *Green Chem.*, 2003, **5**, 280.
- 7 G. W. Huber, J. N. Chheda, C. J. Barrett and J. A. Dumesic, *Science*, 2005, **308**, 1446.
- 8 Y. Nakamura and S. Morikawa, *Bull. Chem. Soc. Jpn.*, 1980, **53**, 3705.
- 9 K. Seri, Y. Inoue and H. Ishida, *Chem. Lett.*, 2000, 22.
- 10 (a) K. Seri, Y. Inoue and H. Ishida, *Bull. Chem. Soc. Jpn.*, 2001, **74**, 1145; (b) F. S. Asghari and H. Yoshida, *Carbohydr. Res.*, 2006, **341**, 2379.
- 11 F. S. Asghari and H. Yoshida, *Ind. Eng. Chem. Res.*, 2006, **45**, 2163.
- 12 J. N. Chheda, Y. Róman-Leshkov and J. A. Dumesic, *Green Chem.*, 2007, **9**, 342.
- 13 C. Moreau, R. Durand, S. Razigade, J. Duhamet, P. Faugeras, P. Rivalier, P. Ros and G. Avignon, *Appl. Catal. A: Gen.*, 1996, **145**, 211.
- 14 T. Welton, *Chem. Rev.*, 1999, **99**, 2071.
- 15 P. Wasserscheid and T. Welton, *Ionic liquids in synthesis*, Wiley-VCH, 2003.
- 16 R. D. Rogers and K. R. Seddon, *Science*, 2003, **302**, 792.
- 17 T. G. Youngs, J. D. Holbrey, M. Deetlefs, M. Nieuwenhuyzen and C. Hardacre, *ChemPhysChem.*, 2006, **7**, 2279.
- 18 C. Villagrán, M. Deetlefs, W. R. Pitner and C. Hardacre, *Anal. Chem.*, 2004, **76**, 2118.
- 19 R. P. Swatloski, S. K. Spear, J. D. Holbrey and R. D. Rogers, *J. Am. Chem. Soc.*, 2002, **124**, 4974.
- 20 A. P. Abbott, T. J. Bell, S. Handa and B. Stoddart, *Green Chem.*, 2005, **7**, 705.
- 21 K. Fukumoto, M. Yoshizawa and H. Ohno, *J. Am. Chem. Soc.*, 2005, **127**, 2398.
- 22 G. H. Tao, L. He, W. S. Liu, L. Xu, W. Xiong, T. Wang and Y. Kou, *Green Chem.*, 2006, **8**, 639.
- 23 M. Avalos, R. Babiano, P. Cintas, J. L. Jiménez and J. C. Palacios, *Angew. Chem. Int. Ed.*, 2006, **45**, 3904.
- 24 A. C. Cole, J. L. Jensen, I. Ntai, K. L. T. Tran, K. J. Weaver, D. C. Forbes and J. H. Davis, Jr., *J. Am. Chem. Soc.*, 2002, **124**, 5962.
- 25 C. Moreau, A. Finiels and L. Vanoye, *J. Mol. Catal. A: Chem.*, 2006, **253**, 165.
- 26 A. P. Abbott, G. Capper, D. L. Davies, R. K. Rasheed and V. Tambyrajah, *Chem. Comm.*, 2003, 70.
- 27 A. P. Abbott, D. Boothby, G. Capper, D. L. Davies and R. K. Rasheed, *J. Am. Chem. Soc.*, 2004, **126**, 9142.
- 28 C. Fayet and J. Gelas, *Carbohydr. Res.*, 1983, **122**, 59.
- 29 A. Chagnes, H. Allouchi, B. Carré and D. Lemordant, *Solid State Ionics*, 2005, **176**, 1419.

# Waste-free process for continuous flow enzymatic esterification using a double pervaporation system

László Gubicza,\* Katalin Bélafi-Bakó, Erika Fehér and Tamás Fráter

Received 13th June 2008, Accepted 7th October 2008

First published as an Advance Article on the web 17th October 2008

DOI: 10.1039/b810009h

The enzyme catalytic esterification reaction of acetic acid and ethanol in [bmim]PF<sub>6</sub> ionic liquid was studied to manufacture natural ethyl acetate by a continuous waste-free process. The optimal parameters of the reaction were determined in batch experiments, and then a continuous set-up was constructed. Ethyl acetate and water formed in the bioreactor were removed by a double pervaporation system using hydrophobic and hydrophilic membranes, respectively. Acetic acid and ethanol were added as they were consumed, thus steady state concentrations in the reactor were maintained and continuous operation for 72 hours long was ensured without any activity loss of the enzyme.

## 1. Introduction

During the last few decades much attention has been paid to the development of new, environmentally friendly solvents. Two new groups of media seem to fulfil the criteria of green principles: ionic liquids (ILs)<sup>1</sup> and supercritical fluids (SCFs).<sup>2</sup> The unique properties of both media are well known from the literature.<sup>3–6</sup> ILs and SCFs can be considered as ideal tailor-made solvents. In the case of ILs the physical and chemical properties, including their polarity, hydrophobicity, viscosity and solvent miscibility can be finely tuned by altering the cation, anion and attached substituents. An ionic liquid can be designed for specific reaction conditions, to modify the enzyme selectivity, or to tailor the reaction rate. SCFs are also highly tuneable media whereby temperature, pressure and density may be altered over a wide range.<sup>7–10</sup>

The increasing demand for clean processes has led to the discovery that biotransformations can also be carried out in ILs and SCFs media. Enzymatic reactions in ILs and SCFs have been investigated over the last few years and a number of critical reviews are available on this special topic.<sup>11–14</sup> The combination of the two media offers an interesting opportunity: SCFs for solute recovery from enzymatic reactions carried out in ILs.<sup>8,15</sup> In particular, reactions catalyzed by lipases and hydrolases have been widely investigated in these solvents. Numerous research has studied the enzymatic production of natural flavour esters. These reactions were realised in organic solvents, solvent-free systems and in the last few years in ILs and SCFs.<sup>16–19</sup> The most

important parameters such as type of enzyme and solvent, effect of acid to alcohol molar ratio, reaction temperature and water activity of the reaction mixture were studied using different model reactions. Only a little attention has been paid to the separation procedure which may be a complicated task in the case of mixtures consisting of acids, alcohols, water and esters due to the formation of azeotropic mixtures.<sup>20,21</sup> The down stream process can be simplified and water production can be avoided by using activated acyl-donors such as vinyl esters instead of acid.<sup>8,18</sup> In the case of natural flavour ester production, however, *natural starting reagents* should be used and the water production can not be avoided. Several methods are known to control water content during the esterification reaction, but these allow only a batch wise process.<sup>21–24</sup> The continuous flow esterification process, where simultaneous removal of both water and ester is realised without any further separation procedure, has not been published in the literature so far.

In this article we describe a general solution to this problem based on the coupling of enzymatic esterification in a bioreactor and a double pervaporation system for continuous products removal. The esterification of acetic acid and ethanol in the presence of a lipase enzyme was studied as a model reaction to demonstrate the applicability of this concept.

## 2. Experimental

### 2.1. Materials

Novozym 435 (immobilised *Candida antarctica* lipase B, CALB) was kindly donated by Novozymes (Bagsvaerd, Denmark). Ionic liquid 1-butyl-3-methylimidazolium hexafluorophosphate ([bmim]PF<sub>6</sub>) (99%) was purchased from IoLiTech GmbH (Denzlingen, Germany). Acetic acid (99–100%), ethanol (99.7%), potassium hydroxide, n-hexane (96%) and other solvents (reagent grade) were from Spektrum 3D Ltd. (Debrecen, Hungary). The membranes “Pervap 2201” and “Pervap 2255–50” were kind gifts from Sulzer Chemtech Ltd. (Winterthur, Switzerland).

### 2.2. Esterification in batch system

Batch experiments were carried out in Eppendorf tubes (1.5 cm<sup>3</sup>). In a typical experiment 5 cm<sup>3</sup> reaction mixture (11.25 mmol ethanol, 3.75 mmol acetic acid and 5.0 mmol water dissolved in [bmim]PF<sub>6</sub>) was prepared in a volumetric flask, and the Eppendorf tubes were filled with 1 cm<sup>3</sup> of the reaction mixture each. The CALB enzyme (50 mg) was added to initiate the reaction. The tubes were incubated at 30–60 °C temperature

Research Institute for Chemical and Process Engineering, University of Pannonia, 8200, Veszprém, Hungary. E-mail: gubicza@mukki.richem.hu; Tel: +36 88 624044; Fax: +36 88 624038



range and shaken at 200 rpm in a GFL 3031 temperature-controlled incubator shaker (GFL GmbH, Burgwedel, Germany). After certain intervals the whole content of an Eppendorf tube was processed by extraction with n-hexane prior to the analysis ( $3 \times 3 \text{ cm}^3$  n-hexane extracts were collected and completed to  $10.0 \text{ cm}^3$  with n-hexane). Blank experiments were performed in the absence of CAL B and no reaction was detected.

### 2.3. Esterification in integrated system

The scheme of the whole reaction system is shown in Fig. 1. The reactor (1) was a magnetic-stirred double-wall vessel ( $150 \text{ cm}^3$ ). An intensive cooler (2) was used to avoid the evaporation of the volatile compounds. The reaction mixture (consisting typically  $2.25 \text{ mol/dm}^3$  ethanol,  $0.75 \text{ mol/dm}^3$  acetic acid and  $1\text{--}2 \text{ mol/dm}^3$  water) was circulated through the pervaporation units equipped with hydrophobic (4) ( $200 \text{ cm}^2$ ) and hydrophilic (5) ( $12 \text{ cm}^2$ ) membranes using a peristaltic pump (3). Both the reactor and the membrane units were thermostated. A vacuum pump (12) was used to keep the system under constant vacuum ( $20 \text{ mmHg}$ ). The permeates were condensed in traps (6) and (7) chilled by dry ice. Further traps (8–11) filled with silicon oil and zeolite were used to protect the vacuum pump from impurities. The pressure in the system was monitored by a manometer (13). For the supplement of the substrates consumed in the reaction, acetic acid and ethanol were fed into the reaction mixture from their storage tanks (14, 15) by peristaltic pumps (16, 17).

### 2.4. Analytical methods

A Hewlett-Packard 5890 GC equipped with HP-FFAP column (Macherey-Nagel) and FID detector was used to determine the composition of the samples (split:  $70 \text{ kPa}$ ,  $\text{N}_2$ :  $19 \text{ cm}^3/\text{min}$ ). Water content of the samples was measured by a Mettler Toledo DL31 type Karl Fischer titrator. The acetic acid content was determined by KOH titration. The samples were diluted with  $5 \text{ cm}^3$  ethanol, titrated by  $0.1 \text{ M}$  KOH in ethanol with Metrohm 785 automata titrator.

## 3. Results and discussion

### 3.1. Results of the batch measurements

Batch wise experiments were carried out to manufacture ethyl acetate with CAL B enzyme and to determine the optimal parameters regarding yield. To design the experiments the information available in the literature for production of similar flavour esters was used. [Bmim]PF<sub>6</sub> ionic liquid was selected as solvent, which was found to be a suitable solvent for several enzyme catalytic reactions. (It is known that degradation of [bmim]PF<sub>6</sub> may occur at higher temperature,<sup>25</sup> but we did not observe any signs of it either in the batch or in the continuous measurements.) The molar ratio of acetic acid–ethanol significantly influenced the yield, since acetic acid has a strong inhibition effect on lipases.<sup>16,18</sup> When an equimolar mixture was applied only 40% ester yield was obtained after 24 hours reaction time. Increasing the amount of alcohol, the yield grew, then beyond 1:3 acid–alcohol molar ratio there was practically no further rise. Therefore this ratio was used in the subsequent experiments.

The initial water content of the reaction mixture also has a strong effect on the progress of the reaction—as was expected.<sup>27,28</sup> Its concentration was varied between 0.5–5.0%. Increasing the initial water content, the initial reaction rate became higher and higher up to 3%, however it showed a considerable decrease at 5%. In this range, around 90% ester yield was obtained. The phenomenon can be explained by the fact that, in the case of the smallest initial water content, the degree of enzyme hydration is not enough for its optimal operation in the beginning of the reaction.<sup>28</sup> Its level, however, grows with the reaction time since water is being formed in the reaction, which may shift the equilibrium at high water content towards the direction of hydrolysis.<sup>27</sup> Thus controlling the water content is very important for effective production of ethyl acetate.

The increase of the reaction temperature definitely enhanced the ethyl acetate yield obtained in a certain time. It is known that the thermostability of CAL B enzyme is better in [bmim]PF<sub>6</sub> ionic liquid than in organic solvents.<sup>11,26</sup> Our primary aim was

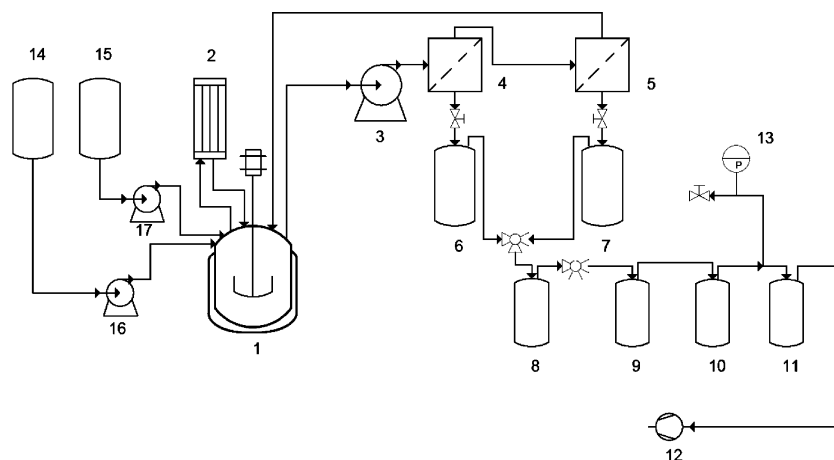


**Fig. 1** System for the continuous enzymatic production of ethyl acetate. 1—Reaction vessel with stirrer; 2—cooler; 3, 16, 17—peristaltic pumps; 4—hydrophobic membrane unit; 5—hydrophilic membrane unit; 6, 7—cooled traps; 8, 9, 10, 11—traps for pump defence; 12—vacuum pump; 13—manometer; 14—ethanol tank; 15—acetic acid tank.

**Table 1** Fluxes of the compounds through the hydrophilic and the hydrophobic membranes

Component	J (mol/m <sup>2</sup> ×h)	
	Hydrophilic membrane	Hydrophobic membrane
Acetic acid	0.004	0.095
Ethanol	0.010	0.581
Ethyl acetate	—	7.505
Water	0.448	—

to confirm the applicability of the integrated system, therefore 40 °C reaction temperature was used, where 86% ethyl acetate yield was obtained in the batch system during 5 hours reaction time. The stability of the enzyme was found to be extremely high in [bmim]PF<sub>6</sub>: after 10 times recycling there was no measurable activity loss.

In the first pervaporation experiments, the most important characteristics of the two membranes (flux and selectivity) were determined using model reaction mixtures. The composition of the reaction mixture was measured every two hours, and after an 8 hour operation the permeates of the hydrophilic and hydrophobic membranes were analyzed as well. From these results, the molar fluxes (J) were calculated and shown in Table 1.

It can be seen that the two membranes removed both the ethyl acetate and the water with a satisfactory flux, while for the other components, ethanol and acetic acid, this was a magnitude lower, which showed that the flux and selectivity properties of these membranes were suitable for the planned integrated process. In this work we did not intend to determine the optimal parameters of the pervaporation, the aim was simply to confirm that continuous removal of the products is possible in this way. It turned out that the ionic liquid was totally rejected by the pervaporation membranes—as was expected from the earlier measurements published in the literature.<sup>21,26</sup>

### 3.2. Experiments with pervaporation and without feed

After the batch experiments, a semi-continuous system was built up where both products were removed by the membranes. The reactions were performed in [bmim]PF<sub>6</sub>, at 40 °C temperature, 10 g/dm<sup>3</sup> enzyme concentration, 1:3 acid/alcohol molar ratio and 2% water content. In the beginning of the reaction, enzyme was added, and then the pervaporation modules were turned on. No substrates (ethanol or acetic acid) were fed into the mixture during the reaction. The concentration profiles obtained at 40 °C are shown in Fig. 2. It can be observed that the concentration of ethyl acetate increased in the first five hours of the experiment (up to 0.45 mol/dm<sup>3</sup>) because of the high initial reaction rate, then it decreased slightly. However, the water content of the reaction mixture started to decrease after 2 hours, indicating that the initial hydration level of the enzyme was not complete. Thus, in the first 2 hours, enzyme was binding water in its monomolecular layer. (In the figure the dotted line shows the water concentration data, which would have been obtained without water removal.) As a consequence, the applied 200 cm<sup>2</sup> hydrophilic and 22 cm<sup>2</sup> hydrophobic membranes were sufficient for the removal of water and ethyl acetate, respectively.

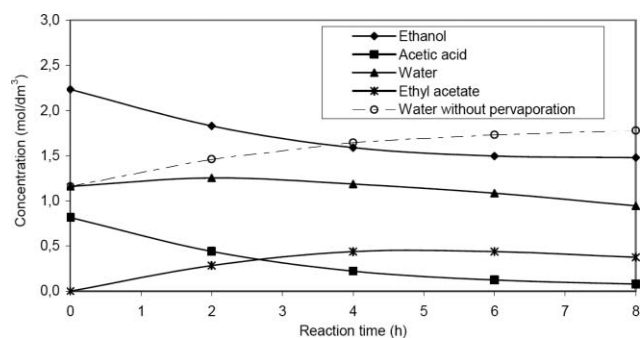


**Fig. 2** Concentration profiles during the batch experiments with pervaporation and without feed ( $T = 40\text{ }^{\circ}\text{C}$ , alcohol/acid molar ratio = 3:1, enzyme concentration = 10 g/dm<sup>3</sup>).

### 3.3. Experiments in continuous system

To realise the desired continuous system, besides the removal of the products, substrate feed was also applied with an adequate rate. Our aim was to achieve steady state concentrations of each compound, so only a minor fluctuation in the composition of the reaction mixture is allowed. According to *LeChatelier's law* for the equilibrium, the maximal reaction rate is achieved at zero product concentration, where all products are removed just after their formation in the reaction. However, in an enzymatic reaction, appropriate water content has to be set for the efficient hydration of the enzyme, thus, only the excess of water has to be removed.

The concentration profiles and the set levels of the compounds of the reaction are shown in Fig. 3. The experiments were carried out altogether over 72 hours, while the formation and removal of ethyl acetate and water were maintained at the same level, and the activity of the enzyme did not change, showing the extreme stability of the enzyme in this ionic liquid. It can be observed that the integration of enzymatic esterification and product removal by the double pervaporation system was successful and continuous operation is possible.

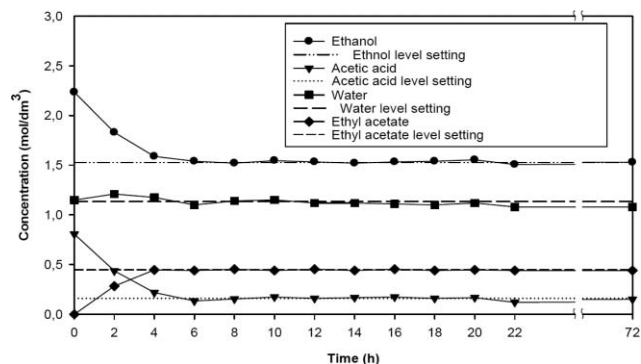


**Fig. 3** Concentration profiles and set levels of the compounds in a 72 hour reaction by both product removal and substrate feed.

## 4. Conclusions

The methodology developed is very promising for the sustainable synthetic biocatalysis in non-conventional media. The operation stability of the enzymes in an appropriate ionic liquid medium is much higher in many cases than in organic

solvents,<sup>11,26</sup> therefore it is worthwhile to develop a continuous system using these stable enzymes. Continuous operation can be maintained by applying continuous reagent feeding and product removal. During the enzymatic manufacture of ethyl acetate from ethanol and acetic acid the activity of the enzyme did not change in the 72 hours reaction time. Ethanol, water and ethyl acetate (both produced in the reaction) form ternary azeotropic mixture, and its separation by e.g. distillation is a complicated, high-energy process, moreover a by-product forms. Using the double pervaporation system the products (ethyl acetate and water) were able to be removed by an environmentally-safe membrane process having a low energy demand. This pervaporation assisted continuous process can be suitable for application to other similar procedures. More compounds and products can be selectively separated by using special membranes, while control of the hydration level of the enzyme can be accomplished by water removal.

## References

- 1 T. Welton, *Green Chem.*, 2008, **10**, 483.
- 2 G. Brunner, *J. Food Eng.*, 2005, **67**, 21–23.
- 3 P. Wasserscheid, T. Welton, (Eds), *Ionic Liquids in Synthesis*, Wiley-VCH, Weinheim, 1<sup>st</sup> edn., 2002.
- 4 P. G. Jessop, W. Leitner, (Eds), *Chemical Synthesis Using Supercritical Fluids*, Wiley-VCH, Weinheim, 1<sup>st</sup> edn., 1999.
- 5 S. Keskin, D. Kayrak-Talay, U. Akman and Ö. Hortascu, *J. Supercrit. Fluid.*, 2007, **43**, 150–180.
- 6 S. Liu and J. Xiao, *J. Mol. Catal. A-Chem.*, 2007, **270**, 1–43.
- 7 D. Das, A. Dasgupta and P. K. Das, *Tetrahedron Lett.*, 2007, **48**, 5635–5639.
- 8 F. J. Hernández, A. P. de los Ríos, D. Gómez, M. Rubio and G. Villora, *Appl. Catal. B-Environ.*, 2006, **67**, 121–126.
- 9 J. Durand, E. Teuma and M. Gómez, *CR. Chim.*, 2007, **10**, 152–177.
- 10 Z. C. Zhang, *Adv. Catal.*, 2006, **49**, 153–237.
- 11 F. van Rantwijk, R. M. Lau and R. A. Sheldon, *Trends Biotechnol.*, 2003, **21**, 131–138.
- 12 J. R. Harjani, P. U. Naik, S. J. Nara and M. M. Sulankhe, *Curr. Org. Synth.*, 2007, **4**, 354–369.
- 13 P. Lozano, G. Villora, D. Gomez, A. B. Gayo, J. A. Sánchez-Conesa, M. Rubio and J. L. Iborra, *J. Supercrit. Fluid.*, 2004, **29**, 121–128.
- 14 R. Bogel-Lukasik, *Monats. Chem.*, 2007, **138**, 1137–1144.
- 15 S. Cantone, U. Hanefeld and A. Basso, *Green Chem.*, 2007, **9**, 954–971.
- 16 A. Güvenc, N. Kapucu, H. Kapucu, Ö. Aydoğan and Ü. Mehmetoglu, *Enzyme Microb. Tech.*, 2007, **40**, 778–785.
- 17 M. Karra-Chaabouni, H. Ghamgui, S. Bezzine, A. Rekik and Y. Garggouri, *Proc. Biochem.*, 2006, **41**, 1692–1698.
- 18 M. D. Romero, L. Calvo, C. Alba, M. Habulin, M. Primozić and Z. Knez, *J. Supercrit. Fluid.*, 2005, **33**, 77–84.
- 19 R. Bogel-Lukasik, N. M. T. Lourenço, P. Vidinha, M. D. R. G. da Silva, C. A. M. Afonso, M. N. da Ponte and S. Barreiros, *Green Chem.*, 2008, **10**, 243–248.
- 20 R. Bogel-Lukasik, V. Najdanovic-Visak, S. Barreiros and M. N. da Ponte, *Ind. Eng. Chem. Res.*, 2008, **47**, 4473–4480.
- 21 P. Izak, N. M. M. Mateus, C. A. M. Afonso and J. G. Crespo, *Sep. Purif. Technol.*, 2005, **41**, 141–145.
- 22 D. J. Benedict, S. J. Parulekar and S. -P. Tsai, *J. Membrane Sci.*, 2006, **281**, 435–445.
- 23 L. Gubicza, N. Nemestóthy, T. Fráter and K. Bélafi-Bakó, *Green Chem.*, 2003, **5**, 236–239.
- 24 M. Noel, P. Lozano, M. Vaultier and J. L. Iborra, *Biotechn. Lett.*, 2004, **26**, 301–306.
- 25 R. P. Swatloski, J. D. Holbrey and R. D. Rogers, *Green Chem.*, 2003, **5**, 361–365.
- 26 O. Ulbert, K. Bélafi-Bakó, K. Tonova and L. Gubicza, *Biocatal. Biotransfor.*, 2005, **23**, 177–183.
- 27 E. J. Günter and A. Zoor, *Biotechnol. Lett.*, 2008, **30**, 925–928.
- 28 D. Barahona, P. H. Pfromm and M. E. Rezac, *Biotechnol. Bioeng.*, 2006, **93**, 318–324.

# Facile solvent free synthesis of polymerised sucrose functionalised polyoxyethylene (23) lauryl ether by microwave irradiation†

Kamalesh Prasad,<sup>\*a</sup> P. Bahadur,<sup>b</sup> Ramavatar Meena<sup>a</sup> and A. K. Siddhanta<sup>a</sup>

Received 20th June 2008, Accepted 10th October 2008

First published as an Advance Article on the web 17th October 2008

DOI: 10.1039/b810514f

One-pot solvent free synthesis of a polymerised sucrose and polyoxyethylene (23) lauryl ether based viscous surfactant by microwave irradiation was achieved.

## Introduction

Recent investigations have shown the possibility for preparation of new gelling materials, similar to those observed in polymer–surfactant systems obtained by mixing surfactants (or lipids) and proteins or polysaccharides in water.<sup>1–4</sup> However, such studies are mainly focused on the possibility to finely tune the properties of gels, solutions and pastes for specific purposes. Studies reported so far deal essentially with water soluble polymers and provide newer means to get new materials including solutions, gels and pastes.<sup>5,6</sup> Surfactants are also being extensively utilised in preparation of various new materials. Temperature responsive hydrogels grafted with an anionic surfactant have been reported by Noguchi *et al.*<sup>7</sup> Surfactants can be modified to impart viscoelasticity and are commonly prepared by mixing in appropriate amounts of anionic, cationic, nonionic and zwitterionic ones either alone or with some polyelectrolytes.<sup>8,9</sup>

Polyoxyethylene (23) lauryl ether or Brij<sup>®</sup> 35 is an extensively studied nonionic surfactant and finds many applications including dissolution of polymers and extraction of proteins from membranes.<sup>10,11</sup>

The microwave irradiation (MW) technique for chemical syntheses has been popular in recent years and there are

many reports of the preparation of new materials using this technique.<sup>12–15</sup> It was found that the rate of reactions and yield of product for the reactions carried out by MW irradiation is superior to the conventional heating techniques.<sup>14,16</sup> MW synthesis for surfactants has not been popular so far except for one report of the technique being used effectively in the synthesis of a polymeric surfactant.<sup>17</sup> It is to be noted that the processes for synthesis of industrially important surfactants require the use of many harmful organic solvents, chemicals, catalysts *etc.* and many of them often consist of a number of steps.

We herein report a facile method for the solvent free synthesis of a polymerised sucrose functionalised polyoxyethylene (23) lauryl ether surfactant, which is highly viscous in nature. Such high viscosity surfactants are useful in polyurethane foam preparation.<sup>18</sup> Attempts are also made to show the self assembly of the surfactant which forms micro spheres. Such assemblies can be useful for drug delivery applications.<sup>19</sup> To the best of our knowledge, this is the first demonstration of the preparation of a viscous surfactant by this simple and one pot manner using this technique (MW). This work will also help to popularise the microwave irradiation technique as an alternative tool to carry out solvent free syntheses in much shorter durations.

The techniques of various analyses can be found in the ESI.†

## Results and discussion

Initially, 10.2 g (29.82 mmol) of sucrose and 11.98 g (10 mmol) of polyoxyethylene (23) lauryl ether were mixed under stirring at 95 °C until a clear solution was obtained followed by addition of 0.015 g (0.0023 mol/L) of potassium persulfate (KPS), and the reaction mixture was microwave irradiated (Star-R, Milestone, Italy) at 120 °C for 300 s with constant stirring. The molar ratio of sucrose to polyoxyethylene (23) lauryl ether was optimized to 1:0.33 to get a stable viscous surfactant. The color of the reaction mixture turned yellowish indicating formation of product which upon precipitation in isopropyl alcohol (IPA) gave the final viscous surfactant (1) (Fig. 1).

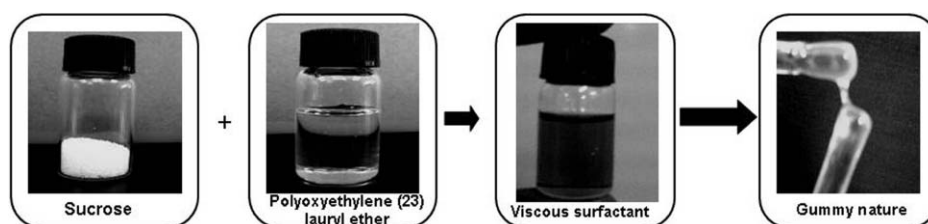


Fig. 1 Photograph of viscous surfactant (1) along with sucrose and polyoxyethylene (23) lauryl ether.

<sup>a</sup>Marine Biotechnology and Ecology Discipline, Central Salt and Marine Chemicals Research Institute (Council of Scientific and Industrial Research), Bhavangar, 364 002, India. E-mail: kamlesh@csmcri.org, drkamaleshp@gmail.com; Fax: +91-278-2567562/2566970; Tel: +91-278-2561354/2567760

<sup>b</sup>Department of Chemistry, Veer Narmad South Gujarat University, Surat, India

† Electronic supplementary information (ESI) available: Syntheses and experimental details, and supplementary figures. See DOI: 10.1039/b810514f



The product was characterized by SEM, XRD, DSC, TGA, GPC and NMR. The yield of the product was 8.8 g. The detailed experimentation for optimization of reaction parameters for the synthesis can be found in the ESI.† In order to get the surfactant with maximum purity, the products obtained by the reaction of sucrose to polyoxyethylene (23) lauryl ether in various molar ratios were subjected to HPLC analyses. The product obtained using a 1:0.33 molar ratio of sucrose to polyoxyethylene (23) lauryl ether gave a single LC peak (ESI†). The plausible mechanism for the formation of surfactant (**1**) is shown in Scheme 1.

The catalyst, KPS, used in the reaction is known to generate free radicals on sugar molecules (C-6) in microwave irradiated reactions;<sup>20–22</sup> although free radical polymerization of sucrose has been described in a few reports, there is no mention about the site of free radical generation on the sucrose molecule.<sup>23,24</sup> Since sucrose has three possible reaction sites for free radical generation and MW is a strong irradiation system, we hence assumed that initially free radicals had generated on C-1' and C-6', which took part in the polymerisation process as shown in Scheme 1. Furthermore, a free radical had generated on the C-6 carbon atom of sucrose and C-58 of polyoxyethylene (23) lauryl ether and gave formation of the final surfactant (**1**). Fig. 2 shows the schematic outlay for the formation of the surfactant. At first, sucrose was polymerised and bound to the POE units of polyoxyethylene (23) lauryl ether (stage 1). On cooling and further treatment with IPA, the exclusion of the unreacted polyoxyethylene (23) lauryl ether molecules took place (stage 2) leaving behind the viscous surfactant (**1**). In order to investigate the possibility of any product formation without using KPS in the way described above, the same reaction was carried out without using KPS keeping other reaction parameters constant. Continuing further, polymerised sucrose was reacted with polyoxy ethylene (23) lauryl ether in the presence of KPS; both the reactions resulted in microscopically heterogeneous colorless products (**2** and **3**). The results indicate that simultaneous formation of the free radicals on sucrose and polyethylene lauryl ether is essential for the formation of homogeneous viscous product. The  $\lambda_{\max}$  (284 nm) measured for **1** (0.02 g/ml) was different from that of polyoxyethylene (23) lauryl ether ( $\lambda_{\max} = 235$  nm), while **2** did not show any UV absorption. The distinct shift of  $\lambda_{\max}$  to a longer wavelength at surfactant concentrations above the critical micelle concentration (cmc = 0.26 mmol/L) indicates an intermolecular interaction between polymerised sucrose and PEO side chain of surfactant.<sup>25</sup> This indicates formation of new bonds in the surfactant (**1**).

The assignment of the <sup>1</sup>H and <sup>13</sup>C NMR shifts for the polyoxyethylene units of polyoxyethylene (23) lauryl ether were done as described by Ribeiro and Dennis.<sup>26</sup> The NMR of sucrose was also compared with that of reported data.<sup>24</sup> <sup>1</sup>H NMR (D<sub>2</sub>O) for **1**,  $\delta = 1.12$  [s, –CH<sub>2</sub>– of lauryl units of poly oxy ethylene (23) lauryl ether ('B' protons), 4H]; 3.18 [t, –CH<sub>2</sub>– of polyoxyethylene (23) lauryl ether ('B' proton attached to oxy ethylene), 2H]; 3.34–3.36 [b, –CH<sub>2</sub>– of polymerised sucrose, 3H]; 3.39–3.42 [b, –(C-6)H<sub>2</sub>– of sucrose, 4H]; 3.44–3.47 [b, –(C-4)H– of sucrose, 4H]; 3.5 [b, –CH<sub>2</sub>– ('C'-protons of polyoxyethylene (23) lauryl ether, 15H)]; 3.60–3.64 [b, –(C-1')H<sub>2</sub>– of sucrose, 6H], 3.84–3.9 [b, (C-5')H of sucrose, 4H]; 4.0 [d, –(C-3')H– of sucrose]; 5.17

[d, –(C-1)H of sucrose]. The presence of a peak at 3.5 indicates formation of an ether linkage between sucrose and polyoxyethylene (23) lauryl ether.

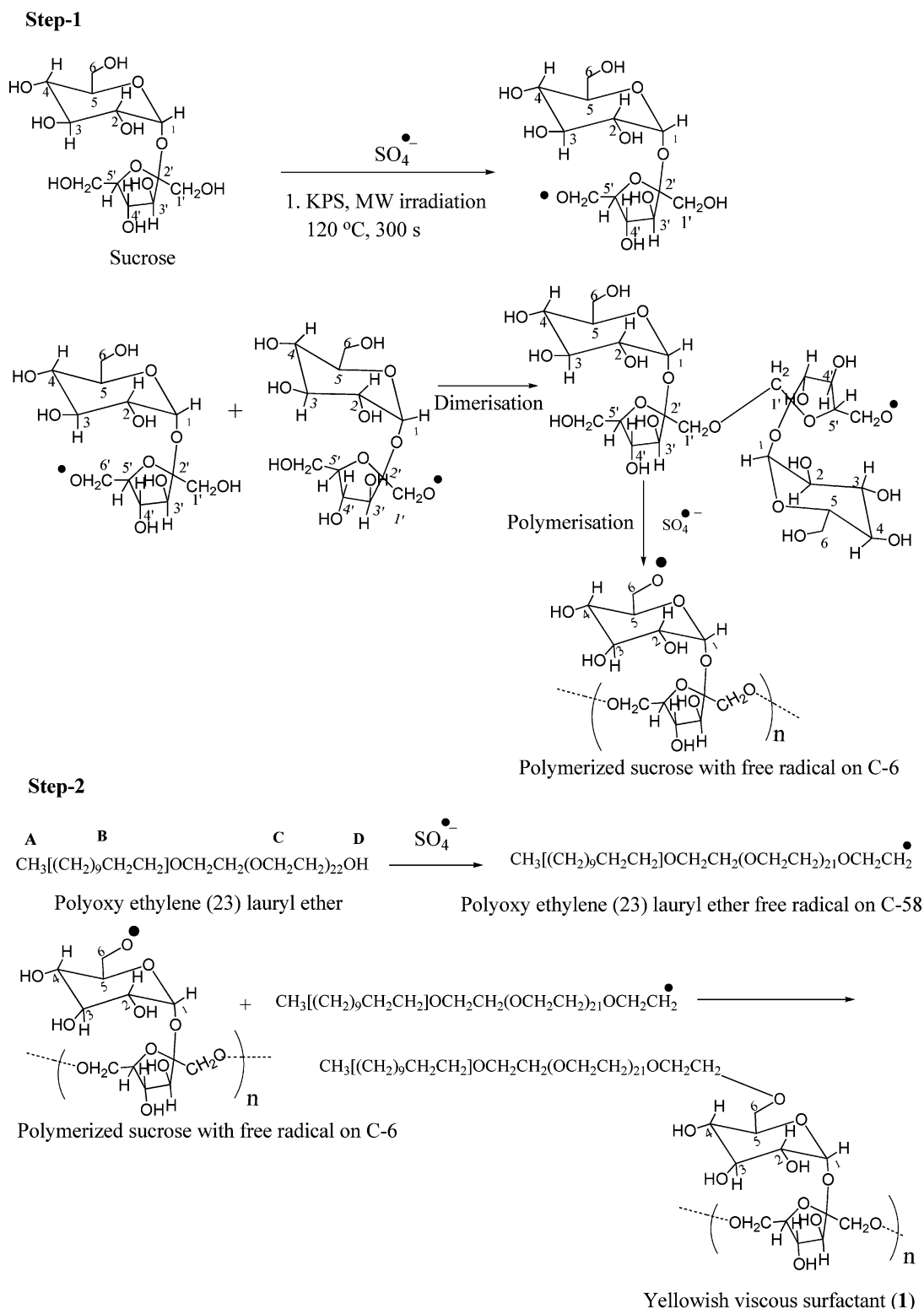
The structure was further confirmed by <sup>13</sup>C NMR. The most significant <sup>13</sup>C NMR signals (D<sub>2</sub>O, d<sub>6</sub>-DMSO as IS) are  $\delta = 25.48$  [lauryl carbons of polyoxyethylene (23) lauryl ether]; 61.93 [(C-3') of sucrose]; 62.78 [(C-6') of sucrose]; 64.9 [(C-6) of sucrose]; 70.12 [(C-3) of sucrose]; 71.0 [(oxyethylene carbons of polyoxyethylene (23) lauryl ether); 79.34 [–CH<sub>2</sub>– attached to oxy ethylene of polyoxyethylene (23) lauryl ether]; 99.60 [(C-4) of sucrose]; 105.93 [(C-2') of sucrose]. There were a total of 39 carbon signals supporting the polymerization of sucrose and the structure of **1** in Scheme 1. Sucrose was separately polymerised and the <sup>13</sup>C NMR (D<sub>2</sub>O, d<sub>6</sub>-DMSO as IS) are  $\delta = 61.33$  [C-6'], 64.46 [C-6], 70.37 [C-3'], 72.45 [C-4], 74.86 [C-3], 76.47 [C-2], 98.60 [C-1], 102.33 [C-2']. There were a total of 25 signals indicating polymerisation process (ESI, Fig S10†). It can be seen from the <sup>13</sup>C NMR data of surfactant (**1**) that the signals shown for the hydrophilic part are not much different from polymerised sucrose, indicating a chemical reaction between sucrose and polyoxyethylene (23) lauryl ether as well as an absence of unreacted polymerised sucrose in the surfactant (**1**). The number of carbon signals observed for polyoxyethylene (23) lauryl ether was 13 and for sucrose it was 12 (ESI†). The  $M_w$  obtained from GPC for **1** was 4402 with poly dispersity index ( $M_w/M_n$ ) equal to 1.18 (ESI†).

### Shear viscosity

The shear viscosity of **1** was found to be 10 times higher over the pure polyoxyethylene (23) lauryl ether. From Scheme 1 it can be seen that the polymerised sucrose moieties were attached to the hydrophilic end of the surfactant, which induced further hydrophilicity in the system and due to the close residency of the polymerised groups, there was always a possibility of self organization of the sucrose units by forming hydrogen bonds among themselves or with polyoxyethylene groups (vide infra SEM images), perhaps responsible for the enhanced viscosity of the product. A more detailed rheological study for the product is ongoing and will be published elsewhere.

### Differential scanning calorimetric studies

Typical significant DSC traces of **1** with sucrose and polyoxyethylene (23) lauryl ether are depicted in Fig. 3. For sucrose, there were two endothermic peaks at temperature 173.0 °C ( $\Delta H = 102$  J/g) and 191.28 °C ( $\Delta H = 82$  J/g). The first endothermic peak was due to the crystalline nature of sucrose and the later might be due to phase transition (Fig. 3(a)). For polyoxyethylene (23) lauryl ether, the phase transition temperature ( $T_g$ ) was 50–94 °C ( $T_m = 86$  °C), which might be due to the evaporation of entrapped water from the surfactant (Fig. 3(b)). For **1**, there was a broad endothermic peak with transition temperature range 50–210 °C ( $\Delta H = 309$  J/g). The broad transition indicated the interaction of sucrose with polyoxyethylene (23) lauryl ether in **1** and the difference observed in the transition temperatures of **1** with polyoxyethylene (23) lauryl ether and sucrose indicates formation of a new compound



**Scheme 1** Plausible mechanism for the formation of surfactant (1).

with different thermal behaviour (Fig. 3(c)). The surfactant upon cooling did not show any transition or crystallization temperature representative of an irreversible viscous system. The reason may be, once the gel was heated surfactant molecules

get detached from the sucrose backbone and upon cooling they did not get associated with sucrose. The phenomenon is not clear yet and may need more experimentation for better understanding.

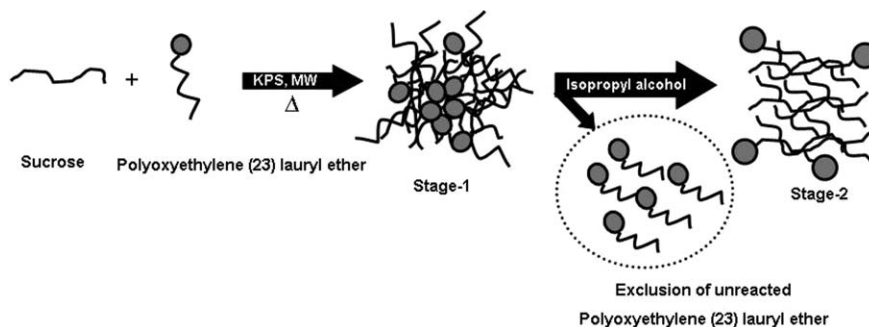


Fig. 2 Schematic diagram for the formation of surfactant (1).

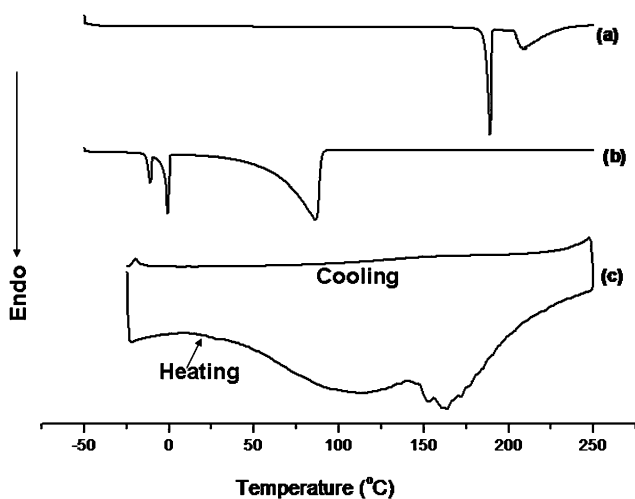


Fig. 3 DSC traces of (a) sucrose (b) polyoxyethylene (23) lauryl ether and (c) surfactant (1).

#### Thermal gravimetric analyses

The TGA profiles for **1** along with sucrose and polyoxyethylene (23) lauryl ether were studied. The first weight loss in the TGA curves for polyoxyethylene (23) lauryl ether and sucrose was 37.1% and 0.46% respectively, the water loss in **1** was similar to polyoxyethylene (23) lauryl ether. The main thermal degradations for polyoxyethylene (23) lauryl ether were in the temperature range of 189.9–326.1 °C (83.7% weight loss); for sucrose it was 205.9–357.2 °C (72% weight loss), while for **1** it was 226.1–325.1 (66.21%). The different onset weight loss temperatures for **1** in comparison to polyoxyethylene (23) lauryl ether and sucrose indicate formation of a new product.<sup>27</sup> The lower degradation rate indicated formation of a stable organized structure in the viscous surfactant and thus supported the result obtained from DSC (ESI, TGA figures†).

#### XRD analyses

The XRD patterns of **1** along with sucrose and polyoxyethylene (23) lauryl ether are depicted in Fig. 4. Sucrose showed a crystalline nature (Fig. 4(a)) with typical diffraction peaks at 8.4°, 13.13°, 16.66° and 25.2°, which got largely disrupted in **1** (Fig. 4(c)) probably due to breaking of hydrogen bonds which are responsible for crystallinity.<sup>28</sup> Although polyoxyethylene (23) lauryl ether also showed amorphous behaviour (Fig. 4(b)), two broad amorphous regions), yet the XRD pattern was different

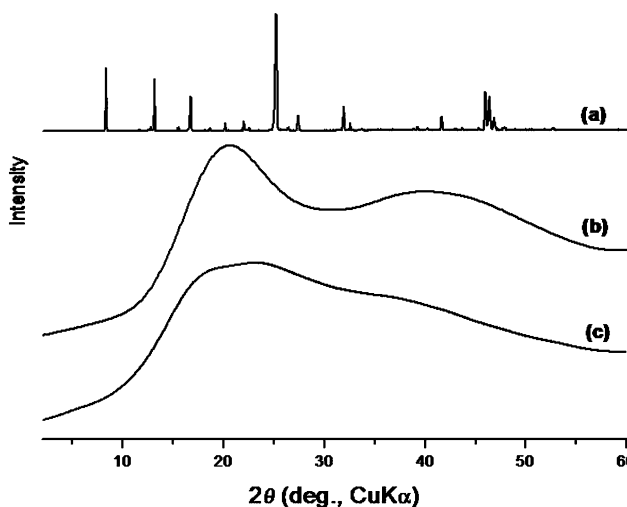


Fig. 4 XRD patterns of (a) sucrose (b) polyoxyethylene (23) lauryl ether and (c) surfactant (1).

from that of **1** (single broad amorphous region) indicating formation of a new product with different molecular association. The average d-spacing for sucrose observed was 2.34, while for **1** this was 4.05 indicating the disintegration of the crystalline phase of sucrose in the surfactant. The crystalline index or the conversion ratio of crystalline into non-crystalline sucrose in the surfactant is not yet clear. The amorphous nature of **1** indicates the association of the polymerised sucrose molecules around the oxy-ethylene chain of polyoxyethylene (23) lauryl ether (Scheme 1). As the self-organization of polyoxyethylene (23) lauryl ether is reported<sup>29</sup> there is a possibility that the self organization of amphiphilic polyoxyethylene (23) lauryl ether was enhanced due to the presence of polymerised sucrose moieties. Micro spheres observed in the SEM images for **1** showed some evidence of such.

#### SEM images

The scanning electron micrographs of **1** along with polymerised sucrose and **2** are shown in Fig. 5. Non-uniform structures for the polymerised sucrose with distorted needle shapes of length 15–20 μm and width 4–6 μm are seen (Fig. 5(a)). The physical mixture of polyoxyethylene (23) lauryl ether and sucrose showed ribbon like shapes (**2**, perhaps polyoxyethylene (23) lauryl ether) molecules and white distorted spheres (possibly sucrose) (Fig. 5(b)) with non-uniform shapes. The product (**1**)

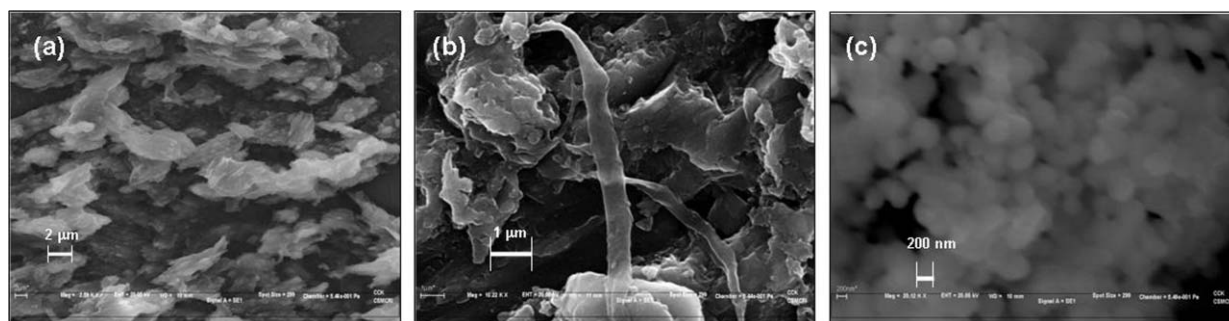


Fig. 5 SEM images (a) polymerised sucrose (b) product (2) and (c) surfactant (1).

showed ordered micro spheres of diameter 200 nm (Fig 5(c)) probably representative of organized polymeric molecules.

### Hydrophilic–lipophilic balance (HLB)

The HLB of polyoxyethylene (23) lauryl ether and **1** was determined using Griffin's method (HLBG).<sup>30</sup> HLBG calculated for the former was found to be 17.18 and is comparable to the reported value<sup>31</sup> and for the later, it was 19.23. Due to the presence of polymerised sucrose units in the side chain, **1** showed a higher HLB value indicating more hydrophilicity.

### Critical micelle concentration (cmc)

The 'cmc' of polyoxyethylene (23) lauryl ether determined by surface tension measurements was found to be 0.045 mmol/L which is similar to the reported values in the literature,<sup>11</sup> and for **1** the 'cmc' was 0.26 mmol/L at 27 °C. The 'cmc' was also determined by a fluorescence technique, where the fluorescence intensity of the first ( $I_1$ ) and third ( $I_3$ ) vibronic peaks ( $I_1/I_3$ ) of the pyrene fluorescence emission spectrum was recorded for polyoxyethylene (23) lauryl ether and **1**. The variation of the intensity ratio for the samples was plotted against the concentration of the surfactants and the break point indicates the 'cmc' value of the systems. The 'cmc' value found for polyoxyethylene (23) lauryl ether and **1** was 0.041 mmol/L and 0.21 mmol/L respectively. Both the values are comparable to the corresponding values determined by surface tension measurements described above.

### Conclusion

In conclusion, we have reported a rapid method for solvent free synthesis of a new viscous surfactant based on sucrose and polyoxyethylene (23) lauryl ether using microwave irradiation. The reaction was carried out in much shorter duration (300 s) in comparison to the 10 h of duration by the conventional heating method and with 40% more yield. The viscosity of the surfactant synthesised by conventional heating was 17.7% lower in comparison to **1** and other physicochemical properties were almost the same (ESI<sup>†</sup>). The structure of the surfactant **1** was determined by NMR and also characterised using various analytical tools. Analytical data supported formation of a new compound and SEM images showed the presence of micro spheres indicating self organization of the surfactant having the potential to be used as drug carriers for various slow release

applications. This is also the first demonstration of a facile solvent free synthesis for obtaining a viscous surfactant. This work will also help to popularise the microwave irradiation technique as an alternative tool to carry out solvent free syntheses over much shorter durations.

### Acknowledgements

The Department of Science and Technology, New Delhi, is acknowledged for financial support (FAST track young scientist project to KP).

### Notes and references

- 1 M. Roversi and C. La Mesa, *J. Colloid Interface Sci.*, 2005, **284**, 470.
- 2 A. Malhotra and J. N. Coupland, *Food Hydrocolloid.*, 2004, **18**, 101.
- 3 K. Prasad, A. K. Siddhanta, A. K. Rakshit, A. Bhattacharya and P. K. Ghosh, *Int. J. Biol. Macromol.*, 2005, **35**, 135.
- 4 K. Prasad, K. Trivedi, R. Meena and A. K. Siddhanta, *Polym. J.*, 2005, **37**, 826.
- 5 S. General and M. Antonietti, *Angew. Chem. Int. Ed.*, 2002, **41**, 2957.
- 6 A. D'Aprano, C. La Mesa and L. Persi, *Langmuir*, 1997, **13**, 5876.
- 7 Y. Noguchi, K. Okeyoshi and R. Yoshida, *Macromol. Rapid Commun.*, 2005, **26**, 1913.
- 8 M. S. Dahayanake, J. Yang, N. Jiang, J. H. Y. Niu, P.-J. Derian, R. Li, and D. Dino, *US Pat.*, 6,258,859, 2001.
- 9 Y. Lapitsky and E. W. Kaler, *Colloids Surf. A.*, 2004, **250**, 179.
- 10 R. Hommel and H. -P. Kleber, *J. Basic Microbiol.*, 1990, **30**, 297.
- 11 N. Vlachy, D. Touraud, K. Kogej and W. Kunz, *J. Colloid Interface Sci.*, 2007, **315**, 445.
- 12 K. Prasad, G. Mehta, R. Meena and A. K. Siddhanta, *J. Appl. Polym. Sci.*, 2006, **102**, 3654.
- 13 V. Singh, A. Tiwari, D. N. Tripathi and T. Malviya, *Tetrahedron Lett.*, 2003, **44**, 7295.
- 14 S. Sinnwell and H. Ritter, *Aust. J. Chem.*, 2007, **60**, 729 and relevant references cited therein.
- 15 M. I. Malik, B. Trathnigg and C. O. Kappe, *Eur. Polym. J.*, 2008, **44**, 144.
- 16 S. Jorge, P. Joaquin and V. -L. Eduardo, *J. Macromol. Sci. Pure Appl. Chem.*, 2006, **43**, 589.
- 17 V. Tomanova, K. Pielichowski, I. Srokova, A. Zoldakova, V. Sasinkova and A. Ebringerova, *Polym. Bull.*, 2008, **60**, 15.
- 18 G. A. Miller, D. L. Kirchner, and S. B. McVey, *US Pat.*, 5,489,617, 1996.
- 19 C. J. Drummond and C. Fong, *Curr. Opin. Colloid Interface Sci.*, 2000, **4**, 449.
- 20 V. Singh, A. Tiwari, P. Shukla, S. P. Singh and R. Sanghi, *React. Funct. Polym.*, 2006, **66**, 1306.
- 21 R. Hoogenboom and Ulrich S. Schubert, *Macromol. Rapid Commun.*, 2007, **28**, 368.
- 22 K. Prasad, R. Meena and A. K. Siddhanta, *J. Appl. Polym. Sci.*, 2006, **101**, 161.
- 23 X. Hou, J. Yang, J. Tang, X. Chen, X. Wang and K. Yao, *React. Funct. Polym.*, 2006, **66**, 1711.



- 
- 24 L. Ferreira, M. M. Vidal, C. F. G. C. Geraldés and M. H. Gil, *Carbohydr. Polym.*, 2000, **41**, 15.
- 25 A. Heredia and M. Bukovac, *J. Agric. Food. Chem.*, 1992, **40**, 2290.
- 26 A. A. Ribeiro and E. A. Dennis, *J. Phys. Chem.*, 1977, **81**, 957.
- 27 M. Murakami, Y. Kaneko and J. Kadokawa, *Carbohydr. Polym.*, 2007, **69**, 378.
- 28 K. Nishinari and M. Watase, *Agric. Biol. Chem.*, 1987, **51**, 3231.
- 29 M. Tomsic, M. Bester-Rogac, A. Jamnik, W. Kunz, D. Tauraud, A. Bergmann and O. Glatter, *J. Phys. Chem. B*, 2004, **108**, 7021.
- 30 W. C. Griffin, *J. Soc. Cosmet. Chem.*, 1954, **5**, 249.
- 31 G. Ben-Et and D. Tatarsky, *J. Am. Oil Chem. Soc.*, 1972, **49**, 499.

# 1-Ethyl-3-methylimidazolium bis{(trifluoromethyl)sulfonyl}amide as solvent for the separation of aromatic and aliphatic hydrocarbons by liquid extraction – extension to C<sub>7</sub>- and C<sub>8</sub>-fractions

Alberto Arce,<sup>a</sup> Martyn J. Earle,<sup>\*b</sup> Héctor Rodríguez,<sup>a,b</sup> Kenneth R. Seddon<sup>b</sup> and Ana Soto<sup>a</sup>

Received 28th April 2008, Accepted 20th August 2008

First published as an Advance Article on the web 21st October 2008

DOI: 10.1039/b807222a

The ionic liquid 1-ethyl-3-methylimidazolium bis{(trifluoromethyl)sulfonyl}amide ([C<sub>2</sub>mim][NTf<sub>2</sub>]) was tested as solvent for the separation of aromatic and aliphatic hydrocarbons containing 7 or 8 carbon atoms (the C<sub>7</sub>- and C<sub>8</sub>-fractions). The liquid–liquid equilibria (LLE) of the ternary systems (heptane + toluene + [C<sub>2</sub>mim][NTf<sub>2</sub>]) and (octane + ethylbenzene + [C<sub>2</sub>mim][NTf<sub>2</sub>]), at 25 °C, were experimentally determined. The performance of the ionic liquid as the solvent in such systems was evaluated by means of the calculation of the solute distribution ratio and the selectivity. The results were compared to those previously reported for the extraction of benzene from its mixtures with hexane by using the same ionic liquid, therefore analysing the influence of the size of the hydrocarbons. It was found that the ionic liquid is also good for the extraction of C<sub>7</sub>- and C<sub>8</sub>-fraction aromatic compounds, just a greater amount of ionic liquid being needed to perform an equivalently efficient separation than for the C<sub>6</sub>-fraction. It is also discussed how [C<sub>2</sub>mim][NTf<sub>2</sub>] performs comparably better than the conventional solvent sulfolane. The original ‘Non-Random Two-Liquid’ (NRTL) equation was used to adequately correlate the experimental LLE data.

## Introduction

In the course of refinery processes, a key separation is that of aromatic and aliphatic hydrocarbons in naphthas, resulting in, on one hand, clean-burning fuels and, on the other hand, the aromatics to be used as major raw materials in plastic, synthetic rubber, and synthetic fibre manufacture.<sup>1,2</sup> Since the early 1990s, an increase in legislation reducing the permissible levels of aromatics in gasoline has led to enhanced research in this separation.<sup>3</sup>

Several alternatives for carrying out the aforementioned separation were developed, including azeotropic distillation, extractive distillation, solvent extraction, crystallisation by freezing, or adsorption on solids. Among other factors, the basic or economical operation of each of these techniques depends on the proportion of aromatics and aliphatics in the stream to be treated. Nevertheless solvent extraction is, by far, more widely applied than either of the other methods mentioned.<sup>1</sup>

Selection of the solvent is, undoubtedly, the most characteristic critical aspect in the design of solvent extraction processes. A number of varied commercial processes for the separation of aromatics and aliphatics are currently in operation, using many different solvents or mixtures of solvents.<sup>1,2</sup> Sulfolane (or, more systematically, 2,3,4,5-tetrahydrothiophene-1,1-dioxide), which offers good thermal and hydrolytic stability, high density and boiling point, and a good balance of solvent properties,<sup>1</sup> is

commonly accepted as the best solvent for the separation of aromatic and aliphatic hydrocarbons.

Over the last decade, ionic liquids have gradually emerged as a novel alternative to traditional organic solvents, for example in reactions and extractions.<sup>4,5</sup> In particular, several ionic liquids have been investigated for the separation of aromatic and aliphatic hydrocarbons by solvent extraction through the determination of the liquid–liquid equilibrium (LLE) of ternary systems.<sup>6–14</sup> In a previous work,<sup>15</sup> we tested the ionic liquid 1-ethyl-3-methylimidazolium bis{(trifluoromethyl)sulfonyl}amide ([C<sub>2</sub>mim][NTf<sub>2</sub>]) for the extraction of benzene from a mixture of benzene and hexane, representatives of the C<sub>6</sub>-fraction of oil. The results were very good, and an explicit comparison with sulfolane showed that this ionic liquid could, in principle, be a successful alternative solvent for the separation of aromatic and aliphatic hydrocarbons by liquid extraction. In this work, we try to confirm the suitability of [C<sub>2</sub>mim][NTf<sub>2</sub>] by expanding the research to the separation of hydrocarbons of the C<sub>7</sub>- and C<sub>8</sub>-fractions. Namely, the ternary systems (heptane + toluene + [C<sub>2</sub>mim][NTf<sub>2</sub>]) and (octane + ethylbenzene + [C<sub>2</sub>mim][NTf<sub>2</sub>]) have been chosen for experimental determination of their LLE at 25 °C. The selection of the working temperature has been made in accordance with the conclusions from our previous paper on the C<sub>6</sub>-fraction.<sup>15</sup>

## Results and discussion

### LLE data

The LLE data for the ternary systems (heptane + toluene + [C<sub>2</sub>mim][NTf<sub>2</sub>]) and (octane + ethylbenzene + [C<sub>2</sub>mim][NTf<sub>2</sub>]),

<sup>a</sup>Department of Chemical Engineering, University of Santiago de Compostela, E-15782, Santiago de Compostela, Spain

<sup>b</sup>The QUILL Centre, The Queen's University of Belfast, Belfast, BT9 5AG, UK. E-mail: quill@qub.ac.uk

at 25 °C, are reported in Tables 1 and 2. No ionic liquid was observed in the upper equilibrium phase of any of the tie-lines of the system with heptane and toluene; however, a small amount could be detected in the upper phase of some equilibrated mixtures of the system with octane and ethylbenzene. The complete absence of ionic liquid in the hydrocarbon-rich phase would be desirable, since it would eliminate the need of a unit for recovering the solvent from the hydrocarbon-rich stream (raffinate) coming out of the extractor in a continuous extraction process. Unfortunately, for the systems studied herein, it seems that a tiny amount of ionic liquid enters the lighter phase, although it is low enough to not be detected in most cases by the technique used. This is consistent with the results from an experiment at a larger scale for a similar system, previously reported,<sup>15</sup> in which a concentration of ionic liquid in the level of a few parts per million could be measured. Nevertheless, the results in the present work with the [C<sub>2</sub>mim][NTf<sub>2</sub>] are better, from that point of view, than those reported by Meindersma *et al.* for analogous systems (heptane + toluene + ionic liquid)

**Table 1** Composition of the experimental tie-line ends, and values of the solute distribution ratio ( $\beta$ ) and selectivity ( $S$ ), for the ternary system (heptane + toluene + [C<sub>2</sub>mim][NTf<sub>2</sub>]) at 25 °C. The mole fractions of heptane, toluene and [C<sub>2</sub>mim][NTf<sub>2</sub>] are represented by  $x_1$ ,  $x_2$  and  $x_3$ , respectively<sup>a</sup>

Upper phase			Lower phase			$\beta$	$S$
$x_1$	$x_2$	$x_3$	$x_1$	$x_2$	$x_3$		
1.000	0.000	0.000	0.023	0.000	0.977	—	—
0.936	0.064	0.000	0.028	0.053	0.919	0.83	27.7
0.793	0.207	0.000	0.025	0.166	0.809	0.80	25.4
0.744	0.256	0.000	0.027	0.204	0.769	0.80	22.0
0.582	0.418	0.000	0.025	0.301	0.674	0.72	16.8
0.459	0.541	0.000	0.023	0.375	0.602	0.69	13.8
0.345	0.655	0.000	0.023	0.435	0.542	0.66	10.0
0.169	0.831	0.000	0.017	0.545	0.438	0.66	6.5
0.068	0.932	0.000	0.008	0.606	0.386	0.65	5.5
0.000	1.000	0.000	0.000	0.654	0.346	0.65	—

<sup>a</sup> Estimated uncertainty:  $\pm 0.011$  mole fraction.

**Table 2** Composition of the experimental tie-line ends, and values of the solute distribution ratio ( $\beta$ ) and selectivity ( $S$ ), for the ternary system (octane + ethylbenzene + [C<sub>2</sub>mim][NTf<sub>2</sub>]) at 25 °C. The mole fractions of octane, ethylbenzene and [C<sub>2</sub>mim][NTf<sub>2</sub>] are represented by  $x_1$ ,  $x_2$  and  $x_3$ , respectively<sup>a</sup>

Upper phase			Lower phase			$\beta$	$S$
$x_1$	$x_2$	$x_3$	$x_1$	$x_2$	$x_3$		
1.000	0.000	0.000	0.015	0.000	0.985	—	—
0.954	0.046	0.000	0.015	0.022	0.963	0.48	30.4
0.816	0.184	0.000	0.016	0.090	0.894	0.49	24.9
0.716	0.282	0.002	0.021	0.141	0.838	0.50	17.0
0.558	0.442	0.000	0.019	0.209	0.772	0.47	13.9
0.471	0.529	0.000	0.022	0.252	0.726	0.48	10.2
0.383	0.617	0.000	0.026	0.297	0.677	0.48	7.1
0.286	0.714	0.000	0.022	0.350	0.628	0.49	6.4
0.202	0.797	0.001	0.017	0.397	0.586	0.50	5.9
0.113	0.887	0.000	0.010	0.436	0.554	0.49	5.6
0.050	0.950	0.000	0.007	0.492	0.501	0.52	3.7
0.000	1.000	0.000	0.000	0.510	0.490	0.51	—

<sup>a</sup> Estimated uncertainty:  $\pm 0.014$  mole fraction.

or (octane + ethylbenzene + ionic liquid) with different ionic liquids,<sup>10,11</sup> since they found larger amounts of ionic liquid in the raffinate phase.

Equilateral triangular diagrams with the graphical representation of the ternary LLE are shown in Fig. 1, where the diagram

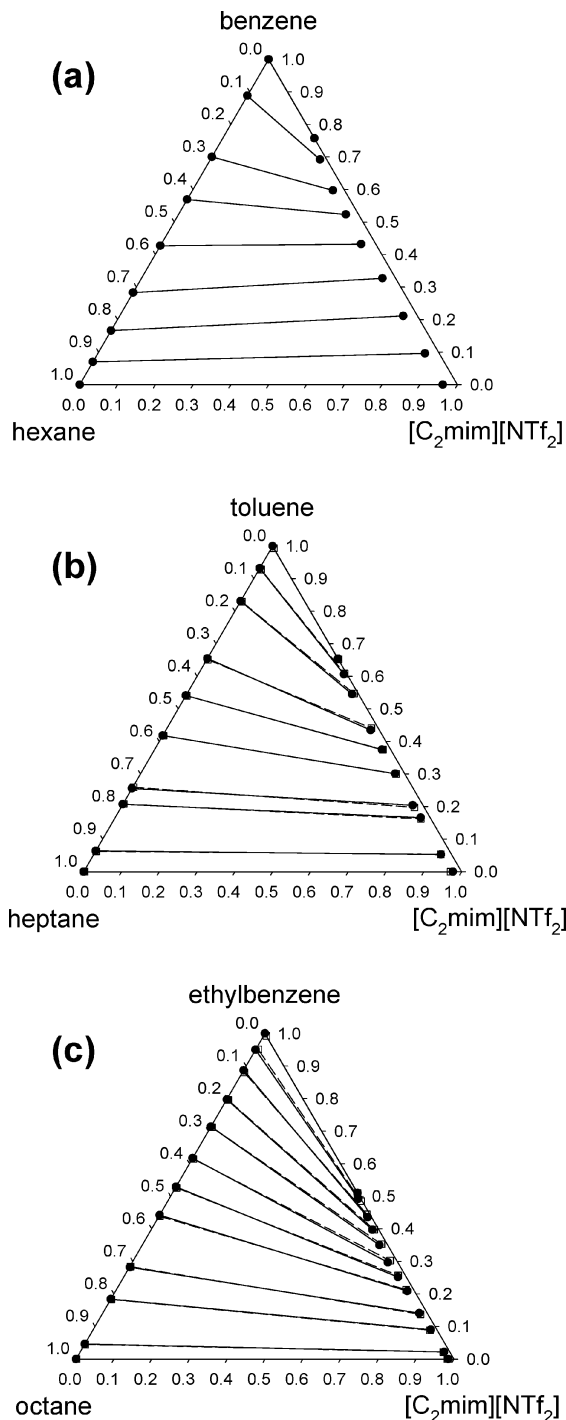


**Fig. 1** Experimental (solid circles, solid lines) tie-lines for the LLE of the ternary systems (a) (hexane + benzene + [C<sub>2</sub>mim][NTf<sub>2</sub>]),<sup>15</sup> (b) (heptane + toluene + [C<sub>2</sub>mim][NTf<sub>2</sub>]), and (c) (octane + ethylbenzene + [C<sub>2</sub>mim][NTf<sub>2</sub>]), at 25 °C. For the novel data provided in this work, the correlated tie-lines (NRTL,  $\alpha = 0.20$  with  $\beta_{\infty,prev}$ ) are also drawn (open squares, dashed lines).

of the system (hexane + benzene + [C<sub>2</sub>mim][NTf<sub>2</sub>]) at the same temperature is also included for the sake of straight visual comparison.<sup>15</sup> As can be seen, all ternary systems correspond to the Type 2 category, according to the classification proposed by Sørensen *et al.*,<sup>16</sup> with two of their constituent pairs exhibiting partial immiscibility, and with only one immiscibility domain across the ternary compositional spectrum. From the tie-lines on the edges of the triangles, it turns out that the solubility of the aromatic hydrocarbons in [C<sub>2</sub>mim][NTf<sub>2</sub>] is much higher than that of the aliphatic hydrocarbons. In good agreement with the minimal level of ionic liquid in the hydrocarbon-rich phase in both systems, already noted, the left ends of the tie-lines lie basically on one of the edges of the triangles.

### Solute distribution ratio and selectivity

The feasibility of using [C<sub>2</sub>mim][NTf<sub>2</sub>] as the solvent for the separation of heptane and toluene, or of octane and ethylbenzene, was evaluated by means of the calculation of classical parameters such as the solute distribution ratio ( $\beta$ ) and the selectivity ( $S$ ). These are respectively defined by the following expressions:

$$\beta = \frac{x_2^{\text{II}}}{x_2^{\text{I}}} \quad (1)$$

$$S = \frac{\frac{x_2^{\text{II}}}{x_1^{\text{II}}}}{\frac{x_2^{\text{I}}}{x_1^{\text{I}}}} \quad (2)$$

where  $x$  stands for the mole fraction, subscripts 1 and 2 refer to the inert (heptane or octane) and solute (toluene or ethylbenzene) compounds, and superscripts I and II indicate the upper phase (raffinate) and lower phase (extract), respectively.

Tables 1 and 2 show the calculated values of  $\beta$  and  $S$  for the systems (heptane + toluene + [C<sub>2</sub>mim][NTf<sub>2</sub>]) and (octane + ethylbenzene + [C<sub>2</sub>mim][NTf<sub>2</sub>]) at 25 °C, respectively. All values of  $\beta$  decrease with an increase in the aromatic content for the system with the pair heptane–toluene, whereas they remain practically constant for the system with octane–ethylbenzene. On the other hand, the selectivity values decrease as the aromatic content increases for both systems.

In Fig. 2, the solute distribution ratios of both ternary systems are represented as a function of the mole fraction of benzene in the organic (less dense) phase. The values for the analogous system (hexane + benzene + [C<sub>2</sub>mim][NTf<sub>2</sub>]) at 25 °C, reported in a previous work,<sup>15</sup> are also plotted for emphasising the effect from the C<sub>6</sub>- to the C<sub>8</sub>-fraction. Whereas for the system with the pair heptane–toluene, a notable decrease in  $\beta$  is observed with increasing the concentration of the aromatic hydrocarbon, for the system with heptane–toluene the decrease is smaller, and for the one with octane–ethylbenzene it remains approximately constant throughout the entire immiscibility domain. Regarding the size (number of carbons) of the hydrocarbons involved in each system, a decrease in  $\beta$  can be observed when moving from the C<sub>6</sub>-fraction to the C<sub>7</sub>-fraction, and to the C<sub>8</sub>-fraction. Therefore, for a feedstream with lighter hydrocarbons, a lesser amount of ionic liquid would be required in the extraction unit. Another interesting feature from Fig. 2 is that, contrary to what happens in the ternary system (hexane + benzene +

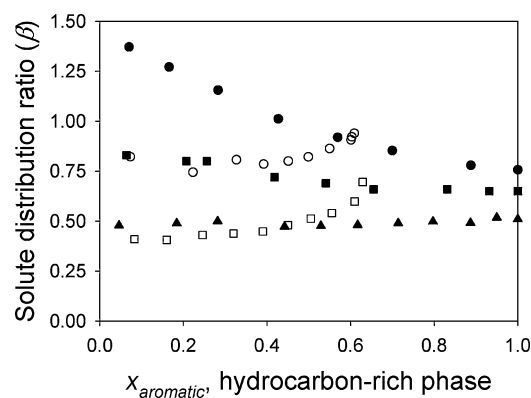


**Fig. 2** Solute distribution ratio, as a function of the mole fraction of solute in the hydrocarbon-rich phase, for the ternary systems (hexane + benzene + [C<sub>2</sub>mim][NTf<sub>2</sub>])<sup>15</sup> (●), (heptane + toluene + [C<sub>2</sub>mim][NTf<sub>2</sub>]) (■), and (octane + ethylbenzene + [C<sub>2</sub>mim][NTf<sub>2</sub>]) (▼), at 25 °C. Values for the systems (hexane + benzene + sulfolane) (○), and (heptane + toluene + sulfolane) (□), at the same temperature, calculated from LLE data in the literature,<sup>18,19</sup> are also plotted for comparison.

[C<sub>2</sub>mim][NTf<sub>2</sub>]), the values of  $\beta$  for the other two systems are always lower than unity; therefore, the solutropy<sup>17</sup> exhibited by the system with the C<sub>6</sub>-fraction (with a change in the sign of the slopes of the tie-lines) disappears as the size of the hydrocarbons involved increases.

Interestingly, a parallel can be established between the evolution of the solute distribution ratio of aromatic hydrocarbons in the ternary systems (aliphatic + aromatic + [C<sub>2</sub>mim][NTf<sub>2</sub>]), and the evolution of the solubilities of both aliphatic and aromatic hydrocarbons in the ionic liquid. These solubility values, taken from the binary tie-lines of the corresponding LLE data sets, and expressed as mole fractions in the ionic liquid-rich phase, are represented in Fig. 3 as a function of the number of carbons of the aromatic or aliphatic hydrocarbons. Of course, the solubilities of the aromatic hydrocarbons in the ionic liquid are very much higher than those of the aliphatic hydrocarbons (please note the two different Y-axis scales in Fig. 3), of slightly above one order of magnitude; but an analogous decreasing

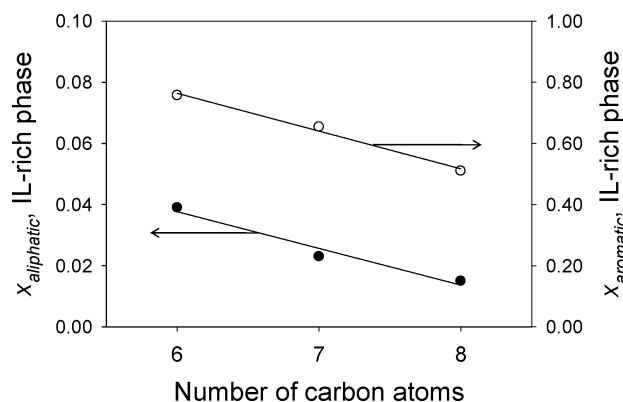


**Fig. 3** Solubility, in mole fraction, of the aromatic (○) and aliphatic (●) hydrocarbons in [C<sub>2</sub>mim][NTf<sub>2</sub>] at 25 °C, as a function of the number of carbons in their molecules. The solid lines correspond to linear fits, and the arrows point to the Y-axis scale which has to be used for each series.



trend, in an approximately linear fashion, is observed with increasing the size of hydrocarbons in both series.

Selectivities, also as a function of the mole fraction of benzene in the organic phase, are plotted in Fig. 4 for all three aforementioned ternary systems. In this case, there is a general decrease of  $S$  with increasing the aromatic content of the system, but no significant differences can be observed when comparing each system with the others. Thus, the separation power of [C<sub>2</sub>mim][NTf<sub>2</sub>] in separating hexane and benzene, already known from previous work,<sup>15</sup> is confirmed with larger aliphatic–aromatic pairs.

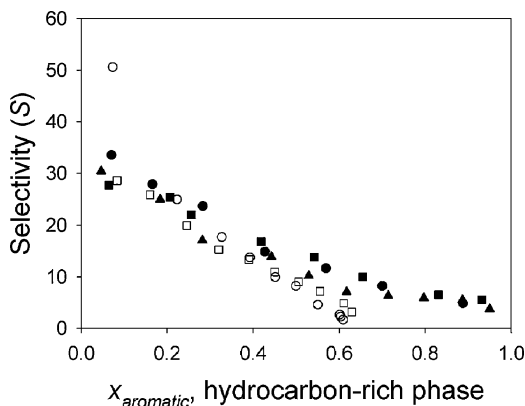


**Fig. 4** Selectivity, as a function of the mole fraction of solute in the hydrocarbon-rich phase, for the ternary systems (hexane + benzene + [C<sub>2</sub>mim][NTf<sub>2</sub>])<sup>15</sup> (●), (heptane + toluene + [C<sub>2</sub>mim][NTf<sub>2</sub>]) (■), and (octane + ethylbenzene + [C<sub>2</sub>mim][NTf<sub>2</sub>]) (▼), at 25 °C. Values for the systems (hexane + benzene + sulfolane) (○), and (heptane + toluene + sulfolane) (□), at the same temperature, calculated from LLE data in the literature,<sup>18,19</sup> are also plotted for comparison.

Meindersma *et al.*<sup>10</sup> studied several ternary systems (heptane + toluene + ionic liquid) at 40 and 75 °C; namely, they investigated the ionic liquids 1-ethyl-3-methylimidazolium ethylsulfate ([C<sub>2</sub>mim][EtSO<sub>4</sub>]), 1,3-dimethylimidazolium methylsulfate ([C<sub>1</sub>mim][MeSO<sub>4</sub>]), 1-butyl-3-methylimidazolium methylsulfate ([C<sub>4</sub>mim][MeSO<sub>4</sub>]), and 1-butyl-4-methylpyridinium tetrafluoroborate ([C<sub>4</sub>pic][BF<sub>4</sub>]). They also used [C<sub>4</sub>pic][BF<sub>4</sub>] in the system with the pair (octane + ethylbenzene) at the same temperatures.<sup>11</sup> A comparison of the performance of those ionic liquids with the [C<sub>2</sub>mim][NTf<sub>2</sub>] used in the present work, *via* the LLE data generated, is obviously desirable. In the case of the systems with the C<sub>7</sub>-fraction, and focusing on the data at the lower temperature (40 °C) because those at the higher temperature (75 °C) are systematically worse, it can be observed that [C<sub>4</sub>mim][MeSO<sub>4</sub>] leads to comparable selectivities; whereas for the other three ionic liquids, the selectivity values are higher than those reported herein for the system with [C<sub>2</sub>mim][NTf<sub>2</sub>]. However, if the solute distribution ratios are calculated from their LLE data, much lower values than those in Tables 1 and 2 will be found, the highest values corresponding to the system with [C<sub>4</sub>pic][BF<sub>4</sub>] but still being half of ours. For the system of [C<sub>4</sub>pic][BF<sub>4</sub>] with the pair (octane + ethylbenzene), again higher selectivities than ours are reported, but simultaneously the calculable solute distribution ratios are comparable at low global concentrations of benzene in the system, then become clearly lower as the aromatic content is increased. Thus, it

would be reasonable to think that [C<sub>4</sub>pic][BF<sub>4</sub>] could in principle perform better than [C<sub>2</sub>mim][NTf<sub>2</sub>] for the targeted separations. Nonetheless, the perfluorinated anion of [C<sub>4</sub>pic][BF<sub>4</sub>] can easily undergo hydrolysis to form hydrofluoric acid, which dissuades from using it as solvent in a scaled-up industrial process; and, additionally, it is a solid at room temperature, which might also be an undesirable factor from the standpoint of handling or treating it in its pure state compared to liquids.

Since sulfolane is widely regarded as the current best solvent for the separation of aromatic and aliphatic hydrocarbon by liquid extraction, a comparison of its performance to that of [C<sub>2</sub>mim][NTf<sub>2</sub>] is also necessary. Thus, solute distribution ratios and selectivities calculated from LLE data reported in the literature for the systems (hexane + benzene + sulfolane) and (heptane + toluene + sulfolane) are also plotted in Figs. 2 and 4.<sup>18,19</sup> No available data were found for the system (octane + ethylbenzene + sulfolane). The comparison of [C<sub>2</sub>mim][NTf<sub>2</sub>] and sulfolane with regard to the extraction of benzene from its mixtures with hexane was already discussed elsewhere.<sup>15</sup> In brief, the only apparent superiority of sulfolane over the ionic liquid occurred in terms of selectivity at low concentration of aromatic hydrocarbons in the system; but, due to the cost of post-extraction stages for solvent recovery, the use of this compound would not be viable from an economical standpoint for the treatment of a feedstream with so low an aromatic content. A similar analysis can be extended to the separation of heptane and toluene, where the selectivity in the system with sulfolane is just slightly higher than that in the system with [C<sub>2</sub>mim][NTf<sub>2</sub>] at low aromatic concentrations; for all other concentrations, better selectivities are observed when using the ionic liquid as solvent, and the solute distribution ratios are also better with the latter throughout the whole concentration range of practical application.

### Data correlation

With the aim of facilitating the computerised treatment of the information provided by the experimental tie-lines, the LLE data of the investigated ternary systems were correlated. Despite being particularly developed for non-electrolytes, the classical ‘Non-Random Two-Liquid’ (NRTL) model was chosen,<sup>20</sup> since it has already been used for appropriately correlating the LLE data of analogous ternary systems involving two hydrocarbons and an ionic liquid.<sup>6–8,10–13,15</sup>

A computer program by Sørensen<sup>21</sup> was used for the calculation of the binary interaction parameters (BIPs) of the NRTL model. This program tries to minimise two objective functions. The first one,  $OF_a$ , is a function of the activities:

$$OF_a = \sum_k \sum_i \left( \frac{a_{ik}^I - a_{ik}^{II}}{a_{ik}^I + a_{ik}^{II}} \right)^2 + Q \cdot \sum_n P_n^2 \quad (3)$$

where  $a$  stands for the activity; superscripts I and II refer to each phase in equilibrium [as in eqn (1) and (2)]; subscript  $i$  indicates the components (1, 2, 3); subscript  $k$  refers to the tie-lines (1, 2, ...  $M$ ; with  $M$  being the total number of experimental tie-lines);  $Q$  is an empirical constant, with a value of  $10^{-6}$  in accordance with Sørensen’s recommendation; and  $P_n$  represents

the adjustable parameters, *i.e.* the BIPs to be determined, with subscript  $n$  taking the values 1, 2, ... 6.

As it does not require any preliminary guess for the BIPs set,  $OF_a$  is used in the first part of the algorithm. In a second stage, the results obtained from the convergence of  $OF_a$  are introduced as the initial parameters estimation for a second objective function,  $OF_b$ , which eventually fits the experimental concentrations:

$$OF_b = \sum_k \min \sum_i \sum_j (x_{ijk} - \hat{x}_{ijk})^2 + Q \cdot \sum_n P_n^2 + \left[ \ln \left( \beta_\infty \cdot \frac{\hat{\gamma}_{s,\infty}^I}{\hat{\gamma}_{s,\infty}^{II}} \right) \right]^2 \quad (4)$$

where  $Q$ ,  $P$ , superscripts I and II, and subscripts  $i$ ,  $k$  and  $n$  have the same meaning than in the expression of  $OF_a$  (although in this case  $Q$  takes a lower value:  $10^{-10}$ ); subscript  $j$  refers to the phases in equilibrium,  $x$  is the mole fraction,  $\beta$  the solute distribution ratio,  $\gamma$  the activity coefficient, and "min" refers to the minimum obtained by the Nelder–Mead method; subscripts  $\infty$  and  $s$  refer, respectively, to infinite dilution conditions and to the solute (the aromatic hydrocarbon); and, finally, the symbol  $\wedge$  on top indicates a calculated value.

The second term on the right hand side on both objective functions is a penalty term designed to reduce the risk of multiple solutions caused by high values of the parameters. The last term in the expression of  $OF_b$  guarantees that the final BIPs set will accurately fit a previously established value of the solute distribution ratio at infinite dilution,  $\beta_{\infty,prev}$ , optionally defined by the user in the data input file.

The goodness of the correlation fit was evaluated by means of the residual function  $F$  and the mean error of the solute distribution ratio,  $\Delta\beta$ , defined as:

$$F = 100 \times \left[ \sum_k \min \sum_i \sum_j \frac{(x_{ijk} - \hat{x}_{ijk})^2}{6M} \right]^{0.5} \quad (5)$$

$$\Delta\beta = 100 \times \left[ \frac{1}{M} \sum_k \left( \frac{\beta_k - \hat{\beta}_k}{\beta_k} \right)^2 \right]^{0.5} \quad (6)$$

where all the symbols and variables have the same meaning as in eqn (3) and (4).

Following a common procedure, the nonrandomness parameter of the model,  $\alpha$ , was set to 0.10, 0.20 and 0.30, covering its most typical range of values. Mimicking the procedure followed by Sørensen,<sup>21</sup> the experimental LLE data of both systems were correlated, using these three values of  $\alpha$ , in two different manners: in a first run the data were correlated without conditioning the resulting value of the solute distribution ratio at infinite dilution; and in a second run, an *a priori* stipulated value of  $\beta_\infty$  was specified ( $\beta_{\infty,prev}$ ), and subsequently optimised by trial and error, with  $\Delta\beta$  being the optimality criterion.

Table 3 summarises the values of the residuals  $F$  and  $\Delta\beta$ , as well as the value of  $\beta_\infty$ , obtained from the data correlation for the two ternary systems (heptane + toluene + [C<sub>2</sub>mim][NTf<sub>2</sub>]) and (octane + ethylbenzene + [C<sub>2</sub>mim][NTf<sub>2</sub>]). The correlation with  $\alpha = 0.10$  provides the worst results in both cases, while the minimum  $F$  and  $\Delta\beta$  values are achieved for either  $\alpha = 0.20$  or

**Table 3** Solute distribution ratio at infinite dilution ( $\beta_\infty$ ), residual function  $F$ , and mean error of the solute distribution ratio ( $\Delta\beta$ ) for the NRTL correlation of the LLE data of the ternary systems (heptane + toluene + [C<sub>2</sub>mim][NTf<sub>2</sub>]) and (octane + ethylbenzene + [C<sub>2</sub>mim][NTf<sub>2</sub>]) at 25 °C, for different values of the nonrandomness parameter  $\alpha$ , both fixing and without fixing a previously optimised value of the solute distribution ratio at infinite dilution,  $\beta_{\infty,prev}$

$\alpha$	$\beta_{\infty,prev}$	$F$	$\Delta\beta$	$\beta_\infty$
Heptane + toluene + [C <sub>2</sub> mim][NTf <sub>2</sub> ]				
0.10	—	0.4970	3.8	1.01
	0.92	0.4548	2.5	0.92
0.20	—	0.2440	3.1	0.97
	0.90	0.3188	2.3	0.90
0.30	—	0.3582	2.8	0.83
	0.88	0.3969	1.8	0.88
Octane + ethylbenzene + [C <sub>2</sub> mim][NTf <sub>2</sub> ]				
0.10	—	0.4970	2.6	0.46
	0.48	0.5003	2.2	0.48
0.20	—	0.3786	2.6	0.46
	0.48	0.3849	2.0	0.48
0.30	—	0.3391	3.5	0.44
	0.48	0.4035	2.1	0.48

$\alpha = 0.30$ . As expected, the correlations with a previously fixed optimum value of  $\beta_\infty$  lead to slightly higher values of the residual  $F$ , but simultaneously to a notable decrease in  $\Delta\beta$ . By comparing the  $\beta_\infty$  values obtained from the correlations with and without  $\beta_{\infty,prev}$ , and checking against the experimental values of  $\beta$  at low concentration of aromatics, an improved correlation of the LLE data in that region is observed. This is especially marked for the system involving the C<sub>7</sub>-fraction hydrocarbons. Just considering the correlations with  $\beta_{\infty,prev}$ , it is clear that the value  $\alpha = 0.20$  performs better than  $\alpha = 0.30$ . The sets of BIPs resulting from the NRTL correlations with  $\alpha = 0.20$  and with a previously fixed value of  $\beta_\infty$ , are shown in Table 4.

The equivalent correlated tie-lines of the experimental ones, generated from the reported BIPs by the computer program, are drawn in Fig. 1(b) and 1(c) for the systems (heptane + toluene + [C<sub>2</sub>mim][NTf<sub>2</sub>]) and (octane + ethylbenzene + [C<sub>2</sub>mim][NTf<sub>2</sub>]), respectively. The visual comparison of both sets of tie-lines for each system supports the general validity of the NRTL correlations carried out. Unfortunately, the model is not able to appropriately correlate either the absence or minimal presence of ionic liquid in the hydrocarbon-rich phase at any global

**Table 4** BIPs ( $\Delta g_{ij}$ ,  $\Delta g_{ji}$ ) of the NRTL model obtained from the correlation of the LLE data of the ternary systems (heptane + toluene + [C<sub>2</sub>mim][NTf<sub>2</sub>]) and (octane + ethylbenzene + [C<sub>2</sub>mim][NTf<sub>2</sub>]) at 25 °C, with  $\alpha = 0.20$  and fixing  $\beta_{\infty,prev}$

Components $i-j$	BIPs	
	$\Delta g_{ij}/J \text{ mol}^{-1}$	$\Delta g_{ji}/J \text{ mol}^{-1}$
Heptane + toluene + [C <sub>2</sub> mim][NTf <sub>2</sub> ]		
Heptane–toluene	−4329.9	5241.6
Heptane–[C <sub>2</sub> mim][NTf <sub>2</sub> ]	12 043	4677.7
Toluene–[C <sub>2</sub> mim][NTf <sub>2</sub> ]	17 281	−4884.6
Octane + ethylbenzene + [C <sub>2</sub> mim][NTf <sub>2</sub> ]		
Octane–ethylbenzene	−1413.9	839.63
Octane–[C <sub>2</sub> mim][NTf <sub>2</sub> ]	12 799	5942.9
Ethylbenzene–[C <sub>2</sub> mim][NTf <sub>2</sub> ]	15 113	−3134.0

composition, and correlated mole fractions as high as 0.007 are registered in both systems for the ionic liquid in that phase.

## Experimental

### Materials

The ionic liquid [C<sub>2</sub>mim][NTf<sub>2</sub>] was synthesised by a meta-thetic reaction between the chloride salt of the desired cation, [C<sub>2</sub>mim]Cl, and the lithium salt of the desired anion, Li[NTf<sub>2</sub>], as reported elsewhere.<sup>15</sup> The final product was characterised by <sup>1</sup>H NMR and <sup>13</sup>C NMR spectroscopy, and its water content was found to be less than 200 ppm by Karl-Fischer titration.

Heptane (Aldrich, 99%), octane (Merck, 99%), toluene (Riedel-de Haën, 99%) and ethylbenzene (Fluka, 99%) were used as received.

### Methods

Several heterogeneous mixtures of the components involved in each ternary system were prepared and placed into jacketed glass cells of 30 cm<sup>3</sup> volume, which were immediately sealed to avoid moisture pickup from the atmosphere. The temperature was kept at 25.0 °C by means of a circulating water bath controlled by an Ultraterm 6000383 thermostat. Such mixtures were magnetically stirred for at least 1 h, and then allowed to settle for a minimum of 4 h, guaranteeing complete splitting of the phases in equilibrium. After that, a sample of each phase was carefully taken and dissolved in deuterated methanol (Aldrich, 99.8+ atom% D, containing 0.03% v/v TMS), then being transferred into nuclear magnetic resonance (NMR) tubes for compositional analysis by spectroscopy.

For the determination of the compositions, a technique based on quantitative integration of the areas under specific peaks in <sup>1</sup>H NMR spectra of the samples was used. This method has already been tested successfully in systems composed of ionic liquids and hydrocarbons, and details of the procedure can be found elsewhere.<sup>15,22</sup> In the particular case of the systems studied in this work, the sets of peaks selected for integration were: for the ionic liquid, the signals corresponding to the methylene and methyl groups bonded to the nitrogen atoms of the imidazolium ring; for heptane or octane, the triplet of the terminal methyl groups; and the signals of the aromatic ring and the methyl group for toluene, or those of the aromatic ring and the methylene group for ethylbenzene. The error in the calculated compositions was estimated from tests with homogeneous samples of the three compounds for each system, prepared by weight, and with global compositions in the vicinity of the immiscibility regions. Although mostly less than 0.010 mole fraction, the maximum deviations found were of 0.014 mole fraction, for any of the investigated systems, in any proportion of their components. The <sup>1</sup>H NMR spectra were recorded on a Bruker DRX-500 spectrometer.

## Conclusions

The LLE of the ternary systems (heptane + toluene + [C<sub>2</sub>mim][NTf<sub>2</sub>]) and (octane + ethylbenzene + [C<sub>2</sub>mim][NTf<sub>2</sub>]) were experimentally determined at 25 °C, and the corresponding solute distribution ratios and selectivities were calculated. The

comparison of these values with those for the ternary system (hexane + benzene + [C<sub>2</sub>mim][NTf<sub>2</sub>])<sup>15</sup> allowed for analysing the influence of the hydrocarbons size (from C<sub>6</sub>- to C<sub>8</sub>-fraction) on the ability of the ionic liquid [C<sub>2</sub>mim][NTf<sub>2</sub>] as extraction solvent for the separation of aromatic and aliphatic hydrocarbons. On one hand, the selectivity values for all three ternary systems are quite similar. However, a gradual decrease in the solute distribution ratios is observed with an increase in the hydrocarbons size, from C<sub>6</sub>-fraction (hexane–benzene) to C<sub>7</sub>-fraction (heptane–toluene), and to C<sub>8</sub>-fraction (octane–ethylbenzene). This behaviour may be related to the solubility trend of the corresponding hydrocarbons in the ionic liquid: although the aromatics are largely more soluble than the aliphatics, in both series a decrease in solubility can be observed as the hydrocarbon fraction increases.

In all cases, a decrease with increasing the aromatic concentration in the system was observed in selectivity, as well as in the solute distribution ratio of the system (heptane + toluene + [C<sub>2</sub>mim][NTf<sub>2</sub>]), although not as strong as in the system (hexane + benzene + [C<sub>2</sub>mim][NTf<sub>2</sub>]). Nevertheless, the solute distribution ratio for the system (octane + ethylbenzene + [C<sub>2</sub>mim][NTf<sub>2</sub>]) remained practically constant regardless of the aromatic concentration.

The straightforward comparison of the extraction parameters of [C<sub>2</sub>mim][NTf<sub>2</sub>] and a reference solvent such as sulfolane showed that the ionic liquid can lead to an equivalent or better performance in practical cases. The negligible volatility of the ionic liquid might facilitate the recovery of the solvent in the raffinate and extract streams coming out of the extractor, thus the extraction unit being economically profitable even at lower concentrations of aromatic hydrocarbons in the feed than the current threshold. Considering work published by Meindersma *et al.*,<sup>10,11</sup> where other ionic liquids were used with the same hydrocarbon pairs as in this paper, it has been discussed that overall [C<sub>2</sub>mim][NTf<sub>2</sub>] can be considered as being superior to those other ionic liquids, or at least as good as them, in spite of leading to lower selectivities; but this can be compensated by other factors, including clearly higher solute distribution ratios, lower viscosity, low melting point and good chemical stability.

The classical NRTL model was proven to acceptably correlate the novel LLE data reported herein. In general, the agreement between experimental and correlated tie-lines for the two systems investigated is remarkable. Nonetheless, the model fails to correlate the minimal presence of [C<sub>2</sub>mim][NTf<sub>2</sub>] in the upper phase, reporting mole fractions of the ionic liquid which are several times higher than those found experimentally.

As a result of the above, the ionic liquid [C<sub>2</sub>mim][NTf<sub>2</sub>] can be confirmed as a potential alternative solvent for the separation of aromatic and aliphatic hydrocarbons. The results for hydrocarbons of the C<sub>7</sub>- and C<sub>8</sub>-fractions are almost identical to those of the C<sub>6</sub>-fraction in terms of selectivity; unfortunately, a larger amount of ionic liquid would be needed if treating feeds rich in the heavier hydrocarbons, because of the lower solute distribution ratios as the molecular weight increases.

## Acknowledgements

The authors are grateful to the Industrial Advisory Board of the QUILL Centre for their support. K. R. S. acknowledges

the EPSRC (Portfolio Partnership Scheme, grant number EP/D029538/1) for support. A. A. and H. R. thank the Ministerio de Educación y Ciencia (Spain) for financial support through project CTQ2006-07687 and the award of an FPI grant with reference BES-2004-5311.

## References

- 1 K. Weissermel and H.-J. Arpe, *Industrial Organic Chemistry*, Wiley/VCH, Weinheim, 4th edn, 2003.
- 2 R. Wennersten, in *Solvent Extraction Principles and Practice*, ed. J. Rydberg, M. Cox, C. Musikas and G. R. Choppin, Marcel Dekker, New York, 2nd edn, 2004, pp. 415–453.
- 3 W. A. Sweeney and P. F. Bryan, in *Encyclopedia of Separation Technology, A Kirk-Othmer Encyclopedia*, ed. A. Seidel, John Wiley & Sons, Hoboken, 2007.
- 4 *Ionic Liquids – Industrial Applications to Green Chemistry*, ed. R. D. Rogers and K. R. Seddon, ACS Symp. Ser. 818, American Chemical Society, Washington DC, 2002.
- 5 *Ionic Liquids as Green Solvents – Progress and Prospects*, ed. R. D. Rogers and K. R. Seddon, ACS Symp. Ser. 856, American Chemical Society, Washington DC, 2003.
- 6 M. S. Selvan, M. D. McKinkey, R. H. Dubois and J. L. Atwood, *J. Chem. Eng. Data*, 2000, **45**, 841–845.
- 7 T. M. Letcher and N. Deenadayalu, *J. Chem. Thermodyn.*, 2003, **35**, 67–76.
- 8 T. M. Letcher and P. Reddy, *J. Chem. Thermodyn.*, 2005, **37**, 415–421.
- 9 N. Deenadayalu, K. C. Ngcongco, T. M. Letcher and D. Ramjugernath, *J. Chem. Eng. Data*, 2006, **51**, 988–991; [Correction: *J. Chem. Eng. Data*, 2007, **52**, 318].
- 10 G. W. Meindersma, A. J. G. Podt and A. B. de Haan, *Fluid Phase Equilib.*, 2006, **247**, 158–168.
- 11 G. W. Meindersma, A. Podt and A. B. de Haan, *J. Chem. Eng. Data*, 2006, **51**, 1814–1819.
- 12 U. Domańska, A. Pobudkowska and M. Królikowski, *Fluid Phase Equilib.*, 2007, **259**, 173–179.
- 13 U. Domańska, A. Pobudkowska and Z. Żolek-Tryznowska, *J. Chem. Eng. Data*, 2007, **52**, 2345–2349.
- 14 C. C. Cassol, A. P. Umpierre, G. Ebeling, B. Ferrera, S. S. X. Chiaro and J. Dupont, *Int. J. Mol. Sci.*, 2007, **8**, 593–605.
- 15 A. Arce, M. J. Earle, H. Rodríguez and K. R. Seddon, *Green Chem.*, 2007, **9**, 70–74.
- 16 J. M. Sørensen, T. Magnussen, P. Rasmussen and A. Fredenslund, *Fluid Phase Equilib.*, 1979, **2**, 297–309.
- 17 J. P. Novák, J. Matouš and J. Pick, *Liquid–liquid equilibria*, Elsevier, Amsterdam, 1987.
- 18 J. Chen, L.-P. Duan, J.-G. Mi, W.-Y. Fei and Z.-C. Li, *Fluid Phase Equilib.*, 2000, **173**, 109–119.
- 19 J. Chen, Z. Li and L. Duan, *J. Chem. Eng. Data*, 2000, **45**, 689–692.
- 20 H. Renon and J. M. Prausnitz, *AIChE J.*, 1968, **14**, 135–144.
- 21 J. M. Sørensen, Ph.D. Thesis, Danmarks Tekniske Højskole, Lingby, Denmark, 1980.
- 22 A. Arce, M. J. Earle, H. Rodríguez and K. R. Seddon, *J. Phys. Chem. B*, 2007, **111**, 4732–4736.



# Extraction of alcohols from water with 1-hexyl-3-methylimidazolium bis(trifluoromethylsulfonyl)imide†

Alexandre Chapeaux, Luke D. Simoni, Thomas S. Ronan, Mark A. Stadtherr and Joan F. Brennecke\*

Received 6th May 2008, Accepted 13th August 2008

First published as an Advance Article on the web 16th October 2008

DOI: 10.1039/b807675h

Ethanol production in the U. S. has increased 36% between 2006 and 2007 (J. M. Urbanchuk, *Contribution of the Ethanol Industry to the Economy of the United States*, LECG, LLC, Renewable Fuels Association, 2008) in response to a growing demand for its use as a commercial transportation fuel. 1-Butanol also shows potential as a liquid fuel but both alcohols require high energy consumption in separating them from water. 1-Butanol, in particular, is considered an excellent intermediate for making other chemical compounds from renewable resources, as well as being widely used as a solvent in the pharmaceutical industry. These alcohols can be synthesized from bio-feedstocks by fermentation, which results in low concentrations of the alcohol in water. To separate alcohol from water, conventional distillation is used, which is energetically intensive. The goal of this study is to show that, using an ionic liquid, extraction of the alcohol from water is possible. Through the development of ternary diagrams, separation coefficients are determined. The systems studied are 1-hexyl-3-methylimidazolium bis(trifluoromethylsulfonyl)imide/ethanol/water, which exhibits Type 1 liquid–liquid equilibrium (LLE) behavior, and 1-hexyl-3-methylimidazolium bis(trifluoromethylsulfonyl)imide/1-butanol/water, which exhibits Type 2 LLE behavior. Based on the phase diagrams, this ionic liquid (1-hexyl-3-methylimidazolium bis(trifluoromethylsulfonyl)imide) can easily separate 1-butanol from water. It can also separate ethanol from water, but only when unreasonably high solvent/feed ratios are used. In addition, we use four excess Gibbs free energy ( $g^E$ ) models (NRTL, eNRTL, UNIQUAC and UNIFAC), with parameters estimated solely using binary data and/or pure component properties, to predict the behavior of the ternary LLE systems. None of the models adequately predicts the Type 1 system, but both UNIQUAC and eNRTL aptly predict the Type 2 system.

## Introduction

Ethanol is used currently as a common solvent and as an additive to gasoline. There is a growing market for transportation fuel that is primarily ethanol (E85). 1-Butanol is currently used primarily as a re-crystallization solvent in the pharmaceutical industry. However, 1-butanol could potentially be used as starting feed for making many common chemicals, and could also be an alternative fuel.<sup>1,2</sup> One of the major hurdles in switching to a biomass-based industry is the production costs (both economic and energetic) of the base alcohols. Purifying an alcohol requires about 6% of the energetic value of the compound itself, with a large portion used in the separation of the alcohol from the fermentation broth, mainly composed of water.<sup>2</sup>

Conventionally, separating alcohols and water requires a series of distillation columns. This method is energetically costly, and much room for improvement exists. Recent development of new membrane technology, such as pervaporation, has improved the efficiency of this separation, although rapid

fouling of the membranes remains a major issue with these methods.<sup>3</sup>

It has been shown that ionic liquids (ILs) have the potential for separating alcohol/water mixtures with simple liquid–liquid extraction,<sup>4</sup> which could be less energetically costly than distillation, and would have limited fouling problems.

ILs are salts with a melting point below 100 °C, which are usually composed of a poorly coordinating, bulky organic cation, and an organic or inorganic anion. Some the properties that make them advantageous for this application are negligible vapor pressure, which allows for recovery and reuse of the IL; a large liquid range, which allows for ease of separation; and, finally, a tunability which allows the creation of ILs that preferentially select alcohols from water.<sup>5,6</sup>

A few groups have studied ternary systems of ILs, alcohols and water. Fadeev *et al.* showed that it was possible to separate 1-butanol and water using 1-butyl-3-methylimidazolium and 1-octyl-3-methylimidazolium hexafluorophosphate.<sup>4</sup> Swatloski *et al.* studied 1-butyl-3-methylimidazolium, 1-hexyl-3-methylimidazolium and 1-octyl-3-methylimidazolium hexafluorophosphate with water and ethanol.<sup>7</sup> 1-Butyl-3-methylimidazolium hexafluorophosphate or bis(trifluoromethylsulfonyl)imide with ethanol, 2-methylpropanol, 1-butanol and water were studied at varying temperatures.<sup>8–10</sup> Hu *et al.* studied 1-hydroxyethyl-3-methylimidazolium and 1-hydroxyethyl-2,3-dimethylimidazolium tetrafluoroborate with 1-butanol and water.<sup>1</sup> Finally, there

Department of Chemical and Biomolecular Engineering, University of Notre Dame, 182 Fitzpatrick Hall, Notre Dame, Indiana, 46556.  
E-mail: jfb@nd.edu

† Electronic supplementary information (ESI) available: Equilibrium data and additional phase diagrams. See DOI: 10.1039/b807675h

is a variety of ternary vapor liquid equilibrium (VLE) data available for ILs with ethanol and water.<sup>11–15</sup>

This study focuses on accurately measuring the fundamental data necessary to design and implement liquid–liquid extraction for the separation of alcohols from water. Presented here are the experimental tie lines for the ternary mixtures of 1-hexyl-3-methylimidazolium bis(trifluoromethylsulfonyl)imide ([hmim][Tf<sub>2</sub>N]) with water and alcohols (ethanol and 1-butanol). [hmim][Tf<sub>2</sub>N] was chosen because it is the IUPAC standard ionic liquid, for which many pure component and binary measurements have been made. In addition, we focus on the modeling of the phase behavior, which is important in the design of real extraction processes.

## Results and discussion

### [hmim][Tf<sub>2</sub>N]/ethanol/water

The ternary phase diagram for [hmim][Tf<sub>2</sub>N]/ethanol/water at 295 K ± 2 K and 1 atm is shown in Fig. 1. The phase equilibrium compositions are tabulated in the ESI.† As can be seen in the figure, the [hmim][Tf<sub>2</sub>N] and water binary system shows a large immiscibility gap, as has been reported previously.<sup>16</sup> The [hmim][Tf<sub>2</sub>N] and ethanol binary system is completely miscible at room temperature. Of course, water and ethanol are completely miscible at room temperature.<sup>17</sup> The ternary system exhibits Type 1 LLE behavior with a large 2-phase region emanating from the IL/water binary.<sup>18</sup>

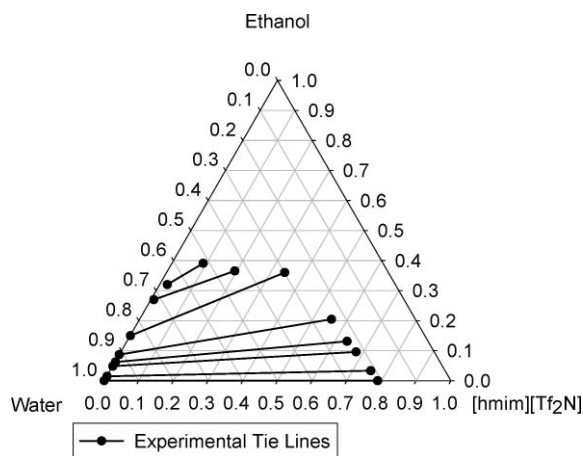


**Fig. 1** The [hmim][Tf<sub>2</sub>N]/ethanol/water system at 295 K and 1 atm (mole fraction).

Addition of ethanol to the IL/water mixture increases the solubility of water in the IL-rich phase, while only slightly increasing the solubility of the IL in the water-rich phase. Comparing this ternary system to published [hmim][PF<sub>6</sub>]/ethanol/water data,<sup>7</sup> the [Tf<sub>2</sub>N]<sup>-</sup> anion increases the size of the two phase immiscibility gap. Therefore, as in the binary data, the [Tf<sub>2</sub>N]<sup>-</sup> anion is more hydrophobic than the [PF<sub>6</sub>]<sup>-</sup> anion, and the mutual solubility with ethanol is increased.

Separation factors, which are a way to measure the potential of a separation between two phases  $\alpha$  and  $\beta$ , are defined as

$$S = \frac{\frac{x_{\text{alcohol}}^{\beta}}{x_{\text{water}}^{\beta}}}{\frac{x_{\text{alcohol}}^{\alpha}}{x_{\text{water}}^{\alpha}}} \quad (1)$$

For low concentrations of ethanol in water (*e.g.*, the maximum concentration of ethanol in water achievable during fermentation is about 4 mol%), the separation factors are around 10, which is quite low. Note that these separation factors and the ternary diagram shown in Fig. 1 are based on mole fraction. Since the molecular weights of the IL and the alcohol are very different, the ternary diagram looks qualitatively different when plotted as mass fraction. This is shown in the ESI.† It is possible to extract ethanol from a dilute ethanol/water mixtures using [hmim][Tf<sub>2</sub>N] but this requires large amounts of solvent (*e.g.*, an equimolar solvent to feed ratio). If one uses a more reasonable equal mass solvent to feed ratio, no separation is possible. Tables of the experimental data, both on a mole and mass basis, are shown in the ESI.†

### IL/1-butanol/water

Fig. 2 is the ternary diagram of [hmim][Tf<sub>2</sub>N]/1-butanol/water at 295 K ± 2 K and 1 atm. [hmim][Tf<sub>2</sub>N] and 1-butanol are completely miscible, but the [hmim][Tf<sub>2</sub>N]/water and 1-butanol/water binary systems are both partially miscible, as has been reported previously.<sup>16,17</sup> A large 2-phase region extends from the IL/water binary to the water/1-butanol binary, indicating a Type 2 LLE phase diagram.<sup>18</sup> The experimental data is shown in tabular form, both on a mole fraction and mass fraction basis, in the ESI.† In addition, the experimental data is plotted on a mass fraction basis in the ESI.†

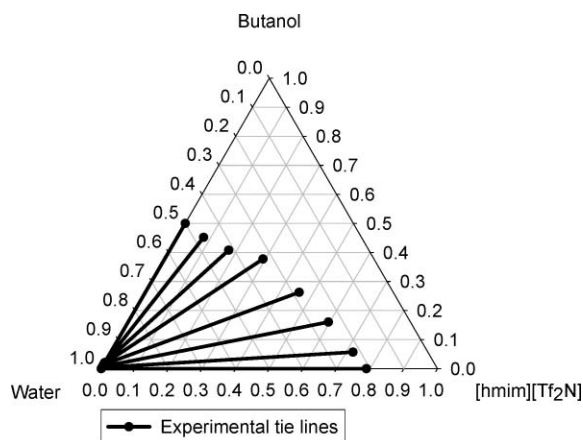


**Fig. 2** The [hmim][Tf<sub>2</sub>N]/1-butanol/water system at 295 K and 1 atm (mole fraction).

Comparing this ternary system to the published [bmim][Tf<sub>2</sub>N]/1-butanol/water system,<sup>9</sup> we observe an increase in the [hmim][Tf<sub>2</sub>N]/water immiscibility and in the mutual solubility of the [hmim][Tf<sub>2</sub>N] and 1-butanol, which is consistent with binary trends.<sup>18–20</sup> We also see the change from a system that exhibits Type 3b LLE behavior to one that exhibits Type 2 LLE behavior, since [hmim][Tf<sub>2</sub>N] and 1-butanol are completely miscible, while [bmim][Tf<sub>2</sub>N] and 1-butanol are not. Further, the solubility of the 1-butanol in the water-rich phase

decreases and an enhancement of the 1-butanol solubility in the IL-rich phase is observed.

Based on this ternary diagram, we conclude that separating 1-butanol and water using [hmim][Tf<sub>2</sub>N] could be easily accomplished using a multistage extractor. Separation factors for low concentrations of 1-butanol in water (*e.g.*, the maximum amount of 1-butanol in water achievable during fermentation is 2 wt%) are around 100. Hu *et al.* reported separation factors for 1-butanol and water between 50 and 250 using hydroxymethylimidazolium based ILs, which extract the water out of the 1-butanol.<sup>1</sup> In general, extracting the water from the 1-butanol would be less attractive than removing the alcohol since this would likely require the energy intensive process of evaporating large amounts of water from the IL.

Using this information, a multistage liquid–liquid extraction calculation was performed by the Hunter–Nash method<sup>21</sup> using the ternary diagram in Fig. 2 Assuming a feed composition of 2 wt% of 1-butanol in water, pure IL as the solvent, setting equal feed and solvent mass flow rates, and requiring 99 wt% fraction water in the final raffinate, it was determined that 4 stages are necessary to remove most of the water. Obviously, the separation would be even easier if a higher solvent/feed ratio were used.

#### Effect of the alkyl chain length on the alcohol

Comparing the ethanol and 1-butanol system, increasing the length of the alkyl chain on the alcohol decreases the solubility of the alcohol in the IL, as described previously, and decreases the mutual solubility of the alcohol and water. In the ternary systems, the separation coefficient of ethanol is smaller than that of 1-butanol. On a molecular level, the van der Waals interactions between the alcohol and the IL are more important in 1-butanol than in ethanol, relative to the hydrogen bonding. This results in a decrease in the mutual solubility of the alcohol and the IL. The longer alkyl chain on the alcohol also decreases the mutual solubility of the water and the alcohol, because the alcohol is more hydrophobic. This decrease in the amount of alcohol in the water-rich phase of the 1-butanol system allows the slopes to tip more steeply towards the water-rich phase.

#### Modeling of ternary system using NRTL/eNRTL/UNIQUAC/UNIFAC

Four different excess Gibbs free energy equations are evaluated for their ability to model the ternary IL/alcohol/water phase behavior: NRTL,<sup>22</sup> UNIQUAC,<sup>23</sup> electrolyte-NRTL (eNRTL),<sup>24</sup> and extended UNIFAC (Dortmund)<sup>25</sup> models. In the case of eNRTL, a new formulation of the model is used, based on a symmetric reference state.<sup>26</sup> The binary parameter estimation, ternary problem formulation, computational methods, and  $g^E$  model forms used to generate the following ternary predictions have been described previously.<sup>26</sup> In addition, the UNIFAC model and parameters for the IL (solvent group size, shape and interaction parameters) can be found elsewhere.<sup>25,27</sup>

Some additional explanation is needed for estimating the interaction parameters when UNIQUAC is used. We have found that when UNIQUAC is applied to binary systems involving an IL, often no parameter solutions yield liquid–liquid phase splitting. To allow the application of UNIQUAC to LLE for systems containing ILs, we follow the approach of Abreu *et al.*,<sup>28</sup>

and redefine the reference species used for determining the relative surface areas  $q_i$ . Conventionally, this reference is the van der Waals –CH<sub>2</sub>– group, but we have allowed the normalization of  $q_i$  to be relative to –CH<sub>2</sub>–, water or ethanol. In practice, the smallest reference species is used to normalize  $q_i$  that will give parameter solutions that predict liquid–liquid equilibrium.

**Ternary liquid–liquid equilibrium predictions.** Our goal is to study the effectiveness with which the excess Gibbs energy models listed above can be used to *predict* ternary liquid–liquid equilibrium solely from binary measurements. Thus, there are two main computational problems involved: 1. Parameter estimation from binary LLE or VLE data and 2. Computation of ternary LLE. The methods used for each of these problems are discussed elsewhere.<sup>26</sup>

Ternary phase diagrams for two systems were predicted: [hmim][Tf<sub>2</sub>N]/ethanol/water and [hmim][Tf<sub>2</sub>N]/1-butanol/water. Both systems are computed at 295 K. Experimentally, the former system exhibits Type 1 LLE behavior, and the latter system exhibits Type 2 LLE behavior, as discussed above.

*Predictions for [hmim][Tf<sub>2</sub>N]/ethanol/water.* The first system, [hmim][Tf<sub>2</sub>N]/ethanol/water at ambient pressure and 295 K, is a Type 1 LLE system. As noted by Anderson and Prausnitz,<sup>29</sup> the quality of the binary VLE data used to obtain model parameters for the two completely miscible binary subsystems will greatly influence the quality of model predictions for Type 1 systems, though correct qualitative results (one distinct phase envelope) are likely to be obtained. For the example considered here, the ternary LLE phase diagram is computed with NRTL, UNIQUAC and eNRTL using parameters obtained from binary measurements.<sup>16,30–32</sup> The estimated interaction parameters for the NRTL, UNIQUAC and eNRTL models are given in Tables 1–4 provide the number of UNIFAC groups for each component, the pure solvent parameters for eNRTL and the physical dimension parameters for UNIQUAC, respectively. The NRTL and eNRTL predictions, superimposed over the experimental tie lines, are shown in Fig. 3, and the UNIQUAC and UNIFAC predictions are shown in Fig. 4. Note that the reference species for the UNIQUAC  $q_i$  parameter is the traditional –CH<sub>2</sub>– group.<sup>23</sup>

Here, all of the models tested provide results that are qualitatively consistent with the experimental data (Type 1). However, NRTL tends to significantly overestimate the size of the two-phase envelope. Nonetheless, it predicts the slope of the tie lines surprisingly well. Overall, UNIQUAC provides better predictions of the phase behavior; the entropic contribution that accounts for mixing components of greatly different size and shape predicts a very accurate binodal curve. We see that the eNRTL and UNIFAC models are not as accurate in predicting neither the location of the binodal curve nor the slopes of the tie line. UNIQUAC and eNRTL most closely capture the correct location of the plait point, whereas UNIQUAC under predicts and eNRTL over predicts. It should be noted that every model used here, with the exception of UNIFAC, suggests that [hmim][Tf<sub>2</sub>N] is better for extracting ethanol from water than supported by the experimental data. In light of a previous study,<sup>26</sup> however, we recommend use of UNIQUAC for Type 1 systems involving imidazolium bis(trifluoromethylsulfonyl)imide-based ILs,

**Table 1** Activity coefficient model binary interaction parameters (J mol<sup>-1</sup>) for ternary diagrams at 295 K

NRTL							
System (components: 1/2/3)	$\Delta g_{12}$	$\Delta g_{21}$	$\Delta g_{13}$	$\Delta g_{31}$	$\Delta g_{23}$	$\Delta g_{32}$	$\alpha_{23}$
[hmim][Tf <sub>2</sub> N]/ethanol/water	-3087.1 <sup>b</sup>	6533.1 <sup>b</sup>	702.08 <sup>a</sup>	21820 <sup>a</sup>	-2568.6	6949.2	0.1448 <sup>32</sup>
[hmim][Tf <sub>2</sub> N]/1-butanol/water	-5222.6 <sup>b</sup>	9210.2 <sup>b</sup>	702.08 <sup>a</sup>	21820 <sup>a</sup>	-2566.9	12505	0.2 <sup>18</sup>
eNRTL, $\rho = 14.9$							
System	$\Delta g_{12}$	$\Delta g_{21}$	$\Delta g_{13}$	$\Delta g_{31}$	$\Delta g_{23}$	$\Delta g_{32}$	$\alpha_{23}$
[hmim][Tf <sub>2</sub> N]/ethanol/water	-8287.1 <sup>b</sup>	14259 <sup>b</sup>	-2707.1 <sup>a</sup>	21287 <sup>a</sup>	-2568.6	6949.2	0.1448 <sup>32</sup>
[hmim][Tf <sub>2</sub> N]/1-butanol/water	-5456.4 <sup>b</sup>	10477 <sup>b</sup>	-2707.1 <sup>a</sup>	21287 <sup>a</sup>	-2566.9	12505	0.2 <sup>18</sup>
UNIQUAC							
System	$\Delta u_{12}$	$\Delta u_{21}$	$\Delta u_{13}$	$\Delta u_{31}$	$\Delta u_{23}$	$\Delta u_{32}$	$q_{\text{ref}}$
[hmim][Tf <sub>2</sub> N]/ethanol/water	2669.4	-760.31	4812.5	151.97	-245.79	1870.2	-CH <sub>2</sub> -
[hmim][Tf <sub>2</sub> N]/1-butanol/water	-377.54	1049.6	6951.4	1582.8	1842.0	2413.5	H <sub>2</sub> O

<sup>a</sup> liquid–liquid equilibrium binary,  $\alpha_{ij} = 0.2$ . <sup>b</sup> VLE binary,  $\alpha_{ij} = 0.3$ .

**Table 2** UNIFAC segments for systems 1 and 2

Component/Group	[hmim][Tf <sub>2</sub> N]	Ethanol	1-Butanol	Water
Imidazolium	1	0	0	0
[Tf <sub>2</sub> N] <sup>-</sup>	1	0	0	0
-CH <sub>2</sub> -	5	1	3	0
-CH <sub>3</sub>	2	1	1	0
-OH	0	1	1	0
H <sub>2</sub> O	0	0	0	1

**Table 3** eNRTL solvent properties

Solvent	Temp/K	<i>M</i>	<i>d</i> /g cm <sup>-3</sup>	$\epsilon$	Reference
Ethanol	295	46.07	0.78	23.7	Smyth and Stoops <sup>37</sup>
<i>n</i> -Butanol	295	74.12	0.80	17.4	Smyth and Stoops <sup>37</sup>
Water	295	18.02	1.00	79.2 <sup>a</sup>	Robinson and Stokes <sup>38</sup>

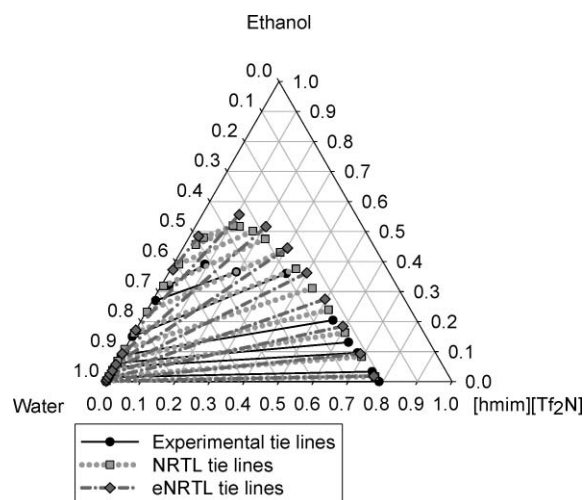
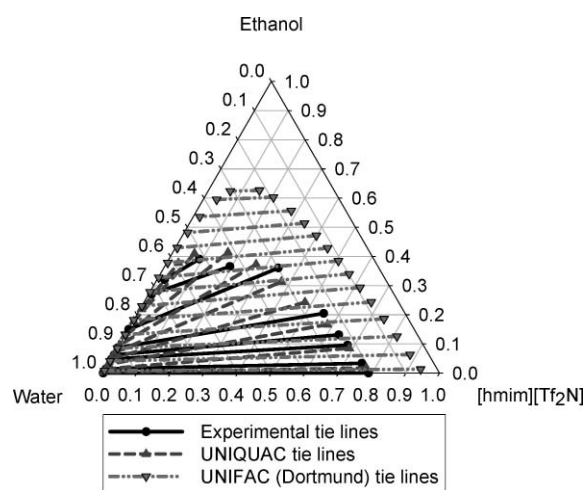
<sup>a</sup> See also Fernandez *et al.* for data on the dielectric constant of water.<sup>39</sup>

**Table 4** UNIQUAC size and shape parameters for ternary diagrams

Component	<i>q</i> reference	<i>r<sub>i</sub></i>	<i>q<sub>i</sub></i>
[hmim][Tf <sub>2</sub> N]	-CH <sub>2</sub> -	12.51	11.62
[hmim][Tf <sub>2</sub> N]	H <sub>2</sub> O	12.51	8.30
Ethanol	-CH <sub>2</sub> -	2.11	1.97
1-Butanol	H <sub>2</sub> O	3.92	2.62
Water	-CH <sub>2</sub> -	0.92	1.40
Water	H <sub>2</sub> O	0.92	1.00

alcohols and water. Finally, although UNIFAC provides the worst results of the models tested, as shown in Fig. 3 and 4, it should be noted that its qualitative agreement with experimental data is impressive since it is a purely predictive group contribution model, with no parameters fit to binary data.

**Predictions for [hmim][Tf<sub>2</sub>N]/1-butanol/water.** The second system, [hmim][Tf<sub>2</sub>N]/1-butanol/water at 295 K and ambient pressure, exhibits Type 2 ternary LLE behavior. For this system, the ternary LLE phase diagrams are predicted with NRTL, UNIQUAC and eNRTL from the binary data.<sup>16,18,33</sup> Furthermore, the UNIFAC prediction is made with group size, shape and interaction parameters that were determined elsewhere.<sup>25,27</sup> Fig. 5 gives NRTL and eNRTL predictions, and Fig. 6 shows UNIQUAC and UNIFAC (Dortmund) predictions, in comparison to the experimental results. The

**Fig. 3** The [hmim][Tf<sub>2</sub>N]/ethanol/water system at 295 K and 1 atm. Both NRTL and eNRTL predict type 1 behavior.**Fig. 4** The [hmim][Tf<sub>2</sub>N]/ethanol/water system at 295 K and 1 atm. Both UNIQUAC and UNIFAC predict type 1 behavior.

estimated interaction parameters for the NRTL, UNIQUAC and eNRTL models given in Table 1–4 provide the number of UNIFAC groups for each component, the pure solvent



parameters for eNRTL and the physical dimension parameters for UNIQUAC, respectively. Note that for the system the reference species for the UNIQUAC  $q_i$  parameter is water.<sup>28</sup>

As seen in Fig. 5 and 6, all models correctly predict Type 2 behavior. In fact, all the models accurately predict this system. The UNIQUAC and eNRTL models provide predictions that match the experimental data within experimental uncertainty. The quality of the predictions is somewhat lower for NRTL, and the UNIFAC model predicts a larger two phase region than is observed experimentally. Note that in Fig. 5 and 6, the slopes of the predicted tie lines are in very good agreement with experiment for all models. Careful examination reveals the best tie lines for the eNRTL model, followed closely by UNIQUAC. As the phase envelope resides closest to the aqueous side of the diagram, where more ionic dissociation is likely, the physical picture is consistent with the eNRTL equation being the most accurate of the models tested.

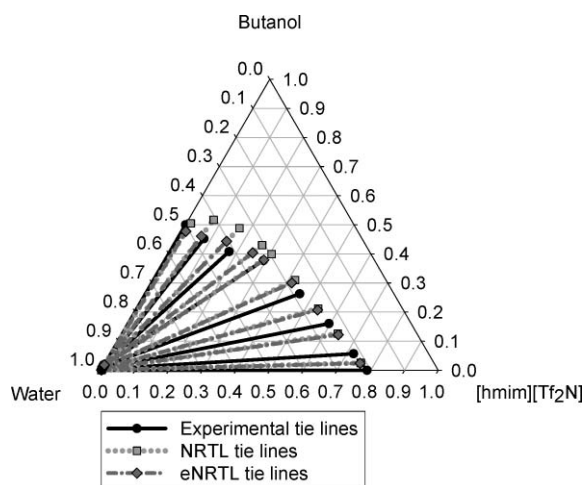


**Fig. 5** The [hmim][Tf<sub>2</sub>N]/1-butanol/water system at 295 K and 1 atm. Both NRTL and eNRTL predict type 2 behavior.

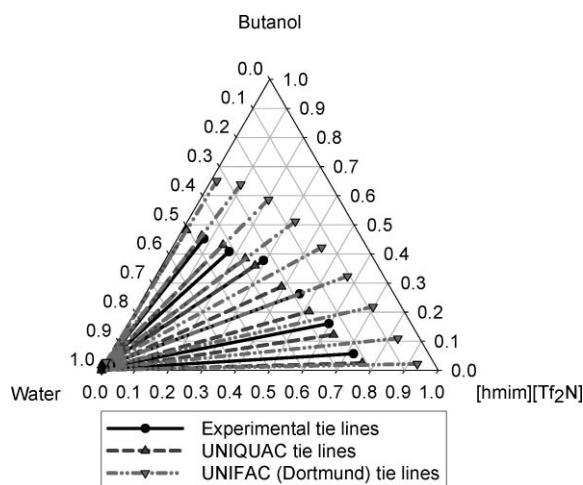


**Fig. 6** The [hmim][Tf<sub>2</sub>N]/1-butanol/water system at 295 K and 1 atm. Both UNIQUAC and UNIFAC predict type 2 behavior.

## Experimental

### Materials

Ethanol (64-17-5, 99.5+% purity, reagent grade, 150 ppm water) and 1-butanol (71-36-3, 99.8+% purity, reagent grade, 600 ppm water) were purchased from Sigma–Aldrich and used as received. The water was deionized by a Millipore purification system (>18 MΩ cm resistivity). [hmim][Tf<sub>2</sub>N] was made according to previously described methods.<sup>20,21,34,35</sup> Standard purification methods were followed and have been described elsewhere.<sup>20,21,36</sup> The bromide content of [hmim][Tf<sub>2</sub>N] was 15 ppm, as measured with Cole–Parmer Bromide Specific Probes (27502–05), which is accurate to ±10 ppm. [hmim][TF<sub>2</sub>N] was dried under vacuum (~1.3 Pa) at 70 °C before use, and the water content, measured by a Karl Fischer coulometer (Metrohm 831 KF Coulometer, accurate within 5 ppm), was below 50 ppm.

### Procedure

To obtain ternary liquid–liquid equilibrium data, samples at various overall compositions of the three components (IL, water, alcohol) were made gravimetrically and placed in air tight vials with a stir bar. They were mixed for about 12 h, such that the stir bar broke the interface to ensure good mixing. The phases in the samples were then allowed to separate for an additional 12 h.

The equilibrium compositions of each phase, described by tie lines on a ternary diagram, were obtained by analyzing the concentrations of all three compounds in each phase. The water content was measured by a Karl Fischer coulometer and the alcohol and IL content were measured with a high pressure liquid chromatograph (Perkin Elmer system: ISS 200 Autosampler, LC 410 Quaternary Pump, Series 200a RI detector, Series 200 Column Oven, Bio-Rad Aminex HPX-87C column). Both phases in each vial were sampled in each of three replicate vials for each feed composition. The estimated uncertainty in the compositions is ±3 mol%. In all cases, the independently determined compositions in each phase summed to one within 5 mol%.

## Conclusion

Developing an understanding of the behavior of ternary systems with ionic liquids is a critical first step in determining their ability to separate systems such as alcohols and water. Further, one must have experimental data with which to compare and evaluate predictive models. In this work, we presented experimental ternary phase diagrams and, based on those experimental results, showed that [hmim][Tf<sub>2</sub>N] should be able to easily separate 1-butanol from water. The separation of ethanol from water with [hmim][Tf<sub>2</sub>N] should be possible, but would require unreasonably high solvent/feed ratios (*e.g.*, equimolar ratio rather than equal mass). Finally, excess Gibb's free energy models based solely on binary data were used to predict the behavior of the systems studied. UNIQUAC was found to be the best model for predicting the Type 1 system (although NRTL provided the most accurate tie lines in this case), and eNRTL and UNIQUAC were the better models for predicting the Type 2 system.

Many possible configurations may be possible for extracting alcohols from fermentation broths, including conventional packed bed columns, as well as supported liquid membranes. Future work will include estimates of energy requirements for the combined liquid extraction/distillation system compared to direct distillation of the alcohol/water systems.

## Acknowledgements

We acknowledge financial support for the project from the National Oceanic and Atmospheric Administration (NOAA). We thank Argonne National Laboratory, Energy Division, Chemical & Biological Technologies Section for initial guidance with this study.

## References

- X. S. Hu, J. Yu and H. Z. Liu, *J. Chem. Eng. Data*, 2006, **51**, 691–695.
- N. Qureshi, S. Hughes, I. S. Maddox and M. A. Cotta, *Bioprocess Biosyst. Eng.*, 2005, **27**, 215–222.
- L. M. Vane, *J. Chem. Technol. Biotechnol.*, 2005, **80**, 603–629.
- A. G. Fadeev and M. M. Meagher, *Chem. Commun.*, 2001, 295–296.
- J. F. Brennecke and E. J. Maginn, *AIChE J.*, 2001, **47**, 2384–2389.
- K. R. Seddon, *Kinet. Catal.*, 1996, **37**, 693–697.
- R. P. Swatloski, A. E. Visser, W. M. Reichert, G. A. Broker, L. M. Farina, J. D. Holbrey and R. D. Rogers, *Green Chem.*, 2002, **4**, 81–87.
- V. Najdanovic-Visak, J. M. S. S. Esperanca, L. P. N. Rebelo, M. N. da Ponte, H. J. R. Guedes, K. R. Seddon and J. Szydlowski, *Phys. Chem. Chem. Phys.*, 2002, **4**, 1701–1703.
- V. Najdanovic-Visak, L. P. N. Rebelo and M. N. da Ponte, *Green Chem.*, 2005, **7**, 443–450.
- V. Najdanovic-Visak, A. Serbanovic, J. M. S. S. Esperanca, H. J. R. Guedes, L. P. N. Rebelo and M. N. da Ponte, *ChemPhysChem*, 2003, **4**, 520–522.
- N. Calvar, B. Gonzalez, E. Gomez and A. Dominguez, *J. Chem. Eng. Data*, 2006, **51**, 2178–2181.
- N. Calvar, B. Gonzalez, E. Gomez and A. Dominguez, *Fluid Phase Equilib.*, 2007, **259**, 51–56.
- N. Calvar, B. Gonzalez, E. Gomez and A. Dominguez, *J. Chem. Eng. Data*, 2008, **53**, 820–825.
- J. F. Wang, C. X. Li and Z. H. Wang, *J. Chem. Eng. Data*, 2007, **52**, 1307–1312.
- J. Zhao, C. C. Dong, C. X. Li, H. Meng and Z. H. Wang, *Fluid Phase Equilib.*, 2006, **242**, 147–153.
- A. Chapeaux, L. D. Simoni, M. A. Stadtherr and J. F. Brennecke, *J. Chem. Eng. Data*, 2007, **52**, 2462–2467.
- R. Stephenson and J. Stuart, *J. Chem. Eng. Data*, 1986, **31**, 56–70.
- Liquid–Liquid Equilibrium Data Collection*, ed. J. M. Sørensen and W. Arlt, Dechema, Frankfurt am Main, 1980.
- J. M. Crosthwaite, S. Aki, E. J. Maginn and J. F. Brennecke, *J. Phys. Chem. B*, 2004, **108**, 5113–5119.
- J. M. Crosthwaite, S. Aki, E. J. Maginn and J. F. Brennecke, *Fluid Phase Equilib.*, 2005, **228–229**, 303–309.
- J. D. Seader and E. J. Henley, *Separation Process Principles*, Wiley, New York, NY, 1998.
- H. Renon and J. M. Prausnitz, *AIChE J.*, 1968, **14**, 135–144.
- D. S. Abrams and J. M. Prausnitz, *AIChE J.*, 1975, **21**, 116–128.
- C. C. Chen, H. I. Britt, J. F. Boston and L. B. Evans, *AIChE J.*, 1982, **28**, 588–596.
- J. Gmehling, J. Li and M. Schiller, *Ind. Eng. Chem. Res.*, 1993, **32**, 178–193.
- L. D. Simoni, Y. Lin, J. F. Brennecke and M. A. Stadtherr, *Ind. Eng. Chem. Res.*, 2007, **47**, 256–272.
- S. Nebig, R. Bölts and J. Gmehling, *Fluid Phase Equilib.*, 2007, **258**, 168–178.
- C. R. A. Abreu, M. Castier and F. W. Tavares, *Chem. Eng. Sci.*, 1999, **54**, 893–896.
- T. F. Anderson and J. M. Prausnitz, *Ind. Eng. Chem. Process Des. Dev.*, 1978, **17**, 561–567.
- Vapor–liquid Equilibrium Data Collection, Chemistry Data Series*, ed. J. Gmehling, U. Onken and W. Arlt, vol. I, parts 1–8, Dechema, Frankfurt/Main, Germany, 1977–1990.
- R. Kato and J. Gmehling, *J. Chem. Thermodyn.*, 2005, **37**, 603–619.
- K. Kurihara, M. Nakamichi and K. Kojima, *J. Chem. Eng. Data*, 1993, **38**, 446–449.
- J. Lachwa, P. Morgado, J. M. S. S. Esperanca, H. J. R. Guedes, J. N. C. Lopes and L. P. N. Rebelo, *J. Chem. Eng. Data*, 2006, **51**, 2215–2221.
- P. Bonhote, A. P. Dias, N. Papageorgiou, K. Kalyanasundaram and M. Gratzel, *Inorg. Chem.*, 1996, **35**, 1168–1178.
- L. Cammarata, S. G. Kazarian, P. A. Salter and T. Welton, *Phys. Chem. Chem. Phys.*, 2001, **3**, 5192–5200.
- C. P. Fredlake, J. M. Crosthwaite, D. G. Hert, S. N. V. K. Aki and J. F. Brennecke, *J. Chem. Eng. Data*, 2004, **49**, 954–964.
- C. P. Smyth and W. N. Stoops, *J. Am. Chem. Soc.*, 1929, **51**, 3312–3329.
- R. A. Robinson and R. H. Stokes, *Electrolyte Solutions*, 2nd edn, Butterworths, London, UK, 1959.
- D. P. Fernández, A. R. H. Goodwin, E. W. Lemmon, J. M. H. Levelt, Sengers and R. C. Williams, *J. Phys. Chem. Ref. Data*, 1997, **26**, 1125–1166.

# It is “2-imino-4-thiazolidinones” and not thiohydantoins as the reaction product of 1,3-disubstituted thioureas and chloroacetylchloride†

Ramesh Yella, Harisadhan Ghosh and Bhisma K. Patel\*

Received 7th May 2008, Accepted 16th September 2008

First published as an Advance Article on the web 21st October 2008

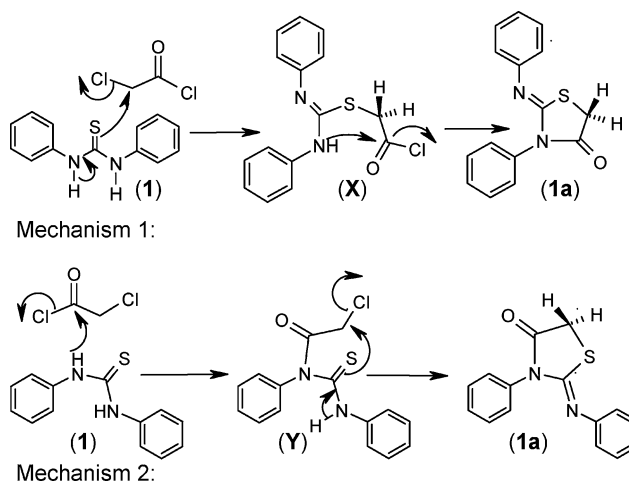
DOI: 10.1039/b807775d

The products obtained by the reaction of 1,3-disubstituted thioureas with chloroacetylchloride are actually 2-imino-4-thiazolidinone derivatives and not thiohydantoins as previously reported (M. Kidwai, R. Venkataraman and B. Dave, *Green Chem.*, 2001, 3, 278). A highly efficient method for the preparation of 2-imino-4-thiazolidinones has been achieved from both symmetrical and unsymmetrical thioureas in the absence of base. The reaction gives a regioselective product for unsymmetrical thiourea which is dependent on the  $pK_a$ 's of the amines. For unsymmetrical thiourea, regioselective 2-imino-4-thiazolidinone formation takes place with the amine attached to the thiourea having lower  $pK_a$  as part of the imino component and the amine having higher  $pK_a$  contributes to the other heterocyclic nitrogen.

## Introduction

The mechanism of thiazole-2-imine formation has not been well understood leading to the proposal of incorrect structures for the products obtained by the reaction of thiourea analogues with  $\alpha$ -haloketones by two independent research groups.<sup>1</sup> Recently, we have suggested a plausible reaction mechanism for the formation of thiazole-2-imine. Our mechanism is supported by isolating the reaction intermediate, confirming its structure and that of the products by X-ray crystallography.<sup>2</sup>

Having understood the reactivity of thioureas towards  $\alpha$ -haloketones, we have reasoned that the products obtained by the reaction of thiourea with chloroacetylchloride under a basic medium should not be thiohydantoins as has been reported.<sup>3</sup> Rather they are expected to have an isomeric 2-imino-4-thiazolidinone skeleton. Our assumption is based on the fact that the sulfur atom (soft nucleophile) of the thiourea will preferentially attack the  $\alpha$ -haloketone (soft electrophile) and NH (hard nucleophile) will attack the carbonyl centre (hard electrophile). Thus we envisaged the following mechanism (Scheme 1) leading to the formation of 2-imino-4-thiazolidinone. The soft nucleophile sulfur of thiourea attacks the soft electrophilic centre chloromethyl carbon giving intermediate **X** as proposed in mechanism 1, Scheme 1. Intramolecular attack of the second NH group of the intermediate **X**, a hard nucleophile will attack the carbonyl carbon of chloroacetylchloride leading to the formation of the expected product **1a**. Alternatively, a second mechanism can not be ruled out where the hard nucleophile NH will attack first the hard electrophilic carbonyl carbon giving intermediate **Y** as shown in mechanism 2, Scheme 1. This is then followed by an intramolecular attack of sulfur on the



**Scheme 1** Plausible mechanism for the formation of 2-imino-4-thiazolidinone.

chloromethyl group leading to the formation of the 2-imino-4-thiazolidinone derivative **1a**.

## Results and discussion

With this assumption, when 1,3-diphenylthiourea **1** was reacted with chloroacetyl chloride under an identical condition as has been described in this journal<sup>3</sup> a product was obtained in mere 45% isolated yield. Proton NMR analysis of the product showed the presence of a doublet at  $\delta = 3.97$  ( $J = 3.6$  Hz) corresponding to two protons. The appearance of the doublet may be due to the non-equivalency of the two protons attached adjacent to a sulfur atom, an observation consistent with the literature.<sup>4</sup> Its HRMS analysis corresponds to a product with molecular formula ( $C_{15}H_{12}N_2O_2S_1$ ). Thus it was difficult to conclude whether the product obtained was 2-imino-4-thiazolidinone as suggested by us or thiohydantoins as has been reported.<sup>3</sup>

Department of Chemistry, Indian Institute of Technology Guwahati, Guwahati, 781 039, Assam, India. E-mail: patel@iitg.ernet.in

† Electronic supplementary information (ESI) available: Spectra. CCDC reference numbers 686655 and 692011. For ESI and crystallographic data in CIF or other electronic format see DOI: 10.1039/b807775d

Interestingly, the compound crystallized out from a mixture of chloroform and hexane (9:1). Crystal X-ray crystallography of the product unequivocally confirmed having the 2-imino-4-thiazolidinone skeleton as shown in Fig. 1, an assumption made by us at the very beginning.<sup>7</sup> The presence of an iminothiazolidinone skeleton can be clearly seen from Fig. 1. The imino group (C=N) C1–N2 (1.266(17) Å) has a shorter bond distance compared to C1–N1 (1.403(16) Å) of the ring system. Furthermore, the C2–S1 (1.801(14) Å) and C1–S1 (1.768(13) Å) bond distances are characteristic of sp<sup>3</sup>-S and sp<sup>2</sup>-S bond distances. The melting point of the isolated compound **1a** was found to be 178 °C, which closely resembles the melting point of 172 °C and 175–176 °C reported by other groups.<sup>5</sup> Surprisingly, the melting point reported is much less (96–97 °C) in this journal for the proposed structure.<sup>3</sup> Had the structure been isomeric thiohydantoin as reported the m.p would have been 218–220 °C as has been reported in the literature.<sup>6</sup> Thus the melting point reported neither corresponds to the proposed thiohydantoin structure nor 2-imino-4-thiazolidinone. We were also surprised with the choice of methanol as the solvent as it will react with chloroacetylchloride to form chloroacetic acid methylester which is expected to be less reactive.

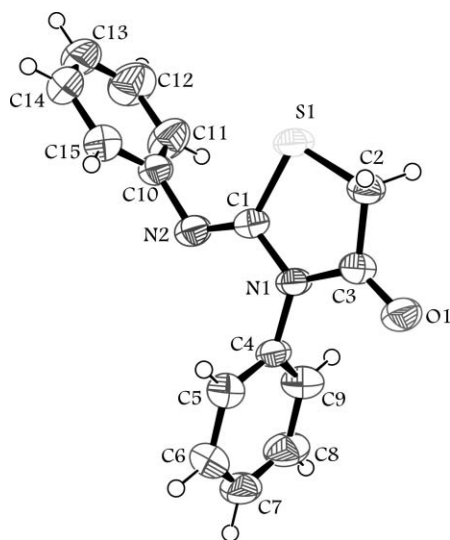
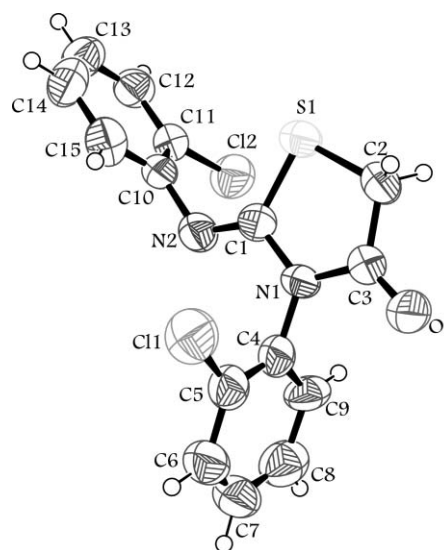


**Fig. 1** ORTEP molecular diagram, with ellipsoid at 50% probability of **1a**.

Having resolved the structural conflict, we wished to develop an efficient method for the preparation of various 2-imino-4-thiazolidinones. In our hands, we obtained a much lower yield (45%) as compared to the literature method (80%).<sup>3</sup> However, when 1,3-diphenylthiourea **1** (1 mmol) was reacted with chloroacetylchloride (1.5 mmol) in the presence of two equivalents of triethylamine under a solvent free condition at room temperature, the desired product **1a** was obtained in 90% isolated yield. This product was identical in all respects (melting point, IR, <sup>1</sup>H and <sup>13</sup>C NMR) to the product obtained by us using K<sub>2</sub>CO<sub>3</sub>-basic alumina under microwave-irradiation. We wanted to see if the reaction can be performed in the absence of a base since chloroacetyl chloride is quite reactive. It was surprising to note that when 1.5 equivalent of chloroacetylchloride was added to 1,3-diphenylthiourea **1**, a sticky solid was obtained.

To this was added acetonitrile (1 mL) to make the medium homogeneous and stirred for 5 minutes. Thin layer chromatography showed complete conversion to product **1a**. After usual workup, the product obtained was again found to be identical (melting point, IR, <sup>1</sup>H and <sup>13</sup>C NMR). Thus the change in the reaction condition has no effect on the reaction path leading to the product formation.

Symmetrical thioureas **2–7** (Table 1) gave their corresponding 2-imino-4-thiazolidinones **1a–7a** in excellent yields under the described reaction conditions. The formation of the 2-imino-4-thiazolidinone skeleton has been further confirmed from the crystal X-ray crystallography of product **5a** (Fig. 2).<sup>8</sup> Here again, the measured bond length C1–N2 (1.282(4) Å) for the imino group is shorter compared to C1–N1 (1.428(4) Å) of the ring system and the C2–S1 (1.834(3) Å) and C1–S1 (1.778(3) Å) bond distances are characteristic of sp<sup>3</sup>-S and sp<sup>2</sup>-S bond distances.

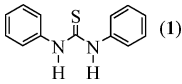
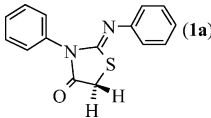
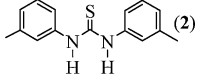
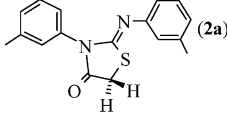
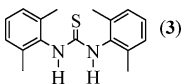
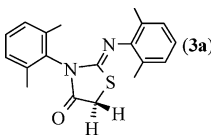
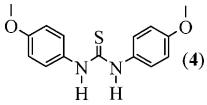
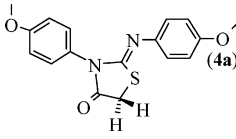
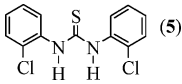
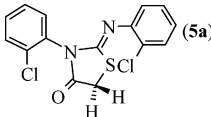
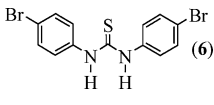
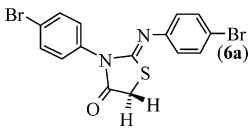
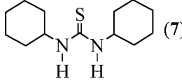
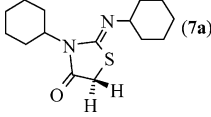


**Fig. 2** ORTEP molecular diagram, with ellipsoid at 50% probability of **5a**.

Having successfully synthesized a series of 2-imino-4-thiazolidinones from symmetrical thioureas, we were interested to investigate the regioselectivity in the reaction for unsymmetrical thioureas. Recently we have found a good correlation between the regioselective N-acylation and the pK<sub>a</sub>'s of the precursor amines attached to the thioureas.<sup>11</sup> A similar observation was also observed during the synthesis of thiazole-2-imine or 2-iminothiazoline.<sup>2b</sup> The larger the difference between the pK<sub>a</sub>'s of the precursor amines in thioureas, the higher is the regioselectivity of N-acylation with preferential acylation taking place towards the amine having lower pK<sub>a</sub>.<sup>11</sup> We wanted to see if this is applicable for the synthesis of 2-imino-4-thiazolidinones as well. When unsymmetrical thiourea **8** (Table 2) containing a phenyl and a *o*-chlorophenyl group attached to the thiourea reacted with chloroacetylchloride it gave a mixture of 2-imino-4-thiazolidinones **8a** and **8b** in the ratio of 36:64. The measured pK<sub>a</sub> of aniline and *o*-chloroaniline respectively are 4.63 and 2.65. Thus as per the mechanism 1, Scheme 1, the amine having lower pK<sub>a</sub> will be a part of the imino component and the other amine attached to the thiourea having higher pK<sub>a</sub> will contribute to the other heterocyclic nitrogen in the 2-imino-4-thiazolidinone



**Table 1** Formation of 2-imino-4-thiazolidinone from 1,3-disubstituted thiourea and chloroacetylchloride

Entry	Thiourea	Product	Yield (%) <sup>a</sup>
1	 (1)	 (1a)	92
2	 (2)	 (2a)	94
3	 (3)	 (3a)	95
4	 (4)	 (4a)	92
5	 (5)	 (5a)	93
6	 (6)	 (6a)	95
7	 (7)	 (7a)	85

<sup>a</sup> Yield of pure isolated product.

skeleton. This assumption has been again demonstrated for thiourea **9**. The ratio (34:66) of the product **9a** and **9b** can be again explained based on the measured  $pK_a$ 's of *p*-methoxy aniline (5.34) and *p*-bromoaniline (3.86). With a larger difference in  $pK_a$ 's attached to thiourea exclusively one product is obtained as has been demonstrated in substrate **10** having aniline ( $pK_a$  4.63) and cyclohexylamine ( $pK_a$  10.66). This has been further demonstrated with two other substrates **11** and **12** having cyclohexylamine ( $pK_a$  10.66) attached to one side and *p*-methoxy aniline ( $pK_a$  5.34) and *p*-bromo aniline ( $pK_a$  3.86) to the other side in thioureas **11** and **12** respectively.

## Conclusion

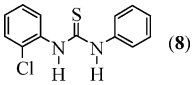
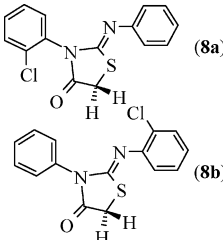
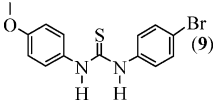
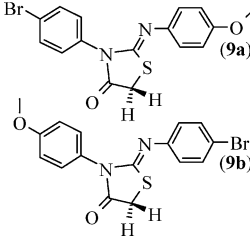
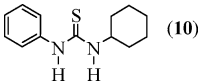
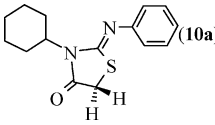
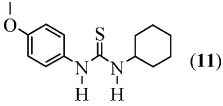
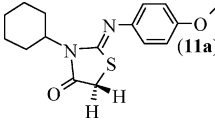
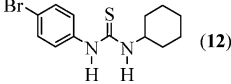
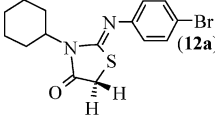
In conclusion, we have unambiguously proved that the reaction of 1,3-disubstituted thioureas with chloroacetylchloride in the presence of basic alumina and  $K_2CO_3$  are 2-imino-4-thiazolidinone derivatives and not thiohydantoin as reported earlier.<sup>3</sup> This reaction can be performed at room temperature

without using any base. Regioselective formation of 2-imino-4-thiazolidinones are observed for unsymmetrical thioureas in which amine attached to the thiourea having lower  $pK_a$  is a part of the imino component and the amine having higher  $pK_a$  is the contributor to the other heterocyclic nitrogen.

## Experimental

All the reagents were commercial grade and purified according to the established procedures. Organic extracts were dried over anhydrous sodium sulfate. Solvents were removed in a rotary evaporator under reduced pressure. Silica gel (60–120 mesh size) was used for the column chromatography. Reactions were monitored by TLC on silica gel 60 GF254 (0.25 mm). NMR spectra were recorded in  $CDCl_3$  with tetramethylsilane as the internal standard for  $^1H$  NMR (400 MHz) and  $CDCl_3$  solvents as internal standard for  $^{13}C$  NMR (100 MHz). IR spectra were recorded in KBr or neat. GC-MS were recorded using a capillary column (30 × 0.25 mm × 0.25 μm) in EI mode. HRMS

**Table 2** Formation of 2-imino-4-thiazolidinone from unsymmetrical 1,3-disubstituted thiourea and chloroacetylchloride

Entry	Thiourea	Product	Yield (%) <sup>a</sup>
8	 (8)	 (8a) (8b)	90 (30:64)
9	 (9)	 (9a) (9b)	92 (34:66)
10	 (10)	 (10a)	93
11	 (11)	 (11a)	90
12	 (12)	 (12a)	91

<sup>a</sup> Yield of pure isolated product.

spectra were recorded on a WATERS LC-MS/MS System, Q-ToF Premier™. Crystal data were collected with a Bruker Smart Apex-II CCD diffractometer using graphite monochromated Mo-K $\alpha$  radiation ( $\lambda = 0.71073 \text{ \AA}$ ) at 298 K. Cell parameters were retrieved using SMART<sup>9</sup> software and refined with SAINT<sup>9</sup> on all observed reflections. Data reduction was performed with the SAINT software and corrected for Lorentz and polarization effects. Absorption corrections were applied with the program SADABS. The structure was solved by direct methods implemented in the SHELX-97<sup>10</sup> program and refined by full-matrix least-squares methods on F2. All non-hydrogen atomic positions were located in difference Fourier maps and refined anisotropically. The hydrogen atoms were placed in their geometrically generated positions. All the colorless crystals were isolated in rectangular shapes from chloroform and hexane mixture (9:1) at room temperature.

#### General procedure

To 1,3-diphenylthiourea **1** (457 mg, 2 mmol) in a 2 mL round bottom flask was added chloroacetylchloride (233  $\mu$ L, 3 mmol)

drop wise. After complete addition of chloroacetylchloride, acetonitrile (1 mL) was added to the reaction mixture and stirred for 10 minutes. Acetonitrile was evaporated and admixed with ethyl acetate (25 mL). The ethyl acetate layer was subsequently washed with saturated sodium bicarbonate solution ( $2 \times 5 \text{ mL}$ ) and water ( $2 \times 5 \text{ mL}$ ). The organic layer was dried over anhydrous Na<sub>2</sub>SO<sub>4</sub> and crystallized from a mixture of chloroform:hexane (8:2) to yield the desired product **1a**.

#### Spectral data

**3-Phenyl-2-phenylimino-thiazolidin-4-one (1a).** Mp: 178 °C (chloroform/hexane: 9/1); yield 92%; <sup>1</sup>H NMR (CDCl<sub>3</sub>, 400 MHz)  $\delta$  (ppm) 3.97 (d, 2H,  $J = 0.8 \text{ Hz}$ ), 6.91 (d, 2H,  $J = 8.4 \text{ Hz}$ ), 7.12 (t, 1H,  $J = 7.2 \text{ Hz}$ ), 7.25–7.54 (m, 7H); <sup>13</sup>C NMR (CDCl<sub>3</sub>, 100 MHz)  $\delta$  (ppm) 32.8, 120.8, 124.6, 127.9, 128.9, 129.1, 129.3, 134.7, 148.0, 154.9, 171.4; IR (KBr) 3049 (m), 1722 (s), 1634 (s), 1591 (s), 1493 (s), 1374 (s), 1270 (m), 1195 (m), 1154 (m), 897 (m), 868 (m), 693 (m), 552 (m); HRMS (ESI): MH<sup>+</sup>, found 269.0564, C<sub>15</sub>H<sub>13</sub>N<sub>2</sub>OS requires 269.3467.

**3-*m*-Tolyl-2-*m*-tolylimino-thiazolidin-4-one (2a).** Mp: 158 °C (chloroform/hexane: 9/1); yield 94%; <sup>1</sup>H NMR (CDCl<sub>3</sub>, 400 MHz) δ (ppm) 2.31 (s, 3H), 2.40 (s, 3H), 3.95 (s, 2H), 6.73 (m, 2H), 6.93 (d, 1H, *J* = 7.6 Hz), 7.17–7.24 (m, 4H), 7.39 (t, 1H, *J* = 7.6 Hz); <sup>13</sup>C NMR (CDCl<sub>3</sub>, 100 MHz) δ (ppm) 21.6, 33.1, 117.9, 121.8, 125.2, 125.6, 128.7, 129.1, 129.4, 130.1, 134.9, 139.2, 139.6, 148.3, 154.9, 171.7; IR (KBr) 2919 (m), 1720 (s), 1638 (s), 1599 (m), 1581(m), 1487 (s), 1370 (s), 1284 (m), 1203 (m), 1132 (m), 936 (m), 800 (m), 691 (m); HRMS (ESI): MH<sup>+</sup>, found 297.0800, C<sub>17</sub>H<sub>17</sub>N<sub>2</sub>O<sub>2</sub>S requires 297.4003.

**3-(2,6-Dimethyl-phenyl)-2-(2,6-dimethyl-phenylimino)-thiazolidin-4-one (3a).** Mp: 188 °C (chloroform/hexane: 9/1); yield 95%; <sup>1</sup>H NMR (CDCl<sub>3</sub>, 400 MHz) δ (ppm) 2.10 (s, 6H), 2.29 (s, 6H), 3.98 (d, 2H, *J* = 2.4 Hz), 6.91 (t, 1H, *J* = 7.4 Hz), 6.99 (d, 2H, *J* = 7.6 Hz), 7.20 (d, 2H, *J* = 7.2 Hz), 7.26 (t, 1H, *J* = 7.4 Hz); <sup>13</sup>C NMR (CDCl<sub>3</sub>, 100 MHz) δ (ppm) 17.9, 18.3, 33.0, 124.4, 128.2, 128.4, 129.0, 129.9, 133.2, 136.2, 145.9, 154.0, 171.0; IR (KBr) 2947 (m), 1718 (s), 1644 (s), 1589 (s), 1473 (s), 1363 (s), 1275 (m), 1247 (m), 1184 (m), 1156 (m), 1086 (m), 873 (m), 764 (m); HRMS (ESI): MH<sup>+</sup>, found 325.1300, C<sub>19</sub>H<sub>21</sub>N<sub>2</sub>O<sub>2</sub>S requires 325.4539.

**3-(4-Methoxy-phenyl)-2-(4-methoxy-phenylimino)-thiazolidin-4-one (4a).** Mp: 135 °C (chloroform/hexane: 9/1); yield 92%; <sup>1</sup>H NMR (CDCl<sub>3</sub>, 400 MHz) δ (ppm) 3.76 (s, 3H), 3.79 (s, 3H), 3.92 (s, 2H), 6.82 (s, 4H), 6.99 (d, 2H, *J* = 8.8 Hz), 7.26 (d, 2H, *J* = 8.8 Hz); <sup>13</sup>C NMR (CDCl<sub>3</sub>, 100 MHz) δ (ppm) 32.9, 55.5, 55.6, 114.4, 114.8, 122.1, 127.5, 129.2, 141.4, 155.2, 156.8, 159.8, 171.8; IR (KBr) 2947 (m), 1725 (s), 1631 (s), 1504 (s), 1370 (s), 1247 (s), 1193 (m), 1031 (m), 832 (m); HRMS (ESI): MH<sup>+</sup>, found 229.0800, C<sub>17</sub>H<sub>17</sub>N<sub>2</sub>O<sub>3</sub>S requires 329.3983.

**3-(2-Chloro-phenyl)-2-(2-chloro-phenylimino)-thiazolidin-4-one (5a).** Mp: 175 °C (chloroform/hexane: 9/1); yield 93%; <sup>1</sup>H NMR (CDCl<sub>3</sub>, 400 MHz) δ (ppm) 4.03 (m, 2H), 6.94 (d, 1H, *J* = 8.0 Hz), 7.06 (m, 1H), 7.22 (m, 1H), 7.35–7.48 (m, 4H), 7.57 (m, 1H); <sup>13</sup>C NMR (CDCl<sub>3</sub>, 100 MHz) δ (ppm) 33.3, 122.0, 125.8, 126.3, 127.6, 128.2, 130.2, 130.7, 131.1, 132.6, 133.0, 145.2, 155.8, 170.6; IR (KBr) 2942 (m), 1731 (s), 1632 (s), 1583 (m), 1478 (s), 1374 (s), 1286 (m), 1201 (m), 1171 (m), 1065 (m), 881 (m); HRMS (ESI): M<sup>+</sup>, found 337.0000, C<sub>15</sub>H<sub>11</sub>Cl<sub>2</sub>N<sub>2</sub>O<sub>2</sub>S requires 337.2290.

**3-(4-Bromo-phenyl)-2-(4-bromo-phenylimino)-thiazolidin-4-one (6a).** Mp: 124 °C (chloroform/hexane: 9/1); yield 95%; <sup>1</sup>H NMR (CDCl<sub>3</sub>, 400 MHz) δ (ppm) 3.99 (s, 2H), 6.79 (d, 2H, *J* = 8.4 Hz), 7.25 (d, 2H, *J* = 8.8 Hz), 7.43 (d, 2H, *J* = 8.8 Hz), 7.64 (d, 2H, *J* = 8.8 Hz); <sup>13</sup>C NMR (CDCl<sub>3</sub>, 100 MHz) δ (ppm) 33.0, 118.0, 122.8, 123.3, 129.8, 132.5, 132.8, 133.6, 146.9, 155.3, 171.1; IR (KBr) 2930 (m), 1718 (s), 1634 (s), 1580 (m), 1487 (s), 1360 (s), 1260 (m), 1190 (m), 1144 (m), 1072 (m), 1012 (m), 869 (m), 830 (m); HRMS (ESI): M<sup>+</sup>, found 426.0100, C<sub>15</sub>H<sub>10</sub>Br<sub>2</sub>N<sub>2</sub>O<sub>2</sub>S requires 426.1310.

**3-Cyclohexyl-2-cyclohexylimino-thiazolidin-4-one (7a).** Gummy; yield 85%; <sup>1</sup>H NMR (CDCl<sub>3</sub>, 400 MHz) δ (ppm) 1.08–1.45 (m, 8H), 1.49–1.76 (m, 10H), 2.30 (m, 2H), 3.02 (m, 1H), 3.66 (d, 2H, *J* = 2.0 Hz), 4.25 (m, 1H); <sup>13</sup>C NMR (CDCl<sub>3</sub>, 100 MHz) δ (ppm) 24.4, 25.4, 25.9, 26.2, 28.0, 32.4, 33.5, 55.6, 61.3, 148.3, 171.9; IR (KBr) 2929 (s), 2854 (s), 1716 (s), 1645 (s),

1450 (s), 1400 (m), 1358 (s), 1337 (s), 1257 (m), 1204 (m), 1138 (m), 1078 (m), 969 (m), 896 (m); HRMS (ESI): MH<sup>+</sup>, found 281.1700, C<sub>15</sub>H<sub>24</sub>N<sub>2</sub>O<sub>2</sub>S requires 281.4415.

**3-(2-Chloro-phenyl)-2-phenylimino-thiazolidin-4-one (8a) + 2-(2-Chloro-phenylimino)-3-phenyl-thiazolidin-4-one (8b).** Yield 90%; <sup>1</sup>H NMR (CDCl<sub>3</sub>, 400 MHz) δ (ppm) 3.91 (m, 4H), 6.90 (m, 3H), 7.01 (m, 1H), 7.08 (m, 1H), 7.16 (m, 1H), 7.30 (m, 3H), 7.32–7.46 (m, 6H), 7.46–7.60 (m, 3H); <sup>13</sup>C NMR (CDCl<sub>3</sub>, 100 MHz) δ (ppm) 32.9, 33.1, 120.9, 121.8, 124.8, 125.6, 127.5, 128.01, 128.03, 128.9, 129.1, 129.2, 129.4, 130.1, 130.5, 130.6, 130.8, 132.78, 132.81, 134.5, 145.2, 147.9, 153.6, 156.8, 170.6, 171.2; IR (KBr) 2986 (m), 1729 (s), 1634 (s), 1592 (s), 1584 (s), 1480 (s), 1373 (s), 1272 (m), 1198 (m), 1158 (m), 1066 (m), 1026 (m), 903 (m), 874 (m); elemental analysis for C<sub>15</sub>H<sub>11</sub>ClN<sub>2</sub>O<sub>2</sub>S: Calcd. C, 59.50; H, 3.66; N, 9.25; S, 10.59. Found: C, 59.34; H, 3.61; N, 9.14; S, 10.64.

**3-(4-Bromo-phenyl)-2-(4-methoxy-phenylimino)-thiazolidin-4-one (9a) + 2-(4-Bromo-phenylimino)-3-(4-methoxy-phenyl)-thiazolidin-4-one (9b).** Yield 92%; <sup>1</sup>H NMR (CDCl<sub>3</sub>, 400 MHz) δ (ppm) 3.78 (d, 2 × 2H, *J* = 0.8 Hz), 3.82 (s, 3H), 3.96 (s, 3H), 6.79 (d, 2H, *J* = 8.0 Hz), 6.85 (s, 4H), 7.01 (d, 2H, *J* = 8.4 Hz), 7.27 (d, 4H, *J* = 8.4 Hz), 7.41 (d, 2H, *J* = 8.0 Hz), 7.63 (d, 2H, *J* = 8.0 Hz); <sup>13</sup>C NMR (CDCl<sub>3</sub>, 100 MHz) δ (ppm) 33.0, 55.6, 114.6, 114.9, 117.8, 122.1, 122.9, 123.1, 127.2, 129.2, 129.8, 132.3, 132.7, 133.9, 141.0, 147.3, 154.4, 157.0, 159.9, 171.3, 171.6; IR (KBr) 2930 (m), 2834 (m), 1728 (s), 1632 (s), 1504 (s), 1487 (m), 1364 (m), 1244 (s), 1190 (m), 1150 (m), 1029 (m), 1013 (m), 875 (m), 830 (m); elemental analysis for C<sub>16</sub>H<sub>13</sub>BrN<sub>2</sub>O<sub>2</sub>S: Calcd. C, 50.94; H, 3.47; N, 7.43; S, 8.50. Found: C, 50.99; H, 3.54; N, 7.39; S, 8.46.

**3-Cyclohexyl-2-phenylimino-thiazolidin-4-one (10a).** Mp: 155 °C (chloroform/hexane: 9/1); yield 93%; <sup>1</sup>H NMR (CDCl<sub>3</sub>, 400 MHz) δ (ppm) 1.18–1.34 (m, 4H), 1.57–1.68 (m, 6H), 3.13 (m, 1H), 3.92 (d, 2H, *J* = 0.8 Hz), 7.20–7.47 (m, 5H); <sup>13</sup>C NMR (CDCl<sub>3</sub>, 100 MHz) δ (ppm) 24.4, 25.5, 32.5, 33.1, 61.5, 127.9, 128.3, 128.8, 135.3, 149.1, 171.4; IR (KBr) 2927 (s), 2853(m), 1724 (s), 1626 (s), 1591 (m), 1496 (m), 1452 (m), 1365 (s), 1233 (s), 1164 (m), 1071 (m), 892 (m), 854 (m); HRMS (ESI): MH<sup>+</sup>, found 275.6200, C<sub>15</sub>H<sub>19</sub>N<sub>2</sub>O<sub>2</sub>S requires 275.3941.

**3-Cyclohexyl-2-(4-methoxy-phenylimino)-thiazolidin-4-one (11a).** Mp: 140 °C (chloroform/hexane: 9/1); yield 90%; <sup>1</sup>H NMR (CDCl<sub>3</sub>, 400 MHz) δ (ppm) 1.26–1.35 (m, 4H), 1.56–1.71 (m, 6H), 3.14 (m, 1H), 3.81 (s, 3H), 3.94 (d, 2H, *J* = 0.8 Hz), 6.95 (d, 2H, *J* = 8.4 Hz), 7.18 (d, 2H, *J* = 8.4 Hz); <sup>13</sup>C NMR (CDCl<sub>3</sub>, 100 MHz) δ (ppm) 24.5, 25.5, 32.4, 33.2, 55.4, 61.6, 114.2, 127.9, 129.0, 149.4, 159.2, 171.6; IR (KBr) 2927 (s), 2852 (m), 1724 (s), 1638 (s), 1514 (s), 1369 (s), 1253 (s), 1234 (m), 1164 (m), 1070 (m), 1025 (m); HRMS (ESI): MH<sup>+</sup>, found 305.1100, C<sub>16</sub>H<sub>21</sub>N<sub>2</sub>O<sub>2</sub>S requires 305.4199.

**2-(4-Bromo-phenylimino)-3-cyclohexyl-thiazolidin-4-one (12a).** Mp: 149 °C (chloroform/hexane: 9/1); yield 91%; <sup>1</sup>H NMR (CDCl<sub>3</sub>, 400 MHz) δ (ppm) 1.18–1.35 (m, 4H), 1.54–1.69 (m, 6H), 3.12 (m, 1H), 3.93 (s, 2H), 7.15 (d, 2H, *J* = 8.8 Hz), 7.55 (d, 2H, *J* = 8.8 Hz); <sup>13</sup>C NMR (CDCl<sub>3</sub>, 100 MHz) δ (ppm) 24.6, 25.7, 32.7, 33.3, 61.7, 122.4, 129.8, 132.3, 134.3, 148.9, 171.3; IR (KBr) 2929 (s), 2853 (m), 1723 (s), 1645 (s), 1489 (s), 1365 (s),

1228 (s), 1069 (m), 816 (m); HRMS (ESI):  $MH^+$ , found 353.0100,  $C_{15}H_{17}BrN_2OS$  requires 353.2823.

## Acknowledgements

B. K. P acknowledges the support of this research from DST New Delhi (SR/S1/OC-15/2006) and CSIR 01(1688)/00/EMR-II. H.G would like to thank CSIR for fellowships and RY would like to thank the institute. Thanks are also due to CIF IIT Guwahati for NMR spectra and DST FIST for the XRD facility.

## References

- (a) R.-S. Zeng, J.-P. Zou, S.-J. Zhi, J. Chen and Q. Shen, *Org. Lett.*, 2003, **5**, 1657; (b) X.-C. Wang, F. Wang, Z. J. Quan, M.-G. Wang and Z. Li, *J. Chem. Res.*, 2005, 689.
- (a) C. B. Singh, S. Muru, V. Kavala and B. K. Patel, *Org. Lett.*, 2006, **8**, 5397; (b) S. Muru, C. B. Singh, V. Kavala and B. K. Patel, *Tetrahedron.*, 2008, **64**, 1931; (c) C. B. Singh, S. Muru, V. Kavala and B. K. Patel, *J. Chem. Res.*, 2007, **64**, 136.
- M. Kidwai, R. Venkataraman and B. Dave, *Green. Chem.*, 2001, **3**, 278.
- S. Erol and I. Dogan, *J. Org. Chem.*, 2007, **72**, 2494.
- (a) H. Singh, A. S. Ahuja and N. Malhotra, *J. Chem. Soc. Perkin Trans 1.*, 1982, 1972; (b) S. Erol and I. Dogan, *J. Org. Chem.*, 2007, **72**, 2494.
- D. M. Wolfe and P. R. Schreiner, *Eur. J. Org. Chem.*, 2007, 2825.
- Crystal data*: for **1a**:  $C_{15}H_{12}N_2OS$ ,  $M_r = 268.33$ , orthorhombic, space group Pbc $a$ ,  $a = 10.9047(2)$ ,  $b = 10.0696(2)$ ,  $c = 24.2827(6)$  Å,  $\alpha = \beta = \gamma = 90.00^\circ$ ,  $V = 2666.39(10)$  Å<sup>3</sup>,  $Z = 8$ ,  $\mu(\text{Mo-K}\alpha) = 0.235$  mm<sup>-1</sup>. Of 21603 reflections measured, 3281 were unique with 2215 having  $I > 2\sigma(I)$ , R indices [ $I > 2\sigma(I)$ ]  $R_1 = 0.346$ ,  $wR_2 = 0.0859$ , GOF on  $F^2 = 0.949$  for 172 refined parameters and zero restraint. C3–O1  $\cdots$  S1 = 3.252 Å. C–H,  $\cdots$   $\pi$  interection C2H  $\cdots$  C Centroid = 3.59 Å and no hydrogen bonding. CCDC # 686655.
- Crystal data*: for **5a**:  $C_{15}H_{10}Cl_2N_2OS$ ,  $M_r = 337.21$ , orthorhombic, space group Pbc $a$ ,  $a = 12.900(4)$ ,  $b = 10.035(4)$ ,  $c = 24.251(8)$  Å,  $\alpha = \beta = \gamma = 90.00^\circ$ ,  $V = 3139.2(18)$  Å<sup>3</sup>,  $Z = 8$ ,  $\mu(\text{Mo-K}\alpha) = 0.545$  mm<sup>-1</sup>. Of 16750 reflections measured, 3513 were unique with 1684 having  $I > 2\sigma(I)$ , R indices [ $I > 2\sigma(I)$ ]  $R_1 = 0.0576$ ,  $wR_2 = 0.0859$ , GOF on  $F^2 = 0.1633$  for 190 refined parameters and zero restraint. C5–Cl1  $\cdots$  O1 = 3.183 Å and no hydrogen bonding. CCDC # 692011.
- SMART V 4.043 Software for the CCD Detector System; Siemens.
- G. M. Sheldrick, *SHELXL-97, Program for the Refinement of Crystal Structures*, University of Göttingen, Göttingen (Germany), 1997.
- C. B. Singh, H. Ghosh, S. Murru and B. K. Patel, *J. Org. Chem.*, 2008, **73**, 2924.



# Microwave assisted synthesis of silicalite—power delivery and energy consumption†

Ko-Yeol Choi,<sup>\*a</sup> Geoffrey Tompsett<sup>b</sup> and W. Curtis Conner<sup>b</sup>

Received 9th June 2008, Accepted 22nd September 2008

First published as an Advance Article on the web 24th October 2008

DOI: 10.1039/b809694e

Silicalite was synthesized by microwave heating and two conventional heating methods: an ethylene glycol bath or an electric oven. The effects of microwave and temperature ramp rate on induction time, crystallization rate, morphology of silicalite and energy consumption were investigated. In a microwave oven the reaction time was significantly reduced due to the rapid heating rate, however, the final yield decreased compared with the conventional methods. When the same temperature ramp rates were used in both microwave heating and conventional heating, the induction time and the crystallization rate were similar and the effect of microwave was found only to enhance the final yield of silicalite. Regardless of the irradiation of microwave the slower temperature ramp rate increased the final yield of silicalite. Energy efficiency was not always high in microwave heating. However, if the temperature ramp rate is carefully controlled, silicalite can be produced with less energy in a microwave reactor.

## Introduction

Zeolites are important heterogeneous catalysts and separation materials used in industry. These materials are typically produced batch-wise using conventional heating taking several days at elevated temperatures.<sup>1,2</sup> A recent American Chemical Society monograph on Green Chemistry<sup>3</sup> recommends for us to “Use methods that minimize the energy required for a reaction to take place. For example... catalysts or **microwave radiation**...”. A more energy efficient and high speed method is desirable to produce these industrially important materials. Previously, Braun *et al.*<sup>4</sup> and Kim *et al.*<sup>5</sup> have reported continuous microwave systems used to prepare zeolites. The energy savings *via* the use of microwaves in engineering and chemistry has recently become a topic of interest. Workers from around the world described the energy savings due to microwave heating in areas such as hydrothermal synthesis of oxides, organic synthesis and ceramics processing.<sup>6</sup> Bagley *et al.*<sup>7</sup> utilized a continuous flow reactor for organic synthesis. These workers calculated energy delivered *via* the magnetron from integrating the power *versus* time profiles.

The enhanced rate of reaction of zeolite synthesis has been demonstrated by many workers for different zeolites. The relative enhancement due to reaction time saving at comparable temperatures has been reviewed for many zeolite types.<sup>1</sup> However, the actual energy consumption has not been reported for these syntheses, as it will depend on the type of oven. The energy

usage of a microwave oven is complex since the oven contains many components that require electricity and therefore have inherent losses to heat. A typical power conversion efficiency of a domestic microwave oven is ~64%. Therefore for a 1100 W oven, only 700 W is actually used by the magnetron operating at full power. The other 400 W are dissipated as heat, mostly in the magnetron tube.<sup>8</sup> Nuchter *et al.*<sup>9</sup> carefully reviewed microwave assisted synthesis. These workers described the energy efficiency factor as the ratio of energy required to reach a certain temperature to the energy input. Nuchter *et al.*<sup>10,11</sup> determined the efficiency of many organic reactions using multimode and monomode microwave systems.

While microwave heating is proven to be an energy efficient process for the significant enhancement in reaction rate for many processes, few workers have reported energy efficiency and energy usage data on the synthesis of zeolites comparing microwave and conventional heating. In this paper, we investigated the energy consumption of typical laboratory synthesis of silicalite using microwave and conventional heating techniques. The rate enhancements for microwave heating compared to conventional heating were investigated using a conventional oven with a high power density and a similar power density heating mantle system. Many engineering parameters are important in microwave synthesis and careful optimisation of these will minimise the energy and time used during the zeolite processing.

## Results and discussion

Microwave heating of a dielectric medium is typically very rapid. The rate of increase in temperature can be controlled precisely using state-of-the-art microwave oven system which can be programmed. Due to the high power density and volumetric heating, elevated temperatures in access of 200 °C can be attained in seconds (depending on the reaction vessel and the materials being heated). Comparatively, convective

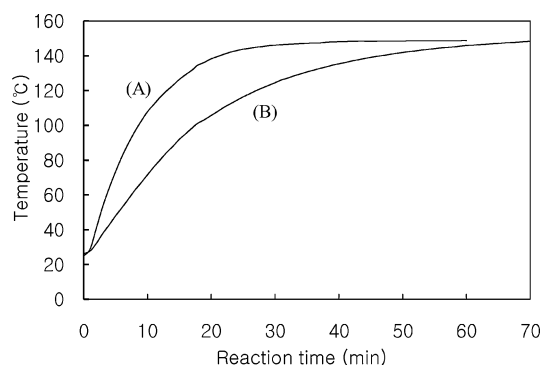
<sup>a</sup>Department of Chemical Engineering, Seoul National University of Technology, 172 Gongneung-dong, Nowon-gu, Seoul, 139-743, Korea. E-mail: kychoi@snut.ac.kr; Fax: +82-2-977-8317; Tel: +82-2-970-6604

<sup>b</sup>Department of Chemical Engineering, University of Massachusetts, Amherst, MA, 01003, USA. E-mail: wconner@ecs.umass.edu; Fax: +1-413-545-1647; Tel: 1-413-545-0316

† Electronic supplementary information (ESI) available: Reaction temperature program used in the microwave oven, SEM photographs of silicalite, and parameters of heating system. See DOI: 10.1039/b809694e

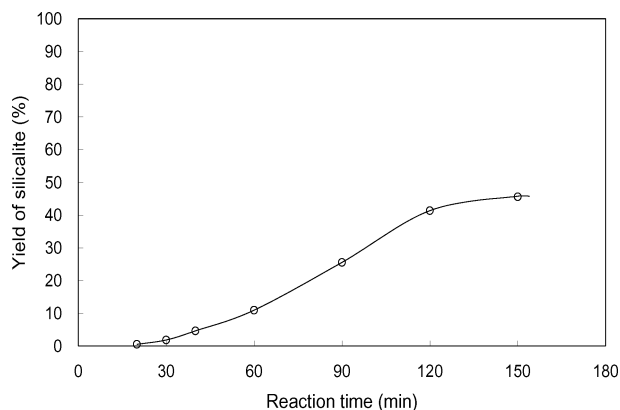
thermal ovens are slow to heat the same liquids due to the poor heat conduction of the air. Conventional systems with improved conduction and higher power density can be employed to accelerated the heating rate, such as described here.

Temperature profiles inside the reactor during the synthesis of silicalite in an ethylene glycol bath and an electric oven were monitored using fiberoptic probes. The profiles are shown in Fig. 1. The time required to reach the temperature of 140–145 °C, which is about 95% of reaction temperature, is 20–30 min in an ethylene glycol bath and 45–55 min in an electric oven, respectively. Although the ambient temperature is similar in both systems, the time for the reactor to reach steady state temperature in the ethylene glycol bath is about 25 min faster than that in the electric oven. However, this temperature ramp rate in the ethylene glycol bath is slow compared with two minutes ramp time for microwave heating. Therefore, the temperature ramp rates in microwave oven, ethylene glycol bath and electric oven shall be referred to in this study as a fast-, an intermediate- and a slow-temperature ramp rate, respectively. The curves in Fig. 1 were divided by five linear segments and used to control the reaction temperature in the microwave oven to have the same temperature profile as in the ethylene glycol bath and in the electric oven. (See ESI.†)



**Fig. 1** Temperature profile in the reactor during the synthesis of silicalite in (A) an ethylene glycol bath and (B) an electric oven.

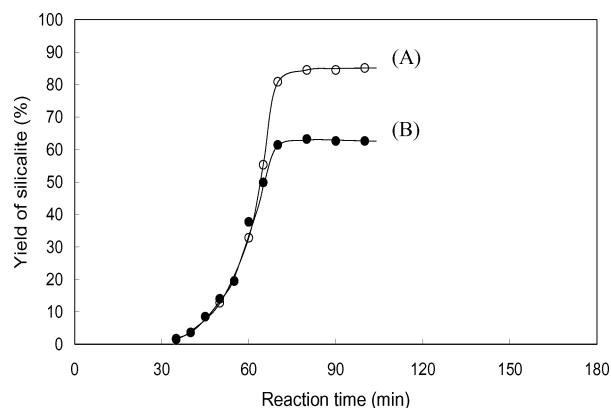
Fig. 2 shows the yield of silicalite synthesized in a microwave oven with a fast ramp rate. This curve exhibits the typical sigmoid nature, which shows a short induction period and a low crystallization rate. The yield of silicalite increases almost



**Fig. 2** Percent yield of silicalite synthesized at 150 °C in a microwave oven with a fast temperature ramp rate.

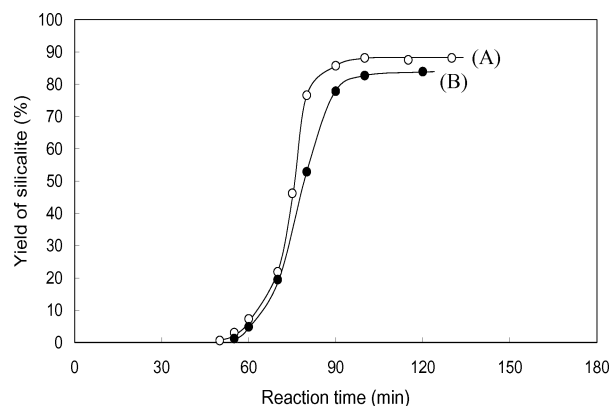
linearly with the reaction time. The final yield of silicalite is 46% after 150 minutes. Although the induction time is reduced significantly in the case of microwave heating with a fast ramp rate, the final yield of silicalite is less than those of silicalites in conventional heating, which will be shown later.

Fig. 3 shows the yield of silicalite synthesized in an ethylene glycol bath and a microwave oven with an intermediate temperature ramp rate. The induction time and the crystallization rate are almost same in both cases, however, the final yield of silicalite is much higher in the microwave oven. It is found from these results that if the same temperature ramp rate is used, the microwave heating does not affect the induction time or the crystallization rate, but enhances the final yield of silicalite. The induction time in this intermediate temperature ramp rate is about 15 minutes longer compared with the result in the microwave oven with a fast temperature ramp rate. However, the rate of crystallization (the slope of curves) are very fast and the reaction has almost finished after 70 minutes of reaction time. The final yield is 63% without irradiation of microwave and 85% with irradiation of microwave, which are much higher values than that in the microwave oven with a fast ramp rate.



**Fig. 3** Percent yield of silicalite synthesized in (A) a microwave oven with an intermediate temperature ramp rate and (B) an ethylene glycol bath.

Fig. 4 shows the yield of silicalite in an electric oven and a microwave oven with a slow temperature ramp rate. The induction time in this slow temperature ramp rate is about



**Fig. 4** Percent yield of silicalite synthesized in (A) a microwave oven with a slow temperature ramp rate and (B) an electric oven.

**Table 1** Summary of silicalite synthesis at 150 °C

Reaction method <sup>a</sup>	Ramp rate	Induction time (min)	Final yield (%)	Crystal size (μm)
MW	fast	20	46	2
EG	intermediate	35	63	1
MW	intermediate	35	85	0.5
EO	slow	55	84	0.5
MW	slow	50	88	0.4

<sup>a</sup> MW: microwave oven, EG: ethylene glycol bath, EO: electric oven.

20 minutes longer compared with an intermediate temperature ramp rate. Concerning the effect of microwave heating, similar results were observed as in the case of intermediate temperature ramp rate. The induction time and the crystallization rate are similar regardless of the irradiation of microwave. The final yield is 84% without irradiation of microwave and 88% with irradiation of microwave, which are higher values than those in an intermediate temperature ramp rate. The crystal growth is still limited by conventional heating.

The results of silicalite synthesis depending on the reaction method are summarized in Table 1. Final crystal size of silicalite was measured from the SEM photographs in the ESI.† For an intermediate temperature ramp rate, there is no microwave effect on the induction time. However, the final yield is much higher and the size of silicalite crystals are larger in the microwave oven than in the ethylene glycol bath. This may be due to the effect of microwave which enhances the crystallization on the surface of silicalite crystals even at low concentration of reactant. The increase of final yield in the microwave oven with a slow temperature ramp rate is not as pronounced as with the intermediate ramp rate. Moreover, the crystal size of silicalite is smaller than that of silicalite in an intermediate one. It can be concluded from the above results that the final yield, the induction time, and the rate of crystallization depend primarily on the temperature ramp rate in the reactor. If the same temperature ramp rate is used, the induction time and the rate of crystallization are similar in both microwave heating and conventional heating. Regardless of the irradiation of microwave, as the temperature ramp rate is fast, the induction time is reduced because of the fast formation of nuclei. However, a larger number of nuclei are produced with a slow temperature ramp rate.

Comparison of parameters in microwave and conventional heating systems used in this study are presented in the ESI.† Energy efficiency during the synthesis of silicalite is related to the kind, volume, and power of heating system. Therefore, energy efficiency will be discussed based on the systems used in this study. Fig. 5 shows power delivery (solid line), energy consumption (dashed line), and temperature inside the reaction vessel (solid circle) for the first one hour during the synthesis of silicalite. Initially, a full power is delivered until the temperature of apparatus reaches at steady state, and then the power is used to control the temperature of apparatus to be constant. The energy consumption during the delivery of a full power is used for the preheating of the apparatus. The energy consumption after preheating is used for the reaction. The slopes of dashed lines represent the rate of energy consumption for each period. The energy consumption for preheating is measured as only 20 Wh in

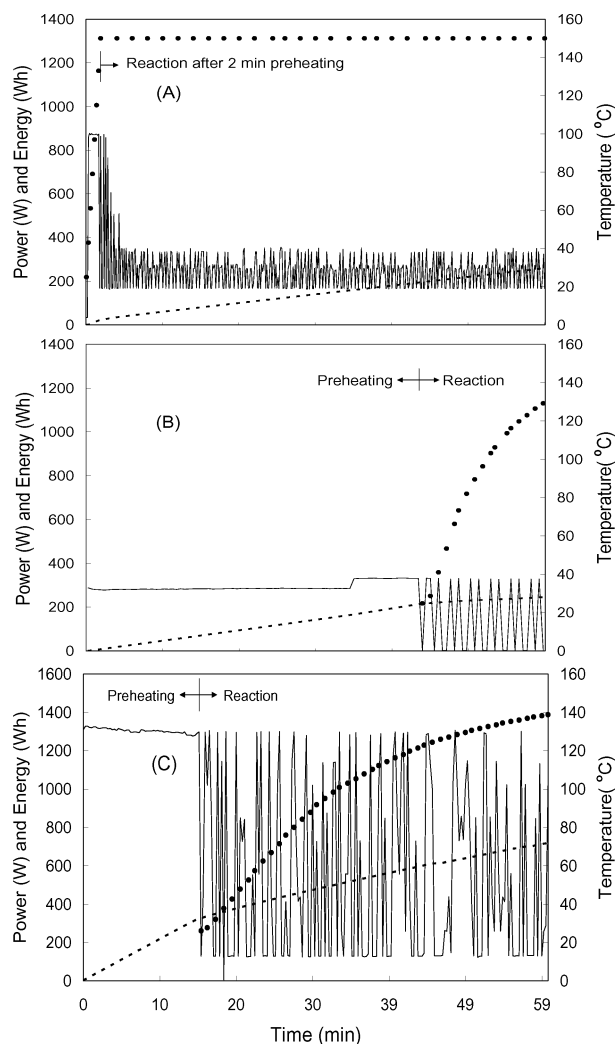


**Fig. 5** Power delivery (solid line), energy consumption (dashed line), and temperature inside the reaction vessel (solid circle) during the first one hour in (A) a microwave oven with a fast temperature ramp rate, (B) an ethylene glycol bath, and (C) an electric oven.

a microwave oven with a fast temperature ramp rate. However, the values of this energy are 210 Wh in an ethylene glycol bath and 320 Wh in an electric oven, which are much higher than that in a microwave oven. The rate of energy consumption for reaction is highest in the electric oven and lowest in the ethylene glycol bath. Therefore, the energy consumption in the electric oven should be highest among the methods used in this study. This highest consumption of energy in the electric oven is due to a high capacity heating element (1200 Watts) as well as a large cavity of the electric oven.

The estimation of energy efficiency between a microwave oven and an ethylene glycol bath is complex. The rate of energy used for the reaction is higher in a microwave oven, but the energy for preheating is higher in an ethylene glycol bath. The energy consumption in these two systems depends on not only the reaction time but also the rate of crystallization related to the temperature ramp rate. The rate of energy consumed only for the reaction is higher in the microwave oven with a fast ramp rate than in the ethylene glycol bath as shown in Fig. 5. Nevertheless, when the yield is less than about 20%, the energy consumption

in the microwave oven with a fast ramp rate is lower than in the ethylene glycol bath as can be seen in Fig. 6. This is because much energy is used for the preheating of the ethylene glycol bath. However, less energy is consumed in the ethylene glycol bath to get more than 20% yield. The lower consumption of energy in the ethylene glycol bath is closely related with the rate of crystallization due to the temperature ramp rate. As shown in Fig. 3, the rate of crystallization is very fast in the ethylene glycol bath compared with that in the microwave oven, which means a significant reduction of energy used for the reaction. On the other hand, the time for the reaction to be completed is longer in the microwave oven because of the slow rate of crystallization. Moreover, the rate of energy consumed for the reaction is higher in the microwave oven. Therefore, the total energy to synthesize more than 20% yield of silicalite is lower in the ethylene glycol bath than in microwave oven.

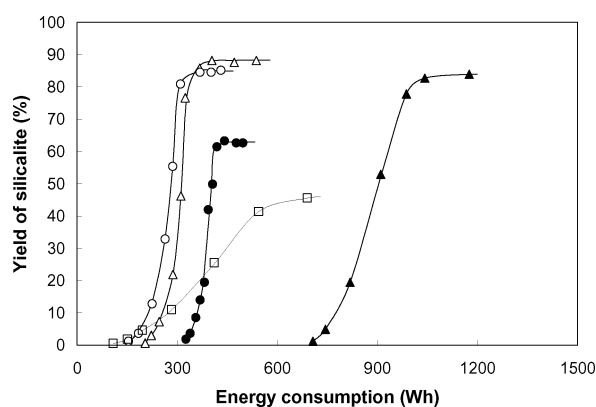


**Fig. 6** Energy consumption for the synthesis of silicalite in a microwave oven with an intermediate temperature ramp rate (○), in a microwave oven with a slow temperature ramp rate (△), in a microwave oven with a fast temperature ramp rate (□), in an ethylene glycol bath (●), and in an electric oven (▼).

These results do not agree with many results saying that microwave heating is more effective than conventional heating for the synthesis of zeolites. In other words, a conventional heating system, if carefully designed, can be more energy effective than a microwave oven. As can be seen in Fig. 6, the most energy efficient system was proven to be the microwave oven with an intermediate temperature ramp rate, followed by the microwave oven with a slow temperature ramp rate, which shows that the energy efficiency is closely related with a temperature ramp rate. Such a high efficiency of energy in the microwave oven with a slow temperature ramp rate can be obtained from not only the small preheating energy compared to the conventional heatings but also the enhancement of crystallization rate due to the control of temperature ramp rate.

## Conclusions

The synthesis of silicalite was carried out using microwave heating as well as conventional heating, namely an ethylene glycol bath or an electric oven. Microwave heating using two minutes ramp time, which was the fastest temperature ramp rate in this study, gave the shortest induction time but the

lowest overall yield of silicalite. Regardless of the irradiation of microwave, the induction time and rate of crystallization were found to depend primarily on the temperature ramp rate in the reactor. If the same temperature ramp rate was used, the induction time and the crystallization rate were similar in both microwave heating and conventional heating. However, the irradiation of microwave enhanced the crystallization at lower concentrations of reactants to give a higher final yield than with conventional heating. A conventional heating system, if carefully designed, can be used to synthesize silicalite with less energy consumption but higher yield than in a microwave, which means that the microwave synthesis is not always energy effective as compared with conventional synthesis. It was found that a ramp rate is very important to the energy efficiency for the synthesis of silicalite in the microwave oven. The microwave oven with an intermediate temperature ramp rate was proven to be the most energy efficient system among all apparatus used in this study. Careful microwave engineering and reaction composition optimization are required to fully utilize the microwave heating effect.

## Experimental

Silicalite solutions were prepared by mixing 25 g tetraethylorthosilicate (98% TEOS, Aldrich) with 26.5 g of 1 M tetrapropylammonium hydroxide solution (TPAOH, Aldrich) and 48.75 g of deionised water. These solutions were stirred for 4 hours in room temperature. The same amount (20 g) of solution was used for all syntheses in this study. Reaction temperature was 150 °C. For a microwave synthesis of silicalite, a MARS<sup>®</sup>-5 microwave oven (CEM Corporation) was used with a 1200 W maximum power. Microwave heating was carried out using 300 W (25% of maximum power) with either two minutes ramp time or the same temperature ramp rate as in ethylene glycol bath or electric oven. An ethylene glycol bath and an electric oven were used for the conventional syntheses. An ethylene glycol bath (self-made) containing 0.6 L ethylene glycol in 1 L glass vessel was heated by an electric heating mantle with 300 W power. A commercial electric oven (Blue M, 1200 W) was also used. The reaction time was measured just after the reactor containing 20 g of solution was put into the ethylene glycol bath or electric oven which was heated up to 150 °C. After the reaction started, the temperature inside the reactor was measured by using a fiber optic temperature sensor or a C-A k-type thermocouple. At the end of the reaction, the reactor was taken out from the apparatus and cooled down to the room temperature. The silicalite was obtained by high speed centrifugal process, washed with distilled water repeatedly, and then dried at 100 °C for further analysis. Energy consumption for all systems was measured by using a power meter (WattsUp Pro). The synthesis yield was evaluated from the mass ratio of the recovered silicalite to the theoretically obtainable silicalite. SEM (JEOL-5400) measurements were made to study the morphology of synthesized silicalite.

## Notes and references

- G. A. Tompsett, W. C. Conner and K. S. Yngvesson, *ChemPhysChem*, 2006, **7**, 296.



- 2 H. Kosslick, H. L. Zubowa, U. Lohse, H. Landmesser, R. Fricke and J. Caro, *Ceramic Trans.*, 1997, **80**, 523.
- 3 M. A. Ryan and M. Tinneland, *Introduction to Green Chemistry*, ACS, Washington DC, 2002.
- 4 I. Braun, G. Schulz-Ekloff, D. Wohrle and W. Lautenschlager, *Micropor. Mesopor. Mat.*, 1998, **23**, 79.
- 5 D. S. Kim, J. M. Kim, J. S. Chang and S. E. Park, *Stud. Surf. Sci. Catal.*, 2001, **135**, 573.
- 6 D. Agrawal, *The Spectrum*, 2006, **1**(3), 1, National Academy of Engineering, Northeastern Regional Meeting, U. S. A.
- 7 M. C. Bagley, R. L. Jenkins, M. C. Lubinu, C. Mason and R. Wood, *J. Org. Chem.*, 2005, **70**, 2003.
- 8 [http://en.wikipedia.org/wiki/Microwave\\_oven](http://en.wikipedia.org/wiki/Microwave_oven), 2007.
- 9 M. Nuechter, B. Ondruschka, W. Bonrath and A. Gum, *Green Chem.*, 2004, **6**, 128.
- 10 M. Nuechter, B. Ondruschka, D. Weiss, R. Beckert, W. Bonrath and A. Gum, *Chem. Eng. Technol.*, 2005, **28**, 871.
- 11 M. Nuechter, U. Mueller, B. Ondruschka, A. Tied and W. Lautenschlaeger, *Chem. Eng. Technol.*, 2003, **26**, 1207.

# Selective oxidation of glucose to gluconic acid over argon plasma reduced Pd/Al<sub>2</sub>O<sub>3</sub>

Xi Liang, Chang-jun Liu\* and Pingyu Kuai

Received 25th March 2008, Accepted 23rd September 2008

First published as an Advance Article on the web 24th October 2008

DOI: 10.1039/b804904a

An argon glow discharge plasma approach was employed to reduce PdCl<sub>2</sub> supported on  $\gamma$ -Al<sub>2</sub>O<sub>3</sub> at ambient temperature. This environmentally benign reduction approach is energy efficient and economically effective. Characterizations using X-ray powder diffraction (XRD), transmission electron microscopy (TEM) and energy dispersive X-ray spectrometer (EDX) confirmed that the ionic Pd could be effectively reduced to the metallic state during this room temperature plasma reduction. The activities of the plasma reduced catalysts were tested for selective oxidation of glucose to gluconic acid with conventional hydrogen reduced catalysts as comparison. The plasma reduced catalyst followed by calcination under argon atmosphere at 500 °C exhibits a higher activity than the hydrogen thermally reduced one. Furthermore, the high stability against leaching of active metal into the reaction medium, observed in the plasma reduced catalysts, is of importance in the potential industrial application.

## Introduction

The use of catalyst and renewable resources has been considered to be part of the principles of green chemistry.<sup>1–3</sup> Oxidation of glucose to gluconic acid with heterogeneous catalyst is a typical example of these green chemistry principles. Gluconic acid, used as an intermediate in the food and pharmaceutical industry and a biodegradable chelating agent, is produced by biochemical oxidation of glucose as the only industrial route. Recent developments, however, have shown the potential of the use heterogeneous catalysts for oxidizing glucose with oxygen or air. Supported Pd and Pt catalysts in the early studies<sup>4–7</sup> showed high selectivity but they were easily deactivated with increasing conversion. The research demonstrated that the deactivation could be caused by the adsorption of reaction products and the oxygen poisoning on the active metal surface. Under slightly alkaline conditions, with the timely consumption of the products, the drastic deactivation can be avoided and high yields can be achieved. Also, promoters, such as Bi, Pb, Ru, Cd, Tl, *etc.*, were added to improve the activity and stability.<sup>8–12</sup> Especially, for the bismuth modified palladium catalyst, with bismuth acting as a co-catalyst to prevent the oxygen poisoning of palladium, an excellent activity and selectivity were obtained. However, the catalyst durability was affected by the leaching of bismuth. In recent years, the gold catalysts with promising results have been extensively developed.<sup>13–17</sup> An important feature of gold is that it is active either in the form of a supported metal or of nanometric colloidal particles. However, aspects such as the nature of the catalyst and the reaction mechanism are still under discussion although many papers have addressed this subject.

Moreover, glucose oxidation is a structure-sensitive reaction, both the initial rate and the deactivation as reaction proceeds are particle-size-dependent.<sup>6,17</sup> Different preparation conditions could result in variation in particle size, morphology, and the metal–support interaction, and then impact on the catalytic behaviors.

One of the basic operations for catalysis is catalyst reduction, since many reactions require metallic nano-particles as the active species. The catalytic properties of metal species are closely related to morphology and particle size, which are normally determined by the conditions of the catalyst reduction. Nowadays, the catalysts are normally reduced by flowing hydrogen at elevated temperatures or by chemical reductants, like formaldehyde and hydrazine. Generally, hydrogen is explosive so special care is required for production, transportation, storage and use, while most chemical reducing agents currently used are hazardous to both the human body and the environment. The production of hydrogen and chemical reducing agents is also expensive, with many wastes generated as by-products. Thus, several alternative reduction technologies have been developed.<sup>18,19</sup>

Recently, our group reported a green, simple and energy efficient glow discharge plasma reduction route to reduce supported metal catalysts using inert gas or even oxygen as the plasma forming gas.<sup>20,21</sup> This novel plasma reduction is operated at ambient temperature. According to the energy balance, the plasma reduction approach significantly reduces the energy consumption and the economic cost as well as emission of the toxic or hazardous materials. The reducibility of metal ions by non-hydrogen plasma can be determined by the value of standard electrode potential of the metal ions. Those metal ions with positive standard electrode potential can be easily reduced by non-hydrogen plasma at ambient temperature, such as Pd, Pt, Au, Ag, Rh, Ir, *etc.*<sup>21</sup>

Key Laboratory for Green Chemical Technology of Ministry of Education, School of Chemical Engineering and Technology, Tianjin University, Tianjin, 300072, China. E-mail: ughg\_cjl@yahoo.com; Fax: +86 22 27890078; Tel: +86 22 27406490

In this paper, the novel argon glow discharge plasma reduced Pd/ $\gamma$ -Al<sub>2</sub>O<sub>3</sub> was tested for the glucose oxidation. This work is the first test of the plasma reduced catalyst for reactions in a liquid medium. Using this greener, efficient and safe reduction method, PdCl<sub>2</sub> supported on  $\gamma$ -Al<sub>2</sub>O<sub>3</sub> was reduced effectively, even when the loading is as high as 3.5 wt%. We confirm that the amounts of Pd leaching, which lead to irreversible deactivation, are much less for the plasma reduced catalysts than that for the hydrogen reduced one. It is attributed to the stronger metal–support interaction in plasma reduced Pd/ $\gamma$ -Al<sub>2</sub>O<sub>3</sub>. We also confirm a particle size effect with the oxidation of glucose over the plasma reduced Pd catalysts.

## Experimental

### Catalyst preparation

The Pd/ $\gamma$ -Al<sub>2</sub>O<sub>3</sub> catalysts were prepared by the incipient wetness impregnation. The  $\gamma$ -Al<sub>2</sub>O<sub>3</sub> powder (Institute of Chemical Engineering, Tianjin, China;  $S_{\text{BET}} = 230 \text{ m}^2 \text{ g}^{-1}$ ) was sieved to above 60 mesh and calcined at 650 °C for 6 h prior to use. It was impregnated with an aqueous solution of PdCl<sub>2</sub> (Tianjin Yingda Noble Reagent Chemical Plant, China; 99% in purity) and hydrochloric acid for 24 h, followed by drying at 110 °C overnight. Then the obtained sample was treated with argon glow discharge plasma. The glow discharge plasma setup and plasma reduction protocol have been described previously in detail.<sup>20,21</sup> Briefly, the sample (about 0.5 g), loaded on a quartz boat, was placed in a quartz tube (i.d. 35 mm) with two stainless steel electrodes (o.d. 30 mm). The system was evacuated by a vacuum pump. When the pressure was adjusted to 50–100 Pa, the glow discharge plasma was generated by applying 900 V to the electrode using a high voltage amplifier (Trek, 20/20B), with argon (>99.999%) as the plasma-forming gas. The signal input for the high voltage amplifier was supplied by a function/arbitrary waveform generator (Hewlett-Packard, 33120A) with a 100 Hz square wave. The current was 4.5 mA. The plasma treatment time was 10 min, and each sample was treated 6 times, with manual mixing of the sample between treatments to ensure even exposure to the plasma. A drop of water was added between the treatments to help the mixing. The gas temperature of plasma was measured by infrared imaging (Ircon, 100PHT), indicating that the treatment was conducted at ambient temperature. The sample reduced by plasma was designated as Pd/Al<sub>2</sub>O<sub>3</sub>(P). The Pd/Al<sub>2</sub>O<sub>3</sub>(P) catalysts calcined at 300 °C and 500 °C under the protection of flowing argon were designated as Pd/Al<sub>2</sub>O<sub>3</sub>(P300) and Pd/Al<sub>2</sub>O<sub>3</sub>(P500) respectively. The conventional hydrogen reduction method was also adopted for comparison, including calcination in air at 300 °C for 6 h and subsequent reduction with hydrogen at 500 °C for 2 h. The sample thus prepared was designated as Pd/Al<sub>2</sub>O<sub>3</sub>(C). The Pd loading amount is 3.5 wt%.

### Catalytic tests

The oxidation reactions were performed in a semi-batch glass reactor (250 mL) equipped with a stirrer, a gas supply system, a burette containing NaOH (1 mol L<sup>-1</sup>) and a pH electrode (HANNA Instruments). The catalyst (0.5 g) and distilled water (50 mL) were introduced into the reactor under nitrogen atmo-

sphere while stirring. When the suspension was brought to the required temperature, 50 mL glucose solution (0.4 mol L<sup>-1</sup>) was added, and nitrogen was fed into the reactor for an additional 15 min to remove oxygen dissolved in the suspension. Thereafter, the reaction was started by substituting oxygen for nitrogen. The acids formed during the oxidation of glucose were neutralized by the addition of aqueous solution of sodium hydroxide. The consumptions of alkali were recorded continuously.

The reaction was conducted at 50 °C, pH value of 9, and under atmospheric pressure. The mixture was stirred at 2000 rpm, and oxygen was bubbled through at 400 mL min<sup>-1</sup>. Under this condition, the reaction rate was not limited by the mass transfer rate.<sup>22</sup> The catalytic tests were terminated when the conversion reached 100% or interrupted after 8 h, and the catalyst powder was removed from the reaction mixture by filtration. The filtrate was then analyzed by HPLC to determine the selectivity.

### Characterization

X-ray diffraction (XRD) analysis was conducted on a Rigaku D/Max-2500 V/PC diffractometer with Cu K $\alpha$  radiation ( $\lambda = 0.154178 \text{ nm}$ ) at a scanning speed of 4° min<sup>-1</sup>. The voltage was 40 kV and the current was 200 mA. Crystalline phases were identified by referencing to the JCPDS data files.

Transmission electron microscopy (TEM) images were recorded with a Philips TECNAI G<sup>2</sup>F20 system equipped with energy dispersion X-ray spectroscopy (EDX) operated at 200 kV.

CO adsorbed diffuse reflectance Fourier transform infrared (DRIFT) spectroscopy was obtained on a Tensor 27 spectrometer (Bruker) equipped with a liquid nitrogen cooled mercury-cadmium-tellurium (MCT) detector, a diffuse reflectance accessory and a high temperature reaction chamber (Praying Mantis, Harrick). The samples were purged at 300 °C by passing helium (20 mL min<sup>-1</sup>) for 1 h. CO adsorption was carried out at 25 °C in flowing 1.11% CO/helium (20 mL min<sup>-1</sup>) for 30 min. After the cell was flushed with helium for another 30 min, the DRIFT spectra were recorded with 64 scans and at a resolution of 4 cm<sup>-1</sup>.

The HPLC analyses were performed on a liquid chromatograph (Agilent 1100 series) coupled with a variable wavelength UV-detector. The reaction products were separated on a BioRad Aminex HPX-87H column thermostated at 30 °C. And H<sub>2</sub>SO<sub>4</sub> (0.005 mol L<sup>-1</sup>) was used as the mobile phase at a fixed flux of 0.4 mL min<sup>-1</sup>. The samples were detected at 200 nm.

The metal content of the Pd/Al<sub>2</sub>O<sub>3</sub> catalysts was determined by optical emission spectroscopy with ICP (VISTA-MPX). Hydrofluoric acid and nitric acid were used for complete digestion of the samples prior to the ICP analysis.

## Results and discussion

### Catalysts characterization

XRD characterizations are conducted to identify the major phase present. Fig. 1a shows the diffraction patterns of the support,  $\gamma$ -Al<sub>2</sub>O<sub>3</sub>. The XRD patterns of the Pd/Al<sub>2</sub>O<sub>3</sub>(P) sample (Fig. 1b) exhibit three broad shoulder peaks centered at  $2\theta = 40.06^\circ$ ,  $46.62^\circ$  and  $68.10^\circ$ . These peaks can be assigned to (111), (200) and (220) reflections of the cubic Pd lattice (JCPDS card, File No. 46–1043), suggesting that the metallic Pd exists in the sample. Namely, the Pd ions have been reduced effectively

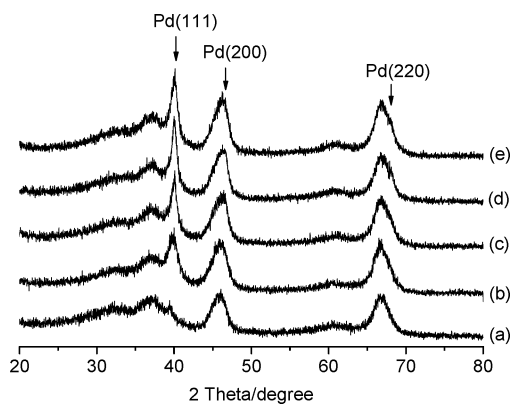


**Fig. 1** XRD patterns of (a)  $\gamma$ - $\text{Al}_2\text{O}_3$ , (b)  $\text{Pd}/\text{Al}_2\text{O}_3(\text{P})$ , (c)  $\text{Pd}/\text{Al}_2\text{O}_3(\text{P}300)$ , (d)  $\text{Pd}/\text{Al}_2\text{O}_3(\text{P}500)$ , (e)  $\text{Pd}/\text{Al}_2\text{O}_3(\text{C})$ .

during the argon glow discharge plasma treatment. And the relatively weak and wide peaks reveal that the nanoparticles of  $\text{Pd}/\text{Al}_2\text{O}_3(\text{P})$  are composed of small crystallites highly dispersed on the support. After calcination under the protection of flowing argon, the diffraction peaks of Pd become sharper and narrower, as shown in Fig. 1c and Fig. 1d, suggesting that some aggregation has occurred during the thermal treatment.  $\text{Pd}/\text{Al}_2\text{O}_3(\text{C})$  also has some aggregation due to the high temperature treatment and shows more intense peaks than  $\text{Pd}/\text{Al}_2\text{O}_3(\text{P})$ . By carefully comparing these patterns, it can be clearly observed that the diffraction peaks of  $\text{Pd}/\text{Al}_2\text{O}_3(\text{P}500)$  are close to those of  $\text{Pd}/\text{Al}_2\text{O}_3(\text{C})$ . According to Scherrer equation, the average sizes of metal crystallites are estimated, as shown in Table 1.

The TEM images of all the samples are shown in Fig. 2. The representative images of  $\text{Pd}/\text{Al}_2\text{O}_3(\text{P})$  reveal that Pd nanoparticles are uniformly distributed on the support (Fig. 2a). A high resolution TEM image of the Pd particle of  $\text{Pd}/\text{Al}_2\text{O}_3(\text{P})$  is given in Fig. 2b. The lattice fringes with  $d = 0.224$  nm are clearly visible, which can be assigned to Pd(111) plane. This result is in good agreement with the aforementioned XRD result. The EDX spectrum (Fig. 2c) provides further evidence of Pd nanoparticles. Fig. 2d–2f illustrate the typical TEM images of  $\text{Pd}/\text{Al}_2\text{O}_3(\text{P}300)$ ,  $\text{Pd}/\text{Al}_2\text{O}_3(\text{P}500)$  and  $\text{Pd}/\text{Al}_2\text{O}_3(\text{C})$ , respectively. They all show some aggregation due to the high temperature treatment. The average particle sizes determined from TEM images are well consistent with the XRD results.

The possible mechanism for the argon glow discharge plasma reduction of ionic Pd to metallic Pd nanoparticles probably involves two processes. One is a direct process. The high energy species generated by the plasma, such as electrons and ions, directly reduce the Pd ions through a recombination process. The second process is an indirect one involving the excitation of the chemisorbed water molecular to generate active species which are able to reduce the Pd ions. This process has been suggested

**Table 1** The average particle sizes and the corresponding initial rates for the catalysts

	$\text{Pd}/\text{Al}_2\text{O}_3(\text{P})$	$\text{Pd}/\text{Al}_2\text{O}_3(\text{P}300)$	$\text{Pd}/\text{Al}_2\text{O}_3(\text{P}500)$	$\text{Pd}/\text{Al}_2\text{O}_3(\text{C})$
$d/\text{nm}$	3.2	5.8	7.1	7.5
$r_0/\text{mmol L}^{-1} \text{min}^{-1}$	3.5	4.5	9.1	9.7

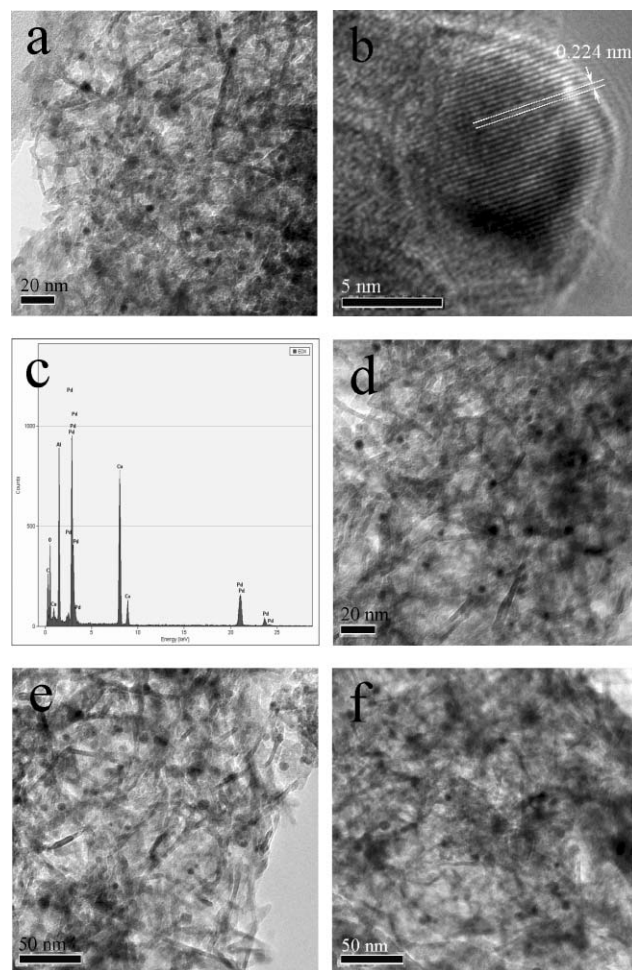


**Fig. 2** TEM results: (a) typical image of  $\text{Pd}/\text{Al}_2\text{O}_3(\text{P})$ , (b) a high resolution TEM image of  $\text{Pd}/\text{Al}_2\text{O}_3(\text{P})$ , (c) EDX spectrum of  $\text{Pd}/\text{Al}_2\text{O}_3(\text{P})$ , (d) typical image of  $\text{Pd}/\text{Al}_2\text{O}_3(\text{P}300)$ , (e) typical image of  $\text{Pd}/\text{Al}_2\text{O}_3(\text{P}500)$ , (f) typical image of  $\text{Pd}/\text{Al}_2\text{O}_3(\text{C})$ .

for the reduction of rhodium, platinum and other metal ions using non-hydrogen glow discharge.<sup>21</sup> In both processes, the reduced Pd could retain some electric charge and repel each other, resulting in the uniform distribution of Pd on the  $\gamma$ - $\text{Al}_2\text{O}_3$  support.

In Fig. 3, the DRIFT spectra of CO adsorption on  $\text{Pd}/\text{Al}_2\text{O}_3(\text{P}500)$  and  $\text{Pd}/\text{Al}_2\text{O}_3(\text{C})$  are included for comparison. The IR bands detected at  $2081 \text{ cm}^{-1}$ ,  $1983 \text{ cm}^{-1}$ ,  $1922 \text{ cm}^{-1}$  and  $1885 \text{ cm}^{-1}$  on  $\text{Pd}/\text{Al}_2\text{O}_3(\text{C})$  can be attributed to a linear CO specie on the palladium atoms and three bridged CO species on different Pd planes respectively.<sup>23</sup> It can be clearly observed that all of the IR bands of  $\text{Pd}/\text{Al}_2\text{O}_3(\text{P}500)$  are much weaker than those of  $\text{Pd}/\text{Al}_2\text{O}_3(\text{C})$ , suggesting that the amount of Pd nanoparticles on  $\text{Pd}/\text{Al}_2\text{O}_3(\text{P}500)$ , able to adsorb CO, is smaller. There are two possibilities for this effect. One is the larger particle sizes; the other is the stronger metal-support interaction. Since the Pd particle size of  $\text{Pd}/\text{Al}_2\text{O}_3(\text{P}500)$  is similar with that of  $\text{Pd}/\text{Al}_2\text{O}_3(\text{C})$  as has been confirmed by XRD and TEM results, the reason for this effect should be the latter, namely,  $\text{Pd}/\text{Al}_2\text{O}_3(\text{P}500)$  has a stronger metal-support interaction than  $\text{Pd}/\text{Al}_2\text{O}_3(\text{C})$ .



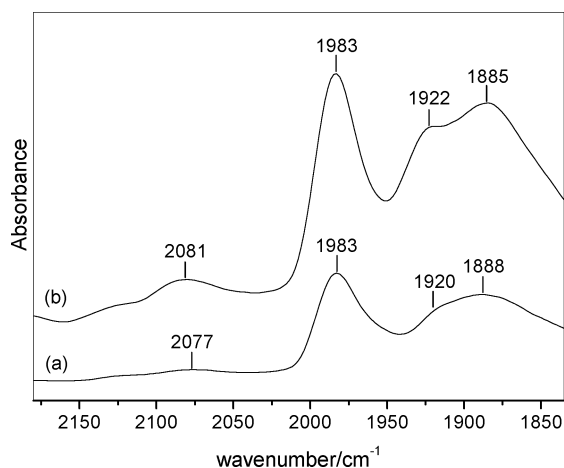


**Fig. 3** DRIFT spectra of CO adsorption on (a) Pd/Al<sub>2</sub>O<sub>3</sub>(P500) and (b) Pd/Al<sub>2</sub>O<sub>3</sub>(C).

### Catalytic activity

The catalysts were tested for selective oxidation of glucose to gluconic acid. The selectivity was determined by analyzing the reaction medium using HPLC. All the catalysts exhibit selectivities above 95% and there are no significant differences among them in selectivities, therefore we will focus our attention on the differences in activities. Since the selectivities to gluconic acid are high enough, the conversions can be conveniently measured from the consumptions of sodium hydroxide which is added to the reaction medium to maintain a constant pH. Fig. 4 gives the conversions as a function of time for all the samples. It is noteworthy that, Pd/Al<sub>2</sub>O<sub>3</sub>(P500) can provide complete conversion within 6 h while the Pd/Al<sub>2</sub>O<sub>3</sub>(C) can only provide a conversion of 95% even at a period of 8 h. What's more, the conversion of Pd/Al<sub>2</sub>O<sub>3</sub>(C) has reached a plateau, implying a low activity.

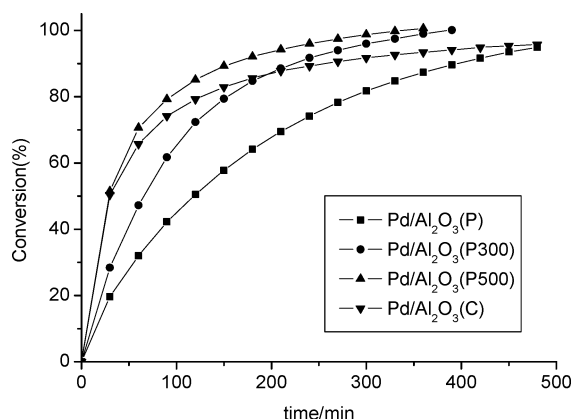


**Fig. 4** Catalytic activity of different catalysts in glucose oxidation. Reaction conditions: [G] = 0.4 mol L<sup>-1</sup>, O<sub>2</sub> flow = 400 mL min<sup>-1</sup>, stirring rate = 1200 rpm, T = 50 °C, PH = 9.

The initial rates determined from the initial slopes of the curves are illustrated in Table 1. It can be concluded that the initial rates are proportional with particle sizes as reported previously for Pd/C.<sup>6</sup> This effect may be ascribed to that the smaller Pd particles have higher oxygen heat of adsorption,<sup>24</sup>

**Table 2** Data of ICP analyses and the amounts of Pd leaching (wt% Pd)

	Pd/Al <sub>2</sub> O <sub>3</sub> (P)	Pd/Al <sub>2</sub> O <sub>3</sub> -(P300)	Pd/Al <sub>2</sub> O <sub>3</sub> -(P500)	Pd/Al <sub>2</sub> O <sub>3</sub> (C)
fresh	3.14	3.10	3.08	3.14
used	3.00	2.99	2.93	2.58
leaching	0.14	0.11	0.15	0.56

*i.e.*, stronger affinities for oxygen, and thus are more prone to oxygen poisoning.

With the reaction proceeding, the decrease of the reaction rates could be caused by catalysts deactivation during the experiment. From Fig. 4, it is obvious that the degrees of deactivation for the four catalysts have the relationships as: Pd/Al<sub>2</sub>O<sub>3</sub>(P) < Pd/Al<sub>2</sub>O<sub>3</sub>(P300) < Pd/Al<sub>2</sub>O<sub>3</sub>(P500) < Pd/Al<sub>2</sub>O<sub>3</sub>(C).

The deactivation depends on a number of factors, the most important two of which are interpreted as follows:

Since the oxidation occurs *via* oxidative dehydrogenation mechanism,<sup>6,25</sup> the organic substrate, oxygen and hydrogen from dehydrogenation of organic substrate are all adsorbed on the metal surface, and there is a delicate balance between them. As the concentration of glucose decreases in the reaction medium, the oxygen coverage will increase, which may lead to a deactivation. This means that the deactivation is directly coupled to the chemical reaction.<sup>26</sup> It well documents the results that the catalyst with a higher initial rate would have a severer deactivation.

However, the Pd/Al<sub>2</sub>O<sub>3</sub>(P500) behaves much more stable than Pd/Al<sub>2</sub>O<sub>3</sub>(C), although both catalysts possess high initial rates. It may be ascribed to another important factor for the deactivation. Because of the presence of gluconic salts, which show strong chelating properties in the reaction medium,<sup>12</sup> the amounts of Pd dissolved in the solution during glucose oxidation have been investigated. Table 2 reveals that, for the plasma reduced catalysts, the amounts of Pd leaching, which may cause an irreversible deactivation, are much less than that for hydrogen reduced catalyst by a factor of 1/4. The less leaching of active metal for plasma reduced catalysts results in the less deactivation in comparison with the hydrogen thermally reduced one. It can be surmised that the stronger metal-support interactions on the plasma reduced catalysts, as confirmed by DRIFT results, cause these effects.

Besides being effective for the catalyst preparation, the plasma reduction route is more energy efficient and economically effective than the thermal hydrogen reduction method. The energy consumption and economy evaluation were conducted based on the procedure described in section of catalyst preparation.

For the glow discharge plasma reduction, the high voltage amplifier, the wave form generator and the vacuum pump will draw their average power at 630 W, 5 W and 370 W, respectively. The total energy consumed during the plasma reduction is 3.618 MJ. The consumption of argon is 0.102 L and the corresponding cost is estimated to be ¥0.0029 (¥ denotes the unit of Chinese Currency RMB Yuan). For the process of plasma reduction with calcination thermally under flowing argon, the energy consumption is 7.698 MJ and the material cost is ¥0.3887.

The average power of the muffle for calcination thermally and the furnace for reduction in the conventional hydrogen reduction

method are 272 W and 425 W, respectively. The total energy consumed during this process is 10.116 MJ. The total cost of argon (8.8 L) and hydrogen (4.8 L) is estimated to be ¥0.4831.

In comparison, the energy consumption and the material cost for the plasma approach are only 35.8% and 0.6% as little as those for the conventional hydrogen reduction. Even including the argon calcination process, the energy consumption and the material cost of the plasma reduction route are only 76.1% and 80.5% of those obtained with the conventional hydrogen reduction. A further economic analysis will be conducted with the planned pilot test.

## Conclusions

The Pd/ $\gamma$ -Al<sub>2</sub>O<sub>3</sub> used for selective oxidation of glucose can be successfully reduced by argon glow discharge plasma at ambient temperature. A size effect has been observed over the plasma reduced catalysts. The plasma reduced catalyst has a small particle size and shows a lower conversion rate compared to the conventional catalyst reduced by hydrogen at elevated temperatures. The calcined plasma reduced Pd/Al<sub>2</sub>O<sub>3</sub> catalyst exhibits a larger particle size and possesses a higher activity than the hydrogen reduced catalyst. It is noteworthy that the stronger metal-support interaction induced by plasma reduction enhances the stability of active metal loaded on the support. This effect, against the irreversible deactivation, is very important for industrial application, because the oxidation in the liquid is normally performed in a continuous mode for a long time and repeatedly recycled. It is expected that the argon glow discharge plasma reduction approach is a promising alternative to conventional reduction method with both fundamental and practical consideration. The plasma reduction at ambient temperature is green, energy efficient and economic effective.

## Acknowledgements

The support from the National Natural Science Foundation of China (under contract 20490203) is greatly appreciated. The

plasma instrument supplied by ABB Switzerland Ltd. is also appreciated.

## Notes and references

- 1 P. Anastas, P. Kazlauskas and G. Sheldrake, *Green Chem.*, 2006, **8**, 677–678.
- 2 H. B. Zhao, J. E. Holladay, H. Brown and Z. C. Zhang, *Science*, 2006, **316**, 1597–1600.
- 3 F. Volgel, M. H. Waldner, A. A. Rouff and S. Rabe, *Green Chem.*, 2007, **9**, 616–619.
- 4 I. Nikov and K. Paev, *Catal. Today*, 1995, **24**, 41–47.
- 5 A. Abbadi, M. Makkee, W. Visscher, J. A. R. van Veen and H. van Bekkum, *J. Carbohydr. Chem.*, 1993, **12**, 573–587.
- 6 M. Besson, P. Gallezot, F. Lahmer, G. Fleche, and P. Fuertes, in *Catalysis of Organic Reactions*, ed. J. R. Kosak, and T. A. Johnson, Marcel Dekker Inc., New York, 1993, pp. 169–180.
- 7 A. Abbadi and H. van Bekkum, *J. Mol. Catal. A*, 1995, **97**, 111–118.
- 8 M. Besson, F. Lahmer, P. Gallezot, P. Fuertes and G. Fleche, *J. Catal.*, 1995, **152**, 116–121.
- 9 M. Wenkin, R. Touillaux, P. Ruiz, B. Delmon and M. Devillers, *Appl. Catal. A*, 1996, **148**, 181–199.
- 10 M. Wenkin, P. Ruiz, B. Delmon and M. Devillers, *J. Mol. Catal. A*, 2002, **180**, 141–159.
- 11 S. Hermans and M. Devillers, *Appl. Catal. A*, 2002, **235**, 253–264.
- 12 S. Karski and I. Witonska, *J. Mol. Catal. A*, 2003, **191**, 87–92.
- 13 S. Biella, L. Prati and M. Rossi, *J. Catal.*, 2002, **206**, 242–247.
- 14 P. Beltrame, M. Comotti, C. D. Pina and M. Rossi, *Appl. Catal. A*, 2006, **297**, 1–7.
- 15 M. Comotti, C. D. Pina, R. Matarrese and M. Rossi, *Angew. Chem. Int. Ed.*, 2004, **43**, 5812–5815.
- 16 M. Comotti, C. D. Pina, E. Falletta and M. Rossi, *J. Catal.*, 2006, **244**, 122–125.
- 17 Y. Onal, S. Schimpf and P. Claus, *J. Catal.*, 2004, **223**, 122–133.
- 18 P. Raveendran, J. Fu and S. L. Wallen, *Green Chem.*, 2006, **8**, 34–38.
- 19 M. N. Nadagouda and R. S. Varma, *Green Chem.*, 2006, **8**, 516–518.
- 20 J. -J. Zou, Y. -P. Zhang and C. -J. Liu, *Langmuir*, 2006, **22**, 11388–11394.
- 21 Z. -J. Wang, Y. Zhao, L. Cui, H. Y. Du, P. Yao and C. -J. Liu, *Green Chem.*, 2007, **9**, 554–559.
- 22 W. Bang, X. Lu, A. M. Duquenne, I. Nikov and A. Bascoul, *Catal. Today*, 1999, **48**, 125–130.
- 23 C. Mondelli, D. Ferri, J. -D. Grunwaldt, F. Krumeich, S. Mangold, R. Psaro and A. Baiker, *J. Catal.*, 2007, **252**, 77–87.
- 24 P. Chou and M. A. Vannice, *J. Catal.*, 1987, **105**, 342–351.
- 25 P. Gallezot, *Catal. Today*, 1997, **37**, 405–418.
- 26 J. M. H. Dirks and H. S. van der Baan, *J. Catal.*, 1981, **67**, 1–13.

# An environmentally benign and catalytically efficient non-pyrophoric Ni catalyst for aqueous-phase reforming of ethylene glycol

Ling-Jun Zhu,<sup>a</sup> Ping-Jun Guo,<sup>a</sup> Xian-Wen Chu,<sup>a</sup> Shi-Run Yan,<sup>a</sup> Ming-Hua Qiao,<sup>\*a</sup> Kang-Nian Fan,<sup>a</sup> Xiao-Xin Zhang<sup>b</sup> and Bao-Ning Zong<sup>\*b</sup>

Received 14th May 2008, Accepted 20th August 2008

First published as an Advance Article on the web 29th October 2008

DOI: 10.1039/b808190e

A non-pyrophoric Ni catalyst (NP Ni) was prepared by alkali leaching of a Ni<sub>50</sub>Al<sub>50</sub> alloy using only ~ 1/10 of the amount of NaOH required for the preparation of the conventional Raney Ni catalyst. Characterizations reveal that the as-prepared NP Ni catalyst can be looked at as a Ni–Al(OH)<sub>3</sub> composite catalyst with Ni in the metallic state and Al(OH)<sub>3</sub> in forms of gibbsite and bayerite. After 100 h on stream in aqueous-phase reforming (APR) of ethylene glycol, phase transformation of gibbsite and bayerite to flake-like boehmite occurred, along with the growth of Ni crystallites and partial oxidation of metallic Ni to Ni(OH)<sub>2</sub>. Under identical reaction conditions for APR of ethylene glycol, the NP Ni catalyst is about 40–52% more active than Raney Ni in terms of the conversion of ethylene glycol to gas products, which is attributed to the stabilizing effect of hydrated alumina on Ni crystallites. The higher selectivity toward H<sub>2</sub> and the lower concentration of CO in the product gas on the NP Ni catalyst are attributed to the activation of water by hydrated alumina which is beneficial to the water-gas shift reaction.

## 1. Introduction

Production of fuel from renewable resources such as biomass has attracted much research interest worldwide. One of the viable routes is the aqueous-phase reforming (APR) of biomass-derived oxygenates, such as glucose, sorbitol, glycerol, and ethylene glycol having a C:O stoichiometry of 1 and a H<sub>2</sub> content relative to carbon higher than one, to H<sub>2</sub> and light alkanes (primarily methane)<sup>1–3</sup> that are feedstocks for proton exchange membrane fuel cell (PEMFC) and direct methane fuel cell (DMFC), respectively. Fuel production by the APR process is carbon-neutral, because the CO<sub>2</sub> byproduct that accompanies the H<sub>2</sub> and alkane production is consumed by biomass growth. Moreover, unlike the steam reforming process that is typically carried out at as high as ~ 900 K, the APR reaction is performed at much lower temperature (~500 K), because the vaporization of water and oxygenates is not required. It is even more attractive that the water-gas shift (WGS) reaction is thermodynamically favored at the low temperature of APR, which can effectively cut down CO, a vital gas for anode materials in fuel cells, in the product gas in a single reactor.<sup>4</sup> In contrast, the steam reforming process requires multi-stage or multiple reactors to achieve low levels of CO.<sup>5</sup> So the APR process is an intriguing energy-efficient and cost-effective green route for the production of renewable fuel from biomass.

APR of ethylene glycol, a sustainable chemical prepared from sugars and sugar-alcohols,<sup>4</sup> to H<sub>2</sub> and light alkanes proceeds mainly in the following pathway: dehydrogenation → C–C cleavage → WGS → methanation/Fischer-Tropsch (F-T) reaction.<sup>1</sup> Since Ni shows high activities for C–C bond scission<sup>6</sup> and methanation,<sup>7</sup> moderate WGS activity,<sup>8</sup> and is much less expensive than the noble Pt, several types of Ni-based catalysts have been prepared and evaluated in APR of ethylene glycol. However, supported Ni catalysts suffered from severe deactivation during APR of ethylene glycol. It is found that Ni supported on Al<sub>2</sub>O<sub>3</sub>, SiO<sub>2</sub>, ZrO<sub>2</sub>,<sup>9</sup> and Ni<sub>3</sub>Sn supported on Al<sub>2</sub>O<sub>3</sub><sup>10</sup> lost ~ 90% of their initial activities after 48 h on stream at 498 K. Skeletal Ni catalysts, such as Raney Ni, showed better stability, losing ~50% of its initial activity over the same period.<sup>9</sup> Although the addition of Sn further improved the stability of Raney Ni due to the improved oxidation/hydration resistance and coking resistance of the NiSn alloy,<sup>9</sup> Sn is adverse to the APR activity. For example, the initial activity of Raney Ni<sub>14</sub>Sn drastically dropped to only about one half of that of Raney Ni.<sup>10,11</sup> In order to improve the activity and stability of the Raney Ni-based catalysts in the APR reaction, it is advisable to develop new generations of dispersed, supported catalysts.<sup>12</sup>

Recently, Petró and co-workers reported that starting from the same Ni–Al alloy as that for the preparation of Raney Ni, a novel non-pyrophoric Ni catalyst (NP Ni) consisting of metallic Ni, gibbsite, and bayerite was obtained.<sup>13,14</sup> This catalyst was prepared in a way similar to that of Raney Ni, with the exception that much less NaOH (~1/10) was used for leaching of Al and consequently, much less waste chemicals were generated for disposal. In liquid phase hydrogenations, the NP Ni catalyst showed the same or higher catalytic activity than Raney Ni.

<sup>a</sup>Department of Chemistry and Shanghai Key Laboratory of Molecular Catalysis and Innovative Materials, Fudan University, Shanghai, 200433, P. R. China. E-mail: mhqiao@fudan.edu.cn; Fax: 86-21-65641740; Tel: 86-21-55664679

<sup>b</sup>Research Institute of Petroleum Processing, Beijing, 100083, P. R. China. E-mail: zongbn@ripp-sinopec.com; Fax: 86-10-82368011; Tel: 86-10-82368011

Considering the attractive catalytic performance of the NP Ni catalyst and its simple and environmentally friendly preparation process, in this work we prepared the NP Ni catalyst for APR of ethylene glycol. Using the same Ni–Al alloy, the Raney Ni catalyst was prepared and tested for comparison. The physicochemical properties of the Raney Ni and NP Ni catalysts before and after 100 h catalytic stability tests were characterized and correlated with their catalytic performances.

## 2. Experimental

### 2.1. Catalyst preparation

The NP Ni catalyst was prepared as described below. Under gentle stirring, 1 g of the Ni–Al alloy powder (Fluka, 50 wt% Ni + 50 wt% Al, 5–20  $\mu\text{m}$ ) was added to an aqueous solution of NaOH (8 ml, 0.31 M) at room temperature. After addition, the mixture was stirred at 363 K for 30 min, and 1 ml of 3.1 M NaOH aqueous solution was added into the mixture and stirred gently at 363 K for 20 min for further alkali leaching. The precipitate was washed to neutrality with distilled water and stored under water for catalytic test.

The Raney Ni catalyst was prepared in the following procedure. One gram of the above Ni–Al alloy powder was added to an aqueous solution of NaOH (10 ml, 6.0 M) at 363 K under gentle stirring. After addition, the reaction system was kept on stirring at 363 K for 1.0 h for further alkali leaching. The precipitate was washed with distilled water to neutrality and stored under water for activity test. For characterizations, both catalysts were washed with ethanol to replace water and stored under ethanol. Since Raney Ni is notorious for its pyrophoricity, care must be taken during sample handling and disposal.

### 2.2. Catalyst characterization

The bulk compositions of the catalysts were determined by inductively coupled plasma-atomic emission spectroscopy (ICP-AES, Hitachi P-4010) after dissolution in aqua regia. The Brunauer-Emmett-Teller (BET) surface area ( $S_{\text{BET}}$ ) and other textural properties were measured by  $\text{N}_2$  adsorption-desorption isotherms at 77 K on a Micromeritics TriStar 3000 apparatus. Powder X-ray diffraction (XRD) was executed on a Bruker AXS D8 Advance X-ray diffractometer using  $\text{Cu K}\alpha$  radiation ( $\lambda = 0.15418 \text{ nm}$ ). The tube voltage was 40 kV and the current was 40 mA. The mean crystallite size of Ni was calculated from the full width at the half maximum (FWHM) of the Ni (111) diffraction peak according to the Scherrer equation.

The surface morphologies were observed by scanning electron microscopy (SEM, Philips XL 30). The distribution of Ni and Al was detected by an energy dispersive X-ray emission analyzer (EDX) attached to the SEM apparatus. The surface composition and chemical state of the catalysts were determined by X-ray photoelectron spectroscopy (XPS, Perkin-Elmer PHI5000C) with a  $\text{Mg K}\alpha$  radiation ( $h\nu = 1253.6 \text{ eV}$ ). Prior to XPS analysis, the surface oxides were removed by Ar ion sputtering. All binding energy (BE) values were calibrated by C 1s peak of contaminant carbon at 284.6 eV with an uncertainty of  $\pm 0.2 \text{ eV}$ .

The active surface areas were determined by  $\text{H}_2$  desorption. After the catalyst was heated at 498 K for 1.0 h under Ar flow (deoxygenated by an Alltech Oxy-trap filter), it was cooled down

to room temperature under Ar. Then  $\text{H}_2$  pulses were injected until the eluted peak area of consecutive pulses was constant. The maximum desorption temperature, 973 K, was achieved at a ramping rate of  $10 \text{ K min}^{-1}$ . The active surface area ( $S_{\text{H}}$ ) was calculated from the volume of  $\text{H}_2$  desorbed by assuming a H/Ni<sub>s</sub> stoichiometry of 1 and a surface area of  $6.5 \times 10^{-20} \text{ m}^2$  per Ni atom.<sup>15</sup>

### 2.3. Activity test

The reactor system for APR of ethylene glycol was established according to the set-up described by Shabaker *et al.*<sup>16</sup> The as-prepared Raney Ni or NP Ni catalyst with water was loaded in the stainless steel tubular reactor with an inner diameter of 6 mm. No additional activation treatment of the catalysts was executed, because Ni in those catalysts has already been in the metallic state. An aqueous solution containing 5 wt% of ethylene glycol was fed into the reactor in an up-flow configuration. Ar was used to regulate the system pressure. The reforming was typically conducted with catalyst containing 0.5 g of Ni, weight hourly space velocity (WHSV, (weight flow rate of the feed solution)  $\times$  (weight fraction of ethylene glycol in the feed)/(weight of Ni in the catalyst)) of  $0.36 \text{ h}^{-1}$ , temperature of 498 K, and system pressure of 2.58 MPa, unless otherwise specified. The stability test was conducted under above-mentioned reaction conditions up to 100 h on stream.

In the APR reaction, gas products were analyzed by an on-line GC122 gas chromatograph.  $\text{H}_2$ , CO, methane, and  $\text{CO}_2$  were separated by a 2 m TDX-01 packed column and examined by a thermal conductivity detector (TCD). Methane, ethane, propane, and butane were separated by a PoraPlot Q capillary column (10 m  $\times$  0.53 mm  $\times$  20  $\mu\text{m}$ ) and examined by a flame ionization detector (FID). Liquid phase effluent was collected and analyzed gas chromatographically using the same PoraPlot Q capillary column and FID detector. The liquid products were also qualified by GC-MS (Finnigan Voyager) with an HP-5 capillary column. The carbon balance was within  $\pm 5\%$  for all catalytic runs.

According to Shabaker *et al.*,<sup>10</sup> in this paper the  $\text{H}_2$  selectivity is defined as:

$$\text{H}_2 \text{ selectivity (\%)} = \left[ \frac{\text{moles of H}_2 \text{ produced}}{\text{moles of C in gas products}} \right] \times \left( \frac{2}{5} \right) \times 100$$

which takes into account of the occurrence of the WGS reaction; and the alkane selectivity is defined as:

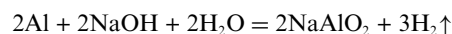
$$\text{Alkane selectivity (\%)} = \left[ \frac{\text{moles of C in gaseous alkanes}}{\text{total moles of C in gas products}} \right] \times 100$$

It should be emphasized that according to the definitions, the summation of the selectivities of  $\text{H}_2$  and alkane does not lead to unity, for they are calculated based on independent hydrogen and carbon balances, respectively.

## 3. Results

### 3.1. Physicochemical properties of the as-prepared catalysts

During alkali leaching, Al in the Ni–Al alloy reacts with NaOH in the equation:





in which  $\text{NaAlO}_2$  is soluble. When the  $\text{NaOH}/\text{Al}$  stoichiometry is lower than 1, besides the reaction depicted above, Al also reacts with water to form insoluble  $\text{Al}(\text{OH})_3$ :



Therefore, it is expected that Raney Ni is mainly composed of metallic Ni (there is also some residual hydrated alumina adsorbed in the spongy structure of Raney Ni<sup>17</sup>), while NP Ni prepared with insufficient amount of NaOH can be taken as a Ni– $\text{Al}(\text{OH})_3$  composite catalyst, as illuminated by Petró *et al.*<sup>13</sup> and our characterizations shown below.

Fig. 1 shows the XRD patterns of the as-prepared Raney Ni and NP Ni catalysts. For Raney Ni, there are only diagnostic (111), (200), and (220) diffractions of fcc Ni at  $2\theta$  of 44.5, 51.8, and 76.3° (JCPDS 04–0850), respectively, and no features due to  $\text{Al}(\text{OH})_3$  were found. For NP Ni, sharp peaks assignable to gibbsite (JCPDS 33–0018) and bayerite (JCPDS 20–0011) were identified, confirming the presence of more  $\text{Al}(\text{OH})_3$  in NP Ni.

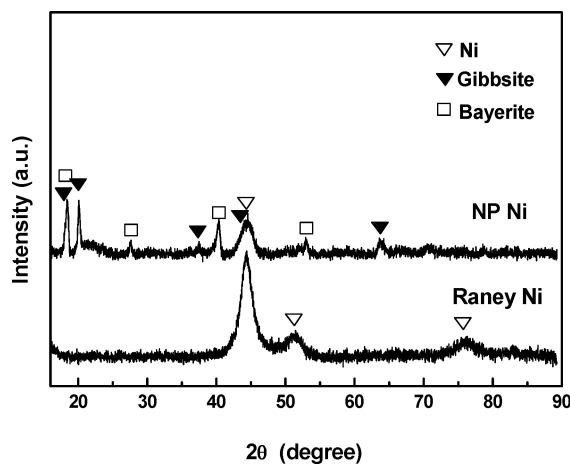


Fig. 1 XRD patterns of the as-prepared Raney Ni and NP Ni catalysts.

Fig. 2 shows the SEM images of the Raney Ni and NP Ni catalysts. The morphological differences between the as-prepared Raney Ni and NP Ni catalysts are readily visible from Figs. 2a and 2b. Raney Ni is constituted by the typical fractured and angular particles (Fig. 2a),<sup>18</sup> while NP Ni is constituted by Ni-rich angular particles and irregularly oriented Al-rich crystal-like particles (Fig. 2b). The Ni-rich region and the Al-rich region of the as-prepared NP Ni catalyst are further illustrated in Figs. 2c and 2d, respectively. Besides the spongy morphology of Ni (Fig. 2c), the Al-rich region (Fig. 2d) contains hexagonal prismatic rods and spiral crystals constructed by plates stacking

perpendicular to the longitudinal axis, which are characteristic morphologies of gibbsite and bayerite, respectively.<sup>19,20</sup>

Table 1 summarizes the compositional and textural properties of the as-prepared Raney Ni and NP Ni catalysts. It is found that NP Ni has a bulk Ni/Al atomic ratio of 0.67, which is much smaller than that of Raney Ni, reflecting that less Al was leached away in the form of soluble  $\text{NaAlO}_2$  during the preparation of NP Ni. Because of the presence of the gibbsite and bayerite crystals, and possibly the blockage of micropores of Ni by them, as compared to Raney Ni, NP Ni exhibited larger average pore size, smaller pore volume and smaller BET surface area that is close to the value of  $48 \text{ m}^2 \text{ g}^{-1}$  derived from the SAXS technique.<sup>14</sup> On the other hand, the new preparation method leads to a better dispersion of Ni. Table 1 shows that the active surface area  $S_{\text{H}}$  with respect to per gram of Ni is  $45 \text{ m}^2$  for NP Ni, while it is only  $16 \text{ m}^2$  for Raney Ni, with the latter value falling well in the range of  $10\text{--}21 \text{ m}^2 \text{ g}^{-1}$  for Raney-type Ni catalysts.<sup>21</sup>

### 3.2. Aqueous-phase reforming of ethylene glycol

**3.2.1. Reaction kinetic results.** Table 2 compares the  $\text{H}_2$  and alkane selectivities and gas and liquid product distributions over the Raney Ni and the NP Ni catalysts at high conversion levels of ethylene glycol for practical considerations. It is found that under the same reaction conditions and after 6 h on stream, the conversion of ethylene glycol and the conversion of ethylene glycol to gas products on the NP Ni catalyst are about 19% and 27% higher than those on Raney Ni, respectively. The NP Ni catalyst also exhibited higher  $\text{H}_2$  selectivity and lower alkane selectivity than Raney Ni, while the distribution of gas products on Raney Ni in this work is qualitatively similar to that reported before.<sup>10</sup> As compared to Raney Ni, NP Ni produced less CO in the outlet gas (below the detection limit of  $\sim 50 \text{ ppm}$ ), which is significant especially for fuel cells in which anode materials are vulnerable to CO poisoning.<sup>22</sup> Moreover, the improved reforming activity and  $\text{H}_2$  selectivity of NP Ni render it a promising alternative as a  $\text{H}_2$ -specific catalyst after proper modifications, such as modification by tin,<sup>2,10</sup> while the activity still remains at an acceptable level.

The novel preparation method also influenced the distribution of liquid products in APR of ethylene glycol, as illustrated in Table 2. On NP Ni, the selectivities to acetaldehyde and acetone were substantially reduced, whereas the selectivity to methanol was enhanced relative to Raney Ni. Methanol is a desirable product, for it still contains a C:O linkage and may be further reformed to  $\text{H}_2$  in high yields.<sup>9</sup> Shabaker *et al.* identified a considerable amount of acetic acid using Raney Ni as the

**Table 1** Physicochemical properties of the as-prepared Raney Ni and NP Ni catalysts (left) and the catalysts after 100 h on stream in APR of 5 wt% ethylene glycol at 498 K, 2.58 MPa, and WHSV of  $0.36 \text{ h}^{-1}$  (right)

Catalyst	Ni/Al (atomic ratio)		$S_{\text{BET}}$ ( $\text{m}^2 \text{ g}^{-1}$ )	$V_{\text{pore}}$ ( $\text{cm}^3 \text{ g}^{-1}$ )	$d_{\text{por}}$ (nm)	$S_{\text{H}}$ ( $\text{m}^2 \text{ g}_{\text{Ni}}^{-1}$ )	$d_{\text{Ni}}^c$ (nm)
	Bulk <sup>a</sup>	Surface <sup>b</sup>					
Raney Ni	4.56/4.60	4.39/0.21	101/17	0.105/0.092	3.4/16.4	16/6	5/23
NP Ni	0.67/0.65	0.10/0.05	40/21	0.060/0.122	4.4/14.8	45/19	4/16

<sup>a</sup> Determined by ICP-AES. <sup>b</sup> Determined by XPS. <sup>c</sup> Ni crystallite size determined by XRD.

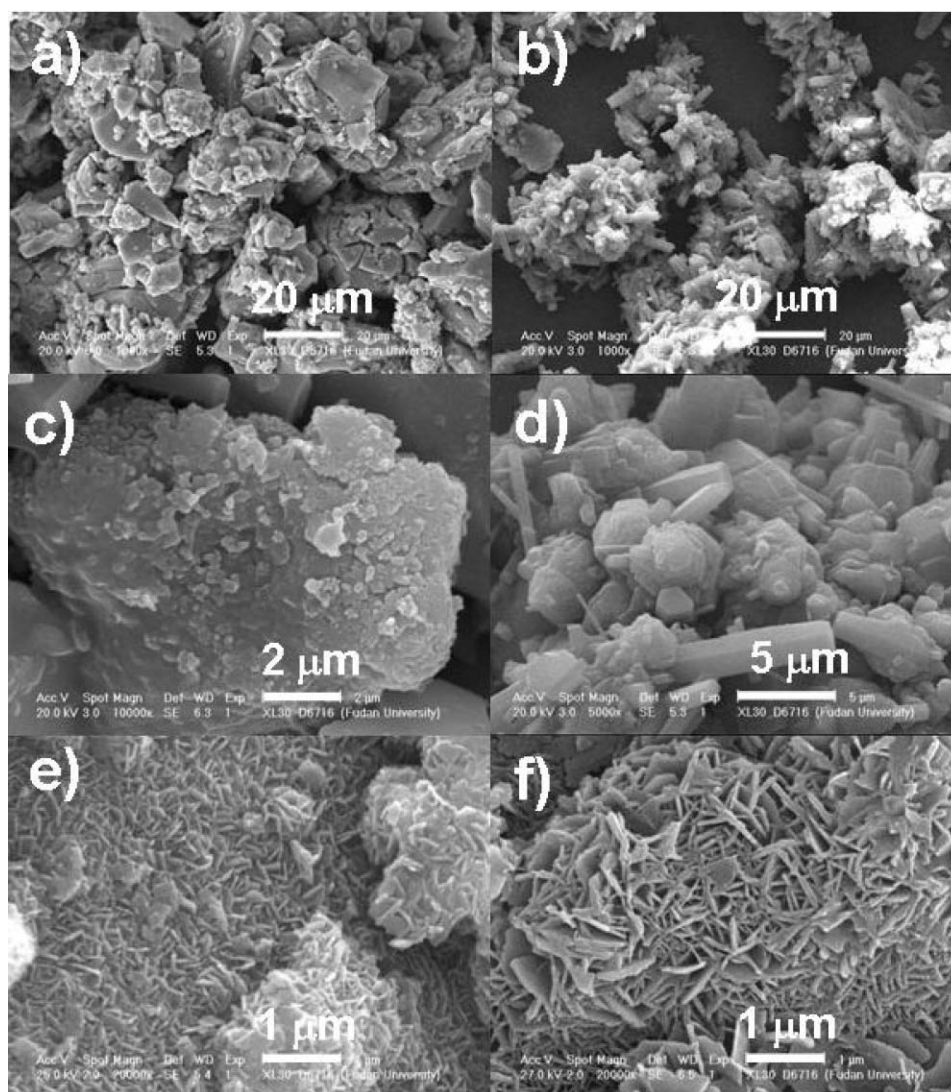


**Fig. 2** SEM images of the as-prepared Raney Ni catalyst (a) and the NP Ni catalyst (b), the Ni-rich region (c) and the Al-rich region (d) of the as-prepared NP Ni catalyst, the Raney Ni catalyst (e) and the NP Ni catalyst (f) after 100 h on stream in APR of 5 wt% ethylene glycol at 498 K, 2.58 MPa, and WHSV of 0.36 h<sup>-1</sup>.

reforming catalyst, which is an undesirable product because of its low reforming reactivity under the reaction conditions of APR<sup>10</sup> and corrosivity that causes the leaching of Ni.<sup>9</sup> In the present case, acetic acid was not detected in the liquid products, which may be attributed to the different origins of Raney Ni or different catalyst activation steps employed in different works.

Table 3 compiles the reaction kinetics data for APR of ethylene glycol over the Raney Ni and NP Ni catalysts at conversions below 10%. As proven by our previous work,<sup>23</sup> the transport limitations can be excluded under the present reaction conditions. In compliance with the situation at high conversions, the conversion of ethylene glycol to gas products on NP Ni is *ca.* 52% higher than that on Raney Ni. It is found that except for the decrement of the production rate of CO, the production rates of CO<sub>2</sub>, H<sub>2</sub>, and alkanes were all increased when using NP Ni as the catalyst. Among them, the increment in the production rates of CO<sub>2</sub> and H<sub>2</sub> is more pronounced than that of alkanes, giving rise to a higher H<sub>2</sub> selectivity on NP Ni. In particular, the production

rates of CO<sub>2</sub> and H<sub>2</sub> were increased to a similar extent, suggesting that their increment was mainly originated from the acceleration of the WGS reaction by the NP Ni catalyst prepared by the new method.

**3.2.2. Catalytic stability.** Fig. 3 depicts the catalytic performances of the Raney Ni and NP Ni catalysts *versus* time-on-stream for APR of ethylene glycol. It shows that Raney Ni exhibited fast deactivation during the first 20 h on stream, lost ~55% of its initial activity over a period of 48 h, and then stayed at ~33% of its initial activity at prolonged reaction times. We noticed that the steady-state activity of the present Raney Ni catalyst is lower than that reported previously,<sup>9</sup> which may be due to the use of different Raney Ni catalysts or experimental differences between different laboratories. The NP Ni catalyst was more active and less prone to deactivation than Raney Ni. After exposure to the reaction condition for 100 h, the NP Ni catalyst still remained ~42% of its initial activity. It has

**Table 2** The catalytic performance of the Raney Ni and NP Ni catalysts in APR of 5 wt% ethylene glycol at 498 K, 2.58 MPa, WHSV of 0.36 h<sup>-1</sup>, and after 6 h on stream

Catalyst	Raney Ni	NP Ni
Carbon in gas effluent (%)	67	94
Carbon in liquid effluent (%)	29 (including 19% unconverted EG)	7
H <sub>2</sub> selectivity (%)	38	47
Methane selectivity (%)	35	31
Alkane selectivity (%)	39	35
Gas products (mol%)		
H <sub>2</sub>	49.4	54.8
CO <sub>2</sub>	31.3	30.2
CO	0.2	n.d. <sup>a</sup>
Methane	18.0	14.1
Ethane	0.9	0.7
Propane	0.2	0.2
Butane	0.02	0.02
Liquid products (mol%, excluding unconverted EG)		
Methanol	66.0	83.3
Ethanol	19.7	15.1
Acetaldehyde	4.2	0.0
Acetone	9.9	1.2
2-Propanol	0.1	0.4

<sup>a</sup> Below the detection limit.

been reported that Raney Ni is more stable than Ni catalysts supported on Al<sub>2</sub>O<sub>3</sub>, SiO<sub>2</sub>, ZrO<sub>2</sub>,<sup>9</sup> and Ni<sub>3</sub>Sn supported on Al<sub>2</sub>O<sub>3</sub> in APR of ethylene glycol,<sup>10</sup> inferring the superior stability of NP Ni to those Ni-based catalysts.

On the other hand, Fig. 3 shows that the H<sub>2</sub> selectivity increased by about 10%, and the alkane selectivity decreased by about 5%, and stabilized after ~ 48 h on stream for both the Raney Ni and NP Ni catalysts. The much less remarkable evolutions of the H<sub>2</sub> and alkane selectivities than that of the catalytic activity imply that the changes in catalytic performances of the Raney Ni and NP Ni catalysts during stability tests is mainly caused by the depletion of the amount of the active sites on the catalysts rather than the change in the nature of the active sites.

### 3.3. Characterization of catalysts after stability test

To gain a better understanding of the changes in the catalytic performances during the stability test, the Raney Ni and NP Ni catalysts were systematically characterized after 100 h on stream. Table 1 shows that the bulk Ni/Al ratios of Raney Ni and NP Ni were virtually unchanged after reaction. Moreover, for both catalysts the effluent Ni and Al concentrations maintained at the level of about 4 and 0.5 wppm, respectively. These facts suggest that the leaching of Ni is not the reason for the decrease of the catalytic activity. It can be attributed to the fact that

**Table 3** Kinetic results for APR of 5 wt% ethylene glycol on the Raney Ni and NP Ni catalysts at 498 K, 2.58 MPa, WHSV of 3.61 h<sup>-1</sup>, and after 6 h on stream

Catalyst	Conv. of EG to gas (%)	Production rate (μmol min <sup>-1</sup> g <sub>Ni</sub> <sup>-1</sup> )/TOF (min <sup>-1</sup> )					Selectivity (%)	
		CO	CO <sub>2</sub>	H <sub>2</sub>	CH <sub>4</sub>	Alkane C	H <sub>2</sub>	Alkane
Raney Ni	5.4	2.3/0.0056	68.4/0.17	151.8/0.37	30.7/0.075	34.8/0.085	58	33
NP Ni	8.2	0.9/0.0008	108.8/0.095	249.5/0.22	43.4/0.038	49.2/0.043	63	31

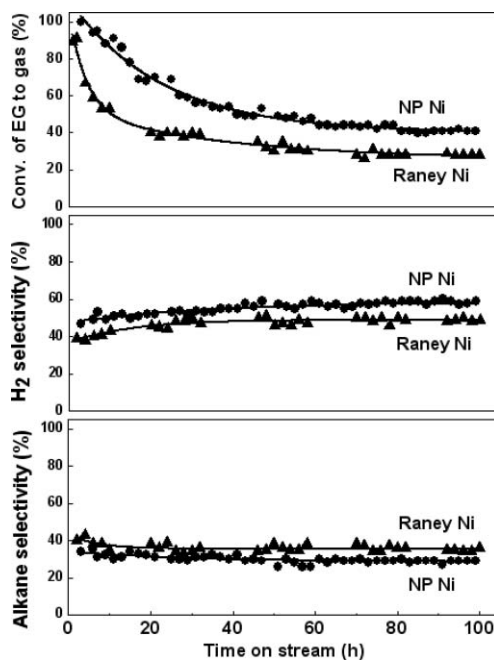


**Fig. 3** The catalytic performance of the Raney Ni and NP Ni catalysts during 100 h on stream in APR of 5 wt% ethylene glycol at 498 K, 2.58 MPa, and WHSV of 0.36 h<sup>-1</sup>.

no acidic products such as acetic acid were formed during the APR process (Table 2). In contrast, the BET surface areas and active surface areas decreased drastically, with the decrement being more drastic for Raney Ni. After reaction, both the BET surface area and the active surface area of NP Ni were larger than those of Raney Ni, which can be related to the better catalytic performance of NP Ni after 100 h on stream in APR of ethylene glycol.

XRD patterns of the Raney Ni and NP Ni catalysts after 100 h on stream are illustrated in Fig. 4. After reaction, the diffraction peaks due to fcc Ni were intensified and sharpened for both catalysts. Based on the Scherrer equation and the Ni (111) diffraction peak, it is calculated that the Ni crystallite size of Raney Ni increased from 5 to 23 nm after reaction, while that of NP Ni increased from 4 to 16 nm, as tabulated in Table 1. On the other hand, after reaction diffractions of gibbsite and bayerite originally on the as-prepared NP Ni catalyst were replaced by diffractions of boehmite (JCPDS 21-1307), indicating that Al(OH)<sub>3</sub> has undergone partial dehydration under the reaction condition of APR. It has been reported that the well-crystallized boehmite is readily synthesized from hydrated alumina by hydrothermal transformation at temperature above 423 K.<sup>24-26</sup> A close inspection of the diffractogram of Raney Ni after reaction can also find the weak diffraction peaks of boehmite at 2θ of

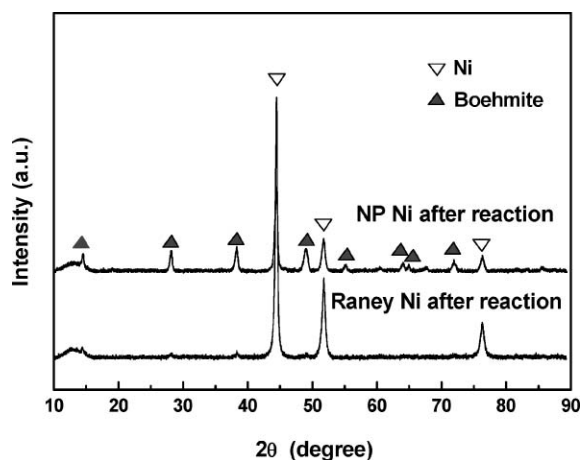


**Fig. 4** XRD patterns of the Raney Ni and NP Ni catalysts after 100 h on stream in APR of 5 wt% ethylene glycol at 498 K, 2.58 MPa, and WHSV of 0.36 h<sup>-1</sup>.

14.5, 28.2, 38.3, and 48.9°, concurrent with the much lower content of Al in Raney Ni.

The formation of boehmite is directly visualized in Figs. 2e and 2f. After 100 h on stream, the prismatic-shaped gibbsite and the spiral-shaped bayerite were diminished, instead, Al-rich flakes (verified by EDX) perpendicular to the catalyst surface were predominant on Raney Ni and NP Ni. The dimension of the boehmite flakes on NP Ni was about 500 nm, while boehmite flakes on Raney Ni were not as well developed, giving particle size of only about 200 nm, consistent again with the much lower content of Al in Raney Ni.

The Ni 2p and Al 2p/Ni 3p XPS spectra of the Raney Ni and NP Ni catalysts before and after 100 h on stream for APR of ethylene glycol are presented in Fig. 5. For the as-prepared Raney Ni and NP Ni catalysts, Ni is in the metallic state with the Ni 2p<sub>3/2</sub> BE of 852.7 eV.<sup>27</sup> After reaction, there is an additional peak at ~ 856.2 eV ascribable to Ni(OH)<sub>2</sub>.<sup>9</sup> For the as-prepared Raney Ni, the Al 2p/Ni 3p XPS spectrum

shows two peaks at BEs of 74.4 and 66.9 eV. It is known that the Al 2p BEs of gibbsite and bayerite are 74.0 and 74.2 eV, respectively, and the Ni 3p BE of metallic Ni is 67 eV.<sup>27</sup> Combining with the XRD and SEM results, these XPS peaks are assigned to Al(OH)<sub>3</sub> and metallic Ni, respectively. In accordance with the bulk composition of Raney Ni, the Ni 3p peak is much stronger than the Al 2p peak. After reaction, the intensity ratio was reversed, and the Al 2p peak shifted to 75.6 eV. Such a high Al 2p BE is unexpected for boehmite or other aluminum oxides, since they usually locate at around 74 eV.<sup>27</sup> We tentatively attribute it to the surface segregation of boehmite which weakened the interaction between boehmite and metallic Ni, resulting in differential charging on the insulating boehmite.

For the NP Ni catalyst, the Al 2p/Ni 3p XPS spectra are identical in peak position before and after reaction. In addition, the Al 2p peak has already been stronger than the Ni 3p peak before reaction, as less Al was leached away from the catalyst. Further intensification of the Al 2p peak relative to the Ni 3p peak occurred after reaction due to the surface segregation of boehmite. The surface compositions of the Raney Ni and NP Ni catalysts before and after reaction were calculated from the intensities of the Ni 3p and Al 2p peaks having similar probing depths and are also included in Table 1.

#### 4. Discussion

XRD, SEM and XPS characterizations disclose that the as-prepared NP Ni catalyst is composed of metallic Ni and a large amount of Al(OH)<sub>3</sub>, *i.e.* gibbsite and bayerite, which can be looked as a Ni–Al(OH)<sub>3</sub> composite catalyst. Although the Raney Ni and NP Ni catalysts are prepared from the same Ni<sub>50</sub>Al<sub>50</sub> alloy and have similar Ni crystallite size, the active surface area of the NP Ni catalyst is larger than that of Raney Ni, suggesting that the presence of gibbsite and bayerite can effectively retard the further agglomeration of Ni crystallites. The larger active surface area of the NP Ni catalyst can account for the higher activities than Raney Ni in previous work<sup>13</sup> and in APR of ethylene glycol

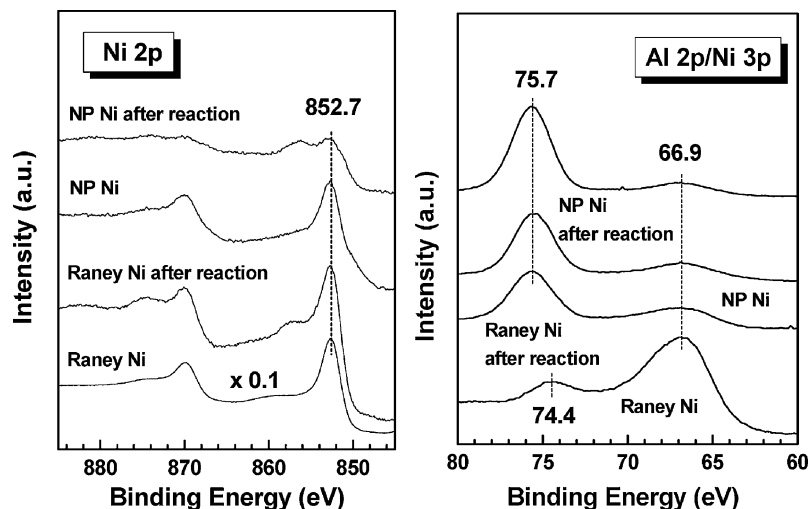


**Fig. 5** Ni 2p and Al 2p/Ni 3p XPS spectra of the Raney Ni and NP Ni catalysts before and after 100 h on stream in APR of 5 wt% ethylene glycol at 498 K, 2.58 MPa, and WHSV of 0.36 h<sup>-1</sup>.



(Tables 2 and 3). Table 3 shows that the conversion of ethylene glycol to gas products is *ca.* 52% higher on NP Ni than on Raney Ni, and the productivities of H<sub>2</sub> and alkanes increase to 249.5 and 49.2  $\mu\text{mol min}^{-1} \text{g}_{\text{Ni}}^{-1}$ , respectively, by using the NP Ni catalyst prepared by the new method. However, the difference in the reforming activity is not as large as that exhibited by the difference in their active surface areas. According to the turnover frequencies (TOFs) listed in Table 3, it turns out that the TOFs on the NP Ni catalyst are smaller than those of the Raney Ni catalyst. Nonetheless, since the nature of the active sites on these two catalysts is unclear, it must be cautioned that overinterpretation of the TOFs may be misleading.<sup>28</sup> Besides, for the NP Ni catalyst, the possibility that some active sites are only accessible by small H<sub>2</sub> molecules rather than bulkier molecules involving in APR of ethylene glycol due to the blockage of hydrated alumina can not be excluded, which will also result in the apparently smaller TOFs.

The new catalyst preparation method can not only improve the reforming activity of the Ni catalyst prepared from the Ni–Al alloy, but also impact on selectivities toward H<sub>2</sub> and alkanes in APR of ethylene glycol. Kinetic data in Table 3 show that on NP Ni the H<sub>2</sub> selectivity is 63%, while it is 58% on Raney Ni, which is in agreement with the results at high conversions (Table 2). Unlike the modification effect of tin on skeletal Ni catalysts which improves the H<sub>2</sub> selectivity with the sacrifice of the reforming activity,<sup>10,11</sup> Table 3 demonstrates an alternative way to improve the H<sub>2</sub> selectivity and the reforming activity concomitantly. Table 3 further reveals that as compared to Raney Ni, the NP Ni catalyst simultaneously accelerates the WGS reaction and the methanation/F-T reaction, with the WGS reaction being enhanced more remarkably than the methanation/F-T reaction.

Moreover, the new catalyst preparation method shows a positive effect on the stability of the Ni catalyst prepared from the Ni–Al alloy. During the stability test, the reforming activity of the Raney Ni catalyst decreased faster than that of the NP Ni catalyst. After 100 h on stream, the Raney Ni and NP Ni catalysts retained 33% and 42% of their initial activities, respectively. Characterizations of the Raney Ni and NP Ni catalysts after 100 h on stream reveal the phase transformation of gibbsite and bayerite to boehmite. Moreover, the growth of the Ni crystallites, the surface segregation of boehmite, and the oxidation of a portion of Ni to Ni(OH)<sub>2</sub> are observed for both catalysts, which are responsible for their activity loss during the APR process. Nonetheless, it seems that such changes are self-constrained, since after *ca.* 80 h on stream the reforming activities are stabilized. It has been reported that the Ni/Al<sub>2</sub>O<sub>3</sub> catalyst prepared by the impregnation method lost  $\sim$  90% of its initial activity over 48 h on stream at 498 K,<sup>9</sup> suggesting a better stabilizing effect of boehmite on Ni crystallites for the NP Ni catalyst prepared by the new method. After reaction, the smaller crystallite size and the larger active surface area than those of Raney Ni evidence the strong interaction between boehmite and Ni crystallites in NP Ni, thus leading to the better activity and stability of the NP Ni catalyst in APR of ethylene glycol.

In a separate experiment, we intentionally treated the as-prepared NP Ni catalyst in a Teflon-lined autoclave at 453 K for 18 h, then used it in APR of ethylene glycol. It is found

that the hydrothermally treated NP Ni catalyst exhibited similar catalytic performance to the NP Ni catalyst after 80 h on stream, suggesting that the evolutions of the reforming activity and selectivities toward H<sub>2</sub> and alkanes during the stability test can be mainly attributed to the occurrence of the hydrothermal process under the APR condition.

The NP Ni catalyst always exhibits higher H<sub>2</sub> selectivities than Raney Ni in both the kinetics and stability tests, signifying that the WGS reaction is more favored on the NP Ni catalyst. According to Shabaker *et al.*,<sup>16</sup> the ratios of the partial pressures  $Q_P$  ( $Q_P = P_{\text{CO}_2}P_{\text{H}_2}/P_{\text{CO}}$ ) at APR conditions indicated in Table 3 are calculated, and the quotient  $Q_P/K_{\text{WGS}}$  ( $K_{\text{WGS}} = P_{\text{CO}_2}P_{\text{H}_2}/P_{\text{CO}}a_{\text{H}_2\text{O}}$ ) denoting the extent of the WGS reaction is determined to be  $\sim$  0.004 and 0.017 for Raney Ni and NP Ni, respectively. The small  $Q_P/K_{\text{WGS}}$  ratios show that the WGS reaction on both catalysts is far from equilibrium, however, it is evident that the extent of the WGS reaction is enhanced when using NP Ni as the catalyst. Although the mechanism of the WGS reaction on Ni is rarely addressed experimentally or theoretically, it is known that Ni represents a borderline case in the periodic table between elements which clearly dissociate H<sub>2</sub>O and those for which only molecular adsorption has been observed.<sup>29</sup> Moreover, the co-adsorbed CO readily induces the breaking of the adsorbed OH group on the Ni(110) surface to oxygen atom which can further combine with CO to form CO<sub>2</sub>.<sup>30</sup> Thus it is rational to assume that on Ni the dissociation of H<sub>2</sub>O to surface OH group is the rate-determining step for the WGS reaction, just like the case on Cu single crystals.<sup>31</sup> The assumption is consistent with the observation by Grenoble *et al.* that the CO order is near zero and the H<sub>2</sub>O order is near 0.5 when using a 5 wt% Ni/ $\gamma$ -Al<sub>2</sub>O<sub>3</sub> catalyst in the WGS reaction.<sup>8</sup> They suggested that H<sub>2</sub>O is activated by the support, thus the supported catalyst is a bi-functional system in the WGS reaction. The similar bi-functional mechanism may also operate on the present NP Ni catalyst constituted by metallic Ni and hydrated alumina, thus justifying its higher WGS activity and lower concentration of CO in the product gas than the Raney Ni catalyst containing much less hydrated alumina.

## 5. Conclusions

The NP Ni catalyst is superior to the Raney Ni catalyst in APR of ethylene glycol to H<sub>2</sub> and alkanes. Under identical reaction conditions, the NP Ni catalyst is *ca.* 40–52% more active in terms of the conversion of ethylene glycol to gas products and *ca.* 9–24% more selective toward H<sub>2</sub> than the Raney Ni catalyst. The stabilizing effect of the hydrated alumina on Ni crystallites is suggested to be responsible for the higher activity and better stability of the NP Ni catalyst. The higher H<sub>2</sub> selectivity and the lower CO concentration in the product gas on the NP Ni catalyst are also attributed to the presence of more hydrated alumina which promotes the dissociation of water and consequently the WGS reaction. Considering the environmentally friendly preparation method, the improved operation safety, the higher activity, and the better stability, the NP Ni catalyst can be a promising candidate for APR of ethylene glycol to H<sub>2</sub> and light alkanes or a starting material to be formulated to a H<sub>2</sub>-specific catalyst by proper modification while still maintaining considerable reforming activity.

## Acknowledgements

This work was supported by the National Basic Research Program of China (2006CB202502), Shanghai Science and Technology Committee (06JC14009), the Fok Ying Tong Education Foundation (104022), the NSF of China (20673025), and State Key Laboratory of Catalytic Material and Reaction Engineering (RIPP, SINOPEC).

## Notes and references

- R. D. Cortright, R. R. Davda and J. A. Dumesic, *Nature*, 2002, **418**, 964.
- G. W. Huber, J. W. Shabaker and J. A. Dumesic, *Science*, 2003, **300**, 2075.
- G. W. Huber, R. D. Cortright and J. A. Dumesic, *Angew. Chem. Int. Ed.*, 2004, **43**, 1549.
- R. R. Davda, J. W. Shabaker, G. W. Huber, R. D. Cortright and J. A. Dumesic, *Appl. Catal. B*, 2003, **43**, 13.
- H. Gunardson, *Industrial Gases in Petrochemical Processing*, Marcel Dekker, New York, 1998.
- J. H. Sinfelt, *Adv. Catal.*, 1973, **23**, 91.
- M. A. Vannice, *J. Catal.*, 1977, **50**, 228.
- D. C. Grenoble, M. M. Estadt and D. F. Ollis, *J. Catal.*, 1981, **67**, 90.
- J. W. Shabaker, D. A. Simonetti, R. D. Cortright and J. A. Dumesic, *J. Catal.*, 2005, **231**, 67.
- J. W. Shabaker, G. W. Huber and J. A. Dumesic, *J. Catal.*, 2004, **222**, 180.
- J. W. Shabaker and J. A. Dumesic, *Ind. Eng. Chem. Res.*, 2004, **43**, 3105.
- J. W. Shabaker, *Ph. D. Dissertation*, University of Wisconsin-Madison, 2004.
- J. Petró, A. Bóta, K. László, H. Beyer, E. Kálmán and I. Dódon, *Appl. Catal. A*, 2000, **190**, 73.
- A. Bóta, G. Goerigk, T. Drucker, H. G. Haubold and J. Petró, *J. Catal.*, 2002, **205**, 354.
- C. H. Bartholomew and R. B. Pannell, *J. Catal.*, 1980, **65**, 390.
- J. W. Shabaker, R. R. Davda, G. W. Huber, R. D. Cortright and J. A. Dumesic, *J. Catal.*, 2003, **215**, 344.
- J. Freil, W. J. M. Pieters and R. B. Anderson, *J. Catal.*, 1969, **14**, 247.
- H. R. Hu, M. H. Qiao, Y. Pei, K. N. Fan, H. X. Li, B. N. Zong and X. X. Zhang, *J. Catal.*, 2004, **221**, 612.
- C. Sweegers, H. C. de Coninck, H. Meekes, W. J. P. van Enckevort, I. D. K. Hiralal and A. Rijkeboer, *J. Cryst. Growth*, 2001, **233**, 567.
- G. Lefevre and M. Fedoroff, *Mater. Lett.*, 2002, **56**, 978.
- B. W. Hoffer, E. Crezee, F. Devred, P. R. M. Mooijman, W. G. Sloof, P. J. Kooyman, A. D. van Langeveld, F. Kapteijn and J. A. Moulijn, *Appl. Catal. A*, 2003, **253**, 437.
- R. A. Lemons, *J. Power Sources*, 1990, **29**, 251.
- F. Z. Xie, X. W. Chu, H. R. Hu, M. H. Qiao, S. R. Yan, Y. L. Zhu, H. Y. He, K. N. Fan, H. X. Li, B. N. Zong and X. X. Zhang, *J. Catal.*, 2006, **241**, 211.
- S. Music, D. Dragevic and S. Popovic, *Mater. Lett.*, 1999, **40**, 269.
- K. M. S. Khalil, *J. Catal.*, 1998, **178**, 198.
- T. Tsuchida, *J. Eur. Ceram. Soc.*, 2000, **20**, 1759.
- J. F. Moulder, W. F. Stickle, P. E. Sobol, and K. D. Bomben, *Handbook of X-ray Photoelectron Spectroscopy*, J. Chastain, (Ed.), Perkin-Elmer, Eden Prairie, MN, 1992.
- M. Boudart, *Chem. Rev.*, 1995, **95**, 661.
- P. A. Thiel and T. E. Madey, *Surf. Sci. Rep.*, 1987, **7**, 211.
- T. Yuzawa, T. Higashi, J. Kubota, J. N. Kondo, K. Domen and C. Hirose, *Surf. Sci.*, 1995, **325**, 223.
- G. C. Wang, L. Jiang, Z. S. Cai, Y. M. Pan, X. Z. Zhao, W. Huang, K. C. Xie, Y. W. Li, Y. H. Sun and B. Zhong, *J. Phys. Chem. B*, 2003, **107**, 557.

# Variables affecting homogeneous acid catalyst recoverability and reuse after esterification of concentrated omega-9 polyunsaturated fatty acids in vegetable oil triglycerides

Matthew B. Boucher,<sup>a</sup> Steven A. Unker,<sup>a</sup> Kyle R. Hawley,<sup>a</sup> Benjamin A. Wilhite,<sup>a</sup> James D. Stuart<sup>b</sup> and Richard S. Parnas<sup>\*a,c</sup>

Received 17th June 2008, Accepted 7th October 2008

First published as an Advance Article on the web 4th November 2008

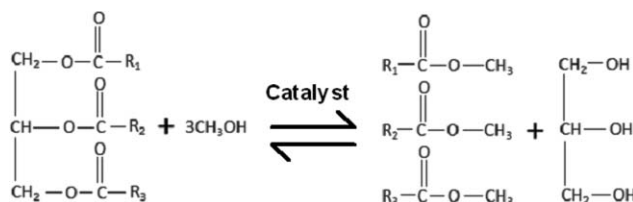
DOI: 10.1039/b810225b

Global concerns regarding greenhouse gas emissions combined with soaring oil prices have driven the search for renewable diesel fuels derived from either virgin or waste vegetable oils, dubbed “bio-diesels”. A key challenge in the emerging bio-diesel industry is cost-effective pre-treatment of waste vegetable oils to reduce free-fatty acid content prior to transesterification. This article reports, for the first time, recoverability and reusability of hydrochloric and sulfuric acid catalysts for efficient pre-treatment of waste cooking oils for subsequent conversion to bio-diesels. Esterification of omega-9 polyunsaturated fatty acids, particularly 18:2,18:3 linoleic acid with methanol and a homogenous acid catalyst was investigated over a range of fatty acid concentrations. It was determined that greater than 95% by weight of each catalyst was recovered after esterification under all conditions investigated. When recovered methanol was used, containing recovered catalyst and water, it was determined that hydrochloric acid catalyzed esterification exhibits a higher tolerance to water accumulation. After sulfuric acid was recovered and re-used, the observed rate constant decreased more than 50% to a value comparable to that observed for hydrochloric acid at more than three times the water concentration.

## Introduction

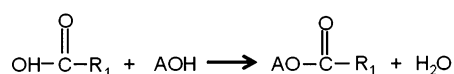
Biomass-derived diesel fuels, termed bio-diesels, can replace petroleum-based diesel fuels with minimum modifications to existing diesel engines, oil heating systems and fuels infrastructure. Biodiesel is non-toxic and biodegradable resulting in less harmful emissions.<sup>1–8</sup> Biodiesel is currently produced *via* transesterification of triglycerides (TG) with an alcohol, preferably methanol due to its favorable kinetics.<sup>9,10</sup> The global transesterification mechanism of TG encompasses three sequential reversible reactions wherein triglycerides (TG) react to form diglycerides (DG), monoglycerides (MG) and final product glycerol (G); the overall reaction is presented in Scheme 1 below.

The source of triglycerides for biodiesel production can range from virgin vegetable oils to waste cooking oils, animal fats, and soapstocks.<sup>9–14</sup> Due to high prices of virgin vegetable oils there is an interest in diversifying feedstock for biodiesel production. Waste cooking oils and animal fats can be used to produce biodiesel; however, they can contain a considerable amount of free fatty acid (FFA).<sup>9–14</sup> The chemical structure of FFA is simply a hydrocarbon chain (C14–C22, 1–3 double bonds),



Scheme 1 Transesterification.

extending from the carboxylic acid group. In base catalyzed transesterification of vegetable oils, FFA will react with the base catalyst *via* reaction shown in Scheme 2 to form soap. Soap formation can cause considerable loss in yield during biodiesel purification steps by emulsion.<sup>15–17</sup>



Scheme 2 Soap formation.

Additionally, the acid value or acid content of biodiesel must meet specifications denoted by ASTM method 644–04 in order to be considered ASTM quality. Any considerable amount of FFA will prevent biodiesel from meeting ASTM standards.<sup>18</sup>

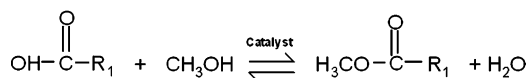
In the interest of producing biodiesel, free fatty acids can be removed from waste cooking oils and animal fats *via* esterification with methanol and catalyst shown in Scheme 3.

Both homogeneous and heterogeneous catalysts have been used for esterification of free fatty acids.<sup>19–23</sup> Homogeneous acids

<sup>a</sup>Department of Chemical Materials and Biomolecular Engineering, University of Connecticut, 97 N. Eagleville Rd., Storrs, CT, 06269-3136, USA. E-mail: rparnas@ims.uconn.edu; Fax: +1 (860)-486-2959; Tel: +1 (860)-486-9060

<sup>b</sup>Department of Chemistry, University of Connecticut, 55 N. Eagleville Rd., Storrs, CT, 06269-3060, USA

<sup>c</sup>Institute of Materials Science, University of Connecticut, 97 N. Eagleville Rd., Storrs, CT, 06269-3136, USA



Scheme 3 Esterification.

such as sulfuric acid, hydrochloric acid, nitric acid, and several others can be used to catalyze esterification.<sup>19,20,24</sup>

When using a homogenous acid catalyst for the esterification of FFA in the presence of triglycerides, the catalyst can be recovered in the methanol layer and re-used. Several variables, however, may affect the recoverability and re-use of the catalyst. For example, if transesterification of triglycerides takes place simultaneously during esterification of FFA, a glycerol layer can form and may result in the loss of the acid catalyst. A study by Goff *et al.*<sup>24</sup> reported acid catalyzed transesterification when sulfuric acid was used as a catalyst, however when other acids were used a glycerol layer was not formed; there was no report, however, of how much catalyst was recovered.

In previous reports, the important engineering questions of catalyst recoverability and reusability were not adequately addressed. Most critically, the presence of water, which is a product of esterification, can have an effect on catalyst activity and reaction equilibrium for future use. There have been several studies which note the effect of water on transesterification of vegetable oils;<sup>24–30</sup> however, there is limited data for effect of water on acid catalyzed esterification of FFA's with methanol in the presence of vegetable oil triglycerides. Liu *et al.*<sup>25</sup> investigated the effect of water on sulfuric acid catalyzed esterification of acetic acid. Liu *et al.* report that there is a decrease in initial reaction kinetics with an increase in initial water concentration, and that the loss in strength of catalytic protons is due to water solvation.

The present study compares sulfuric acid and hydrochloric acid as catalysts for the esterification of linoleic acid with methanol in the presence of soybean oil triglycerides. Catalyst recoverability after esterification was investigated at several different initial concentrations of linoleic acid in soybean oil. The effect of water, as a product of esterification, was investigated by re-using the recovered methanol layer for esterification of linoleic acid in the presence of soybean oil. The affect of accumulating water in the methanol layer was further investigated by repeating experiments and changing initial water concentrations.

## Experimental

Temperature was held constant at 70 °C for all experiments. Linoleic acid concentrations ranged from 2–15 wt% of the initial soybean oil-fatty acid mixture. Acid catalyst concentration was held constant at 1 wt% of soybean oil triglycerides, and initial methanol concentration was approximately a 6:1 molar ratio with respect to soybean triglycerides. Table 1 provides the six formulations used, where 400 g of soy oil were used in each case.

Reactions were carried out in a 1 L three-neck round bottom flask with a water-cooled reflux condenser to minimize methanol losses. The flask was submerged in a water bath placed on a temperature-controlled magnetic stirring hotplate (Fisher Scientific). The reaction temperature was monitored by thermocouple as well as mercury thermometer, and held within  $\pm 1$  °C. Agitation was provided by a magnetic stirrer (1.5 in.  $\times$

Table 1 Initial conditions of six experimental formulations

Experiment #	Acid Catalyst	Vol. of Acid soln. (mL)	Wt. Linoleic Acid (g)
1	H <sub>2</sub> SO <sub>4</sub> (97%)	2.25	8.20
2	H <sub>2</sub> SO <sub>4</sub> (97%)	2.25	21.0
3	H <sub>2</sub> SO <sub>4</sub> (97%)	2.25	70.8
4	HCl (36%)	9.15	8.20
5	HCl (36%)	9.15	21.0
6	HCl (36%)	9.15	70.8

0.75 in. diameter) at 700 RPM. Experiment 5 was repeated at 800 rpm and the initial rate of disappearance of linoleic acid was compared to the same experiment conducted at 700 rpm to verify that the mixing was sufficient to prevent bulk mass transfer limitations.

Virgin soybean oil (400 grams of Whole Harvest's 100% Soy Product) was loaded into the reaction flask and heated to 70 °C. The desired amount of Linoleic acid (Acros Organics, 60%, Tech grade (32% Oleic acid, 8% saturated C:18 fatty acid)) was measured separately and added to the reaction flask. Methanol (111  $\pm$  0.5 mL of (99.9% HPLC grade, Fischer Scientific)) was measured into a separate 250 mL flask. The amount of added methanol was calculated to correspond exactly to a 6:1 molar ratio of Methanol:TG for the case of pure triolein (MW 885 g/mol). However, since the molecular weight of Soybean TG is typically reported in the range of 860 to 880 g/mol,<sup>30,31</sup> the actual molar ratio employed in all the experiments below is more accurately 5.95:1. The methanol:Linoleic acid molar ratios were 93.7, 36.6, and 10.86 for FFA levels of 2, 5, and 15 wt%, respectively. Concentrated acid catalyst solution was added to the 250 mL flask using a graduated pipette and mixed with the methanol. Both reagent grade hydrochloric acid (12 Molar- 36%) and sulfuric acid (18 Molar- 97%) were used as catalysts for each experiment. The acid solution volume was adjusted to add acid at 1 wt% of the Soybean TG, or 4  $\pm$  0.1 g.

Ten (10) mL samples were withdrawn periodically and immediately quenched in an ice bath for 5 minutes. Samples were then centrifuged (Thermo Electron Corp. model HN SII) at 4000 rpm for 2 minutes. After centrifugation the methanol layer was removed from the sample in a 250 mL separatory funnel and discarded. To remove any residual methanol and acid, the oil phase was washed with distilled water in a 250 mL separatory funnel by adding 50 mL of distilled (DI) water, shaking vigorously, and allowing to settle for 5 minutes. After settling the water layer was discarded and the sample was centrifuged again for 2 minutes at 4000 rpm to remove residual water.

The samples were prepared for gas chromatography following ASTM 6584-00 method for analysis of free and total glycerine content in biodiesel.<sup>32</sup> The derivatized solution was injected (1  $\mu$ l) into a Hewlett-Packard 5890 Series II Gas Chromatograph equipped with Quadrex Aluminum Clad column with 1 meter retention gap and employing a flame ionization detector to determine fatty acid methyl-ester, glycerol and glyceride (tri-, di-, mono-) concentrations. Computer-assisted analysis of resulting chromatograms was performed using Chem-Station software (Hewlett-Packard, now Agilent Technologies). Samples were also prepared for titration following ASTM method D664-00 for acid number of biodiesel samples.<sup>18</sup> After allowing the diluted



sample to mix for one minute, titrant was added drop by drop until the permanent light pink endpoint was reached.

### Recoverability experiments

Experiments 1–6 were repeated in order to investigate the recoverability of the unreacted methanol and acid catalyst. Recoverability experiments were conducted as described above but no samples were withdrawn. The reactants were mixed at 70 °C for the period of time required for the concentration of linoleic acid to reach approximately 0.2 wt%, with the time estimated from the results of experiments 1–6. After stopping agitation, the reaction flask was placed in an ice bath where the phases were allowed to separate for 2 hours. The oil phase was decanted using a 1 L separatory funnel. A sample of the oil phase was washed and prepared for titration as previously described.

The recovered methanol layer was decanted into a 100 mL graduated cylinder to measure its volume. The recovered methanol phase was prepared for titration as 10% (by volume) aqueous methanol solutions, where 10 mL of the recovered methanol layer was added to 90 mL of DI water in a 100 mL graduated cylinder. Titrant was made by dissolving 44 grams of potassium hydroxide pellets (87.9%, JT Baker) in 392 mL of DI water to make a 1.74 M KOH solution. Titrant was added drop by drop until the phenolphthalein endpoint was reached.

### Reusability experiments

For the initial condition of 5% linoleic acid (experiments 2 and 5), the recovered methanol layer containing the recovered acid catalyst and water, was re-used with a new mixture of 5% linoleic acid in 400 g of soybean oil triglycerides. Due to loss of methanol by consumption, partitioning, and small amounts of evaporation, a small amount of fresh methanol was added to match the volume of methanol initially used, 111 mL. No water was removed from the recovered methanol. Samples were withdrawn periodically and treated as previously described.

To investigate multiple re-use of the methanol and acid where further accumulation of water in the methanol layer is expected, experiments 2 and 5 were also repeated adding different concentrations of DI water to the methanol and acid before the reaction. Samples were drawn periodically and treated as previously described.

## Results and discussion

In experiments 1–6, samples were monitored for FFA, bound glycerine (MG, DG, TG) and free glycerine (G). Fig. 1 shows a typical data set, specifically from experiment 2 at the initial condition of 5 wt% initial linoleic acid with sulfuric acid catalyst.

Reproducibility was verified by repeating several of the experiments, and the measured values of the chemical composition remained within 5% of initial measurements in all cases. As shown in Fig. 1, there was significant conversion of FFA to methyl ester. Transesterification of soybean triglycerides did not nearly reach completion; however, there was notable conversion of triglycerides to diglycerides and methyl ester. The majority of transesterification took place after esterification already had reached equilibrium. It was noted that conversion of TG → DG was less than 5% for all of experiments 1–6 before the

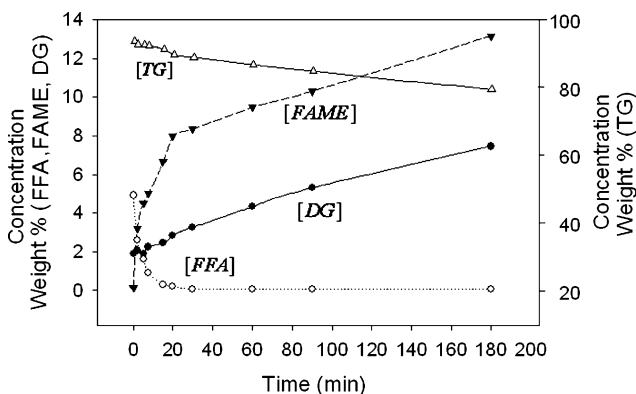


**Fig. 1** Representative data collection for experiment 2. Note that since negligible amounts of monoglyceride and glycerol were present, they do not appear in the figure. (○) Linoleic Acid [FFA]; (▲) Methyl ester [FAME]; (●) Diglyceride [DG]; (△) Triglyceride [TG].

concentration of FFA reached 0.2 wt%. Fig. 2(a) shows the concentration of linoleic acid with time, using H<sub>2</sub>SO<sub>4</sub> as the catalyst, at different initial concentrations of linoleic acid. Fig. 2(b) displays the equivalent plot using HCl as a catalyst.

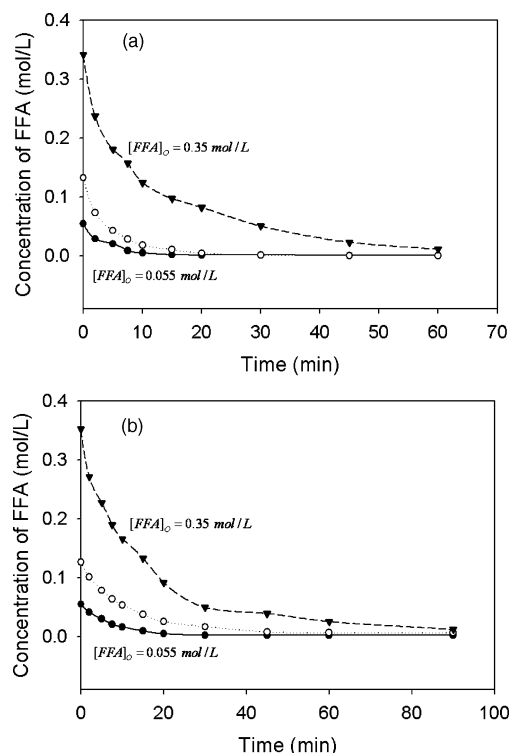


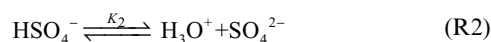
**Fig. 2** FFA concentration vs. time at different initial linoleic acid concentrations, (▲) [FFA]<sub>0</sub> = 0.35 mol/L; (○) [FFA]<sub>0</sub> = 0.13 mol/L; (●) [FFA]<sub>0</sub> = 0.055 mol/L. (a) Acid catalyst H<sub>2</sub>SO<sub>4</sub>. (b) Acid catalyst HCl.

### Catalyst recoverability

Recoverability of each acid was determined by repeating experiments 1–6, but withdrawing no samples. Experiments were allowed to run until the concentration of linoleic acid reached 0.2 wt% for experiments 1, 2, 4 and 5, and 0.5 wt% for experiments 3 and 6. After rapidly cooling the final reaction

mixture, it was allowed to separate for two hours, after which each phase was titrated as previously described. After settling, the observed phases were a methanol rich phase containing water and acid catalyst, and an oil rich phase. Slight differences were observed after decanting; a lighter yellow color was observed after esterification of 15 wt% FFA in Soybean Oil with H<sub>2</sub>SO<sub>4</sub>, and a darker orange after using HCl; also observed by Goff *et al.*<sup>24</sup> The dark orange color was not observed when initial FFA concentration was 5 wt% or less.

The concentration of sulfuric acid in the aqueous layer was calculated using an equation provided from a study conducted by Evans *et al.*<sup>33</sup> on the electrolytic dissociation of sulfuric acid in aqueous methanol. The dissociation of sulfuric acid in water (R1–R2) is shown below.



Evans and co-workers reported a strong effect on the dissociation constant of sulfuric acid in 10–20% aqueous methanol. The equation used to calculate the second dissociation constant ( $K_2$ ), as reported by Evans *et al.*<sup>33</sup> is shown below.

$$\text{p}K_2 = 1.669 + 0.0336m + 0.0126T \text{ (}^\circ\text{C)} \quad (1)$$

In equation (1),  $m$  is the volume% of methanol in the aqueous solution and  $T$  is the temperature of the solution during titration. It was assumed that the first dissociation for sulfuric acid is in effect infinity and goes to completion. The resulting mol balance for the titration is shown in equation (2) below.

$$n_{\text{OH}^-, \text{ added}} = (2n_{\text{SO}_4^{2-}} + n_{\text{HSO}_4^-})_{\text{in solution}} \quad (2)$$

In equation (2),  $n$  represents number of moles. The equilibrium equation for the second dissociation is shown below.

$$K_2 = \frac{[\text{H}_3\text{O}^+][\text{SO}_4^{2-}]}{[\text{HSO}_4^-]} \quad (3)$$

Between equations (2) and (3) there are two unknowns,  $[\text{HSO}_4^-]$  and  $[\text{SO}_4^{2-}]$  in the sample, which can be solved for using the system of two equations. Table 2 summarizes the results from the recoverability experiments.

In order to examine reusability of each catalyst, experiments 2 and 5 were repeated and the methanol layer was recovered after 2 hours of decanting. Methanol was added to the aqueous

layer in order to make up for methanol consumed by reaction and methanol lost by partitioning in the oil phase and small amounts of evaporation loss. It was assumed that all water produced by esterification ended up in the methanol layer. The methanol/acid/water mixture was then re-used to treat the same amount of linoleic acid as the first run (5 wt% linoleic acid in 400 g Soybean Oil). To investigate further accumulation of water in the methanol layer, experiments 2 and 5 were also repeated adding different concentrations of DI water to the methanol and acid before the reaction. Samples were drawn periodically and treated as previously described.

Fig. 3(a) displays the concentration of linoleic acid with time for esterification catalyzed by H<sub>2</sub>SO<sub>4</sub> for the initial run compared to its re-use and experiments with increased initial

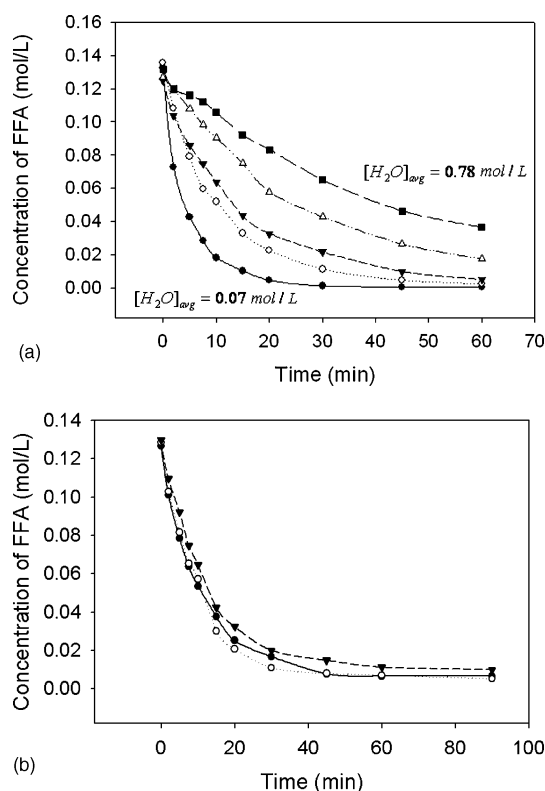


**Fig. 3** FFA concentration vs. time with  $[\text{FFA}]_0 = 0.13 \text{ mol/L}$  for various water concentrations. (a) Acid catalyst H<sub>2</sub>SO<sub>4</sub>: (●) Initial run  $[\text{H}_2\text{O}]_{\text{avg}} = 0.07 \text{ mol/L}$ ; (○) Re-use  $[\text{H}_2\text{O}]_{\text{avg}} = 0.20 \text{ mol/L}$ ; (▲)  $[\text{H}_2\text{O}]_{\text{avg}} = 0.33 \text{ mol/L}$ ; (△)  $[\text{H}_2\text{O}]_{\text{avg}} = 0.52 \text{ mol/L}$ ; (■)  $[\text{H}_2\text{O}]_{\text{avg}} = 0.78 \text{ mol/L}$ . (b): Acid catalyst HCl: (●) Initial run  $[\text{H}_2\text{O}]_{\text{avg}} = 0.60 \text{ mol/L}$ ; (○) Re-use  $[\text{H}_2\text{O}]_{\text{avg}} = 0.75 \text{ mol/L}$ ; (▲)  $[\text{H}_2\text{O}]_{\text{avg}} = 0.90 \text{ mol/L}$ .

**Table 2** Summary of recoverability experiment results

Catalyst	Initial FFA Concentration (mol/L)	Rxn Time (min)	%FFA Final	Catalyst Recovered (g)	Volume of Methanol Layer Recovered (mL)
H <sub>2</sub> SO <sub>4</sub> (97%)	0.055	10	0.18	3.92	82
H <sub>2</sub> SO <sub>4</sub> (97%) <sup>a</sup>	0.13	20	0.19 ± 0.05	3.86 ± 0.04	74 ± 1
H <sub>2</sub> SO <sub>4</sub> (97%)	0.35	60	0.48	3.75	66
HCl (36%)	0.055	20	0.19	3.96	93
HCl (36%) <sup>a</sup>	0.13	60	0.23 ± 0.04	3.97 ± 0.02	84 ± 1
HCl (36%)	0.35	90	0.53	3.86	81

<sup>a</sup> Results are an average of 3 repeated experiments.

water concentration; Fig. 3(b) is a similar plot for experiments where HCl was used for the catalyst. Because water is being continuously produced by esterification, water concentrations are denoted as average water concentration throughout the experiment.

The effect of water, accumulated in the methanol phase during esterification, on the re-use of the catalyst and methanol was determined by comparing the observed rate constant between runs. The rate expression employed was a second order, elementary, reversible relationship shown in equation (4).

$$r_{\text{FFA}} = \{k_{\text{FFA}}[\text{A}]\}[\text{FFA}][\text{MeOH}] - \{k_{\text{FFA}}^{-1}[\text{A}]\}[\text{FAME}][\text{H}_2\text{O}] \quad (4)$$

In equation (4), [A] is the concentration of the acid catalyst; because the catalyst is not consumed during the reaction [A] is a constant and can be combined with the rate constant  $k_{\text{FFA}}$ . Equation (4) can be written in terms of FFA conversion, where the equation for conversion is given below.

$$x = \frac{[\text{FFA}]_0 - [\text{FFA}]}{[\text{FFA}]_0} \quad (5)$$

Combining equations (4) and (5) the rate expression can be written in terms of FFA conversion. Due to a large molar excess of methanol, the concentration of methanol is assumed to be constant at its initial concentration. Reverse hydrolysis can be neglected, as suggested by Liu *et al.*,<sup>25</sup> yielding the rate expression below.

$$\frac{dx}{dt} = \{k_{\text{FFA}}[\text{A}]\} (1-x)(\mathcal{R}-x) \quad (6)$$

In equation (6)  $\mathcal{R}$  is the ratio of the initial methanol concentration to the initial FFA concentration, ( $[\text{MeOH}]_0/[\text{FFA}]_0$ ). Integrating equation (6) from  $t = 0$  to  $t$  and substituting  $k_{\text{FFA}}[\text{A}] = k_1$ , the following expression can be used to linearize initial FFA concentration data in order to yield a rate constant from the slope.

$$\ln\left(\frac{\mathcal{R}-x}{1-x}\right) - \ln(\mathcal{R}) = k_1[\text{FFA}]_0 t \quad (7)$$

Fig. 4(a) displays the linearization of the initial FFA conversion data when  $\text{H}_2\text{SO}_4$  was used for a catalyst and the initial concentration of FFA was 5 wt%; individual data sets are at different initial water concentrations. Fig. 4(b) shows the equivalent plot where HCl was used as the catalyst.

Using best fit slopes from Fig. 4(a) and (b), a rate constant was derived, and the effect of average water concentration on the observed rate constant was examined. Fig. 5 shows the affect of water concentration on the observed rate constant for both catalysts. Because HCl was purchased as a 36% aqueous solution, the first data point is at a relatively high water concentration of 0.60 mol/L.

The sensitivity of  $\text{H}_2\text{SO}_4$  to water displayed in Fig. 5 is in contrast to the lack of sensitivity noted by Kusdiana and Saka.<sup>34</sup> The differences in the results illustrated here compared to those previous results is easily explained because Kusdiana and Saka allowed their system 48 hours to react and measured total conversion rather than just conversion of free fatty acid. Perhaps they were observing equilibrium conversions rather than initial free fatty acid reaction rates as illustrated above.

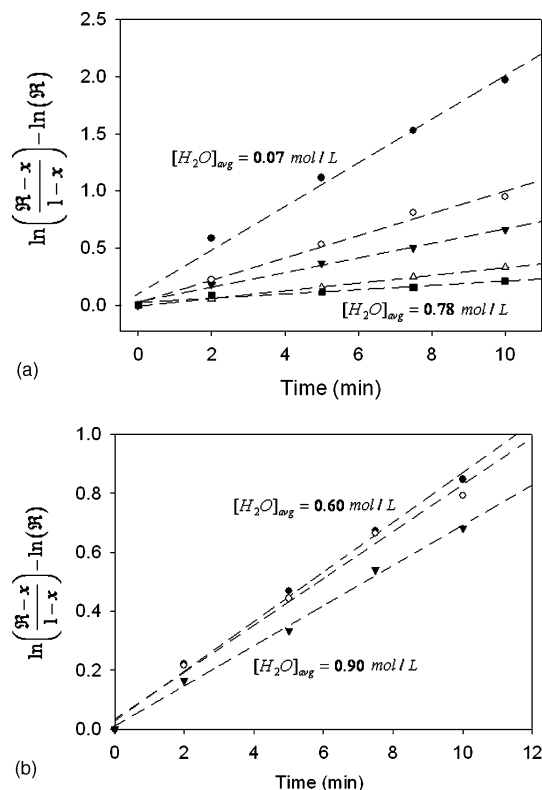


**Fig. 4** The initial rate of FFA consumption plotted according to equation (7) with  $[\text{FFA}]_0 = 0.13$  mol/L for various water concentrations. (a) Acid catalyst  $\text{H}_2\text{SO}_4$ : (●) Initial run  $[\text{H}_2\text{O}]_{\text{avg}} = 0.07$  mol/L; (○) Re-use  $[\text{H}_2\text{O}]_{\text{avg}} = 0.20$  mol/L; (▲)  $[\text{H}_2\text{O}]_{\text{avg}} = 0.33$  mol/L; (△)  $[\text{H}_2\text{O}]_{\text{avg}} = 0.52$  mol/L; (■)  $[\text{H}_2\text{O}]_{\text{avg}} = 0.78$  mol/L. (b) Acid catalyst HCl: (●) Initial run  $[\text{H}_2\text{O}]_{\text{avg}} = 0.60$  mol/L; (○) Re-use  $[\text{H}_2\text{O}]_{\text{avg}} = 0.75$  mol/L; (▲)  $[\text{H}_2\text{O}]_{\text{avg}} = 0.90$  mol/L.

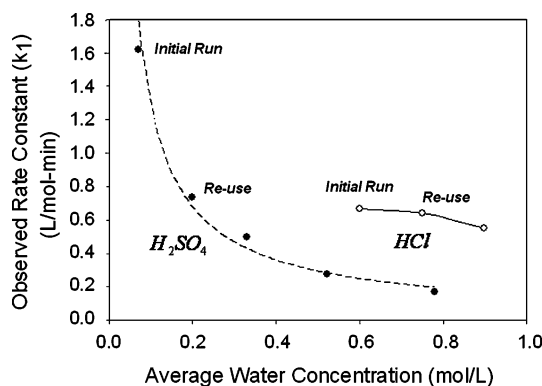


**Fig. 5** The esterification rate constant  $k_1$  vs. water concentration at 70 °C: (●)  $\text{H}_2\text{SO}_4$  (○) HCl.

The experiments above were conducted with HCl and  $\text{H}_2\text{SO}_4$  levels that range from 11 wt% to 50 wt% with respect to the FFA. Those levels, which correspond to 1 wt% with respect to the soybean triglycerides, are quite high for homogeneous catalysis of FFA. Note, however, that the chemical system of reactions is quite complex as the HCl and  $\text{H}_2\text{SO}_4$  slowly catalyze the transesterification of the triglycerides as well as more rapidly catalyze the esterification of the free fatty acids.

Several additional experiments were therefore conducted at lower HCl and  $\text{H}_2\text{SO}_4$  levels. Experiments 2 and 5 (Table 1)

contained 5 wt% FFA relative to triglycerides and 20 wt% acid catalyst relative to the FFA. Additional experiments were conducted with 5 wt% FFA and with acid catalyst levels of 2, 4, and 10 wt% with respect to FFA in order to verify that the results depicted above for FFA are not simply due to an overabundance of acid catalyst. Various amounts of water were added to the reaction mixtures for comparison with the results above.

Just as above, HCl activity was less sensitive to the water than H<sub>2</sub>SO<sub>4</sub> activity, but the formulations using low levels of catalyst converted FFA too slowly for industrial needs. For example, the mixture containing 2 wt% H<sub>2</sub>SO<sub>4</sub> (wrt FFA) and roughly 0.5 wt% water reduced the FFA from 5 wt% to 1.8 wt% after 90 minutes, whereas at 20 wt% H<sub>2</sub>SO<sub>4</sub> (wrt FFA) the FFA was reduced from 5 wt% to 1.8 wt% in less than 5 minutes. The mixture containing 2 wt% HCl and 0.5 wt% water reduced the FFA from 5 wt% to 1.8 wt% in roughly 30 minutes and to 0.3 wt% in 90 minutes, about 1/3 the conversion rate of the case with 20 wt% HCl.

A final comparison between HCl and H<sub>2</sub>SO<sub>4</sub> is worth noting in that an experiment was conducted where the number of moles of HCl and H<sub>2</sub>SO<sub>4</sub> was matched. At 4 wt% HCl and 10 wt% H<sub>2</sub>SO<sub>4</sub>, the number of moles is the same due to differences in molecular weight. Using a water content of approximately 2 wt%, the experiment with HCl reduced the FFA content from 5 wt% to roughly 2.2 wt% in 30 minutes, while the experiment with H<sub>2</sub>SO<sub>4</sub> reduced the FFA content from 5 wt% to roughly 2.9 wt% in 30 minutes. Thus, we observe that if significant levels of water reside in the mixture, HCl may be more effective than H<sub>2</sub>SO<sub>4</sub>, and high levels of acid may be used since recovery and recycle are quite straightforward.

## Conclusion

Increasing interest has been invested in renewable, environmentally benign alternative fuels due to greenhouse gas emissions and towering oil prices. Biodiesel is renewable, and an immediate replacement for petroleum diesel. A key challenge in economically efficient biodiesel production is the utilization of waste cooking oils and animal fats with high concentrations of free fatty acids. Homogenous acid catalysts have been employed for the esterification of FFA for treatment of waste oils, however in many cases they are not recovered and re-used.

In biodiesel production, it is important to limit waste streams and recover important reactants. After acid catalyzed esterification of free fatty acids in the presence of triglycerides, methanol can be recovered simply by phase separation. The re-use of catalyst can be limited by the formation of a glycerol layer and its tolerance to accumulating water produced by esterification in the methanol layer.

Within the range of conditions investigated in this study it was determined that transesterification is negligible when either sulfuric acid or hydrochloric acid are used to catalyze the esterification of polyunsaturated 18:2,18:3 linoleic acid in the presence of soybean oil triglycerides. Greater than 95% by weight of the catalyst was recovered in the methanol layer under all conditions investigated.

It was found that HCl exhibits a higher tolerance for accumulating water in the methanol layer. After H<sub>2</sub>SO<sub>4</sub> was

recovered and re-used, the observed rate constant decreased more than 50% to a value comparable to that observed for HCl at more than three times the water concentration.

## Notes and references

- 1 A. Boehman and R. McCormick, *Fuel Processing Technology*, 2007, **88**(7), 641–642.
- 2 J. Szybist, J. Song and M. Alam, *Fuel Processing Technology*, 2007, **88**(7), 679–691.
- 3 S. Koonin, *Science*, 2006, **311**(5760), 435–436.
- 4 J. Song, M. Alam and A. Boehman, *Combust. Sci. and Tech.*, 2007, **179**, 1991–2037.
- 5 Y. Zhang and A. Boehman, *Energy & Fuels*, 2007, **21**, 2003–2012.
- 6 K. Bullard, *National Biodiesel Conference and Expo, Fort Lauderdale*, 2005, available at: <http://www.nps.gov/renew/npsbiodiesel.htm>.
- 7 J. McDonald, B. Cantrell and W. Watts, *CIM Bulletin*, 1997, **90**(1015), 91–95.
- 8 C. Peterson, D. Reece and J. Thompson, *Biomass and Bioenergy*, 1996, **10**(5/6), 331–336.
- 9 T. Issariyakul, M. Kulkarni and A. Dalai, *Fuel Processing Technology*, 2007, **88**(5), 429–436.
- 10 K. Demirbas and S. Karlioglu, *Energy Sources, Part A: Recovery, Utilization, and Environmental Effects*, 2007, **29**(2), 133–141.
- 11 M. Canakci and H. Sanli, *Journal of Industrial Microbiology & Biotechnology*, 2008, **35**(5), 431–441.
- 12 B. Nas and A. Berkta, *Energy Sources, Part B: Economics, Planning and Policy*, 2007, **2**(1), 63–71.
- 13 M. Math and G. Irfan, *Journal of Scientific & Industrial Research*, 2007, **66**(9), 772–776.
- 14 M. Canakci and J. Van Gerpen, *Transactions of the ASAE*, 2001, **44**(6), 1429–1436.
- 15 P. Vasudevan and M. Briggs, *Journal of Industrial Microbiology & Biotechnology*, 2008, **35**(5), 421–430.
- 16 A. Abdullah, N. Razali and H. Mootabadi, *Environmental Research Letters*, 2007, **2**(3).
- 17 S. Mahajan, S. Konar and D. Boocock, *Journal of the American Oil Chemists' Society*, 2007, **84**(2), 189–195.
- 18 *Standard Test Method for Acid Number of Petroleum Products by Potentiometric Titration, D664-04*, ASTM International, West Conshohocken, PA, USA, 2004.
- 19 M. Berrios, J. Siles and M. Martin, *Fuel*, 2007, **86**, 2383–2388.
- 20 E. Sendzikiene, V. Makareviciene, P. Janulis and S. Kitrys, *Eur. J. Lipid Sci. Technol.*, 2004, **106**, 831–836.
- 21 R. Tesser, M. Di Serio and E. Santacesaria, *Ind. Eng. Chem. Res.*, 2005, **44**, 7978–7982.
- 22 J. Marchetti, V. Miguel and A. Errazu, *Fuel*, 2007, **86**, 906–910.
- 23 J. Ni and F. Meunier, *Applied Catalysis A: General*, 2007, **333**, 122–130.
- 24 M. Goff, N. Bauer and G. Suppes, *Journal of the American Oil Chemists' Society*, 2004, **81**(4).
- 25 Y. Liu, E. Lotero and J. Goodwin, *Journal of Molecular Catalysis A: Chemical*, 2006, **245**(1–2), 132–140.
- 26 M. Canakci and J. Gerpen, *Trans. ASAE*, 1999, **42**, 1203–1210.
- 27 B. Freedman, E. Pryde and T. Mounts, *J. Am. Oil Chem. Soc.*, 1984, **61**, 1638–1643.
- 28 F. Ma, L. Clements and M. Hanna, *Trans ASAE*, 1998, **41**, 1261–1264.
- 29 S. Romano, *Trans ASAE*, 1982, **4**, 106–116.
- 30 E. Lotero, Y. Liu, D. Lopez, K. Suwannakarn, D. Bruce and J. Goodwin, *Ind. Eng. Chem. Res.*, 2005, **44**(14), 5353–5363.
- 31 C. Gonzalez, J. M. Resa, J. Lanz and M. Iglesias, *J. Food Eng.*, 2006, **77**, 152–161.
- 32 *Test Method for Determination of Free and Total Glycerin in B-100 Biodiesel Methyl Esters by Gas Chromatography, D6584-00*, ASTM International, West Conshohocken, PA, USA, 2000.
- 33 J. Evans and C. Monk, *Transactions of the Faraday Society*, 1953, **49**, 415–17.
- 34 D. Kusdiana and S. Saka, *Bioresource Technology*, 2004, **91**, 289–295.



# Synthesis of cyclic carbonates from epoxides and CO<sub>2</sub> catalyzed by potassium halide in the presence of $\beta$ -cyclodextrin

Jinliang Song, Zhaofu Zhang, Buxing Han,\* Suqin Hu, Wenjing Li and Ye Xie

Received 29th August 2008, Accepted 7th October 2008

First published as an Advance Article on the web 4th November 2008

DOI: 10.1039/b815105a

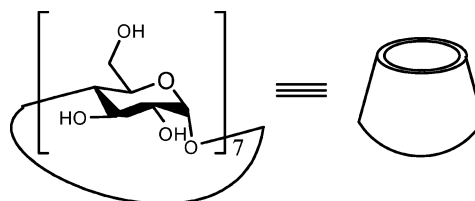
Development of efficient, cheap and non-toxic catalysts for cycloaddition of CO<sub>2</sub> with epoxides to produce five-membered cyclic carbonates under greener reaction conditions is still a very attractive topic. In this work, cycloaddition of CO<sub>2</sub> with propylene oxide (PO) to propylene carbonate (PC) catalyzed by potassium halide (KCl, KBr, and KI) in the presence of  $\beta$ -cyclodextrin was studied at various conditions. It was discovered that potassium halide and  $\beta$ -cyclodextrin ( $\beta$ -CD) showed excellent synergetic effect in promoting the reactions, and KI- $\beta$ -CD catalytic system was the most efficient among them. The optimal temperature for the reaction was around 120 °C, and the reaction rate reached maximum at about 6 MPa at this temperature. The reaction could be completed in 4 h with very high selectivity. The decrease of the yield of PC was not noticeable after KI- $\beta$ -CD was reused five times, indicating that the catalyst was very stable. KI- $\beta$ -CD catalytic system was also very active and selective for cycloaddition of CO<sub>2</sub> with other epoxides, such as glycidyl phenyl ether, epichlorohydrin, and styrene oxide. The mechanism for the synergetic effect is discussed.

## Introduction

Chemical conversion of carbon dioxide (CO<sub>2</sub>) into useful organic compounds has attracted much attention in recent years because CO<sub>2</sub> is an inexpensive, nontoxic, and abundant C<sub>1</sub> feedstock.<sup>1–3</sup> Cycloaddition of CO<sub>2</sub> with epoxides to produce five-membered cyclic carbonates is one of the most successful routes because cyclic carbonates can be used as aprotic polar solvents, precursors for producing polycarbonates, fine chemical ingredients, etc.<sup>4–8</sup> Numerous catalysts have been developed for the coupling reaction of CO<sub>2</sub> and epoxides, such as alkali metal salts,<sup>9–11</sup> metal oxides,<sup>12,13</sup> transition metal complexes,<sup>14–17</sup> Schiff base,<sup>18,19</sup> ion-exchange resins,<sup>20</sup> functional polymers,<sup>21,22</sup> quaternary ammonium and phosphonium salts,<sup>23–26</sup> ionic liquids,<sup>27,28</sup> lanthanide oxochloride,<sup>29,30</sup> gold nanoparticles supported on resins.<sup>31</sup> However, many of these catalyst systems suffer from low catalyst stability or reactivity, the need for cosolvent, extreme conditions.

Among the above catalysts, alkali metal salts are an important type of catalyst for the cycloaddition of CO<sub>2</sub> with epoxides.<sup>9–11</sup> Endo *et al.*<sup>10</sup> reported that alkali metal salts could be used as catalyst for the synthesis of cyclic carbonates using crown ether as co-catalyst. Although the reaction could be conducted at low temperature (100 °C) and low CO<sub>2</sub> pressure, organic solvent, N-methylpyrrolidinone (NMP), was used and crown ether was a toxic reagent. Recently, Huang *et al.*<sup>11</sup> described that alkali metal salts could catalyze cycloaddition of CO<sub>2</sub> with epoxides effectively in the presence of PPh<sub>3</sub> and phenol without solvents.

In recent years, using  $\beta$ -cyclodextrin ( $\beta$ -CD) as reaction catalyst has gained much interest.<sup>32,33</sup>  $\beta$ -CD, which is a cyclic oligosaccharide consisting of seven glucose units (Scheme 1), exerts a microenvironmental effect that can lead to selective reactions.  $\beta$ -CD catalyzes reactions by supermolecular catalysis through noncovalent bonding. Some catalytic reactions can be carried out in the presence of  $\beta$ -CD.<sup>34–42</sup> Surendra *et al.*<sup>43</sup> reported that  $\beta$ -CD and epoxides could form a cyclodextrin-epoxide complex through hydrogen bonding, which could activate the epoxides.



Scheme 1 General structure of  $\beta$ -cyclodextrin.

Development of efficient catalysts for cycloaddition of CO<sub>2</sub> with epoxides using cheap and non-toxic reagents and conducting the reactions under solvent-free conditions is still an attractive topic. In this work, we conducted the reactions using potassium halide as the catalysts in the presence of  $\beta$ -CD under solvent-free conditions, and discovered that the salts and  $\beta$ -CD showed excellent synergetic effect for the reactions. To our knowledge, this is the first work to combine these two kinds of compounds for the reactions. We believe that the simple, cheaper, and ecologically safer route to synthesize cyclic carbonates has great potential in industrial application.

Beijing National Laboratory for Molecular Sciences (BNLMS), Centre for Molecular Science, Institute of Chemistry, Chinese Academy of Sciences, Beijing, 100190, China. E-mail: hanbx@iccas.ac.cn; Fax: 86-10-62562821

**Table 1** Coupling of CO<sub>2</sub> and PO catalyzed by different catalysts<sup>a</sup>

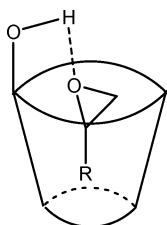
Entry	Catalyst	Yield (%) <sup>c</sup>
1	None	0
2 <sup>b</sup>	β-CD	0
3	KCl	0
4	KBr	3
5	KI	27
6 <sup>b</sup>	KCl + β-CD	4
7 <sup>b</sup>	KBr + β-CD	48
8 <sup>b</sup>	KI + β-CD	98

<sup>a</sup> Typical reaction conditions: a stainless reactor of 22 ml, 20 mmol PO with 2.5 mol% catalyst, CO<sub>2</sub> pressure 6 MPa, reaction temperature 120 °C, reaction time 4 h. <sup>b</sup> 0.1 g β-CD was added. <sup>c</sup> Yields were determined by GC *versus* an internal standard.

## Results and discussion

### Effect of catalysts

The activity of various catalysts was tested using the reaction of PO and CO<sub>2</sub> to produce propylene carbonate (PC), and the results are summarized in Table 1. No product was detected without catalyst or when β-CD only was used as the catalyst (entries 1, 2). Potassium halide could catalyze the cycloaddition alone, but the yield of PC was very low (entries 3–5). When β-CD was added, the yield of PC was enhanced (entries 6–8). It has been reported by Shi<sup>11</sup> that the epoxy ring can be activated through the forming of hydrogen bonding with phenol. In our system, hydrogen bonding exists between β-CD and epoxides<sup>43</sup> (Scheme 2), and this could be the reason that the yield of PC increased dramatically when β-CD was added. The order of the activity of potassium halide was found to be KI > KBr > KCl (entries 3–5, 6–8), which is consistent with the order of the nucleophilicity of the halide ions. Furthermore, the leaving ability of the halide anions is another important factor, which has great influence on the catalytic activity, and the activity increases with the leaving ability. The leaving ability of the halide anions is I<sup>-</sup> > Br<sup>-</sup> > Cl<sup>-</sup>, which is consistent with the order of the nucleophilicity of these anions.<sup>10,44</sup> Therefore, KI was selected as the catalyst to study the effect of reaction conditions on the reaction in the presence of β-CD.



**Scheme 2** Cyclodextrin-epoxide complex formed through hydrogen bonding.

### Effect of CO<sub>2</sub> pressure on the yield of PC

Fig. 1 shows the effect of CO<sub>2</sub> pressure on the yield of PC at 120 °C with a reaction time of 2 h. The yield of PC strongly depended on CO<sub>2</sub> pressure. The yield increased with increasing pressure in the low pressure range and reached a maximum

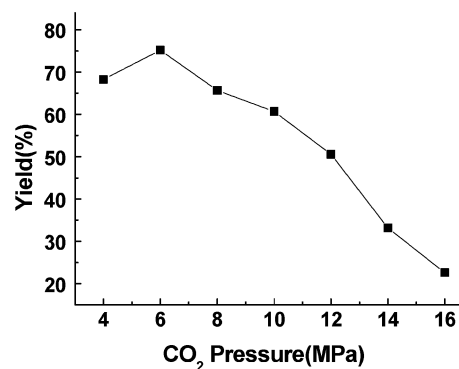


**Fig. 1** Effect of CO<sub>2</sub> pressure on PC yield. Reaction condition: 20 mmol PO with 2.5 mol% KI, 0.1 g β-CD, reaction temperature 120 °C, reaction time 2 h.

at about 6 MPa, and then decreased further with increasing pressure. In this work, it was observed that there were two phases in the reaction system by using a view cell reported previously.<sup>45</sup> The top phase was a CO<sub>2</sub>-rich phase and the bottom phase was a PO-rich phase. The concentration of the CO<sub>2</sub> in the bottom phase increased with increasing pressure, and this was the reason that the yield of PC increased with increasing pressure at low pressure. However, too high CO<sub>2</sub> pressure causes a low concentration of the epoxide in the vicinity of the catalyst, and may retard the interaction between epoxide and the catalyst,<sup>46</sup> resulting in a low yield of the product. Therefore, the optimized CO<sub>2</sub> pressure for our catalyst system was 6 MPa.

### Influence of reaction temperature on PC yield

Fig. 2 demonstrates the dependence of the yield of PC on temperature at CO<sub>2</sub> pressure of 6 MPa in the temperature range of 100–140 °C, and the reaction time was 4 h. It was shown that the activity of the catalyst was strongly affected by the reaction temperature. The yield of PC increased with increasing temperature, and reached 98% at 120 °C, then the PC yield kept almost constant with further increase of temperature, hinting that 120 °C is the optimal temperature for the reaction.

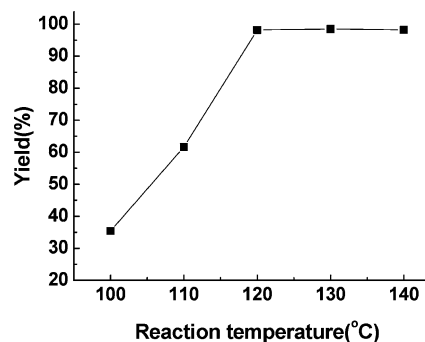


**Fig. 2** Influence of reaction temperature on PC yield. Reaction condition: 20 mmol PO with 2.5 mol% KI, 0.1 g β-CD, CO<sub>2</sub> pressure 6 MPa, reaction time 4 h.

### Influence of reaction time

The dependence of the yield of PC on reaction time is presented in Fig. 3. The reaction was performed in the presence of 2.5 mol%

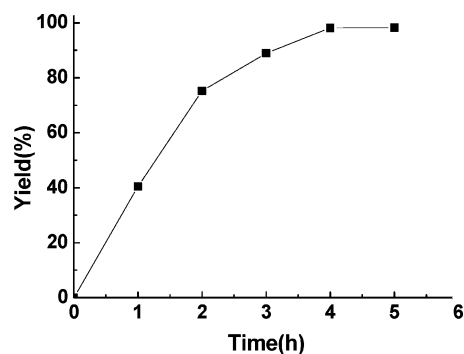


**Fig. 3** The dependence of PC yield on reaction time. Reaction conditions: 20 mmol PO with 2.5 mol% KI, 0.1 g  $\beta$ -CD, CO<sub>2</sub> pressure 6 MPa, reaction temperature 120 °C.

catalyst KI and 0.1 g  $\beta$ -CD at 120 °C under CO<sub>2</sub> pressure 6 MPa. In a relatively short reaction time, the conversion of PO was incomplete and the PC yield was low. It can be seen that a yield of 98% could be achieved at 4 h. No further increase in the yields of PC was observed with prolonged reaction time. Therefore, the reaction time of 4 h was suitable for this system.

#### Catalyst recyclability

The reusability of the catalyst was also examined using PO as the substrate at the optimized reaction conditions and the results are shown in Fig. 4. The decrease of the yield of PC was not considerable after reused five times, indicating that the catalyst was very stable.

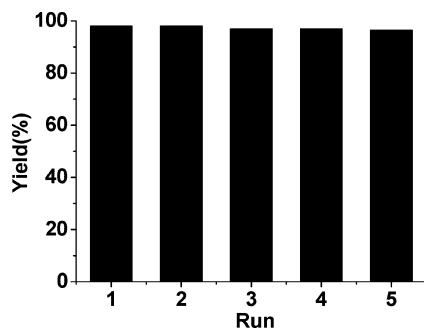


**Fig. 4** Reuse of the catalyst. Reaction condition: 20 mmol PO with 2.5 mol% KI, 0.1 g  $\beta$ -CD, CO<sub>2</sub> pressure 6 MPa, reaction temperature 120 °C, reaction time 4 h.

#### Various Substrates

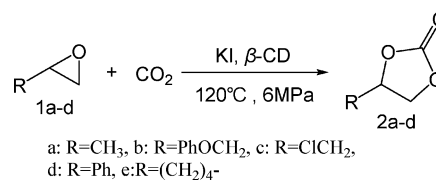
Using KI as the catalyst in the presence of  $\beta$ -CD, cycloaddition of CO<sub>2</sub> with other epoxides (Scheme 3) were also studied at 120 °C and 6 MPa without using any solvent and the results are summarized in Table 2. The catalyst system was found to be applicable to a variety of terminal epoxides, producing the corresponding cyclic carbonates with yields of 93–99%. Propylene oxide (**1a**, Table 1) and glycidyl phenyl ether (**1b**) gave cyclic carbonates in nearly 100% yield. Epichlorohydrin (**1c**) showed less activity and required a longer time (8 h) to give product **2c** in a high yield (93%), which may result from the reduced electron density of the epoxide oxygen atom caused by the electron-withdrawing CH<sub>2</sub>Cl group. A much longer reaction

**Table 2** Various carbonates synthesis catalyzed by KI in the presence of  $\beta$ -CD<sup>a</sup>

Entry	Epoxides	Products	Reaction time (h)	Yield (%)
1			4	99
2	<b>1b</b> 	<b>2b</b> 	8	93
3	<b>1c</b> 	<b>2c</b> 	12	94
4	<b>1d</b> 	<b>2d</b> 	24	< 3
	<b>1e</b> 	<b>2e</b> 		

<sup>a</sup> Reaction conditions: 20 mmol epoxide with 2.5 mol% KI, CO<sub>2</sub> pressure 6 MPa, reaction temperature 120 °C, 0.1 g  $\beta$ -CD.

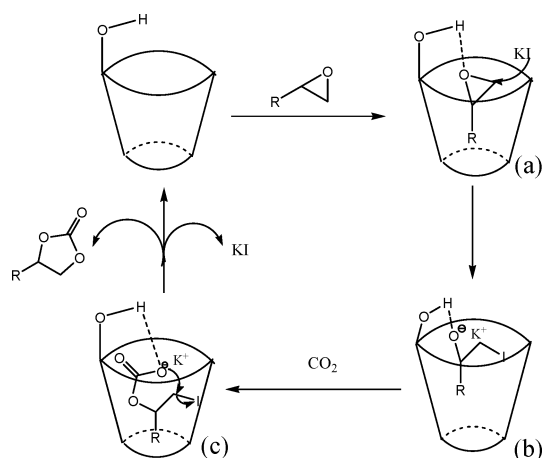
time (12 h) was needed to get a high product yield (94%) when styrene oxide (**1d**) was used as substrate, which is probably due to the low reactivity of its  $\beta$ -carbon center. When cyclohexene oxide (**1e**) was used as the reactant, the yield was very low even the reaction time was prolonged to 24 h. This may partially result from the weak interaction between cyclohexene oxide and  $\beta$ -CD due to the high steric hindrance of cyclohexene oxide and  $\beta$ -CD in our catalytic system. The low activity of cyclohexene oxide<sup>47</sup> also contributed the low yield.



**Scheme 3** Coupling of CO<sub>2</sub> with different epoxides.

#### Mechanism

It has been suggested by Huang and Shi<sup>11</sup> that hydrogen bonding can activate the ring-opening reaction of epoxides. In our catalyst system, there was a hydrogen bonding donor ( $\beta$ -CD). Based on the results discussed above, we propose a possible mechanism for the formation of cyclic carbonates, which is shown in Scheme 4. Firstly, the coordination of PO with  $\beta$ -CD through hydrogen bonding to form the cyclodextrin-epoxide complex (a in Scheme 4) and this step can activate the epoxy ring. Secondly, the I<sup>-</sup> anion of KI attacks the less hindered carbon atom of the activated ring, followed by ring opening reaction step (b in Scheme 4). Then, the interaction was occurred between the oxygen anion of the opened epoxy ring and CO<sub>2</sub> and this can form an alkylcarbonate anion (c in Scheme 4), which



**Scheme 4** The plausible reaction mechanism for the cycloaddition of CO<sub>2</sub> with epoxide catalyzed by KI and  $\beta$ -CD.

is stabilized *via* the hydrogen bonding. Finally, corresponding cyclic carbonates are achieved through the intramolecular cyclic step, and meanwhile, the catalyst is regenerated. From the discussion above, we think that the synergistic effect of iodide anion and  $\beta$ -CD may be the main reason for the high catalytic activity of the catalyst system.

## Conclusions

We found that cyclic carbonates can be formed in high yield from the reaction of epoxides with CO<sub>2</sub> in the presence of catalytic amounts of KI and  $\beta$ -CD without using any organic solvent. In the KI- $\beta$ -CD catalytic system, KI is the active catalyst and  $\beta$ -CD acted as a hydrogen bonding donor to accelerate the ring-opening reaction, and they show excellent synergetic effect to catalyze the reactions. The catalytic system can be reused at least five times without noticeable decrease in activity and selectivity. The greener, inexpensive, active, selective and stable catalytic system has potential application for synthesizing cyclic carbonates from CO<sub>2</sub> and epoxides.

## Experimental

### Materials

CO<sub>2</sub> was supplied by Beijing Analytical Instrument Factory with a purity of 99.995%. Propylene oxide, epichlorohydrin,  $\beta$ -cyclodextrin, potassium iodide, potassium chloride, potassium bromide were analytical grade and produced by Beijing Chemical Reagents Company. Other epoxides were purchased from ACROS ORGANICS. All chemicals were used as received.

### Cycloaddition reaction

All the cycloaddition reactions were conducted in a 22 mL stainless steel reactor equipped with a magnetic stirrer. We describe the procedures for the cycloaddition of propylene oxide (PO) because the procedures for reactions of other epoxides are similar. In the experiment, desired amounts of catalyst,  $\beta$ -cyclodextrin and PO were added into the reactor. The reactor was sealed and put into a constant-temperature air bath of desired temperature. CO<sub>2</sub> was then charged into the reactor until

the desired pressure was reached, and the stirrer was started. After a certain time, the reactor was placed into ice water and CO<sub>2</sub> was released slowly passing through a cold trap containing ethyl acetate to absorb the trace amount of reactant and product entrained by CO<sub>2</sub>. After depressurization, ethyl acetate in the cold trap and internal standard dodecane were added into the reactor. The reaction mixture was analyzed by GC (Agilent 6820) equipped with a flame-ionized detector. The purity and structure of the product at some typical experimental conditions were also checked by <sup>1</sup>H NMR and GC-MS. The products of other epoxides were analyzed at room temperature on a Bruker 400 MHz <sup>1</sup>H NMR spectrometer using CDCl<sub>3</sub> as the solvent. In the experiments to test the reusability of the catalyst, the catalyst was recovered by centrifugation, washed using ethyl ether to remove the product and dodecane, and then dried under vacuum for 12 h at 60 °C before reused. Spectral characterizations of the products (**2b–d**) are as follows:

**4-Phenylloxymethyl-1,3-dioxolan-2-one (2b).** <sup>1</sup>H NMR (CDCl<sub>3</sub>, 400 MHz)  $\delta$  (ppm) 4.15 (dd,  $J = 3.6, 10.5$  Hz, 1H), 4.24 (dd,  $J = 4.4, 10.5$  Hz, 1H), 4.54 (dd,  $J = 6.0, 8.5$  Hz, 1H), 4.62 (t,  $J = 8.4$  Hz, 1H), 5.00–5.05 (m, 1H), 6.91 (d,  $J = 8.2$  Hz, 2H), 7.02 (t,  $J = 7.4$  Hz, 1H), 7.31 (t,  $J = 8.2$  Hz, 2H).

**4-Chloromethyl-1,3-dioxolan-2-one (2c).** <sup>1</sup>H NMR (CDCl<sub>3</sub>, 400 MHz)  $\delta$  (ppm) 3.75 (dd,  $J = 3.6, 12.3$  Hz, 1H), 3.84 (dd,  $J = 4.9, 12.3$  Hz, 1H), 4.42 (dd,  $J = 5.7, 8.8$  Hz, 1H), 4.62 (t,  $J = 8.7$  Hz, 1H), 5.00–5.06 (m, 1H).

**4-Phenyl-1,3-dioxolan-2-one (2d).** <sup>1</sup>H NMR (CDCl<sub>3</sub>, 400 MHz)  $\delta$  (ppm) 4.35 (t,  $J = 8.2$  Hz, 1H), 4.80 (t,  $J = 8.4$  Hz, 1H), 5.68 (t,  $J = 8.0$  Hz, 1H), 7.36–7.45 (m, 5H).

## Acknowledgements

This work was supported by the National Key Basic Research Project of China (2006CB202504) and Chinese Academy of Sciences (KJCX2.YW.H16).

## Notes and references

- D. H. Gibson, *Chem. Rev.*, 1996, **96**, 2063.
- C. Song, *Catal. Today*, 2006, **115**, 2.
- T. Sakakura, J. C. Choi and H. Yasuda, *Chem. Rev.*, 2007, **107**, 2365.
- A. A. G. Shaikh and S. Sivaram, *Chem. Rev.*, 1996, **96**, 951.
- M. Yoshida and M. Ihara, *Chem. Eur. J.*, 2004, **10**, 2886.
- J. Bayardon, J. Holz, B. Schöffner, V. Andrushko, S. Verevkin, A. Preetz and A. Börner, *Angew. Chem. Int. Ed.*, 2007, **46**, 5971.
- J. H. Clements, *Ind. Eng. Chem. Res.*, 2003, **42**, 663.
- S. Fukuoka, M. Kawamura, K. Komiya, M. Tojo, H. Hachiya, K. Hasegawa, M. Aminaka, H. Okamoto, I. Fukawa and S. Konno, *Green. Chem.*, 2003, **5**, 497.
- T. Zhao, Y. Han and Y. Sun, *Phys. Chem. Chem. Phys.*, 1999, **12**, 3047.
- N. Kihare, N. Hara and T. Endo, *J. Org. Chem.*, 1993, **58**, 6198.
- J. W. Huang and M. Shi, *J. Org. Chem.*, 2003, **68**, 6705.
- K. Yamaguchi, K. Ebitani, T. Yoshida, H. Yoshida and K. Kaneda, *J. Am. Chem. Soc.*, 1999, **121**, 4526.
- T. Yano, H. Matsui, T. Koike, H. Ishiguro, H. Fujihara, M. Yoshihara and T. Maeshima, *Chem. Comm.*, 1997, 1129.
- W. J. Kruper and D. V. Dellar, *J. Org. Chem.*, 1995, **60**, 725.
- X. B. Lu, Y. J. Zhang, K. Jin, L. M. Luo and H. Wang, *J. Catal.*, 2004, **227**, 537.
- J. Meléndez, M. North and R. Pasquale, *Eur. J. Inorg. Chem.*, 2007, 3323.
- F. Li, C. Xia, L. Xu, W. Sun and G. Chen, *Chem. Comm.*, 2003, 2042.



- 18 Y. M. Shen, W. L. Duan and M. Shi, *Eur. J. Org. Chem.*, 2004, 3080.  
19 T. Aida and S. Inoue, *J. Am. Chem. Soc.*, 1983, **105**, 1304.  
20 Y. Du, F. Cai, D. L. Kong and L. N. He, *Green Chem.*, 2005, **7**, 518.  
21 J. He, T. Wu, Z. Zhang, K. Ding, B. Han, Y. Xie, T. Jiang and Z. Liu, *Chem. Eur. J.*, 2007, **13**, 6992.  
22 Y. Xie, Z. Zhang, T. Jiang, J. He, B. Han, T. Wu and K. Ding, *Angew. Chem. Int. Ed.*, 2007, **46**, 7255.  
23 H. Yasuda, L. N. He, T. Sakakura and C. Hu, *J. Catal.*, 2005, **233**, 119.  
24 Y. Du, J. Q. Wang, J. Y. Chen, F. Cai, J. S. Tian, D. L. Kong and L. N. He, *Tetrahedron Lett.*, 2006, **47**, 1271.  
25 L. N. He, H. Yasuda and T. Sakakura, *Green Chem.*, 2003, **5**, 92.  
26 W. N. Sit, S. M. Ng, K. Y. Kwong and C. P. Lau, *J. Org. Chem.*, 2005, **70**, 8583.  
27 H. Kawanami, A. Sasaki, K. Matsui and Y. Ikushima, *Chem. Comm.*, 2003, 896.  
28 A. Zhu, T. Jiang, B. Han, J. Zhang, Y. Xie and X. Ma, *Green Chem.*, 2007, **9**, 169.  
29 H. Yasuda, L. N. He and T. Sakakura, *J. Catal.*, 2002, **209**, 547.  
30 H. Yasuda, L. N. He and T. Sakakura, *Stud. Surf. Sci. Catal.*, 2003, **136**, 259.  
31 F. Shi, Q. Zhang, Y. Ma, Y. He and Y. Deng, *J. Am. Chem. Soc.*, 2005, **127**, 4182.  
32 K. Takahashi, *Chem. Rev.*, 1998, **98**, 2013.  
33 R. Breslow and S. D. Dong, *Chem. Rev.*, 1998, **98**, 1997.  
34 K. Surendra, N. S. Krishnaveni, Y. V. D. Nageswar and K. R. Rao, *J. Org. Chem.*, 2003, **68**, 4994.  
35 W. K. Chan, W. Y. Yu, C. M. Che and M. K. Wong, *J. Org. Chem.*, 2003, **68**, 6576.  
36 N. S. Krishnaveni, K. Surendra and K. R. Rao, *Adv. Synth. Catal.*, 2004, **346**, 346.  
37 N. S. Krishnaveni, K. Surendra and K. R. Rao, *Chem. Comm.*, 2005, 669.  
38 N. S. Krishnaveni, K. Surendra, M. S. Reddy, Y. V. D. Nageswar and K. R. Rao, *Adv. Synth. Catal.*, 2004, **346**, 395.  
39 A. Schlatter, M. K. Kundu and W. D. Woggon, *Angew. Chem. Int. Ed.*, 2004, **43**, 6731.  
40 M. A. Reddy, L. R. Reddy, N. Bhanumathi and K. R. Rao, *New J. Chem.*, 2001, **25**, 359.  
41 H. B. Ji, D. P. Shi, M. Shao, Z. Li and L. F. Wang, *Tetrahedron Lett.*, 2005, **46**, 2517.  
42 B. Kaboudin and M. Sorbiun, *Tetrahedron Lett.*, 2007, **48**, 9015.  
43 K. Surendra, N. S. Krishnaveni and K. R. Rao, *Tetrahedron Lett.*, 2004, **45**, 6523.  
44 Y. Zhou, S. Hu, X. Ma, S. Liang, T. Jiang and B. Han, *J. Mol. Catal. A: Chem.*, 2008, **284**, 52.  
45 H. F. Zhang, B. X. Han, Z. S. Hou and Z. M. Liu, *Fluid Phase Equilib.*, 2001, **179**, 131.  
46 X. B. Lu, J. H. Xiu, R. He, K. Jin, L. M. Luo and X. J. Feng, *Appl. Catal. A: Gen.*, 2004, **275**, 73.  
47 T. Sakai, Y. Tsutsumi and T. Ema, *Green Chem.*, 2008, **10**, 337.

**Retracted article: An efficient and practical synthesis of chiral imidazolium ionic liquids and their application in an enantioselective Michael reaction**

Wen-Hua Ou and Zhi-Zhen Huang

*Green Chem.*, 2006, **8**(8), 731–734 (DOI: 10.1039/b604801c)

We, the named authors, hereby retract this Green Chemistry paper. Signed: Wen-Hua Ou and Zhi-Zhen Huang, Nanjing, China, June 2008. Retraction endorsed by Sarah Ruthven, Editor. Retraction published 13 June 2008.

**Ionic liquids *via* efficient, solvent-free anion metathesis**

Peter D. Vu, Andrew J. Boydston and Christopher W. Bielawski

*Green Chem.*, 2007, **9**(11), 1158–1159 (DOI: 10.1039/b705745h)

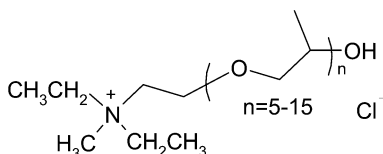
Since the publication of our manuscript (*Green Chem.*, 2007, **9**, 1158), we have become aware of related anion metathesis methodologies, see: WO 2006/063653, WO 2006/063654, WO 2006/063655, and WO 2006/063656.

**Designing enzyme-compatible ionic liquids that can dissolve carbohydrates**

Hua Zhao, Gary A. Baker, Zhiyan Song, Olarongbe Olubajo, Tanisha Crittle and Darkeysha Peters

*Green Chem.*, 2008, **10**(6), 696–705 (DOI: 10.1039/b801489b)

An error was found in Scheme 1 on page 698. The correct version is given below.



The Royal Society of Chemistry apologises for these errors and any consequent inconvenience to authors and readers.

**Additions and corrections can be viewed online by accessing the original article to which they apply.**

Number 1  
in the field



# years of publishing!

## *Green Chemistry...*

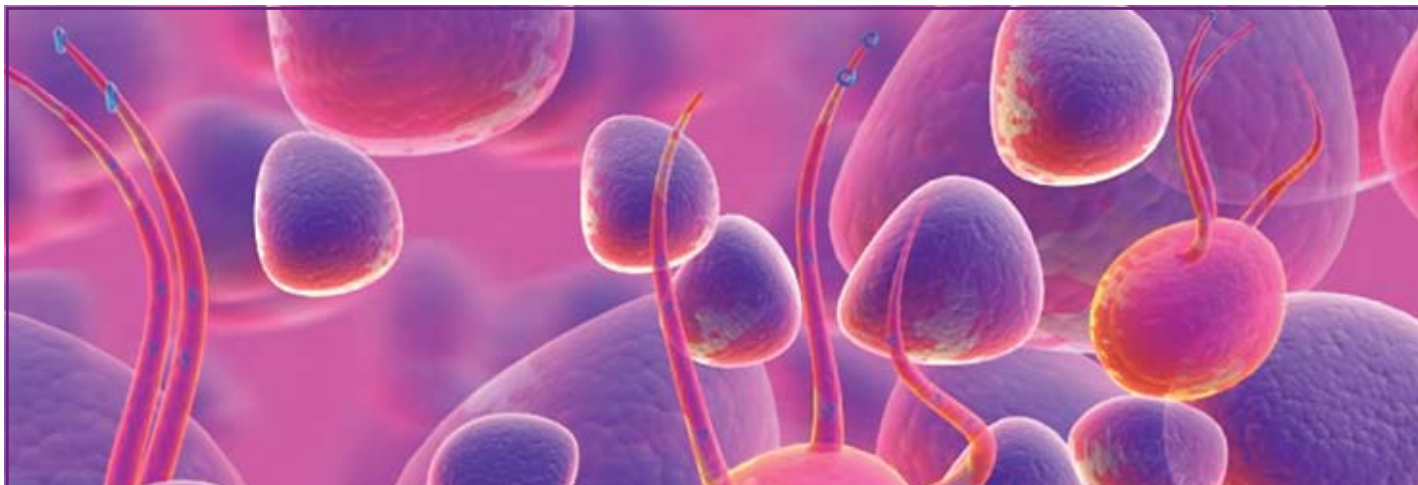


- The most highly cited *Green Chemistry* journal, Impact factor = 4.836\*
- Fast publication, typically <90 days for full papers
- Full variety of research including reviews, communications, full papers and perspectives.

Celebrating 10 years of publishing, *Green Chemistry* offers the latest research that reduces the environmental impact of the chemical enterprise by developing alternative sustainable technologies, and provides a unique forum for the rapid publication of cutting-edge and innovative research for a greener, sustainable future

*...for a sustainable future!*

\* 2007 Thomson Scientific (ISI) Journal Citation Reports ®



*Integrative Biology* would like to congratulate the 2008 recipients of the

## Nobel Prize in Chemistry

The prize was awarded to Roger Y. Tsien, Osamu Shimomura and Martin Chalfie for outstanding contributions in chemistry for their work in the development of the gene marker green fluorescent protein (GFP).

"We are all immensely pleased that 2008 Nobel Prize winner Roger Tsien is an Editorial Board member for *Integrative Biology*; his work typifies the quality of material we are seeking in the development of biology through new tools and technologies."

Harp Minhas, managing editor of *Integrative Biology*

### Submit your work to *Integrative Biology*

Launching January 2009, *Integrative Biology* provides a unique venue for elucidating biological processes, mechanisms and phenomena through quantitative enabling technologies at the convergence of biology with physics, chemistry, engineering, imaging and informatics.

Submissions are welcomed via ReSource, our homepage for authors and referees. [www.rsc.org/resource](http://www.rsc.org/resource)



Professor Roger Y. Tsien, Editorial Board, *Integrative Biology*

Go online Today!